



Natural Resources
Canada

Ressources naturelles
Canada

**GEOLOGICAL SURVEY OF CANADA
OPEN FILE 8135**

**Analysis of piston cores and high-resolution sub-bottom
profiler data, Baffin Bay slope, Nunavut**

D.C. Campbell, K.A. Jenner, J. Higgins, and D.J.W. Piper

2017



Canada



GEOLOGICAL SURVEY OF CANADA OPEN FILE 8135

Analysis of piston cores and high-resolution sub-bottom profiler data, Baffin Bay slope, Nunavut

D.C. Campbell, K.A. Jenner, J. Higgins, and D.J.W. Piper

2017

© Her Majesty the Queen in Right of Canada, as represented by the Minister of Natural Resources, 2017

Information contained in this publication or product may be reproduced, in part or in whole, and by any means, for personal or public non-commercial purposes, without charge or further permission, unless otherwise specified.

You are asked to:

- exercise due diligence in ensuring the accuracy of the materials reproduced;
- indicate the complete title of the materials reproduced, and the name of the author organization; and
- indicate that the reproduction is a copy of an official work that is published by Natural Resources Canada (NRCan) and that the reproduction has not been produced in affiliation with, or with the endorsement of, NRCan.

Commercial reproduction and distribution is prohibited except with written permission from NRCan. For more information, contact NRCan at nrcan.copyrightdroitdauteur.nrcan@canada.ca.

doi:10.4095/300835

This publication is available for free download through GEOSCAN (<http://geoscan.nrcan.gc.ca/>).

Recommended citation

Campbell, D.C., Jenner, K.A., Higgins, J., and Piper, D.J.W., 2017. Analysis of piston cores and high-resolution sub-bottom profiler data, Baffin Bay slope, Nunavut; Geological Survey of Canada, Open File 8135, 179 p. doi:10.4095/300835

Publications in this series have not been edited; they are released as submitted by the author.

Preface

This Open File report summarizes a set of 20 piston cores, up to 822 cm long, taken from the continental slope of Baffin Bay, Canada, in water depths between 833 and 1715 m. It provides down-core lithostratigraphy, physical properties measurements, core photography and core X-radiography, in addition to high-resolution seismic data over most core sites, selected grain size data and portable X-ray fluorescence data. Preliminary along-slope correlation between cores and AMS radiocarbon ages are also provided. Further information on these cores is available through the Expedition Database at http://ed.gdr.nrcan.gc.ca/index_e.php

Acknowledgments

We thank Dan Meagher, Jesse Sherwin and Meaghan MacQuarrie for assistance with core processing and core logging and Jessica Parkinson and Simon Poirier for core data compilation. Owen Brown completed grain size analyses and Linda Fan assisted with these analyses and plotted the grain size data. We also thank Kate Jarrett for assistance with core subsampling.

Authors' addresses

D.C. Campbell, K.A. Jenner, J. Higgins, and D. J.W. Piper are all from the Geological Survey of Canada (Atlantic), Bedford Institute of Oceanography, P.O. Box 1006, Dartmouth, N.S. B2Y 4A2

Authors' e-mails

Calvin.Campbell@canada.ca

Kimberley.Jenner@canada.ca

Jenna.Higgins@canada.ca

David.Piper@canada.ca

Contents

1.0 Introduction.....	11
2.0 Methods.....	12
2.1 Shipboard operations	12
2.2 Core processing at GSC (Atlantic)	13
2.2.1 Multi Sensor Core Logger (MSCL).....	14
2.2.2 Core Photography	17
2.2.3 Reflectance Spectrophotometry	17
2.2.4 Sample Description	18
2.2.5 Discrete core measurements	18
2.2.6 Core data compilation	20
2.2.7 Radiocarbon Dating	21
2.2.8 Portable X-ray Fluorescence (pXRF) Spectrometer	22
2.2.9 Grain Size Measurements	23
3.0 Results, Core Summaries and Acoustic stratigraphic setting	23
3.1 The northern Baffin Island slope	24
3.2 The slope off Clyde River.....	33
3.3 The slope off Home Bay	35
3.4 The slope off Disko Bugt.....	45
4.0 Baffin Bay Slope Lithofacies.....	50
4.1 Lithofacies 1 (L1) - Diamicton	50
Interbedded Mud and Weakly Stratified Diamicton.....	51
Graded Diamicton.....	52
4.2 Lithofacies 2 (L2) – Laminated Red Brown Mud	53
Parallel Laminated and Rhythmically Laminated Mud	54
Parallel Laminated Red Brown Mud and Very Fine Sand with IRD	54
4.3 Lithofacies 3 (L3) - Tan Carbonate Mud.....	55
4.4 Lithofacies 4 (L4) - Bioturbated Brown Mud.....	57
References.....	59
Tables and Figures	60

List of Tables

All tables appear at the end of the report.

Table 1. Cores used in this study.

Table 2. Radiocarbon results used in this study.

List of Figures

All figures appear at the end of the report.

Figure 1.1. Location map of Baffin Bay showing 2013029 core locations (white circles) and 2013029 sub-bottom profiler coverage (black lines). White lines indicate high resolution seismic reflection profiles collected by the GSC prior to the 2013 expedition. Boxes indicate the 4 geographic regions discussed in the text. Bathymetric contour interval is 200 m.

Figure 3.1. Regional map showing core locations and seismic coverage for the northern Baffin Bay slope region. 2013029 core locations are indicated by white circles and 2013029 sub-bottom profiler coverage by black lines. White lines indicate high resolution seismic reflection profiles collected by the GSC prior to the 2013 expedition. Bathymetric contour interval is 200 m.

Figure 3.2a. 3.5 kHz sub-bottom profile showing the regional acoustic facies of the northern Baffin Island slope region and location of piston cores 2013029-063 & 2013029-064.

Figure 3.2b. 3.5 kHz sub-bottom profile showing the regional acoustic facies of the northern Baffin Island slope region and location of piston cores 2013029-059 & 2013029-060.

Figure 3.2c. 3.5 kHz sub-bottom profile showing the regional acoustic facies of the northern Baffin Island slope region and location of piston cores 2013029-061 & 2013029-062.

Figure 3.2d. 3.5 kHz sub-bottom profile showing the regional acoustic facies of the northern Baffin Island slope region and location of piston cores 2013029-057 & 2013029-058.

Figure 3.3. 3.5 kHz sub-bottom profile showing the acoustic stratigraphy and location of core 2013029-063.

Figure 3.4. Core plot summary legend.

Figure 3.5a. Core plot summary for piston core 2013029-063.

Figure 3.5b. Core plot summary for trigger weight core 2013029-063.

Figure 3.6a. Photography and X-radiography compilation for piston core 2013029-063.

Figure 3.6b. Photography and X-radiography compilation for trigger weight core 2013029-063.

Figure 3.7. 3.5 kHz sub-bottom profile showing the acoustic stratigraphy and position of core 2013029-064.

Figure 3.8a. Core plot summary for piston core 2013029-064.

Figure 3.8b. Core plot summary for trigger weight core 2013029-064.

Figure 3.9a. Photography and X-radiography compilation for piston core 2013029-064.

Figure 3.9b. Photography and X-radiography compilation for trigger weight core 2013029-064.

Figure 3.10. Down-core pXRF analysis for piston core 2013029-064. Tan highlighting indicates tan carbonate mud; rose highlighting indicates rose mud; gold brown highlighting indicates gold brown mud; light brown highlighting indicates light brown mud associated with an increase in the pXRF Ca/Ti ratio.

Figure 3.11. Representative grain size spectra plots of each lithofacies.

Figure 3.12. 3.5 kHz sub-bottom profile showing the acoustic stratigraphy and position of core 2013029-059.

Figure 3.13. Down-core pXRF analysis for piston core 2013029-059. Tan highlighting indicates tan carbonate mud; rose highlighting indicates rose mud; gold brown highlighting indicates gold brown mud.

Figure 3.14a. Core plot summary for piston core 2013029-059.

Figure 3.14b. Core plot summary for trigger weight core 2013029-059.

Figure 3.15a. Photography and X-radiography compilation for piston core 2013029-059.

Figure 3.15b. Photography and X-radiography compilation for trigger weight core 2013029-059.

Figure 3.16. 3.5 kHz sub-bottom profile showing the acoustic stratigraphy and position of core 2013029-060.

Figure 3.17a. Core plot summary for piston core 2013029-060.

Figure 3.17b. Core plot summary for trigger weight core 2013029-060.

Figure 3.18a. Photography and X-radiography compilation for piston core 2013029-060.

Figure 3.18b. Photography and X-radiography compilation for trigger weight core 2013029-060.

Figure 3.19. 3.5 kHz sub-bottom profile showing the acoustic stratigraphy and position of core 2013029-061.

Figure 3.20a. Core plot summary for piston core 2013029-061.

Figure 3.20b. Core plot summary for trigger weight core 2013029-061.

Figure 3.21a. Photography and X-radiography compilation for piston core 2013029-061.

Figure 3.21b. Photography and X-radiography compilation for trigger weight core 2013029-061.

Figure 3.22. Down-core pXRF analysis for piston core 2013029-061. Tan highlighting indicates tan carbonate mud; rose highlighting indicates rose mud; gold brown highlighting indicates gold brown mud.

Figure 3.23. 3.5 kHz sub-bottom profile showing the acoustic stratigraphy and position of core 2013029-062.

Figure 3.24a. Core plot summary for piston core 2013029-062.

Figure 3.24b. Core plot summary for trigger weight core 2013029-062.

Figure 3.25a. Photography and X-radiography compilation for piston core 2013029-062.

Figure 3.25b. Photography and X-radiography compilation for trigger weight core 2013029-062.

Figure 3.26. 3.5 kHz sub-bottom profile showing the acoustic stratigraphy and position of core 2013029-057.

Figure 3.27a. Core plot summary for piston core 2013029-057.

Figure 3.27b. Core plot summary for trigger weight core 2013029-057.

Figure 3.28a. Photography and X-radiography compilation for piston core 2013029-057.

Figure 3.28b. Photography and X-radiography compilation for trigger weight core 2013029-057.

Figure 3.29. 3.5 kHz sub-bottom profile showing the acoustic stratigraphy and position of core 2013029-056.

Figure 3.30a. Core plot summary for piston core 2013029-056.

Figure 3.30b. Core plot summary for trigger weight core 2013029-056.

Figure 3.31a. Photography and X-radiography compilation for piston core 2013029-056.

Figure 3.31b. Photography and X-radiography compilation for trigger weight core 2013029-056.

Figure 3.32. Regional map showing core locations and seismic coverage for the Clyde River region. 2013029 core locations are indicated by white circles and 2013029 sub-bottom profiler coverage by black lines. White lines indicate high resolution seismic reflection profiles collected by the GSC prior to the 2013 expedition. Bathymetric contour interval is 200 m.

Figure 3.33. Regional acoustic facies of the Clyde River slope region.

Figure 3.34. 3.5 kHz sub-bottom profile showing the acoustic stratigraphy and position of core 2013029-053.

Figure 3.35a. Core plot summary for trigger weight core 2013029-053.

Figure 3.35b. Photography and X-radiography compilation for trigger weight core 2013029-053.

Figure 3.36. 3.5 kHz sub-bottom profile showing the acoustic stratigraphy and position of core 2013029-052.

Figure 3.37a. Core plot summary for piston core 2013029-052.

Figure 3.37b. Core plot summary for trigger weight core 2013029-052.

Figure 3.38a. Photography and X-radiography compilation for piston core 2013029-052.

Figure 3.38b. Photography and X-radiography compilation for trigger weight core 2013029-052.

Figure 3.39. 3.5 kHz sub-bottom profile showing the acoustic stratigraphy and position of core 2013029-073.

Figure 3.40a. Core plot summary for piston core 2013029-073.

Figure 3.40b. Core plot summary for trigger weight core 2013029-073.

Figure 3.41a. Photography and X-radiography compilation for piston core 2013029-073.

Figure 3.41b. Photography and X-radiography compilation for trigger weight core 2013029-073.

Figure 3.42. Regional map showing core locations and seismic coverage for the Home Bay region. 2013029 core locations are indicated by white circles and 2013029 sub-bottom profiler

coverage by black lines. White lines indicate high resolution seismic reflection profiles collected by the GSC prior to the 2013 expedition. Bathymetric contour interval is 200 m.

Figure 3.43a. 3.5 kHz sub-bottom profile showing the regional acoustic facies on the slope off Home Bay and location of piston cores 2013029-074 & 2013029-075.

Figure 3.43b. 3.5 kHz sub-bottom profile showing the regional acoustic facies on the slope off Home Bay and location of piston cores 2013029-047 & 2013029-048.

Figure 3.44. 3.5 kHz sub-bottom profile showing the acoustic stratigraphy and position of core 2013029-074.

Figure 3.45a. Core plot summary for piston core 2013029-074.

Figure 3.45b. Core plot summary for trigger weight core 2013029-074.

Figure 3.46a. Photography and X-radiography compilation for piston core 2013029-074.

Figure 3.46b. Photography and X-radiography compilation for trigger weight core 2013029-074.

Figure 3.47. Down-core pXRF analysis for piston core 2013029-074. Tan highlighting indicates tan carbonate mud; rose highlighting indicates rose mud.

Figure 3.48. 3.5 kHz sub-bottom profile showing the acoustic stratigraphy and position of core 2013029-075.

Figure 3.49a. Core plot summary for piston core 2013029-075.

Figure 3.49b. Core plot summary for trigger weight core 2013029-075.

Figure 3.50a. Photography and X-radiography compilation for piston core 2013029-075.

Figure 3.50b. Photography and X-radiography compilation for trigger weight core 2013029-075.

Figure 3.51. Hunttec profile showing the acoustic stratigraphy and position of core 2013029-076.

Figure 3.52a. Core plot summary for piston core 2013029-076.

Figure 3.52b. Core plot summary for trigger weight core 2013029-076.

Figure 3.53a. Photography and X-radiography compilation for piston core 2013029-076.

Figure 3.53b. Photography and X-radiography compilation for trigger weight core 2013029-076.

Figure 3.54. Hunttec profile showing the acoustic stratigraphy and position of core 2013029-077.

Figure 3.55a. Core plot summary for piston core 2013029-077.

Figure 3.55b. Core plot summary for trigger weight core 2013029-077.

Figure 3.56a. Photography and X-radiography compilation for piston core 2013029-077.

Figure 3.56b. Photography and X-radiography compilation for trigger weight core 2013029-077.

Figure 3.57. Down-core pXRF analysis for piston core 2013029-077. Tan highlighting indicates tan carbonate mud; gold brown highlighting indicates gold brown mud; light brown highlighting indicates light brown mud associated with an increase in the pXRF Ca/Ti ratio.

Figure 3.58. Hunttec profile showing the acoustic stratigraphy and position of core 2013029-079.

Figure 3.59a. Core plot summary for piston core 2013029-079.

Figure 3.59b. Core plot summary for trigger weight core 2013029-079.

Figure 3.60a. Photography and X-radiography compilation for piston core 2013029-079.

Figure 3.60b. Photography and X-radiography compilation for trigger weight core 2013029-079.

Figure 3.61. Down-core pXRF analysis for piston core 2013029-079. Tan highlighting indicates tan carbonate mud; light brown highlighting indicates light brown mud associated with an increase in the pXRF Ca/Ti ratio.

Figure 3.62. 3.5 kHz sub-bottom profile showing the acoustic stratigraphy and position of core 2013029-047.

Figure 3.63. Core plot summary for piston core 2013029-047.

Figure 3.64. Photography and X-radiography compilation for piston core 2013029-047.

Figure 3.65. 3.5 kHz sub-bottom profile showing the acoustic stratigraphy and position of core 2013029-048.

Figure 3.66a. Core plot summary for piston core 2013029-048.

Figure 3.66b. Core plot summary for trigger weight core 2013029-048.

Figure 3.67a. Photography and X-radiography compilation for piston core 2013029-048.

Figure 3.67b. Photography and X-radiograph compilation for trigger weight core 2013029-048.

Figure 3.68. Regional map showing core locations and seismic coverage for the Disko Bugt region. 2013029 core locations are indicated by white circles and 2013029 sub-bottom profiler coverage by black lines. White lines indicate high resolution seismic reflection profiles collected by the GSC prior to the 2013 expedition. Bathymetric contour interval is 200 m.

Figure 3.69. 3.5 kHz sub-bottom profile showing the regional acoustic facies of the Disko Bugt slope region and location of piston cores 2013029-046, 2013029-082 & 2013029-084.

Figure 3.70. 3.5 kHz sub-bottom profile showing the acoustic stratigraphy and position of core 2013029-046.

Figure 3.71a. Core plot summary for piston core 2013029-046.

Figure 3.71b. Core plot summary for trigger weight core 2013029-046.

Figure 3.72a. Photography and X-radiography compilation for piston core 2013029-046.

Figure 3.72b. Photography and X-radiography compilation for trigger weight core 2013029-046.

Figure 3.73. 3.5 kHz sub-bottom profile showing the acoustic stratigraphy and position of core 2013029-082.

Figure 3.74a. Core plot summary for piston core 2013029-082.

Figure 3.74b. Core plot summary for trigger weight core 2013029-082.

Figure 3.75a. Photography and X-radiography compilation for piston core 2013029-082.

Figure 3.75b. Photography and X-radiography compilation for trigger weight core 2013029-082.

Figure 3.76 Down-core pXRF analysis for piston core 2013029-082. Tan highlighting indicates tan carbonate mud; light brown highlighting indicates light brown mud associated with an increase in the pXRF Ca/Ti ratio.

Figure 3.77. 3.5 kHz sub-bottom profile showing the acoustic stratigraphy and position of core 2013029-084.

Figure 3.78a. Core plot summary for piston core 2013029-084.

Figure 3.78b. Core plot summary for trigger weight core 2013029-084.

Figure 3.79a. Photography and X-radiography compilation for piston core 2013029-084.

Figure 3.79b. Photography and X-radiography compilation for trigger weight core 2013029-084.

Figure 4.1. Summary figure of core lithofacies from the western margin of Baffin Bay.

Figure 4.2. North to south along-slope variations of lithostratigraphy in cores from the western margin of Baffin Bay.

Figure 4.3. Examples of diamicton lithofacies.

Figure 4.4. Examples of laminated red brown mud lithofacies.

Figure 4.5. Examples of tan carbonate mud and bioturbated brown mud lithofacies.

1.0 Introduction

Baffin Bay forms an elongated ocean basin (1300 km long; 450 km wide) that connects northward to the Arctic Ocean via several Canadian Arctic Channels and southward to the Labrador Sea and the North Atlantic by way of Davis Strait (Figure 1.1). The continental shelf along the western side of Baffin Bay is 40-60 km wide and up to 300 m deep. Along the eastern side of Baffin Bay the continental shelf width increases to 200-240 km with an average depth of 500 m, except toward the southern end of the bay where the depth decreases to 300 m. Numerous u-shaped transverse troughs, 20-200 km wide and up to 700 m deep, extend out across the continental shelf to the shelf break as subsea fjord extensions. The continental slope is narrow and steep, passing rapidly out onto the relatively smooth Baffin Bay basin abyssal plain (Aksu and Piper, 1987). Unlike many other passive continental margins, Baffin Bay slope does not exhibit well-developed canyon systems, extending from the shelf break, that feed the deeper basin. The deepest, central portion of the basin reaches ~2300 m water depth.

Twenty-eight piston cores were collected onboard CCGS Hudson during expedition 2013029, predominantly along the western slope of Baffin Bay but also at the mouth of Disko Bugt, on the southeastern margin of Baffin Bay. In addition, 4200 line-kms of 3.5 kHz sub-bottom profiler data were collected with the Knudsen hull-mounted system (Campbell, 2014). This Open File documents the late Quaternary lithostratigraphy identified from 21 of these piston cores taken from Baffin Bay slope (Table 1) and presents the along-slope variation of specific lithofacies throughout the western side of the Baffin Bay margin. The cores used in this study sampled a variety of seismic stratigraphic targets, selected using high-resolution sub-bottom profiler data, to enable the development of a slope lithostratigraphic framework.

2.0 Methods

2.1 Shipboard operations

Piston core and sub-bottom profile records presented in this report were collected in August and September 2013 during CCGS Hudson Expedition 2013029 (Campbell, 2014). Core samples were acquired using the AGC Long Coring Facility. The sub-bottom profiler data were from a Knudsen 3260 system. On-board processing of cores samples entailed sectioning the cores into 1.5 m lengths, measurement of sediment strength using a handheld TORVANE® on the section ends, and collection of constant volume samples from the section ends. Core sections were then sealed and stored upright in refrigerated storage to await further analysis at the Geological Survey of Canada (Atlantic) laboratories.

2.2 Core processing at GSC (Atlantic)

(modified from Weitzman et al., 2014)

The initial steps in core processing at the GSC(A) Core Processing Laboratory are the non-destructive measurements of whole-core X-radiography and the Multi Sensor Core Logger (MSCL). Whole core X-radiography enables the evaluation of core quality and the semi-quantitative assessment of sediment structure and composition. The core is brought to ambient room temperature after X-radiography is completed and it is run through the MSCL for measurement of whole core sediment physical properties at a standard 1 cm down-core resolution. Following whole-core analysis, the plastic liner is cut longitudinally using the GSC(A) Duits splitter. The sediment core is then split longitudinally by pulling a piece of fine wire through the sediment along the cuts in the plastic core liner. The two core halves are designated archive and working and are temporarily covered with plastic wrap. Each half is labelled with an up arrow, cruise number, sample number and section information.

Metre tape is placed along the length of the split core section to indicate down-core depth. The archive half is photographed, measured for colour reflectance, and described visually. The working half is immediately measured for physical properties, before the core dries, at intervals of 10 cm for velocity and shear strength and 50 cm for bulk density and water content.

Additional samples are taken depending on the specific core-site objectives. The core halves are re-covered with plastic wrap, sealed in labeled plastic core sleeving, placed in labelled plastic D-tubes and stored at 4°C in the GSC(A) GSC-A Marine Geoscience Collection Facility.

2.2.1 Multi Sensor Core Logger (MSCL)

The MSCL measures compressional (P) wave velocity in a transverse direction, bulk density and magnetic susceptibility. The MSCL consists of two tracks with a sensor stand in between them; one track has a motorized pusher that pushes whole core sections through the sensor stand and onto the passive track. The sensor stand includes a core detection laser, a gamma ray emitter and detector, two rolling p-wave transducers, and a magnetic susceptibility solenoid; all sensor offset distances from the laser are known. Both the motor and the sensors in the stand are connected to an electronics rack that includes a computer for automating the system.

Whole core sections are placed in front of the pusher on the motorized track, their lengths are automatically measured by breaking the detection laser, and are then incrementally pushed past each sensor for measurement. Measurements from each sensor are taken after each increment of travel. A piece of plastic core liner filled with distilled water is run through the MSCL every four or five sections of core to check the precision of the MSCL system.

The quality of the bulk density and velocity values is dependent on: 1) an accurate measure of sediment thickness, 2) the degree of sediment saturation, and 3) the presence of air voids between the sediment and plastic core liner. The magnitude of magnetic susceptibility values is dependent on the type of sediment and the volume of material within the coil. Identical cores containing the same sediment but of varying diameters will give different magnetic susceptibility values but will show the same down-core profile.

Compressional Wave Velocity (PWL)

The P-wave logger system consists of two spring loaded compressional wave transducers (PWT) and two laser distance transducers attached to the PWT mountings. The PWTs are pushed against either side of the core as it moves between the transducers. A short 500 kHz compressional wave pulse is produced at the transmitting transducer at a repetition rate of 1 kHz. This wave pulse travels through the core and is detected by the receiving transducer and the time of flight of the wave pulse is measured. The two laser distance transducers measure the displacement of the active faces of the PWT transducers. The diameter of the sediment core is calculated by subtracting the liner thickness from the measured distance between the distance transducers. This calculation assumes that the core liner is filled with sediment. The P-wave travel time delay caused by the core liner and the electronics of the system is calculated using a distilled water standard of known diameter and temperature. The measured sediment P-wave travel time is corrected for the P-wave travel time delay. The sediment P-wave velocity is calculated as the sediment diameter/corrected P-wave travel time.

Gamma Ray Attenuation (GRA)

The GRA unit measures the bulk density of the sediment. It comprises a 10 millicurie ¹³⁷Cesium capsule housed in a 150 mm ø primary lead shield with 2.5 and 5 mm collimators and a sodium iodide scintillation detector housed in a 100 mm ø collimated lead shielding. The source and detector are mounted on opposite sides of the core as it moves through the central unit assembly. A narrow (pencil size) beam of gamma rays with energies principally at 0.662 MeV is emitted from the ¹³⁷Cesium source and passes through the diameter of the sediment core. At these energy levels Compton scattering is the primary mechanism for the attenuation of the gamma rays in

most sedimentary material. The incident photons are scattered by collision with electrons encountered in the core and there is a partial energy loss. The attenuated gamma-ray beam is measured by the scintillation detector. The Compton scattering of the photons is directly related to the number of electrons in the path of the gamma ray beam. A two-phase model representing the mineral and interstitial water of fully saturated marine sediment is assumed for the MSCL GRA calibration. Aluminum is assumed to have an attenuation coefficient similar to common minerals found in marine sediments and represents the mineral phase. Distilled water represents the interstitial water phase. A calibration standard consisting of different thicknesses of aluminum and distilled water is used to calibrate the GRA. The measure of density of the sediments assumes that the marine sediment is fully saturated and completely fills the core liner. The diameter of the sediment is determined using the measured displacement between the laser distance transducers and the thickness of the liner. Sediment density is calculated using the calibration coefficients and the measured diameter of the sediment.

Magnetic Susceptibility (MS)

A Bartington loop sensor (MS2B) measures the magnetic susceptibility of the sediment. It is mounted to minimize the effects of magnetic or metallic components of the MSCL system. An oscillator circuit in the sensor loop produces a low intensity non-saturating, alternating magnetic field. Changes in the oscillator frequency caused by material that has a magnetic susceptibility is measured and converted into magnetic susceptibility values. Air measurements taken at the beginning and end of each section are used to correct the measurements for equipment drift during each section run.

2.2.2 Core Photography

The archive half of the core is photographed using a Nikon D300 12.3 megapixel digital camera. Overlapping digital photographs are taken at two scales. The first is a close up image covering a 30 cm interval with a 5 cm overlap, and the second is a long shot image covering a 90 cm interval with a 25 cm overlap. The images are saved in raw, tiff and jpg formats.

2.2.3 Reflectance Spectrophotometry

High accuracy measurements of spectral reflectance of split core are made over wavelengths of 400 to 700 nm using the Konica Minolta Spectrophotometer CM 2600d. Tristimulus values X, Y and Z are derived from the colour reflectance spectra according to the Commission Internationale d'Eclairage (CIE) method. The $L^*a^*b^*$ system (CIELAB) represents coordinates in 3 dimensional space where the L^* is the vertical axis representing lightness and a^* b^* are horizontal radii representing chromaticity. The L^* value ranges from zero (black) to 100 (white). The a^* value represents green (-) to red (+) and the b^* value represents blue (-) to yellow (+). Munsell colour is calculated but there is no international standard for converting Tristimulus values to Munsell HVC notation.

A zero calibration is performed to compensate for the effects of any change in the optical system and changes in ambient and internal temperature. White calibration is done using a white ceramic calibration cap and sets the maximum reflectance to 100 %. Zero calibrations are performed daily and white calibrations are performed routinely at the beginning of each section.

Prior to spectral reflectance measurements the archive half of the core is carefully covered with Glad ClingWrap™ taking care to minimize the presence of air bubbles between the sediment and the wrap. Measurements are taken at 5 cm intervals where possible.

2.2.4 Sample Description

Written laboratory descriptions for the sediment cores include: 1) condition of sample (e.g. cracks, disturbance, oxidation), 2) consistency of sample (e.g. soft, hard, firm) 3) reaction to 10% hydrochloric acid which indicates the presence of calcium carbonate, 4) colour, based on Munsell soil colour charts and 5) visual core description consisting of colour, texture, grain size, stratification, depositional contacts, bedforms, sedimentary and post-sedimentary structures, presence of organic material, shells, bioturbation and any other visible feature. Lithologic summaries were created on the basis of sedimentary facies developed from visual sediment colour, spectrophotometry data, sediment structures, sediment texture and shear strength and, in some cores, pXRF data.

2.2.5 Discrete core measurements

Discrete velocity

The split core P-wave logger system has four transducer probes that are carefully inserted into the split core section and measure compressional wave velocity in both longitudinal and transverse directions to the axis of the core. There is a P-wave travel time delay caused by the electronics of the system which is calculated for each set of transducers by measuring the distance between the transducers and measuring the travel time in distilled water at a known

temperature. The measured sediment P-wave travel time is corrected for the P-wave travel time delay. The sediment P-wave velocity is calculated as the sediment diameter/corrected P-wave travel time. Longitudinal and transverse velocity measurements are taken at standard 10 cm intervals.

Discrete Shear Strength

Split core undrained shear strength measurements are made using a motorized miniature vane shear apparatus. A four bladed vane is inserted to a constant depth within clayey, split-core intervals and rotated at a constant rate of 90°/min until sediment failure.

The difference in rotational strain between the top and bottom of a linear spring (deflection angle) is measured and the torque required to shear the cylindrical surface around the vane is calculated. Routine calibration of the system is not necessary. Each vane has a vane blade constant dependent on the geometry of the blade, and each spring has a spring constant that relates the deflection angle to the torque. Peak and remoulded shear strength values are calculated according to ASTM Method D 4648. Peak shear strength measurements are taken at standard 10 cm intervals. Two to three measurements of remoulded shear strength are taken per section. Onboard measurements of whole-core peak shear strength are taken from the top and base of each whole-core section using a hand-held TORVANE®.

Constant volume sampling

Constant volume samples are taken using a stainless steel cylinder of known volume. The cylinder is gently introduced into the sediment at a constant rate. The cylinder is then carefully removed from the core and trimmed using a wire saw. The sediment is extruded from the cylinder, weighed, dried at 105°C for 24 hours and weighed again. Bulk density and water content values are calculated according to ASTM Method D2216-98.

2.2.6 Core data compilation

MSCL data, spectral reflectance, shear strength and constant volume data for individual cores are compiled as Excel workbooks. Each workbook consists of individual worksheets containing the original unedited physical property datasets and a worksheet of the compiled physical property dataset. The compiled dataset is imported into Kaleidagraph and poor quality data is masked. The edited, good quality, data is saved as a tab delimited text file and plotted. The graphic lithology, MSCL, spectral reflectance, and discrete onboard and laboratory physical property data plots are compiled in a CoreIDRAW letter size core plot summary file.

Down-core summaries are a synthesis of MSCL data, spectral reflectance measurements, geotechnical measurements and detailed core descriptions. Lithologies are interpreted using core descriptions, core photography, X-radiography, MSCL data plots, discrete geotechnical measurements and limited pXRF data.

2.2.7 Radiocarbon Dating

Radiocarbon dating was carried out on a total of eight samples. Six samples underwent accelerator mass spectrometry (AMS) at the National Ocean Sciences Accelerator Mass Spectrometry (NOSAMS) facility of the Woods Hole Oceanographic Institution. Calcareous foraminifers were hand-picked from the >106 μm fraction. In five of the six samples, the foraminifer populations extracted consisted of mixed benthic taxa; in one sample, the population consisted of planktic foraminifers dominated by *Neogloboquadrina pachyderma* left-coiled. The total weight of carbonate extracted ranged from 1.1 to 4.9 mg (Table 2).

An additional sample, at the base of core 2013029 077 (638-643.5 cm), was sent to the Keck AMS Laboratory at the University of California at Irvine because of the unusually small sample size (Table 2). An eighth sample, containing mollusc shell fragments, from 2013029 073, was analysed at the Institute of Arctic and Alpine Research Laboratory, University of Colorado at Boulder, Colorado.

Dates reported on core plot summaries and in the text are conventional radiocarbon ages which have been calibrated with the online software Calib 7.1 using the Marine13 calibration curve of Reimer et al. (2013) and a ΔR of 220 ± 20 to account for regional air-sea reservoir differences (Coulthard et al., 2010). All calibrated radiocarbon ages are reported as 1σ .

One AMS date, taken from core 062, may be unreliable. The sample was taken from a gold brown mud bed underlying thin stratified diamicton and is ~20,000 cal years BP older than ages immediately overlying the stratified diamicton in nearby core 064 (Table 2). The biogenic content of the sample was poor and the > 106 μg fraction contained detrital particles. There is also inconsistency with the age of 15,894 calibrated years BP which is ~2,000 calibrated years BP older than the underlying age of 13,804 calibrated years BP.

2.2.8 Portable X-ray Fluorescence (pXRF) Spectrometer

An Olympus Innov-X Delta Premium 6000 spectrometer is mounted on a vertical motorized arm of an MSCL, configured for analyzing split cores, to facilitate high-resolution down core elemental data. Generally, the instrument is capable of measuring many elements from Mg through U, however, they are not all measured simultaneously. Different settings are used depending on which elements are being targeted for study. The down-core resolution and measurement times of the instrument are also user-defined. In this study, pXRF data were collected at 1cm down-core resolution using Soil Mode with 30 second dwell times for each of beams 2 and 3.

Because there are a number of sources of error that are inherent when taking pXRF measurements of marine core samples (i.e. matrix effects, water content, sample inhomogeneity, uneven split core surface) it is widely accepted that these pXRF measurements are semi-quantitative and should be considered as such during interpretation. All pXRF data herein are presented as ratios of elemental abundances.

2.2.9 Grain Size Measurements

Grain size analyses for the sand and mud fractions of samples were completed using a Beckman Coulter Laser LS-230 laser diffraction analyser with a grain size analysis range of 0.4 to 2000 microns. In preparation for laser analysis, the samples were dried and then washed at 63 microns. The < 63 micron fraction (mud) was freeze dried prior to analysis; the > 63 micron to < 2000 micron fraction (sand) was microsplit. The >2000 micron fraction (gravel) was dry sieved at ¼ phi intervals. Data were then processed and merged at 1/5th phi midpoint intervals and converted to microns. These data were then plotted using Grapher 7 software and imported into the grain size spectra format developed in CorelDraw X5.

3.0 Results, Core Summaries and Acoustic stratigraphic setting

The cores in this study are grouped into four areas based on their geographic setting: 1) the northern Baffin Island slope which covers the slope off Pond Inlet, Buchan Trough and Scott Trough, 2) the central Baffin Island slope off Clyde River, 3) the southern Baffin Island slope off Home Bay, and 4) the slope off Disko Fan. The acoustic facies are based on 3.5 kHz sub-bottom profiles. All core descriptions are based on a review of core photography, X-radiography, MSCL data plots, discrete geotechnical measurements, grain size data and limited pXRF data.

3.1 The northern Baffin Island slope

The northern Baffin Island slope spans the continental slope seaward of Pond Inlet, Buchan Trough, Scott Trough and the intervening banks; 2013029 cores in this region are located on or in the vicinity of trough mouth fans (Figure 3.1).

Acoustic facies

3.5 kHz data from the northern Baffin Island slope shows a consistent acoustic facies that is composed of an acoustically transparent or stratified unit overlying a reflective unit. The upper unit tends to drape the underlying unit and shows subtle thickening in lows (Figures 3.2a, 3.2b, 3.2c, 3.2d). The upper unit tends to be less than 10 ms two-way travel time (twtt) thick while the underlying unit extends to the limit of acoustic penetration.

2013029-063 piston core 72.455251 N; -72.906995 W; 833 m WD; Slope North of Buchan Trough; 382 cm (opened). The acoustic target is a stratified sequence over a strong reflection (Figure 3.3).

A basal dark grey ungraded diamicton, to 295 cm (Figures 3.4, 3.5a and 3.6a), is overlain by a thin, distinctly laminated reddish brown, gold brown and medium grey brown mud to 270 cm (Figure 3.6a). The lighter gold brown-coloured interval, between 285 and 275 cm may correlate to a more pronounced gold-brown bed between 455 and 445 cm in core 064. Between 270 and 245 cm is a dark grey brown, weakly-bedded diamicton. A sharp contact, based on colour, separates this sequence from overlying tan-coloured carbonate-rich beds with heavy ice-rafted detritus (IRD) between 245 cm and 100 cm (Figure 3.5b and 3.6b). A distinctive sequence of

medium brown mud overlain by rose mud and then grey mud occurs within this carbonate interval, from 195 to 185 cm, and can be correlated between most cores, southward to Home Bay. From 100 cm to 65 cm, stratification develops within the IRD-rich tan mud interval, with the introduction of less IRD-rich brown mud. Medium brown mud, with < 5 % IRD, continues from 65 cm to the top of the core.

2013029-064 piston core

72.426113 N; -72.769305 W; 875 m WD; Slope North of Buchan Trough; 713 cm (opened). The acoustic target is a thick transparent unit overlying a prolonged strong reflector (Figure 3.7).

The base of the core (713 cm) to 585 cm consists of a very dark grey brown, fining upward, graded diamicton (Figures 3.8a and 3.9a).

Between 585 and 524 cm, X-radiography shows a coarse IRD-rich, weakly thick-bedded, tan-brown interval (devoid of grading) which becomes increasingly weakly laminated and darker brown in colour toward a sharp upper contact. Down-core pXRF analyses indicate that this interval has an increased Ca/Ti ratio, indicative of increased calcium carbonates (Figure 3.10, tan highlighting). The overlying interval, to 450 cm, consists of a distinctly laminated and rhythmically laminated reddish brown mud (Figure 3.11) with < 1 cm thick IRD-rich beds near the base and the top of the interval. Between 455 and 445 cm the laminated mud is a distinctive gold brown (Figure 3.10, gold highlighting) and correlates visually with a gold brown bed between 205 and 195 cm in core 059. A sharp contact at 440 cm separates the gold brown mud from an overlying 60 cm thick very dark grey brown IRD-rich mud (to 385 cm). The top of the

very dark grey brown mud at 385 cm forms a sharp colour contact which can be correlated between several cores southward to Home Bay. From 385 cm to 183 cm is a distinct carbonate-rich sequence of light tan pebbly, sandy mud (Figure 3.11) associated with an increase in the Ca/Ti pXRF profile (Figure 3.10), and thin medium brown mud containing the distinctive sequence of medium brown mud, rose mud (Figure 3.10, rose highlighting) and grey mud (320 to 310 cm). The tan carbonate mud interval becomes weakly stratified with medium brown mud at 215 cm. At 183 cm, IRD concentration is abruptly reduced. A few granules persist to 155 cm. The top 183 cm of core consists of medium brown bioturbated and vaguely laminated mud with < 5 % IRD (Figure 3.11, 3.8b and 3.9b).

2013029-059 piston core

71.856891 N; -70.952513 W; 1084 m WD; Slope north of Scott Trough; 502 cm (opened). The acoustic target is a stratified sequence over a mass transport deposit (MTD) on a small slope terrace (Figure 3.12).

Between 502 and 428 cm, two ~20 cm thick very dark grey brown intervals of diamicton are separated by a 10 cm thick, faintly-laminated light gold brown mud (Figure 3.13, lower gold highlighting). The diamicton is sharply overlain by distinctly coloured, laminated and rhythmically laminated reddish brown mud from 428 to 205 cm, punctuated with rare, thin IRD-rich beds (Figure 3.14a). This interval correlates well visually with the stratified interval in core 064, between 520 and 450 cm, and in core 060, between 424 and 348 cm. Slightly elevated pXRF Ca/Ti ratios occur within laminated red brown mud between 425 cm and 413 cm and between 222 cm and 215 cm. The stratified mud is capped by a 10 cm light, gold brown bed

which correlates visually to a gold brown mud between 455 and 445 cm in core 064. Between 195 and 132 cm, three 8 to 20 cm thick, very dark brown diamicton beds are separated by two 10 cm thick very dark grey brown stratified intervals with < 5% disseminated IRD (Figure 3.15a). A sharp colour contact separates this diamicton interval from an overlying 32 cm thick, laminated to thin bedded carbonate-rich IRD mud with faint red brown laminae (Figure 3.13, tan highlighting). Within this carbonate mud is the distinctive sequence of medium brown mud, rose mud and grey mud (108-102 cm) which can be correlated between cores southward to Home Bay. Fifteen centimetres of very dark grey brown, low IRD, bioturbated mud with < 5 % fine disseminated IRD separates this lower tan carbonate mud interval from the top 82 cm of massive to very weakly thin bedded, IRD-rich tan carbonate mud (Figure 3.14b and 3.15b).

2013029-060 piston core

71.867328 N; -70.867066 W; 1191 m WD; Slope north of Scott Trough; 487.0 cm (opened). The acoustic target is a well stratified sequence with probable erosion near the seabed (Figure 3.16).

From the base of the core to 444 cm, the sediments comprise vaguely laminated dark grey brown diamicton with a sharp upper contact (Figure 3.17a). The diamicton is overlain by faintly laminated light gold brown and subtly mottled mud with a gradational upper contact based on colour. Reddish brown laminated mud occurs between 424 cm and 348 cm (Figure 3.18a) and is sharply overlain by a weakly stratified gold brown and brown mud to 328 cm which is visually similar to the gold brown mud in core 059 (between 205 cm and 195 cm) and the gold brown mud in core 062 (between 166 and 156 cm). A thin dark grey brown diamicton that grades upward, sharply overlies this gold brown mud to 276 cm and is also sharply overlain by very

well stratified and distinctly colour-laminated reddish brown mud to 133 cm, becoming gold brown coloured from 133 cm to 127 cm. Within the graded diamicton a whole-round core sample was taken from 318 cm to 293 cm. Between 247 and 173 cm these muds contain convolute lamination, wavy laminae and rare foresets. A sharp contact separates this laminated mud from overlying tan-coloured IRD-rich carbonate mud to 2 cm (Figure 3.17b and 3.18b). A whole-round core sample was taken between 166 cm and 140 cm. Orange brown mud occurs at the top 2 cm of the core. Coring disturbance between 100 cm and 60 cm may have homogenized the brown, rose and grey colour sequence identified in several other cores.

2013029-061 piston core

71.919041 N; -70.458838 W; 1635 m WD; slope north of Scott Trough; 315 cm (opened). The acoustic target is a well stratified sequence (Figure 3.19).

The base of the core to 190 cm consists of distinctly stratified grey brown to dark grey brown, wavy laminated mud with distinct contacts based on colour and texture (Figures 3.20a and 3.21a). Most mud beds are IRD-rich and contain abundant mud clasts and are interpreted as diamicton; others contain < 5 % fine IRD and are devoid of mudclasts. These latter mud beds increase in frequency up-core. At 206 to 201 cm is a distinctive dark brown and gold brown mud couplet which is visually different from the gold brown mud beds observed in northward cores. In core 062, however (at 235-228 cm), the gold brown mud correlation is much more obvious. Between 190 and 183 cm there is a gradual upward change into distinctly laminated reddish brown mud. Here the IRD is finer and is interlaminated with reddish brown mud. From 183 to 135 cm reddish brown mud is distinctly laminated in X-radiographs but appears massive in core

photographs. Further northward in core 064, this same reddish brown mud is colour laminated and thicker. Between 135 cm and 131 cm red brown laminated mud is associated with a slightly elevated pXRF Ca/Ti ratio. A granular dark grey brown mud between 138 and 125 cm may correlate with the upper dark grey brown diamicton in core 064 between 440 and 385 cm and similar looking dark grey brown mud immediately underlying tan carbonate mud in several other cores. Between 125 and 83 cm, a carbonate-rich tan mud (Figure 3.22) with high concentrations of IRD contains a much less vivid version of the brown, rose, grey colour sequence identified in several other cores. Grey mud with a thin reddish top, from 83 to 72 cm, separates this lower carbonate-rich tan mud from the upper carbonate and IRD-rich tan mud. Tan carbonate mud gradually decreases up-core (Figure 3.22) to ~ 23 cm where it becomes brown mud with IRD (Figures 3.20b and 3.21b). The top 12 cm of core consists of orange brown, massive mud with < 10 % fine IRD.

2013029-062 piston core

71.924568 N; -70.413305 W; 1648 m WD; slope north of Scott Trough; 319 cm (opened). The acoustic target is a local high that is poorly stratified; possibly an MTD (Figure 3.23).

The base of the core to 210 cm consists of distinctly stratified grey brown to dark grey brown mud with sharp bedding contacts based on colour and texture (Figures 3.24a and 3.25a). Most mud beds are IRD-rich, contain mud clasts and are interpreted as stratified diamicton. Some thin beds are massive with < 5 % IRD; these massive beds increase in thickness and frequency up core. At 235 cm to 228 cm a distinctive dark brown mud and gold brown mud couplet correlates to a similar dark brown and gold brown mud couplet between 206 and 201 cm in core 061 and

between 263 and 258 cm in core 056 (core disturbance in core 056 makes this correlation less clear). Grey brown muds are laminated between 215 and 208 cm and gradually become reddish brown in colour. From 208 to 166 cm, reddish brown mud appears massive in core photographs but is distinctly laminated in X-radiographs, defined by very fine sand or coarse silt laminae with some thin beds containing higher IRD concentrations. This reddish brown mud correlates to a reddish brown mud in core 061 (183 to 135 cm) and can be correlated to reddish brown mud in core 056 between 417 and 385 cm. Between 203 and 166 cm, laminae are frequently undulating with rare cross-cutting relationships and one instance of microfaulting at 204-201 cm. A distinctive gold brown mud between 166 cm and 156 cm tentatively correlates with the light gold brown mud in core 061, between 141 and 138 cm. An age of 33,975 cal years BP from mixed benthic foraminifera (Table 2) may be too old since the > 106 μg fraction contained detrital particles. Laminated dark grey brown mud with a sharp upper contact into carbonate-rich tan mud, to 120 cm, overlies the gold brown mud bed. The lower IRD-rich carbonate tan mud interval between 120 and 80 cm contains the brown, rose and grey colour sequence which correlates between other cores, south to Home Bay. Grey mud with a slight reddish top, between 80 and 67 cm, separates this lower carbonate-rich interval from the upper carbonate-rich interval which continues to the top of the core with some mixing of brown mud in X-radiography (Figures 3.24b and 3.25b).

2013029-057 trigger weight core

71.701388 N; -69.148798 W; 1713 m WD; off of Scott Trough Slope; 153 cm (opened). The acoustic target is a probable glacigenic debris flow deposited on top of stratified reflections (Figure 3.26).

Only 31.5 cm were retrieved from the piston core, consisting of weakly stratified to massive tan carbonate mud with < 25 % fine IRD (Figures 3.27a and 3.28a). Parallel stratification is visually apparent in core between 25 and 18 cm as alternating dark brown and medium brown laminae.

The trigger weight core (Figures 3.27b and 3.28b) consists of tan carbonate mud from the base of the core at 153 cm to 23 cm. Angled, laminated dark brown mud occurs within this interval, from 141 to 140 cm, 131 to 130 cm and 118 to 107 cm. In all instances the dark brown mud has a bedding contact angle (BCA) of < 090° suggesting either core disturbance or mass transport of the sediment. From 20 cm to 8 cm the sediments consist of brown bioturbated mud with scattered very fine IRD. The colour changes abruptly to orange brown mud at 8 cm which continues to the top of the core.

2013029-056 piston core

71.687403 N; -69.106078 W; 1715 m WD; off of Scott Trough Slope; 464.5 cm (opened). The acoustic target is a well stratified sequence (Figure 3.29).

The base of the core to 430 cm comprises a dark grey brown diamicton (Figure 3.11) with a distinct upper contact into reddish brown laminated mud and interbedded fine IRD-rich mud beds (< 5 cm) (Figures 3.30a and 3.31a). The laminated mud interval continues to 385 cm and consists of < 5 cm thick beds of fine IRD-rich clayey silt, separated by thicker distinctly laminated mud with sparse, fine IRD (Figure 3.11). Microfaulting at 045°, with offsets on the order of 1-2 cm, is also evident. Similar looking reddish brown muds are found in core 064 (from 524 to 455 cm - here laminated reddish brown muds are capped by a distinctive gold brown bed)

and core 059 (428 to 205 cm with a similar appearance to core 064) but in core 056 the reddish brown laminated mud interval is much thinner. Above 385 cm, to 318 cm, the diamicton is poorly sorted and distinctly stratified with most clasts < 1 cm in diameter (Figures 3.11 and 3.31a). Some beds are internally laminated; others are massive and up to 17 cm thick. Between 318 and 292 cm the clast size increases to a maximum of 5 cm in diameter and the basal contact is distinctive because of the coarseness of the clasts. Clasts are less than 1 cm ϕ between 292 and 273 cm.

A sharp contact, based on colour and texture, separates the top of the diamicton at 273 cm from weakly stratified gold brown mud and interbedded brown sandy mud to 238 cm. Here, the core is somewhat fluidized. Within this fluidized interval is the contact between underlying diamicton and overlying tan carbonate mud.

Tan carbonate-rich sediments between 238 and 193 cm contain the distinctive sequence of brown, rose and grey mud identified in most other cores north of Home Bay. Above this lower tan carbonate mud, between 193 and 163 cm, is a brown mud with < 5 % fine IRD and granules and a slightly reddish brown top. A distinct contact based on colour and texture separates this brown mud from overlying, moderately IRD-rich tan carbonate mud to 90 cm (Figures 3.11, 3.30b and 3.31b). A gradual contact, defined by colour and an upward reduction in IRD, occurs between tan carbonate mud and overlying weakly bioturbated brown mud to 40 cm (Figure 3.11). A sharp contact separates this brown mud from distinctly orange-brown weakly bioturbated mud to the top of the core.

3.2 The slope off Clyde River

The slope off Clyde River forms a broad fan that extends into Baffin Bay. The shelf in this region is cut by Clyde Trough and another trough that extends seaward from McBeth Fiord. A terrace is apparent at ~1200 m water depth along the slope in this area. Cores from 2013029 in this region are located on the terrace (Figure 3.32).

Acoustic facies

3.5 kHz data from the slope off Clyde River show a consistent acoustic facies that is composed of an acoustically transparent or stratified unit overlying a reflective unit. The upper unit tends to drape the underlying unit and shows subtle thickening in lows (Figure 3.33). The upper unit tends to be less than 10 ms (twtt) thick while the underlying unit extends to the limit of acoustic penetration.

2013029-053 trigger weight core

71.696770 N; -66.395751 W; 1349 m WD; Slope off Clyde River; 165 cm (opened). The acoustic target is a thick post-glacial sequence on the mid-slope terrace (Figure 3.34).

Only an angular clast was recovered in the piston core. The entire trigger weight core consists of brown, moderately bioturbated and very faintly laminated homogeneous mud with $\sim < 2\%$ fine, isolated IRD (Figures 3.35a and 3.35b).

2013029-052 piston core

70.635813 N; -66.247913 W; 1251 m WD; Slope off Clyde River; 183.5 cm (opened). The acoustic target is post-glacial sediments over an erosional unconformity (Figure 3.36).

A light tan, IRD-rich carbonate (Figure 3.11) occurs at the base of the core from 183.5 cm to 87 cm (Figures 3.37a, 3.37b, 3.38a, and 3.38b). Red brown clasts within the tan carbonate mud, between 162 and 151 cm, appear to correlate to the rose bed within the well-developed brown, rose and grey colour sequence in cores north to Lancaster Sound. The very dark grey brown mud from 151 cm to 149 cm correlates to the same mud within tan carbonate mud in cores from Lancaster Sound to Home Bay. A distinct colour contact at 98 cm separates underlying carbonate from overlying medium brown, weakly bioturbated mud. IRD diminishes upward within medium brown mud to 72 cm above which brown mud is moderately to extensively bioturbated with rare, isolated IRD (Figure 3.11). Orange brown mud occurs at the top 2 cm of the core.

2013029-073 piston core

70.208068 N; -65.320780 W; 1022 m WD; Slope off Clyde River; 428.0 cm (opened). The acoustic target is a hummocky seabed, possibly an MTD (Figure 3.39).

The base of the core from 428 to 137 cm comprises a very dark grey brown, massive diamicton with a sharp upper contact based on both colour and texture (Figures 3.40a and 3.41a). Unlike the diamicton at the base of other cores, the percentage of clasts in this diamicton appears to be slightly less. The overlying gold brown sequence between 137 and 118 cm consists of interlaminated mud and very fine sand. The correlation of this gold brown coloured interval with

other cores is unclear. A thin lighter brown mud with < 5 % fine IRD overlies the gold brown mud and very fine sand to 103 cm. Tan carbonate mud (Figure 3.11) occurs between 103 and 16 cm and contains a very faint light brown, rose and grey colour sequence and overlying distinctive grey brown mud which grades to light reddish brown at the top of the bed (Figure 3.11). This is the same sequence found in 2013029 cores north to Lancaster Sound. The upper tan carbonate mud interval begins at 61 cm and contains about 20 % IRD. Orange brown mud with < 10 % IRD begins at 16 cm and continues to the top of the core (Figures 3.40b and 3.41b).

3.3 The slope off Home Bay

The region termed the slope off Home Bay extends from Home Bay in the north to Padloping Trough in the south. In this part of the Baffin Island margin, the shelf is narrower and the shelf break forms a broad embayment. Here, the shelf is cut by the large Home Bay Trough and a number of smaller transverse troughs. Cores from 2013029 are located within this region along the slope, both on trough mouth fans and on areas of the slope between fans (Figure 3.42).

Acoustic facies

3.5 kHz data and older Hunttec DTS sparker data from the slope off Home Bay show much more acoustic penetration than on the slope north of this region (Figures 3.43a, 3.43b). The acoustic facies ranges from well stratified to chaotic and there is evidence for both glacial debris flows and normal slope failure deposits.

2013029-074 piston core

69.523171 N; -64.645093 W; 1482 m WD; Isabella Bank; 592.0 cm (opened). The acoustic target is a stratified sequence (Figure 3.44).

The base of the core to 378 cm consists of a massive very dark grey brown diamicton with a number of clasts (Figures 3.11, 3.45a and 3.46a). From 378 cm to 368 cm the diamicton is a medium brown colour with a sharp upper contact, based on colour and texture, into interlaminated and thin bedded light grey, olive and light brown muds to 348 cm. Bedding contacts are somewhat diffuse and may be bioturbated. Muds of this colour have not been seen in any of the 2013029 slope cores taken north of core 074 to Lancaster Sound. From 348 to 344 cm medium to dark brown clast-rich mud is similar in appearance to the top of the upper diamicton in several other cores to the north - the upper contact is distinct based on colour and directly underlies tan carbonate-rich muds. The carbonate-rich mud interval between 344 and 316 cm contains the brown, rose and grey colour sequence identified in other cores, although the rose and grey beds are thinner and less vivid. Thin bedded brown mud with black mottling and a slight reddish top occurs from 316 to 298 cm and can also be correlated with other, more northern cores. The upper tan carbonate mud begins at 298 and extends to 232 cm. It is crudely thick-bedded from 250 cm upward with a sharp upper contact at 232 cm. The decrease in the pXRF Zr/Rb profile within this tan carbonate bed (Figure 3.47) suggests correlation to the uppermost tan carbonate mud in core 077. Between 232 cm and 215 cm the carbonate and IRD contents decrease rapidly as tan mud grades to brown mud. Brown, bioturbated mud (Figure 3.11) continues to 2 cm (Figures 3.45b and 3.46b). The top 2 cm of core consists of orange brown mud.

2013029-075 piston core

69.547883 N; -64.643330 W; 1484 m WD; Isabella Bank; 704.0 cm (opened). The acoustic target is an MTD with drape (Figure 3.48).

The base of the core to 675 cm consists of massive very dark grey brown diamicton with a low degree of clasts (Figures 3.49a and 3.50a) which may be part of an overlying MTD sequence. A whole-round core sample was taken between 675 cm and 647 cm. Above 675 cm and continuing to 440 cm, the core consists of an MTD composed of interbedded, distinctly laminated to thin bedded dark brown and medium brown mud, with BCAs between 035° and 045°. Between 675 and 594 cm laminated mud is interbedded with massive brown mud beds up to 8 cm thick. Fine clasts, < 4 mm in diameter are scattered throughout this interval. From 594 cm to 440 cm laminated brown mud is punctuated by < 10 cm thick, predominantly monomictic (although some are polymictic), clast-supported mudclast conglomerates. The mudclasts are mainly dark grey brown (with rare medium brown-coloured clasts), unsorted, subrounded to subangular and < 1 cm in diameter. Toward the top of the MTD above 500 cm, mudclast conglomerates are replaced by clast-supported diamicton beds with clasts < 5 mm ϕ . Laminated beds between the diamicton beds have BCAs of 090°. Contacts are sharp and based on both colour and texture. From 590 cm to 570 cm and from 477 cm to 450 cm, the laminae have a wispy appearance and there are faint planar cross laminae between 487 cm and 485 cm and between 480 cm and 475 cm.

Above 440 cm, immediately overlying the MTD, is a thin, faintly laminated to massive, light grey mud which may correlate to the distinctive olive and grey mud beds between 378 cm and 348 cm in core 074. A distinct contact at 427 cm, based on colour and texture, separates the lower half of the core from the overlying tan carbonate mud sequence. This contact is correlatable with the top of the diamicton in most cores north to Lancaster Sound.

The interval from 427 cm to about 275 cm contains the tan, detrital carbonate-rich mud sequence which includes the brown, rose and grey colour sequence (402 cm to 395 cm) identified in most other northern cores. Within this tan carbonate mud sequence, a whole-round core sample was taken between 382 cm and 358 cm. The top of the carbonate sequence is defined by the relative absence of IRD in X-radiographs at 275 cm, although the colour changes from tan to brown at 310 cm. Brown mud continues to the top of the core and is weakly to moderately bioturbated with faint remnant parallel lamination (Figure 3.49b and 3.50b). A third whole-round core sample was taken between 224 cm and 200 cm.

2013029-076 piston core

68.288243 N; -64.007485 W; 1040 m WD; Alexander Bank; 101.5 cm (opened). The acoustic target is an MTD at the base of a 150 m high scarp (Figure 3.51).

The base of the core to the sharp, angled contact at 50 cm consists of interlaminated very dark grey brown mud alternating with massive very dark grey brown mud with fine clasts in beds < 10 cm thick (Figures 3.52a and 3.53a). Parallel laminae appear well developed in X-radiographs. The upper contact is sharp with a BCA of 045°. Distinctive orange brown sediments with a low

degree of bioturbation occur above this contact to the top of the core. X-radiography shows these sediments to be distinctly laminated from 50 cm to 30 cm and laminated, wispy laminated and thin-bedded above 30 cm. The entire core has a very high shear strength (Figure 3.52a), when compared with other cores and is interpreted as an MTD. The trigger weight core is 16 cm thick and disturbed (Figures 3.52b and 3.53b).

2013029-077 piston core

68.308682 N; -63.794663 W; 1153 m WD; Alexander Bank; 649.5 cm (opened). The acoustic target is a thick stratified sequence (Figure 3.54).

The base of the core to 625 cm consists of dark grey brown interlaminated silt and clay interbedded with thin, very fine sand to coarse sand and granule beds (Figures 3.55a and 3.56a). Whole-round core was subsampled between 622 cm and 598 cm. Above 598 cm to 548 cm, the core consists of distinctive interbedded light grey mud and fine sand, olive grey mud and medium brown mud and coarse sand. Medium brown muds are laminated in X-radiography and frequently display wavy laminae (593 cm to 588 cm). Medium brown coarse sand is ripple laminated and faintly climbing ripple-laminated (573 cm to 567 cm). Light grey and olive grey muds appear massive and bioturbated and are interrupted by wavy fine sand beds. Here, bedding contacts with mud are diffuse. A sharp contact separates the underlying light grey, olive and brown mud sequence from overlying distinctly colour laminated reddish brown mud with interbedded gold brown mud which continues to 457 cm. X-radiography shows that these reddish brown muds are predominantly parallel laminated with lesser instances of wavy laminae and ripple cross-laminae. Down-core pXRF analysis shows a slight increase in the Ca/Ti ratio

between 529 cm and 510 cm (Figure 3.57) which is associated with a gold brown mud bed at the top of the interval.

Between 457 cm and 427 cm is another light grey, olive grey and medium brown mud sequence punctuated with 2 coarse sand and granule beds < 1 cm thick. Again, these muds appear predominantly massive and bioturbated with blurred remnant lamination and rare, faint laminae evident in X-radiography.

From 427 cm to 323 cm is a second distinctly colour laminated reddish brown mud interval with two additional gold mud beds. As in the lower reddish brown mud interval, these muds are also distinctly parallel laminated – becoming rhythmically laminated between 355 cm and 333 cm. Rare, angled laminae occur between 332 cm and 327 cm. A grain size curve of reddish brown mud between 343 and 344 cm is presented in Figure 3.11. As in the lower reddish brown mud interval, there is also a slight increase in the pXRF Ca/Ti ratio within these muds between 400 cm and 386 cm (Figure 3.57) associated with a gold brown mud bed in core.

A third light grey, olive and brown mud interval occurs between 323 cm and 275 cm. Like the lower two instances of this sequence, the mud appears massive except for infrequent, parallel laminated coarser sand and granule beds (305 cm, 290 cm and 275 cm). Perhaps the mud is extensively bioturbated. Microfaulting is seen in X-radiography between 312 cm and 308 cm. It is possible that this light grey, olive and brown mud interval correlates to a similar coloured interval in core 074 between 378 cm and 348 cm. However, core 077 contains a reddish brown mud interval (Figure 3.11) overlying this upper light grey, olive and brown mud interval which is

not present in core 074 so the correlation is not entirely clear. A sharp contact separates this sequence from a third sequence of distinctly colour laminated reddish brown muds with rare silty laminae to 228 cm. Here, X-radiography shows the muds to be predominantly parallel laminated but without the distinctive rhythmic laminae and crisp contacts of the underlying reddish brown mud interval. A third, more pronounced increase in the pXRF Ca/Ti ratio occurs between 273 cm and 252 cm (Figure 3.57).

Between 228 cm and 207 cm is a distinctive, moderately to extensively bioturbated grey brown mud devoid of IRD with the exception of a thin IRD-rich bed between 216 cm and 214 cm. This mud contains black mottles and is visually similar to the brown muds found above the colour sequence in other 2013029 cores. However, X-radiography and pXRF data (Figure 3.57), specifically an increase in the Zr/Rb trace, show this to be a unique, bioturbated mud. Above this bioturbated brown mud, at 207 cm and continuing to 180 cm, is a lighter coloured IRD-rich brown mud with very fine, wispy sandy laminae at the base of the interval. This IRD-rich mud is the fourth interval containing a slightly elevated pXRF Ca/Ti ratio (Figure 3.57). It is interpreted as a carbonate mud on figure 3.57 because of the pXRF Ca/Ti ratio and the stratigraphic position of this mud. A whole-round core sample was collected between 180 cm and 172 cm. A thin bioturbated interval, devoid of IRD continues to 163 cm. Here, X-radiography and pXRF data, specifically a decrease in the Zr/Rb trace, show that this upper grey brown, bioturbated mud correlates to the grey brown, bioturbated mud beginning at 316 cm in core 074, just above the colour sequence. In cores to the north, this same grey brown, bioturbated mud separates the lower tan carbonate mud containing the brown, rose, grey colour sequence, from the upper tan carbonate. However, in core 077, the lower carbonate interval and colour sequence are missing.

This grey brown, bioturbated mud has a sharp upper contact with tan carbonate mud based on both colour and texture.

The overlying tan carbonate mud is IRD-rich and continues to 123 cm. It is weakly thin-bedded based on the intensity of IRD events and becomes more mud-rich to the top of the interval. The down-core pXRF Ca/Ti profile shows a well-developed peak when compared to lower Ca/Ti events (Figure 3.57). IRD rapidly decreases between 123 and 113 cm. Above 113 cm, to the top of the core, is a thin bedded, moderately to weakly bioturbated, light to medium brown mud (Figure 3.55b and 3.56b). A grain size curve for the brown mud is presented in Figure 3.11.

2013029-079 piston core

68.152065 N; -63.673306 W; 1078 m WD; Alexander Bank; 254 cm (opened). The acoustic target is a shallow MTD (Figure 3.58).

From the base of the core at 254 cm, to 206 cm, the sediments consist of medium grey brown muds with vague thin beds defined by colour and very fine IRD (Figures 3.59a and 3.60a).

Above 206 cm to 155 cm the sediments are virtually devoid of IRD, browner in colour, and are faintly laminated and moderately bioturbated with visible black mottling. Bioturbation lessens at 180 cm and laminae and thin beds are more clearly defined. The contact at 155 cm separates underlying brown muds from overlying tan carbonate mud and is defined by a distinct change in both colour and texture. This same contact has been identified in most other cores north to Lancaster Sound. Like core 077 to the north, core 079 does not have the brown, rose and grey colour sequence within tan carbonate mud, identified in cores north of Home Bay.

From 155 cm to 123 cm, the tan carbonate mud is characterized by a high degree of IRD at the base of the interval which lessens upward. The pXRF Ca/Ti trace of this tan carbonate mud is very similar to the tan carbonate mud in core 077 beginning at 163 cm (Figure 3.61). Above 123 cm (Figures 3.59b and 3.60b) there is a gradual colour change from tan to light brown. X-radiographs indicate that there are still episodic pulses of very fine IRD deposition to 55 cm, after which the sediments are moderately bioturbated, faintly bedded and devoid of IRD to the top of the core. Two additional Ca/Ti pulses are shown in the pXRF data at 60 cm and 30 cm within brown mud. The Ca/Ti event at 60 cm is associated with fine, wispy silt laminae in X-radiography; the Ca event at 30 cm is unremarkable in both core and X-radiography.

2013029-047 piston core

67.630128 N; -62.050921 W; 919 m WD; Slope off of Qikiqtarjuaq; 384 cm (opened). The acoustic target is a layered MTD (Figure 3.62).

From the base of the core at 384 cm to 55 cm, the sediment consists of massive very dark grey brown diamicton with ~ 30-40 % randomly distributed subrounded to subangular clasts < 20 mm in diameter (Figures 3.63 and 3.64). X-radiographs suggest vague bedding but this is due to manipulation of the wire over clasts during splitting, resulting in pseudo, angled lineations. Between about 55 cm and 21 cm, there appears to be a slight reduction in the number of clasts. A distinctive, sharp colour contact at 21 cm, with a BCA of ~ 060°, separates the diamicton from overlying orange brown mud and fine clasts with diameters < 1cm. X-radiography shows this contact as a fine line with no distinction in grain size above and below the contact. The top 7 cm

of core consists of orange brown mud devoid of clasts. There was no sediment recovered in the trigger weight core.

Core 047 is similar in appearance to core 076 – very dark grey brown diamicton sharply underlies orange brown mud with fine clasts. Unlike core 076, the shear strength for core 047 is within the normal range. Both cores targeted MTDs.

2013029-048 piston core

67.605618 N; -61.967451 W; 935 m WD; Slope off of Qikiqtarjuaq; (822.5 cm opened). The acoustic target is a transparent stratified interval (Figure 3.65).

The base of the core to 723 cm consists of interbedded, medium to thin bedded very dark brown silt and clayey silt with distinct tan, silty sand laminae, rare granule-rich laminae and isolated shell fragments (Figures 3.66a and 3.67a). Microfaulting occurs between 802 and 807 cm.

Between 723 cm and 577 cm, X-radiography shows the clayey silt to be faintly laminated to massive and moderately to extensively bioturbated, with < 5 % fine IRD.

Between 577 cm and 547 cm the clayey silt is faintly stratified with many contacts appearing diffuse and blurred. IRD increases to < 10 % and also coarsens with some angular clasts reaching 6 cm by 3 cm in size. Above 547 cm to 420 cm, IRD is reduced to < 2 %, and is mostly very fine, except at 460 cm where IRD increases to about 10 %. The sediments appear extensively bioturbated. A whole-round core sample was taken from 505 cm to 481 cm. Between 420 cm and 390 cm fine IRD increases to < 5 % within massive, extensively bioturbated clayey silt. A fine

IRD-rich bed occurs from 390 cm to 384 cm. Between 384 cm and 185 cm brown, parallel laminated clayey silt, devoid of IRD, is moderately bioturbated toward the base of the interval and extensively bioturbated toward the top. As bioturbation increases upward, laminae become faint. Two whole-round core samples were taken from this interval between 355 cm and 332 cm and between 205 cm and 190 cm. From 290 to 275 cm laminae are wavy-laminated and rarely cross-laminated, or perhaps microfaulted.

A gradational contact in both colour and texture, over 10 cm, separates lower brown clayey silt at 185 cm from upper tan carbonate, IRD-rich mud to 125 cm. This interval is characterized by distinct parallel laminae and $> \sim 40\%$ medium to coarse IRD. A second gradational contact separates IRD-rich mud from overlying brown mud and is defined by an upward decrease in fine IRD. Thin-bedded to laminated, medium brown silty clay with less than about 15 % disseminated fine IRD, continues from 125 cm to 17 cm (Figures 3.66b and 3.67b). Between 17 cm and 2 cm brown mud is devoid of IRD and contains wispy laminae. The top 2 cm of core consists of orange brown mud.

3.4 The slope off Disko Bugt

The slope off Disko Bugt consists of a large trough mouth fan. Three piston cores were collected in this region during cruise 2013029. They targeted glaciomarine and post-glacial sediments, as well as sediments that occur below a regional erosional unconformity (Figure 3.68).

Acoustic facies

3.5 kHz data from the slope off Disko Bugt show an acoustically transparent or stratified unit overlying a more reflective stratified unit. The two units are separated by a distinct erosional unconformity (Figure 3.69).

2013029-046 piston core

67.802350 N; -59.374205 W; 1248 m WD; Off of Disko Bugt; 492 cm (opened). The acoustic target is an acoustically stratified interval over an unconformity (Figure 3.70).

The base of the core to 473 cm consists of medium brown, laminated to thin bedded clayey silt, coarse silt and IRD-rich medium sand (Figures 3.71a and 3.72a). A distinct contact separates this interval from overlying wavy and parallel laminated brown silt to 426 cm. The core is subtly colour-laminated; X-radiography shows that primary bedding contacts are blurred. Isolated shell fragments are rare. Between 426 cm and 410 cm, brown mud contains up to ~ 15 % fine disseminated IRD and gradually becomes slightly tan coloured upward. Above 410 cm, to 372 cm, laminae are faint. IRD drops to < 5 % and is more variable in size with one clast reaching 5 cm ϕ . Isolated, tan mudclasts are less than 5 mm ϕ . The upper contact into more brown mud is gradual. Between 372 cm and 338 cm laminae are still faint and appear wispy, IRD is rare and the sediments are moderately bioturbated with isolated shell fragments and faint, black mottling. Above 338 cm to ~265 cm the sediments consist of moderately bioturbated, faintly laminated tan brown clayey silt with fine IRD (< 5 %), shell fragments at 325 cm and 305 cm and isolated light brown mudclasts. Laminae become more faint and fine IRD lessens upward. A distinct tan brown mud occurs between 315 cm and 321 cm. Above about 265 cm to about 210 cm, brown

mud is more faintly laminated and contains only scattered fine IRD. Between 210 and the top of the core brown mud is moderately bioturbated (Figure 3.71b and 3.72b). Rare IRD occurs between 57 cm and 43 cm. Above 40 cm the sediments are faintly colour-laminated.

2013029-082 piston core

67.781908 N; -59.539071 W; 1352 m WD; Off of Disko Bugt; 643 cm (opened). The acoustic target is an acoustically stratified interval over an unconformity; a thicker stratified unit than in core 046 (Figure 3.73).

A whole-round core sample was collected from 643 cm to 613 cm. Between 613 cm and 597 cm, the sediments consist of medium grey brown very fine silty sand with angled parallel laminations defined by a BCA of 080° (Figures 3.74a and 3.75a). A sharp upper contact separates this silty sand from overlying moderately bioturbated, medium grey brown clayey silt with faint parallel laminae, wavy laminae and rare angled laminae to 540 cm. Bedding contacts appear diffuse.

Between 540 cm and 522 cm laminae are faint and the degree of bioturbation increases slightly.

A distinct upper contact at 522 cm is defined the introduction of shell fragments which continue to 387 cm. Here, dark grey brown clayey silt is medium to thin bedded and internally parallel laminated. Again laminae are moderately bioturbated and faint with blurred contacts, however, beds are defined by textural changes, infrequent lighter brown beds and shell accumulations on X-radiography. A whole-round core sample was taken between 499 cm and 472 cm.

Microfaulting occurs between 440 cm and 430 cm. Above 387 cm, to 365 cm, medium brown clayey silt is distinguished by less bioturbation, an absence of shells, more well-developed wavy laminae and rare angled laminae. There is a fairly distinct colour change to light brown clayey

silt at 365 cm which coincides with the introduction of fine IRD in X-radiography and a distinct increase in the Ca/Ti pXRF profile (Figure 3.76). Between 365 cm and 325 cm, light brown clayey silt contains ~30 % IRD at the base, decreasing to ~5 % IRD upward. Bedding is vague. A whole-round core sample was taken between 348 cm and 338 cm. Above 325 cm to 265 cm bedding is faint and dark grey mottling is evident on core photographs. A distinct tan carbonate mud occurs between 265 cm and 258 cm and this is associated with a thin but well-defined peak in the Ca/Ti pXRF ratio and a higher concentration of IRD. The Ca/Ti pXRF ratio is weakly elevated up to about 215 cm and X-radiography shows that the core also contains < 15 % fine IRD up to about 215 cm. Moderately bioturbated brown clayey silt with faint primary laminae and < 2 % fine IRD (Figures 3.74b and 3.75b) continues from ~215 cm to the top of the core. A whole-round sample was taken between 200 cm and 177 cm.

2013029-084 piston core

67.777421 N; -59.582088 W; 1359 m WD; Off of Disko Bugt; 725 cm (opened). The acoustic target is an acoustically stratified interval over an unconformity; thinner upper unit when compared to core 046 (Figure 3.77).

From the base of the core to 592 cm, the sediments consist of grey brown, distinctly ripple-laminated very fine sand in bedsets up to 40 cm thick (Figures 3.78a and 3.79a). Cross-lamination is especially evident in X-radiography, with individual bedsets defined by higher concentrations of detrital organics or by light wispy laminae. Between 592 cm and 518 cm the sediments are finer (clayey silt) and moderately bioturbated, although blurred parallel lamination and rarer ripple cross-lamination are visible in X-radiography. Between 518 cm and 500 cm, the

sediments coarsen to very fine sand, bioturbation is weak and ripple-lamination and parallel lamination are more clear. Above 500 cm to 472 cm, bioturbation is moderate, the grain size appears to be sandy, clayey silt and blurred parallel laminated intervals, up to 4 cm thick, are interbedded with 10 cm thick cross-laminated bedsets. Between 472 cm and 355 cm bioturbation is moderate to strong within grey brown clayey silt. Massive, burrow-homogenized intervals, up to 30 cm thick, are interbedded with 15 cm thick parallel laminated intervals displaying blurred bedding contacts. At 355 cm to 290 cm, bioturbation decreases, and the sediments are distinctly parallel laminated with rare wavy lamination, ripple cross-lamination and angled bedding. Above 290 cm, to 210 cm, bioturbation within clayey silt is moderate to strong. The sediments are faintly parallel laminated but primary bedding is blurred by bioturbation.

A sharp contact separates underlying bioturbated clayey silt from clean, parallel laminated and ripple cross-laminated very fine sand to 175 cm. The character of this interval is similar to that of the sediments at the base of the core. A sharp contact separates underlying very fine sand from overlying thin bedded silty clay. At 147 cm there is a distinct colour change from underlying grey brown clayey silt to light brown clayey silt containing IRD which continues to 128 cm. Here beds are defined by IRD concentrations, which do not exceed ~30 %, and IRD clast size - most IRD is fine and less than 5 mm in diameter. A thin brown mud, between 128 cm and 122 cm, underlies a distinctive tan coloured IRD-rich mud to 117 cm. This tan mud may correlate to a similar tan mud bed in core 082, between 265 cm and 258 cm. Light brown clayey silt with IRD overlies the tan mud bed to 101 cm.

A distinct contact separates IRD-rich sediments at 101 cm from overlying massive brown mud to the top of the core (Figures 3.78b and 3.79b). With the exception of scattered, fine IRD to 60 cm and an IRD-rich bed between 76 cm and 78 cm, brown mud is massive and burrow homogenized. The colour changes to orange brown mud at three centimeters and continues to the top of the core.

4.0 Baffin Bay Slope Lithofacies

Four sedimentary facies have been identified from 14 stratigraphic cores, taken along the western slope of Baffin Bay, on the basis of grain size, colour, sedimentary features, physical properties measurements and pXRF analyses (Figure 4.1). The across-slope correlation of these core lithofacies is shown in Figure 4.2. Detailed descriptions of each lithofacies are presented below.

4.1 Lithofacies 1 (L1) - Diamicton

Dark grey brown diamicton occurs at the base of all sediment cores collected north of Home Bay, that exceed 2 m in length (Figure 4.2). There is also a thin, younger diamicton found in 7 piston cores located just seaward of Scott Inlet and north to Pond Inlet.

Three types of diamicton were observed – poorly sorted, massive mud and sand with granules and clasts; mud beds interbedded with weakly to moderately stratified, poorly-sorted, mud and sand with granules and clasts; and clast-rich, matrix-poor diamicton grading to matrix-

dominated, clast-poor diamicton. The basal diamicton is thicker than most instances of the upper diamicton, enabling the identification of physical properties trends down core.

Massive, Poorly Sorted Diamicton

Massive, poorly sorted, matrix-dominated diamicton occurs at the base of cores 073 and 074 (Figure 4.3) and is characterized by slightly elevated and variable shear strengths between 10 and 45 kPa, higher but uniform bulk densities and slightly higher but relatively uniform magnetic susceptibilities (Figure 3.45a). The Ca/Ti pXRF ratio is relatively uniform and low (Figure 3.47). Dark grey brown clayey, silty, sand contains disseminated granules and isolated yellowish, dark grey, medium grey and rose subrounded to subangular clasts up to 90 mm ϕ . Northward, the basal diamicton of core 063 is similar both in appearance and in down-core physical properties trends to L1 in cores 073 and 074. At 330 cm the diamicton consists of 10 % gravel, 37 % sand and 53 % mud. Grain size spectra for cores 063 and 074 are presented in Figure 3.11.

Interbedded Mud and Weakly Stratified Diamicton

Seaward of Scott Trough, at core 056, L1 is characterized by mud beds interbedded with weakly to moderately stratified, poorly sorted, matrix-dominated diamicton. Mud beds are < 15 cm thick, reddish brown and internally parallel laminated and microfaulted. Diamicton intervals are 5 to 95 cm thick and characterized by massive diamicton beds, up to 32 cm thick, and weakly stratified diamicton intervals, also up to 32 cm thick. Here down-core bulk density and P-wave velocity profiles are more variable than in cores 073 and 074; the magnetic susceptibility is considerably higher and X-radiography shows a visible increase in disseminated granules and a concomitant decrease in the number of large clasts.

In cores 059 and 060, 64 km to the north, reddish brown laminated mud increases to a thickness of 2.5 m (Figure 4.2), resulting in a thinner upper diamicton. This upper diamicton is finer than the basal diamicton and is used only to establish trends in grain size, colour and sedimentary features.

The basal diamicton in core 059 is only 20 cm thick and is massive; in core 060 the basal diamicton is 45 cm thick and weakly stratified with scattered subangular granules and pebbles up to 3 cm in length. Just seaward and in 500 m deeper water, within cores 061 and 062, the basal diamicton is weakly stratified and distinctly interbedded with both massive and laminated brown muds which increase in thickness toward the top of the diamicton (Figure 4.3), resulting in variable down-core bulk densities, P-wave velocities and shear strengths (Figure 3.20a). The diamicton bed at 248-240 cm in core 061 consists of 2 % gravel in a sandy (22 %) mud (76 %) matrix with isolated subangular to subrounded pebbles up to 4 cm ϕ . Both the thickness and coarseness of diamicton beds diminish upward.

Graded Diamicton

Ninety-eight km north, in core 064, the lower diamicton is well graded and clast-supported with subangular clasts up to 70 mm in length, 55 % gravel (>2 mm), 19 % sand and 26 % mud, grading upward to a matrix-supported diamicton characterized by fine granules (2 %) and sand (31 %) in a silty clay (66 %) matrix (Figure 4.3). Clasts do not show preferred alignment or orientation. A sharp contact separates this lower diamicton from an overlying carbonate-rich mud.

The upper diamicton in core 060 is also normally graded and distinguished by a distinctive dark brown colour and sharp upper and lower contacts. At 53 cm thick, the base of the diamicton contains 16 % gravel in a sandy (13 %), mud (71 %) matrix. Clasts are subangular and without clast orientation. The base of the diamicton grades upward into dark brown sandy (5 %) mud (94 %) with 1 % fine gravel.

4.2 Lithofacies 2 (L2) – Laminated Red Brown Mud

Laminated red brown mud is sandwiched between diamicton within the lower part of all sediment cores taken between Scott Trough and Pond Inlet. The thickest interval of L2 (3.73 m) was intersected in core 077, south of Home Bay, in the absence of diamicton (Figure 4.2). Northward, L2 is thickest in cores 059 (2.3 m) and 060 (2.45 m), thinning in deeper water in cores 061 (0.5 m) and 062 (0.45 m). Further north, just south of Pond Inlet, red brown laminated mud thins again to 0.80 m, (core 064), and to 0.20 m, (core 063). It is not evident in Pond Inlet cores. In cores 059, 060, 061, 062, 063, 064 and 077 laminated red brown mud is associated with distinctive gold brown mud beds < 10 cm thick. L2 is distinguished by a slight increase in the colour a* trace, low magnetic susceptibility, low shear strength and a relatively low bulk density. In core, it is distinctly to poorly colour laminated and, less commonly, massive looking. X-radiography elucidates parallel laminated to thin bedded mud, on a 1 mm to 20 mm scale, with slightly coarser silty to very fine sand laminae. A 1 cm grain size sample at 170-171 cm in core 061 consists of 45 % silt and 54 % clay (Figure 3.11).

X-radiography of L2 from representative cores - 077, 060 and 062 - (Figure 4.4) reveals three types of laminated red brown mud - rhythmically laminated and parallel laminated mud with rare angled beds; parallel laminated mud with wavy beds, load features, and angled laminae; and parallel laminated bedsets comprised of interlaminated mud and basal silty to very fine sand laminae with fine IRD.

Parallel Laminated and Rhythmically Laminated Mud

Parallel laminated red brown mud with infrequent low-angled laminae is the most prevalent type of L2, occurring in cores 056, 059, 060, 063, 064 and 077 (Figure 4.4, core 077). Alternating clay and silt laminae are of variable thicknesses, from 1-3 mm, display sharp to diffuse and wispy bedding contacts and are up to 193 cm thick. Occasionally, laminated red brown mud is interrupted by distinct rhythmically laminated clay and silt forming bedsets up to 5 cm thick (Figure 4.4, core 077 335-340 cm). Bedset bounding surfaces are not necessarily sharp but are defined by the absence of rhythmic laminae. Less commonly, laminated red brown mud is disrupted by faintly laminated mud bedsets, < 8 cm thick, characterized load features and faint ripple laminae (core 060) (Figure 4.4).

Parallel Laminated Red Brown Mud and Very Fine Sand with IRD

Parallel laminated bedsets, < 23 cm thick, are visible only on x-radiographs and are comprised of interlaminated clay and silty to very fine sand (Figure 4.4; core 062). Coarser laminae appear discrete with relatively sharp upper and lower contacts and occur every 5-20 mm; some sandy

laminae contain coarse sand and IRD; other sandy laminae define planar cross-lamination or wavy beds. Interlaminated mud between the sandy laminae is distinguished by subtle changes in texture. Rarely, vague, laminated mud couplets, up to 4 mm thick, occur. This type of red brown mud was only identified in cores 061 and 062 where it directly overlies stratified diamicton facies. In X-radiography there is a gradual decrease in coarse IRD-rich beds from underlying stratified diamicton into laminated red brown mud and very fine sand with IRD.

4.3 Lithofacies 3 (L3) - Tan Carbonate Mud

Tan carbonate mud occurs toward the top of all sediment cores, sharply overlying either laminated red brown mud of L2 or the diamicton of L1, with the exception of cores 079 and 048. It is characterized by a high L* colour value, a high P-wave velocity and a high bulk density (Figures 3.45a, 3.20a and 3.8a). X-radiography shows tan carbonate mud to be predominantly massive and poorly sorted with weak stratification visible in some cores (Figure 4.5). Subangular to angular IRD (> 2 mm), between 6 and 29 %, is disseminated within a sandy mud matrix. Grain size spectra are presented in Figure 3.11.

Two distinctive units are recognized within L3. Toward the base of tan carbonate mud is a very distinctive brown, rose and grey colour sequence up to 6 cm thick (Figure 4.5). This colour sequence has been identified in all cores from just south of Pond Inlet (core 063) to just north of Home Bay (core 074) (Figure 4.2). Above this colour sequence is a thin tan carbonate mud overlain by a distinctive massive to faintly bedded grey brown mud, up to 30 cm thick, with < 1 % IRD, black mottling, and a reddish top (Figure 4.5). This brown grey mud has been recognized

in all cores which contain the brown, rose and grey colour sequence in addition to core 077, within Home Bay, and core 079, just south of Home Bay.

The upper tan carbonate mud is generally < 0.8 m in thickness and is predominantly massive with some occurrences of weak stratification observed in X-radiographs. The contact with underlying brown grey mud is gradational over 3-5 cm in core, but is striking because of the visual colour change; in X-radiographs the contact is diffuse with IRD increasing upward over a 5 cm interval. The percentage of IRD within the upper tan carbonate mud interval is consistent until the upper 0.5 m of L3. Here X-radiography shows an upward decrease in IRD and a defined upper limit of IRD where it is overlain by L4. In most cores, however, isolated IRD persists for another 30 to 90 cm within the upper bioturbated brown mud facies.

There is a gradual decrease in tan carbonate mud bed thickness from north to south along the western margin of Baffin Bay. In core 064 the upper and lower tan carbonate mud interval, combined, is ~ 2.0 m thick whereas south of Home Bay tan carbonate mud thins to about 0.5 m and the brown, rose and grey colour sequence, identified in all cores north of Home Bay, has not been recognized.

Several AMS radiocarbon ages provide timing for the deposition of tan carbonate mud (Table 2) although some of the ages appear reversed. The top of the lower tan carbonate interval, just beneath the brown, rose and grey colour sequence, is dated at 13,804 cal yrs BP in core 064 (Figure 3.8a). The brown, rose and grey colour sequence is missing in core 077, to the south. However, on the basis of X-radiography and pXRF data we have correlated the upper grey

brown, black mottled mud in core 077 (172 cm to 163 cm) to the grey brown mud just above the brown, rose and grey colour sequence in all cores north of Home Bay (Figure 4.2; Figure 4.5). An age of 14,013 cal yrs BP just beneath the lower grey brown bioturbated mud in core 077 is consistent with the 13,804 cal yrs BP age beneath the brown, rose and grey colour sequence in core 064. Tan carbonate mud overlying grey brown mottled mud in core 064 (Figure 3.8a) was dated at 15,894 cal yrs BP which is almost 2,000 calibrated years older than the underlying age and according to our correlation should be just younger than about 13,000 cal yrs BP. It is possible that the mixed benthic foraminifera contained some reworked tests. The top of the tan carbonate mud interval in core 077 is just younger than 11,327 cal yrs BP (Table 2).

4.4 Lithofacies 4 (L4) - Bioturbated Brown Mud

Medium brown mud, often containing numerous *Zoophycos* burrows, occurs within the top 2 m of most sediment cores and directly overlies tan carbonate mud (Figures 4.2 and 4.5). Here the contact with tan carbonate mud is gradational over 5 to 10 cm as much of the underlying IRD rapidly diminishes. Infrequent, disseminated IRD often persists for another 0.5 m within bioturbated brown mud before disappearing completely. Down-core magnetic susceptibility and P-wave velocity are relatively constant; bulk density increases gradually toward the base of L4 (Figures 3.8a and 3.55a).

The mud is very weakly stratified to massive, and often mottled, with primary bedding contacts modified by bioturbation. In some cases the mud is completely burrow-homogenized and looks

massive. In core photography, horizontal burrows are commonly dark brown to black and appear as specs or interrupted, wispy laminae. A representative grain size spectra plot is presented in Figure 3.11. In water depths greater than 1000 m, L5 is gradationally overlain by a distinctive orange brown hemipelagic mud, less than 40 cm thick, and commonly, less than 15 cm thick. The contact into orange brown mud occurs over an interval of 3 to 5 cm. Toward the base of brown mud, mixed benthic foraminifera returned an age of 9,629 cal yrs BP (Table 2) and this is consistent with the calibrated radiocarbon age near the top of underlying tan carbonate mud. This age is just below the top of the last few scattered granules within bioturbated brown mud.

References

- Aksu, A.E. and Piper, D.J.W. 1987. Late Quaternary sedimentation in Baffin Bay. *Can. J. Earth Sci.*, **24**, 1833-1846.
- Campbell, D. C. 2014. CCGS Hudson Expedition 2013-029 geological hazard assessment of Baffin Bay and biodiversity assessment of Hatton Basin, August 14-September 16, 2013. Geological Survey of Canada, *Open File 7594*, 124 p. doi:10.4095/293694
- Coulthard, R.D., Furze, M.F.A., Pienkowski A.J., Nixon, F.C. and England, J.H. 2010. New marine ΔR values for Arctic Canada. *Quaternary Geochronology*, **5**, 419-434.
- Reimer, P.J., Bard, E., Bayliss, A., Beck, J.W., Blackwell, P.G., Ramsey, C.B., Buck, C.E., Cheng, H., Edwards, R.L., Friedrich, M., Grootes, P.M., Guilderson, T.P., Hafliðason, H., Hajdas, I., Hatté, C., Heaton, T.J., Hoffmann, D.L., Hogg, A.G., Hughen, K.A., Kaiser, K.F., Kromer, B., Manning, S.W., Niu, M., Reimer, R.W., Richards, D.A., Scott, E.M., Southon, J.R., Staff, R.A., Turney, C.S.M. and van der Plicht, J. 2013. INTCAL 13 and marine 13 radiocarbon age calibration curves 0-50,000 years cal BP. *Radiocarbon*, **55**, 1869-1887.
- Weitzman, J.; Ledger, S.; Stacey, C. D.; Strathdee, G.; Piper, D. J. W.; Jarrett, K. A. and Higgins, J. 2014. Logs of short push cores, deep-water margin of Flemish Cap and the eastern Grand Banks of Newfoundland. Geological Survey of Canada, *Open File 7148*, 389 p. doi:10.4095/293871

Tables and Figures

Table 1- Piston cores collected during Hudson 2013-029 used in this study.

Station Number	Core type	Latitude (north)	Longitude (west)	water depth (m)	split core length (cm)	Chronology	Geographic Location	Notes
046	Piston	67.802350	-59.374205	1248	492.0		off of Disko Bugt	
047	Piston	67.630128	-62.050921	919	254.0		slope off of Qikiqtarjuaq	
048	Piston	67.605618	-61.967451	935	822.5		slope off of Qikiqtarjuaq	
052	Piston	70.635813	-66.247913	1251	183.5		slope off of Clyde River	
053	TWC	70.696770	-66.395751	1349	0.0		slope off of Clyde River	PC recovered only an angular clast; TWC used
056	Piston	71.687403	-69.106078	1715	464.5		off of Scott Trough slope	
057	Piston	71.701388	-69.148798	1713	31.5		off of Scott Trough slope	PC recovered only 31.5 cm; TWC used
059	Piston	71.856891	-70.952513	1084	502.0		slope north of Scott Trough	
060	Piston	71.867328	-70.867066	1191	487.0		slope north of Scott Trough	
061	Piston	71.919041	-70.458838	1635	315.0		slope north of Scott Trough	
062	Piston	71.924568	-70.413305	1648	318.5	¹⁴ C AMS	slope north of Scott Trough	
063	Piston	72.455251	-72.906995	833	382.0		slope north of Buchan Trough	
064	Piston	72.426113	-72.769305	875	713.0	¹⁴ C AMS	slope north of Buchan Trough	
073	Piston	70.208068	-65.320780	1022	428.0		slope off of Scott Trough	
074	Piston	69.523171	-64.645093	1482	592.0		Isabella Bank	
075	Piston	69.547883	-64.643330	1484	704.0		Isabella Bank	
076	Piston	69.288243	-64.007485	1040	101.5		Alexander Bank	
077	Piston	63.308682	-63.794663	1153	649.5	¹⁴ C AMS	Alexander Bank	
079	Piston	68.152065	-63.673306	1078	254.0		Alexander Bank	
082	Piston	67.781908	-59.539071	1352	643.0		off of Disko Bugt	
084	Piston	67.777421	-59.582088	1359	725.0		off of Disko Bugt	

Table 2- Radiocarbon results used in this study.

Radiocarbon Ages Cruise 2013029 Cores

Expedition number	Station number	New core number	Information on core			Information on dated sample			Laboratory Number	Conventional radiocarbon age (radiocarbon years BP)	Calibrated radiocarbon age in years BP (1 σ ; Delta R = 220)		Median	Lithofacies			
			Core type	Latitude	Longitude	Water depth (m)	top depth (cm)	bottom depth (cm)			Material dated	Species where known			Weight dated (mg)	Minimum	Maximum
2013029	062	Piston	71.924568	-70.413305	1648	158	162	F	mixed benthic foraminifera assemblage	1.4	OS-118357	30,500	470	33,600	34,418	33,975	upper diamicton
2013029	064	Piston	72.426113	-72.769305	875	135	140	F	mixed benthic foraminifera assemblage	2.9	OS-118358	9200	35	9,553	9,676	9,629	Holocene mud
2013029	064	Piston	72.426113	-72.769305	875	275	280	F	mixed benthic foraminifera assemblage	1.4	OS-118649	13,850	95	15,752	16,042	15,894	upper tan carbonate mud
2013029	064	Piston	72.426113	-72.769305	875	330	335	F	mixed benthic foraminifera assemblage	3.9	OS-117862	12,500	45	13,731	13,875	13,804	tan carbonate (below colour sequence)
2013029	073	Piston	70.208068	-65.320780	1022	123	125	F	mollusc shell fragments	~4-5	CURL-21050	19,900	80	23,066	23,365	23,219	gold sand bed within gold mud and immediately overlying diamicton
2013029	077	Piston	63.308682	-63.794663	1153	137	142	F	mixed benthic foraminifera assemblage	4.9	OS-117723	10,550	40	11,226	11,396	11,327	tan carbonate mud (just below brown Holocene mud)
2013029	077	Piston	63.308682	-63.794663	1153	200	205	F	mixed planktonic foraminifera assemblage	1.7	OS-118359	12,750	55	13,936	14,094	14,013	bioturbated brown grey mud (at base of tan carbonate mud)
2013029	077	Piston	63.308682	-63.794663	1153	638	643.5	F	planktonic foraminifera (Neogloboquadrina pachyderma (Nps))	0.09	UCIAMS 181265	37,900	1600	40,108	42,862	41,461	basal grey brown mud

Notes

Radiocarbon dates were converted to calibrated years BP using the online software Calib 7.1 (<http://calib.qub.ac.uk/calib/calib.html>) and the Marine 13 calibration curve of Reimer et al. (2013).

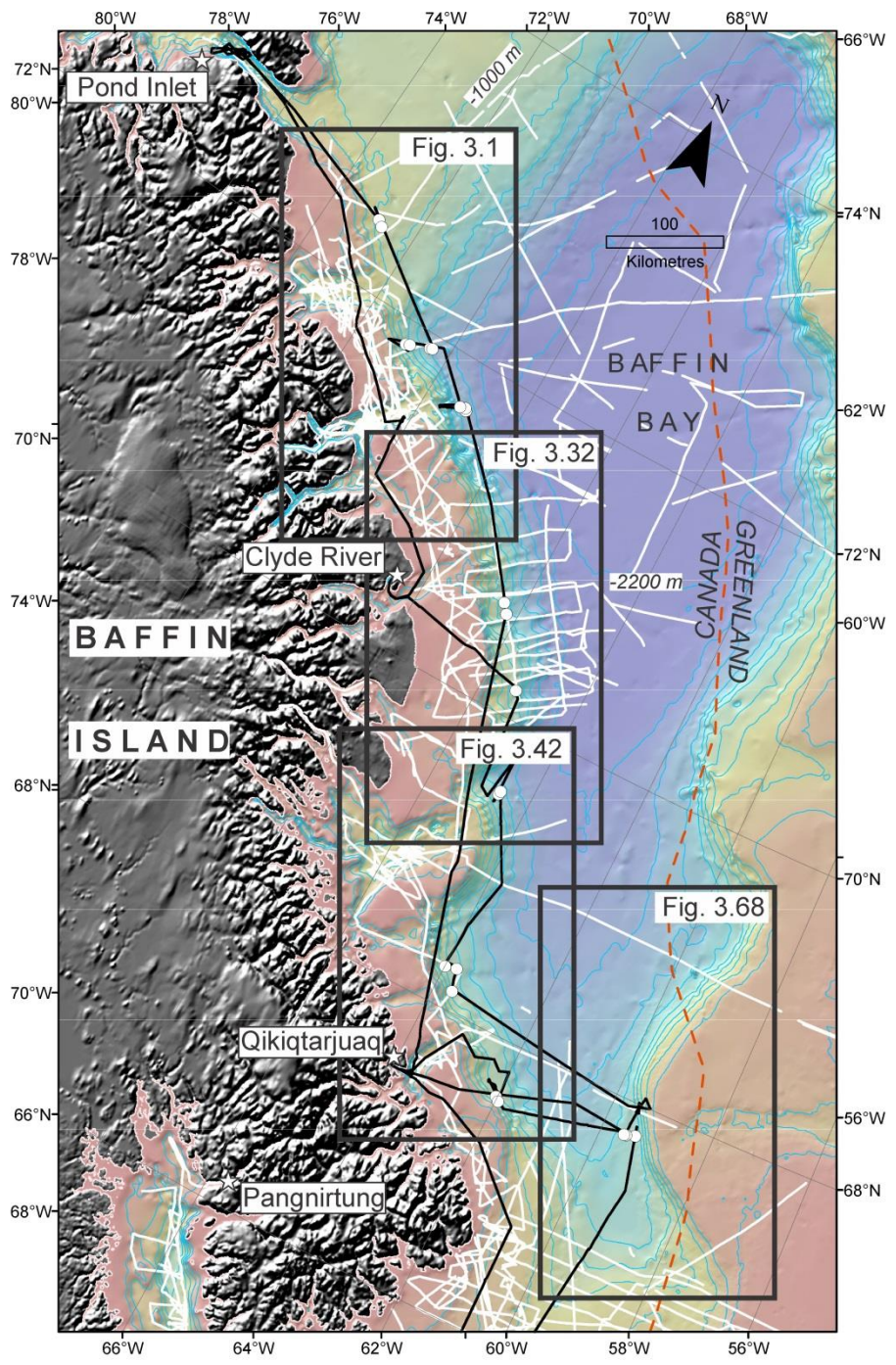


Figure 1.1. Location map of Baffin Bay showing 2013029 core locations (white circles) and 2013029 sub-bottom profiler coverage (black lines). White lines indicate high resolution seismic reflection profiles collected by the GSC prior to the 2013 expedition. Boxes indicate the 4 geographic regions discussed in the text. Bathymetric contour interval is 200 m.

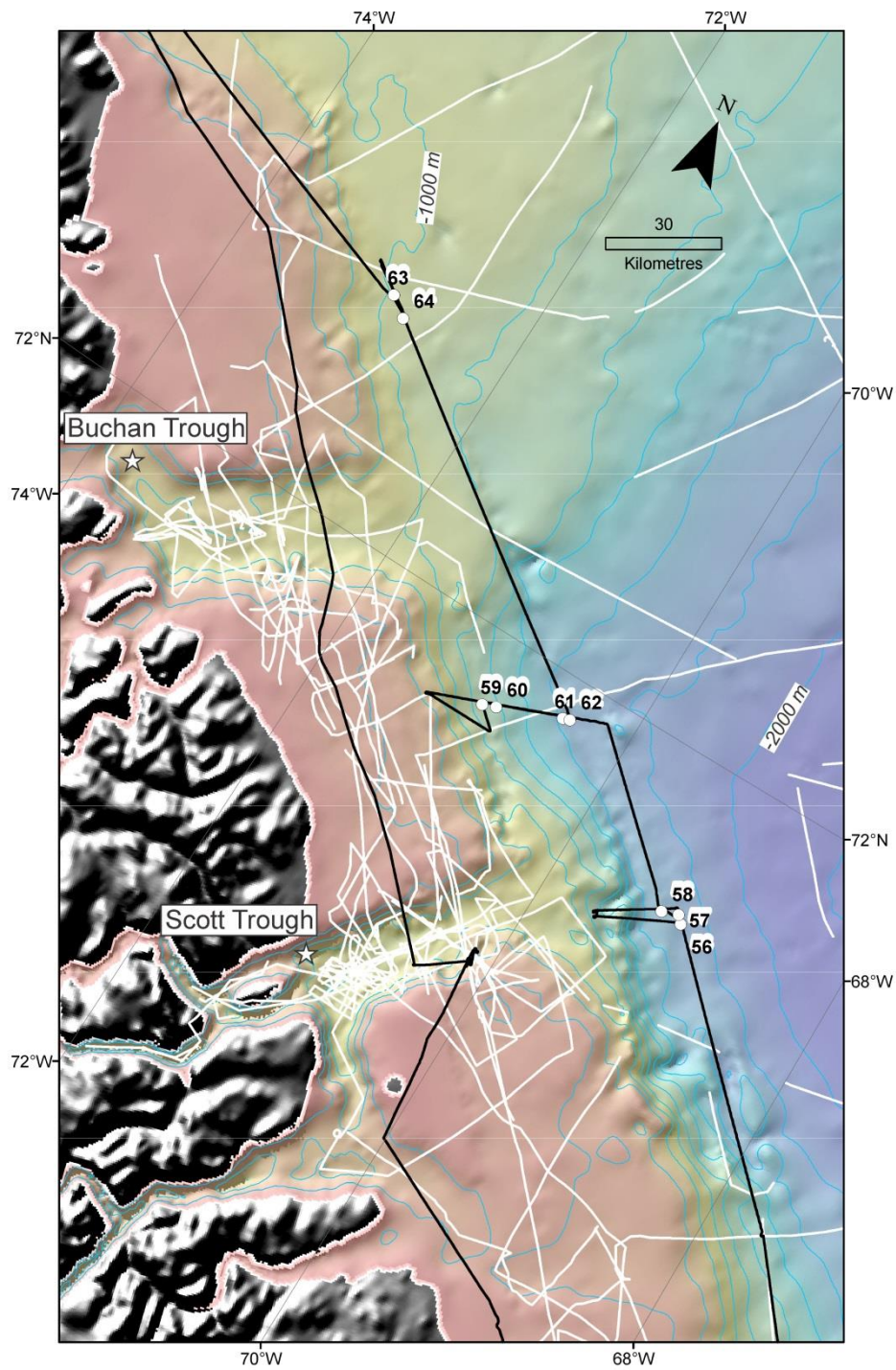


Figure 3.1. Regional map showing core locations and seismic coverage for the northern Baffin Bay slope region. 2013029 core locations are indicated by white circles and 2013029 sub-bottom profiler coverage by black lines. White lines indicate high resolution seismic reflection profiles collected by the GSC prior to the 2013 expedition. Bathymetric contour interval is 200 m.

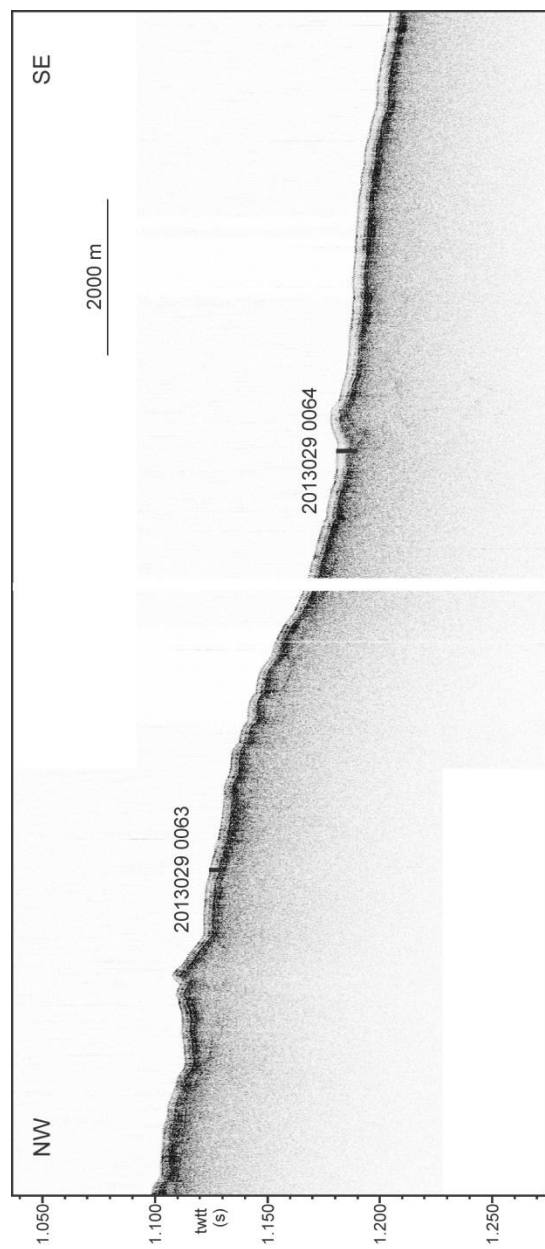


Figure 3.2a. 3.5 kHz sub-bottom profile showing the regional acoustic facies of the northern Baffin Island slope region and location of piston cores 2013029-063 & 2013029-064.

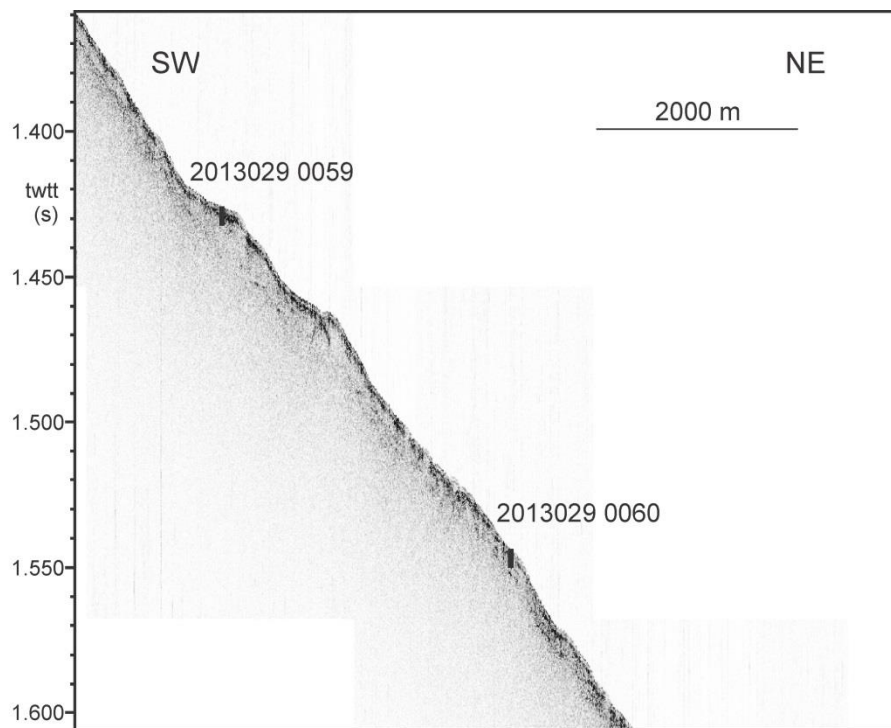


Figure 3.2b. 3.5 kHz sub-bottom profile showing the regional acoustic facies of the northern Baffin Island slope region and location of piston cores 2013029-059 & 2013029-060.

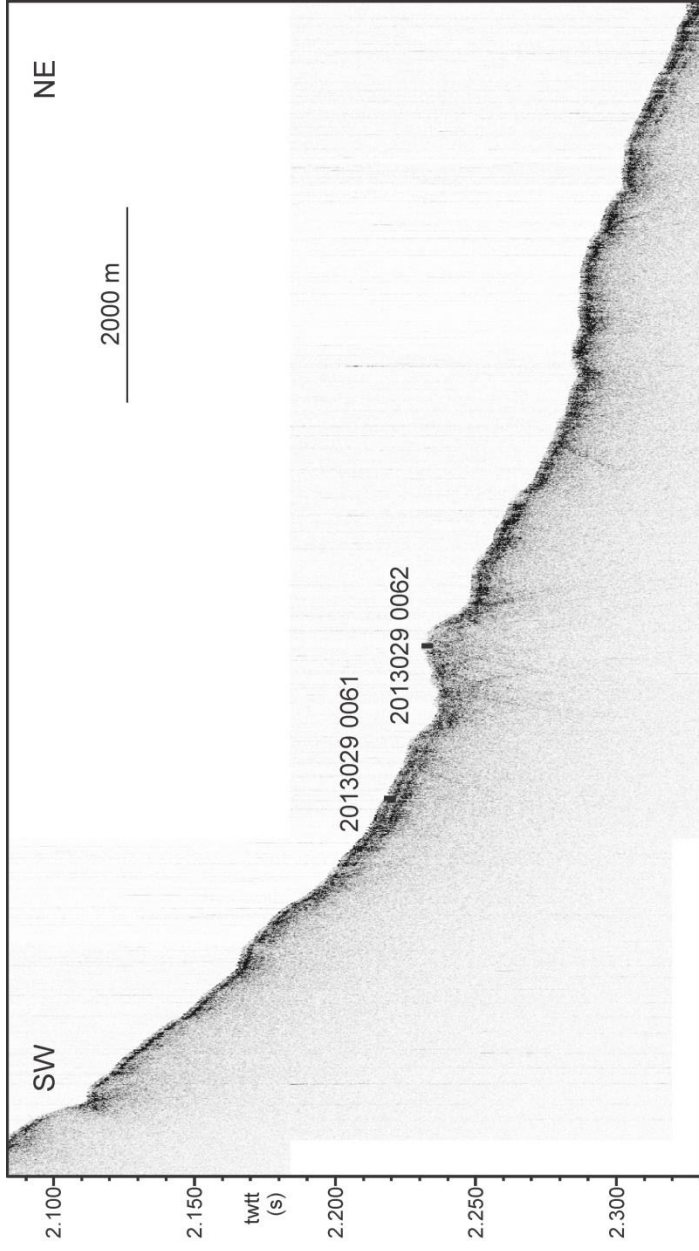


Figure 3.2c. 3.5 kHz sub-bottom profile showing the regional acoustic facies of the northern Baffin Island slope region and location of piston cores 2013029-061 & 2013029-062.

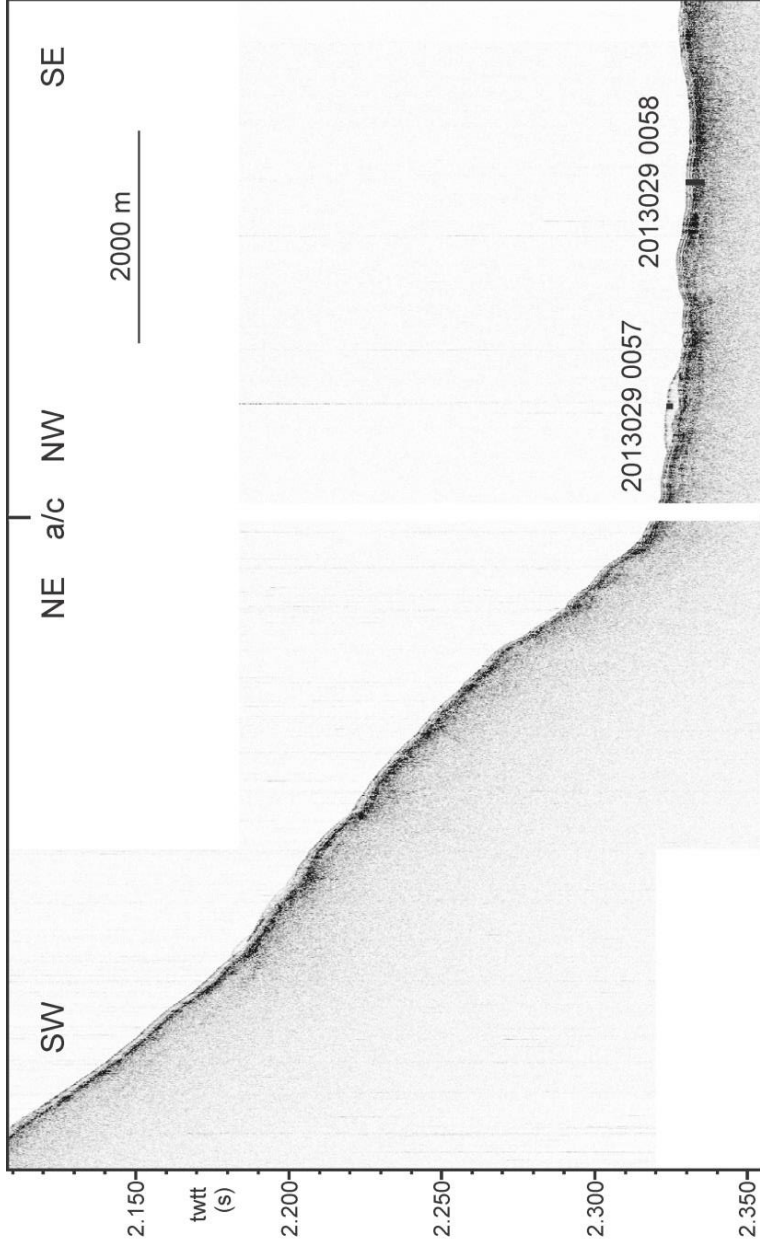


Figure 3.2d. 3.5 kHz sub-bottom profile showing the regional acoustic facies of the northern Baffin Island slope region and location of piston cores 2013029-057 & 2013029-058.

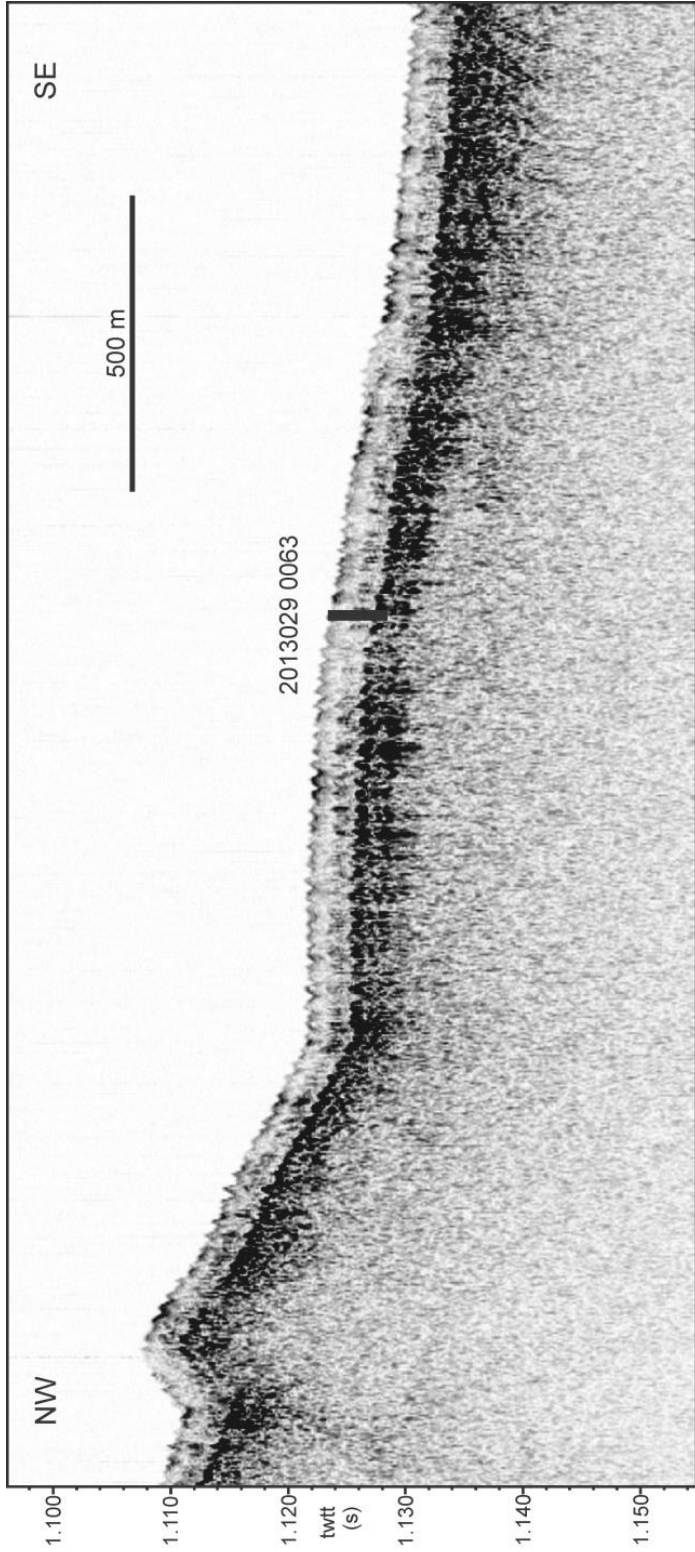




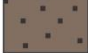
























Figure 3.3. 3.5 kHz sub-bottom profile showing the acoustic stratigraphy and location of core 2013029-063.

Lithology Legend

	Orange brown mud
	Orange brown mud with low IRD
	Tan carbonate mud
	Tan carbonate mud with low IRD
	Tan carbonate mud with high IRD
	Light brown carbonate-rich mud with IRD
	Brown mud
	Brown mud with low IRD
	Brown mud with high IRD
	Grey mud
	Rose mud
	Medium brown mud
	Gold brown mud
	Gold brown mud with low IRD
	Stratified red brown mud
	Stratified red brown mud with low IRD
	Stratified red brown mud with high IRD
	Light gold brown mud
	Light grey mud
	Olive grey mud
	Light brown sand/silt laminae
	Dark grey brown mud
	Dark grey brown sandy mud
	Dark grey brown mud with low IRD
	Dark grey brown mud with high IRD

} Colour sequence

Mass Transport Deposit Lithofacies

	Clast-supported mudclast conglomerate
	Matrix-dominated mudclast conglomerate
	Matrix-supported mudclast conglomerate
	Diamicton
	Folded mud interval
	Stratified mud interval

Symbol Legend

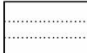
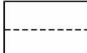








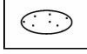


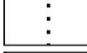

	Gradational contact
	Distinct contact
	Sharp contact
	Erosional contact
	Laminations/thin beds
	Bioturbation
	Ripple cross lamination
	Bivalve
	Shell fragment
	Mudclast
	Sand bleb/lens
	Radiocarbon age (calibrated)
	Fining upward
	Core disturbance
	Whole round core subsample

Figure 3.4. Core plot summary legend.

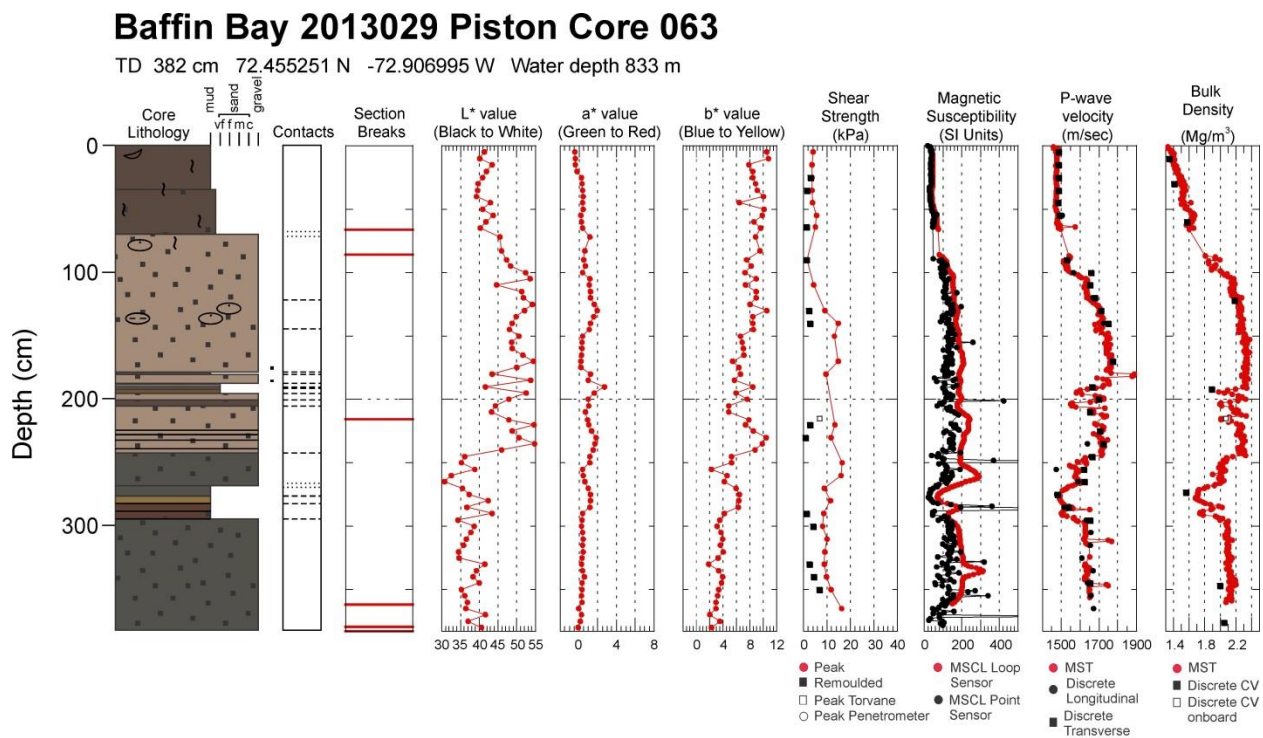


Figure 3.5a. Core plot summary for piston core 2013029-063.

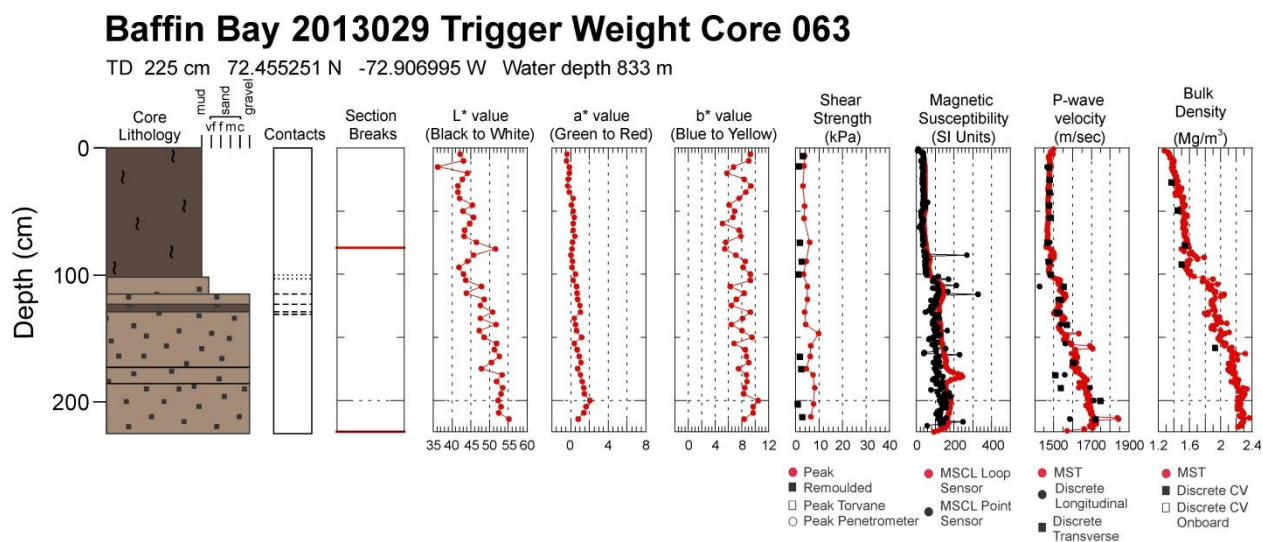


Figure 3.5b. Core plot summary for trigger weight core 2013029-063.

2013029 063 PC

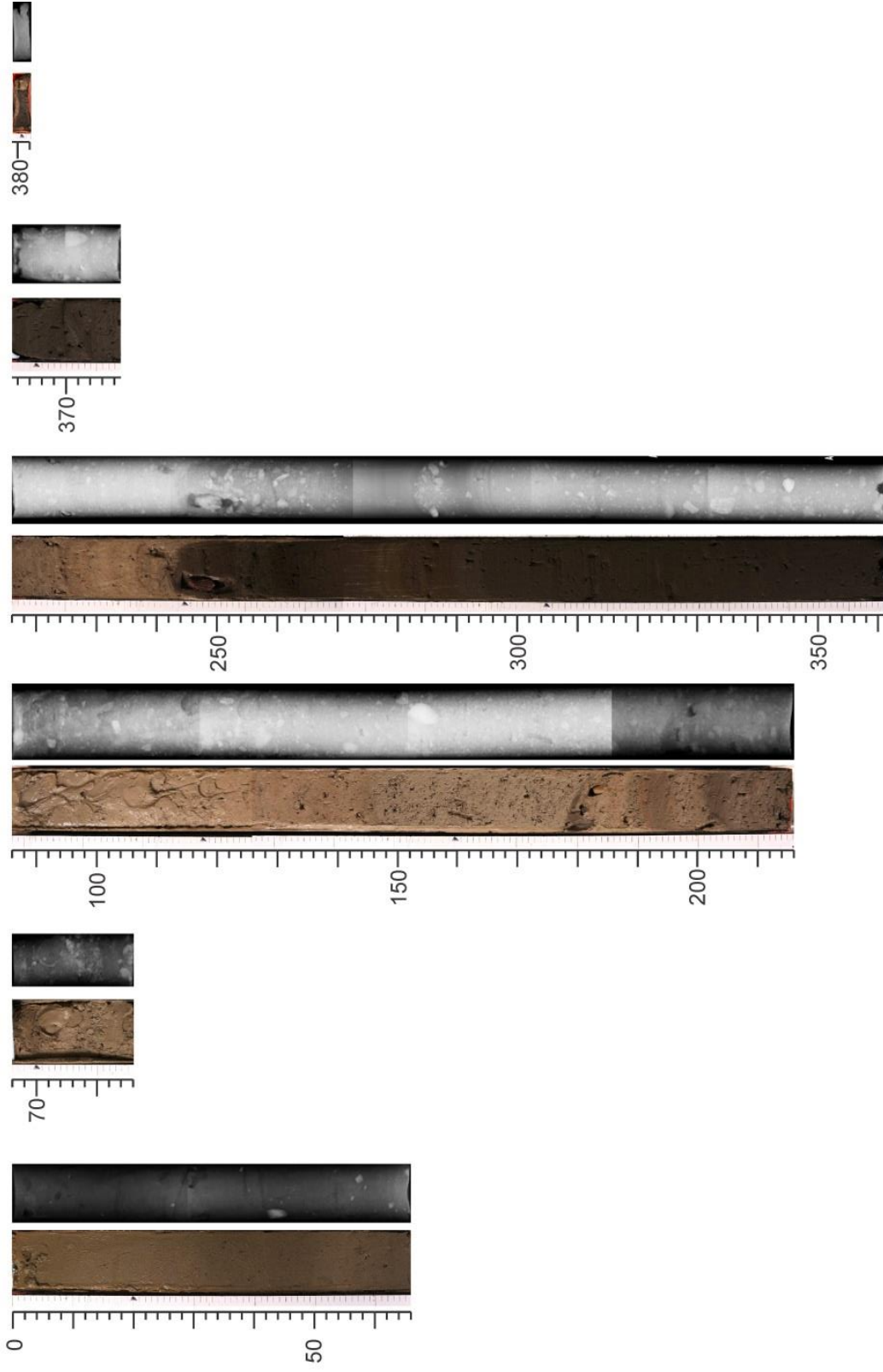


Figure 3.6a. Photography and X-radiography compilation for piston core 2013029-063.

2013029 063 TWC

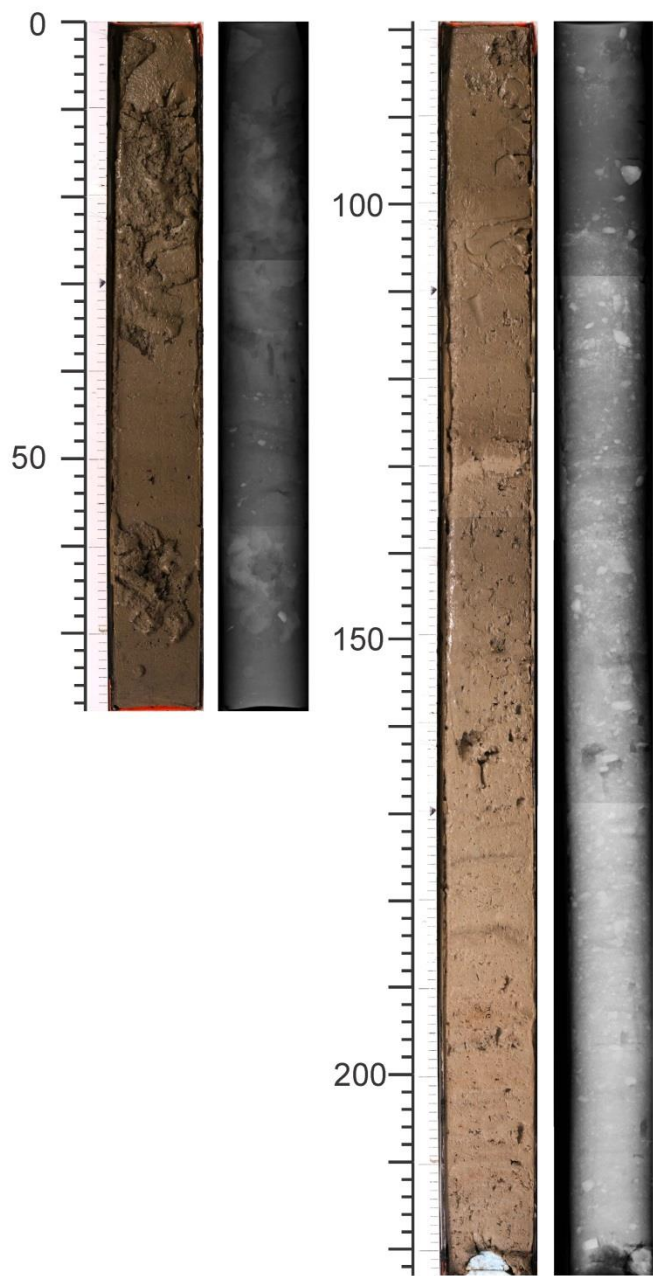


Figure 3.6b. Photography and X-radiography compilation for trigger weight core 2013029-063

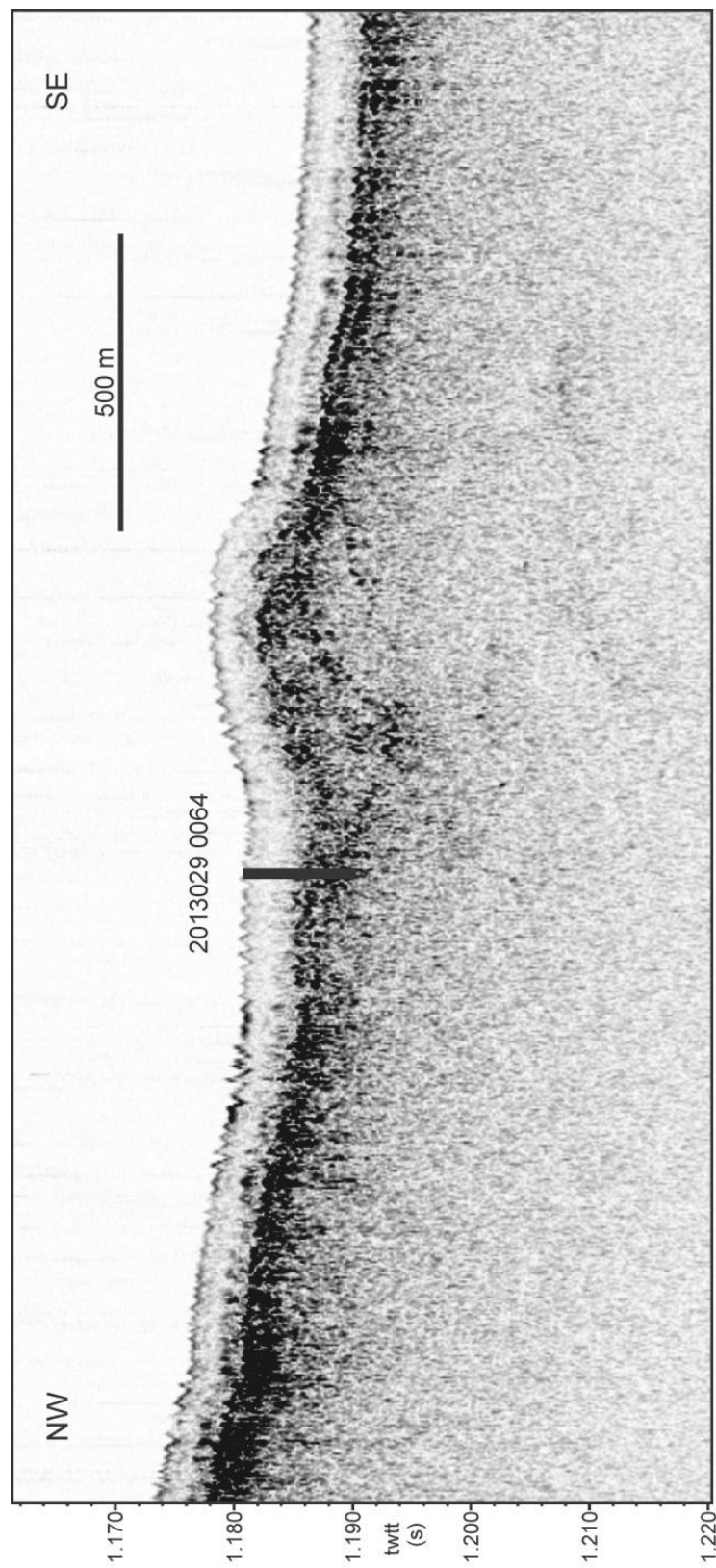


Figure 3.7. 3.5 kHz sub-bottom profile showing the acoustic stratigraphy and position of core 2013029-064.

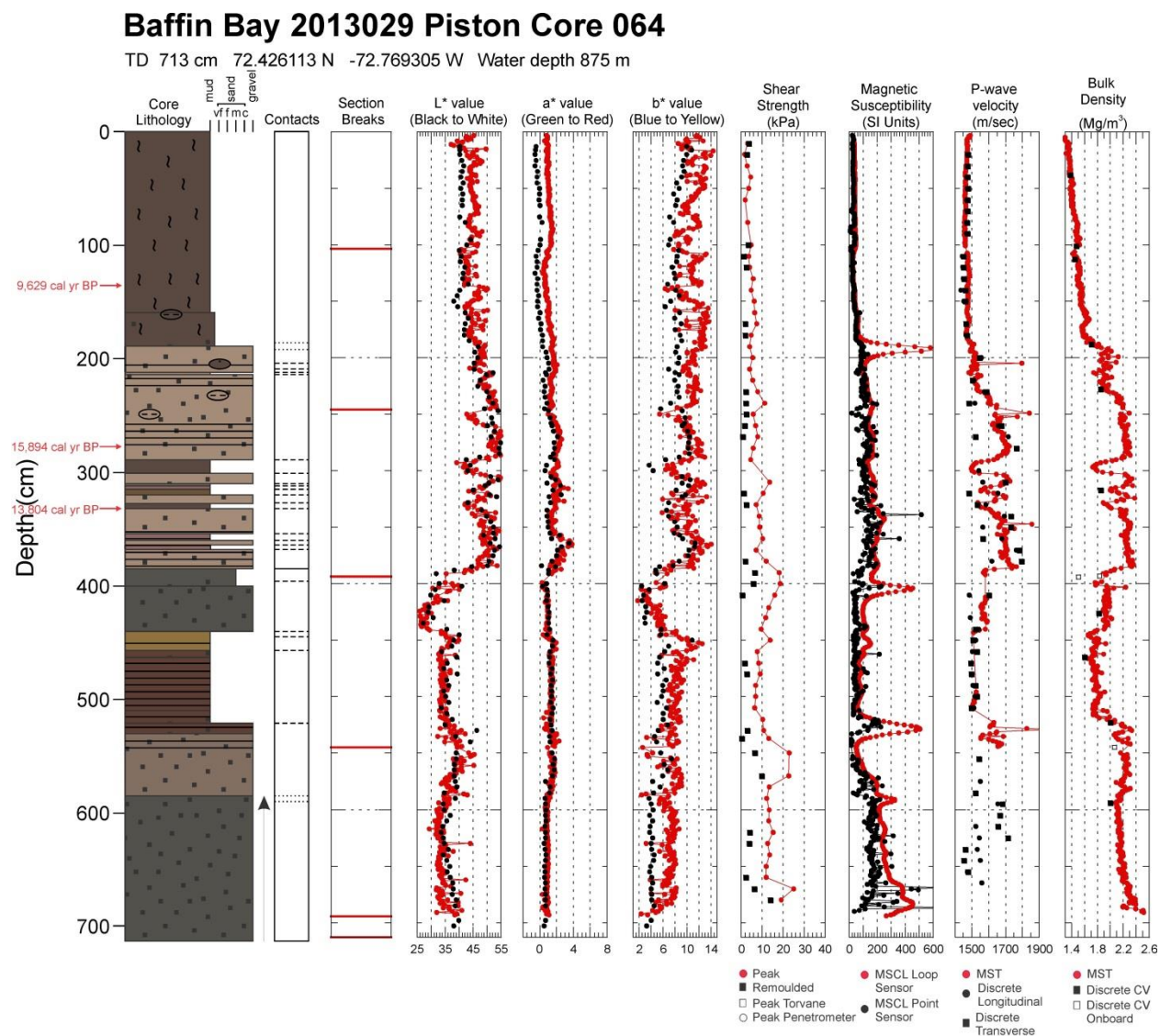


Figure 3.8a. Core plot summary for piston core 2013029-064.

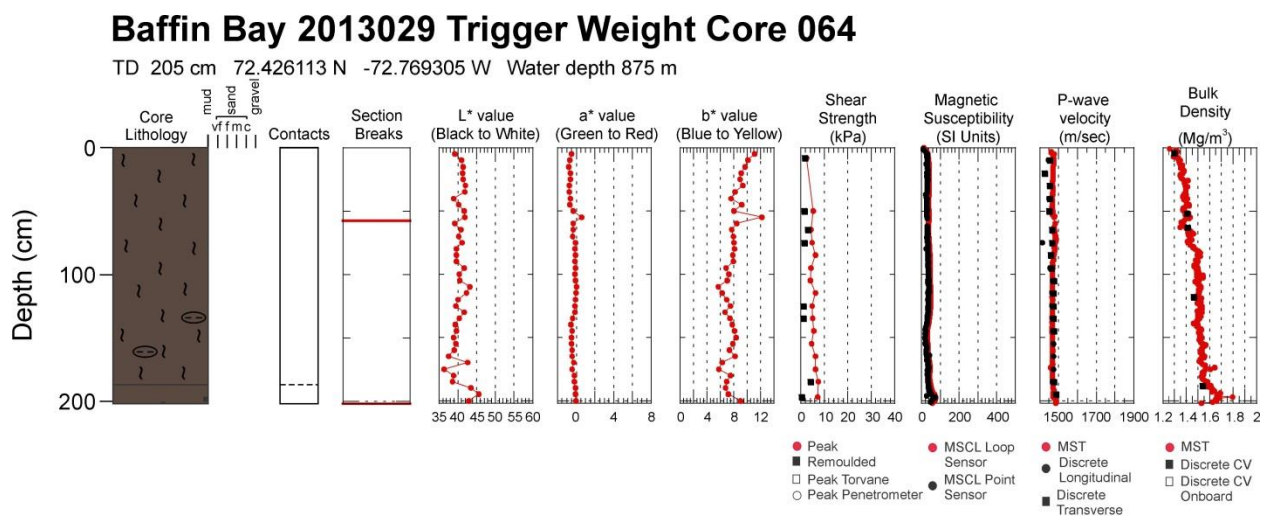


Figure 3.8b Core plot summary for trigger weight core 2013029-064.

2013029 064 PC

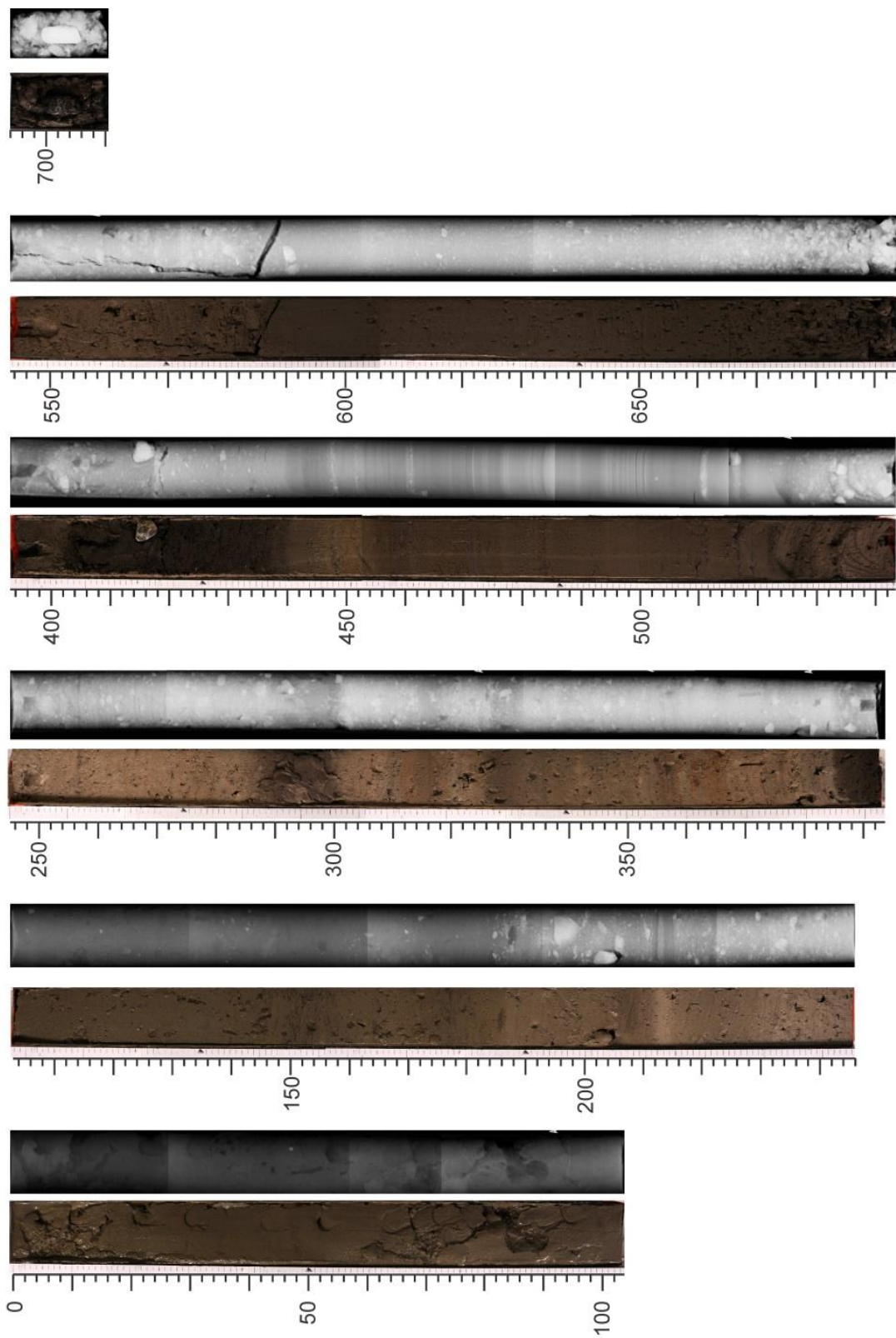


Figure 3.9a. Photography and X-radiography compilation for piston core 2013029-064

2013029 064 TWC

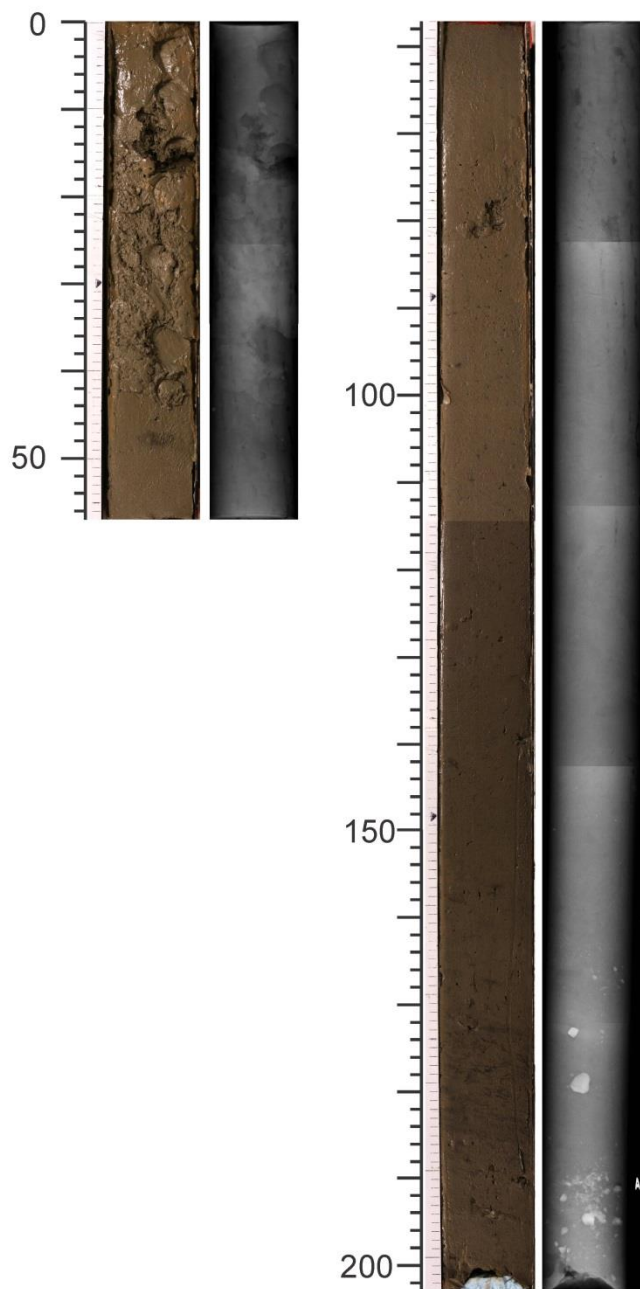


Figure 3.9b. Photography and X-radiography compilation for trigger weight core 2013029-64.

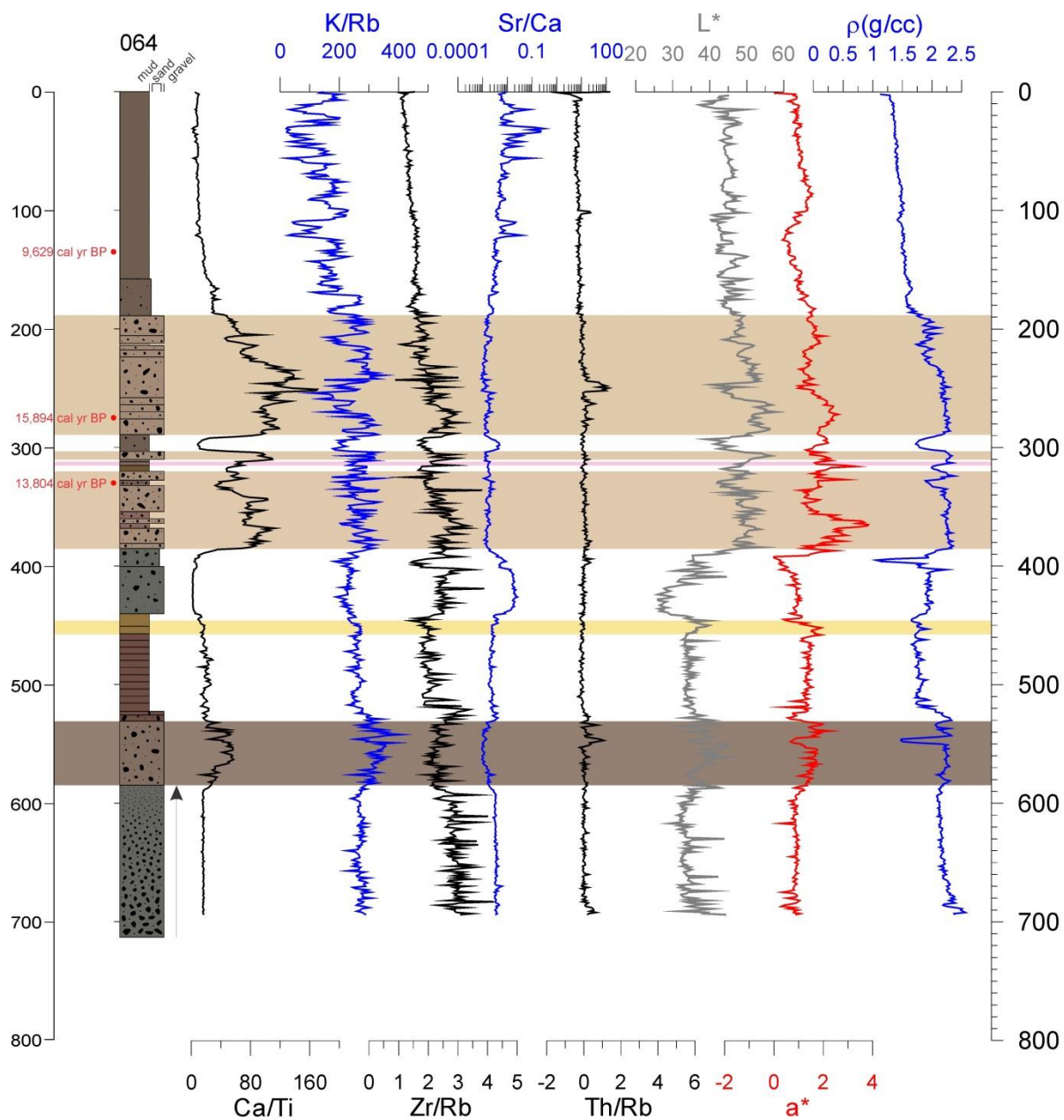


Figure 3.10. Down-core pXRF analysis for piston core 2013029-64. Tan highlighting indicates tan carbonate mud; rose highlighting indicates rose mud; gold brown highlighting indicates gold brown mud; light brown highlighting indicates light brown mud associated with an increase in the pXRF Ca/Ti ratio.

2013029 Grain Size Facies Plots

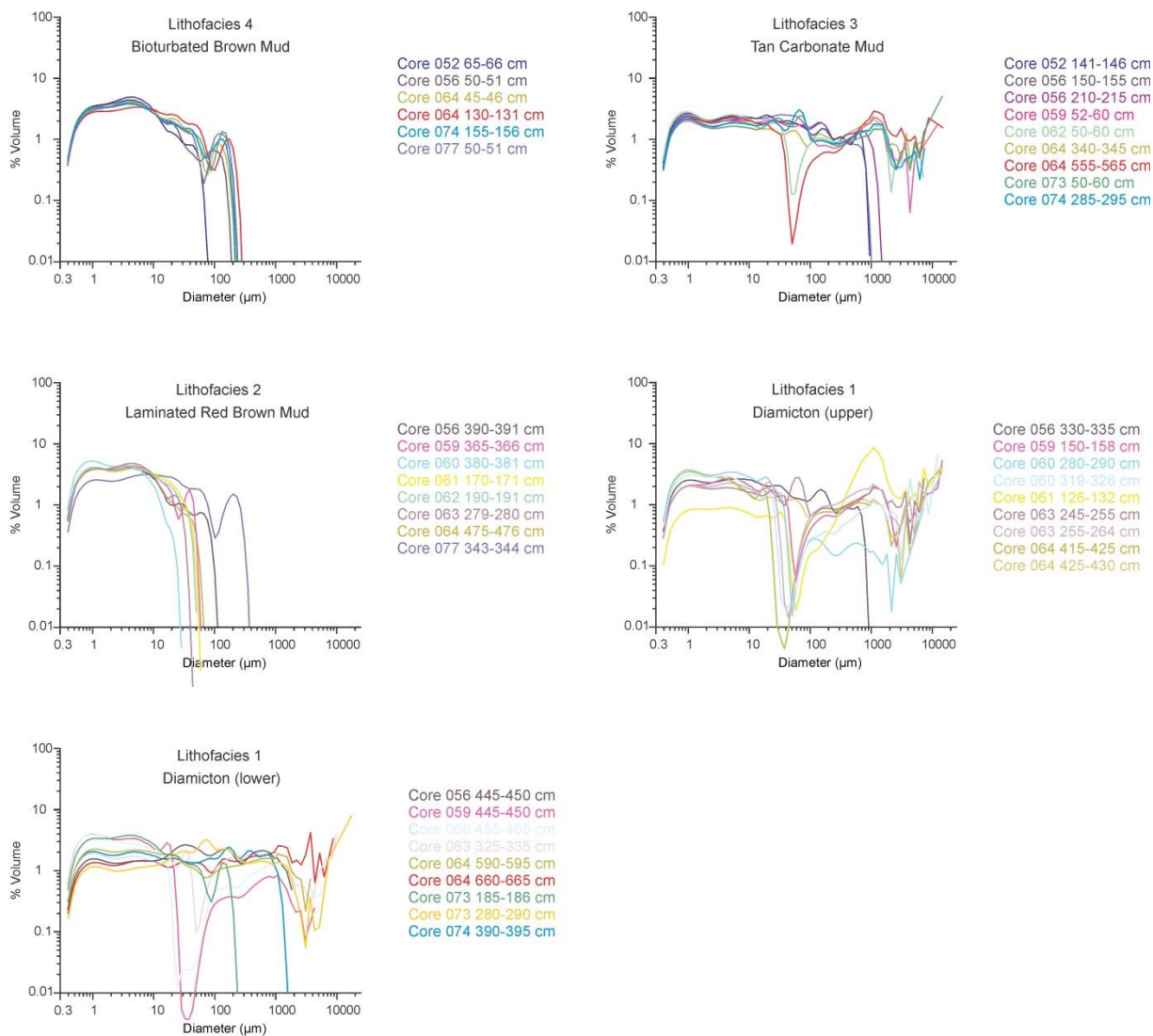


Figure 3.11. Representative grain size spectra plots of each lithofacies.

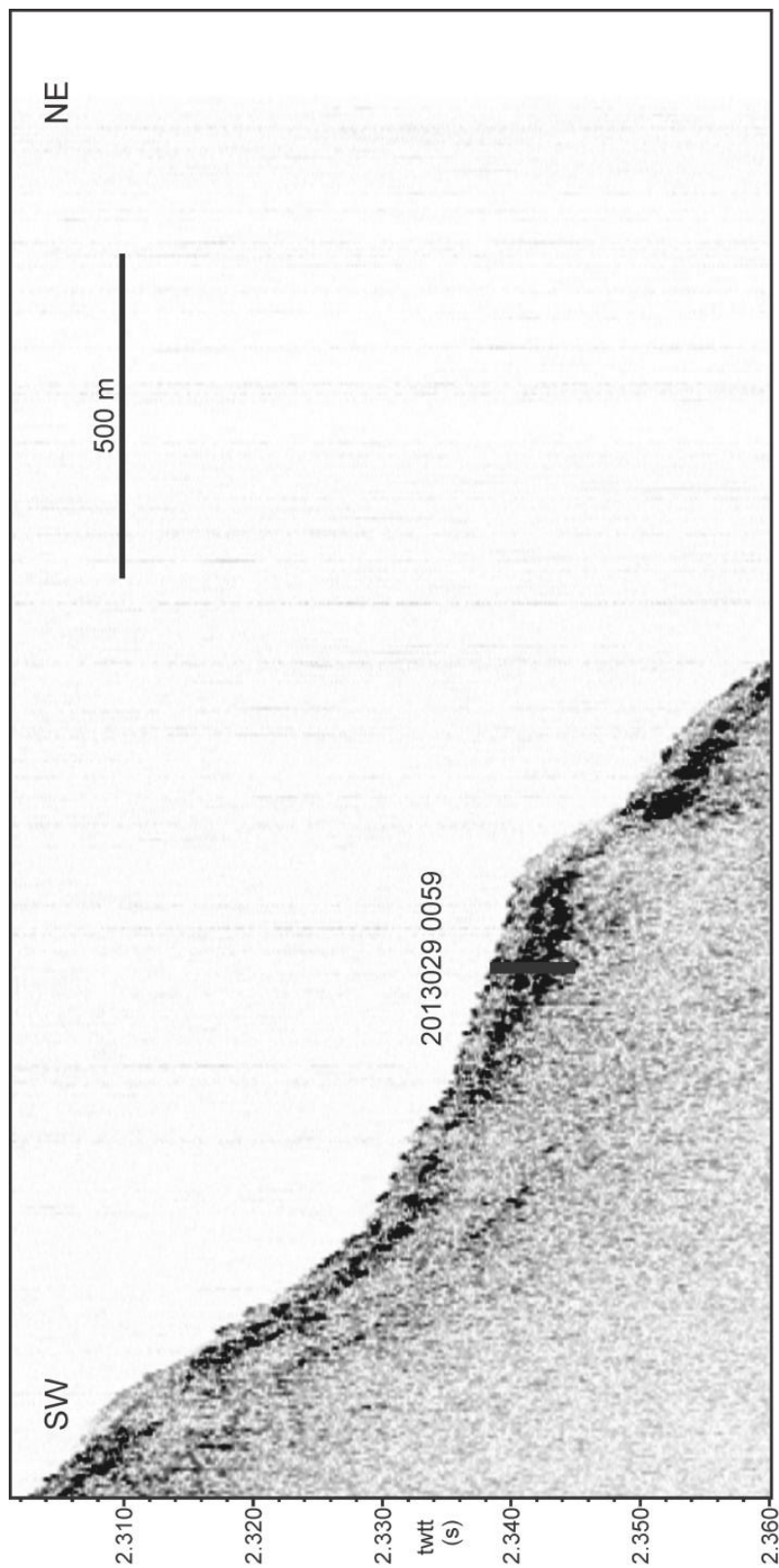


Figure 3.12. 3.5 kHz sub-bottom profile showing the acoustic stratigraphy and position of core 2013029-059.

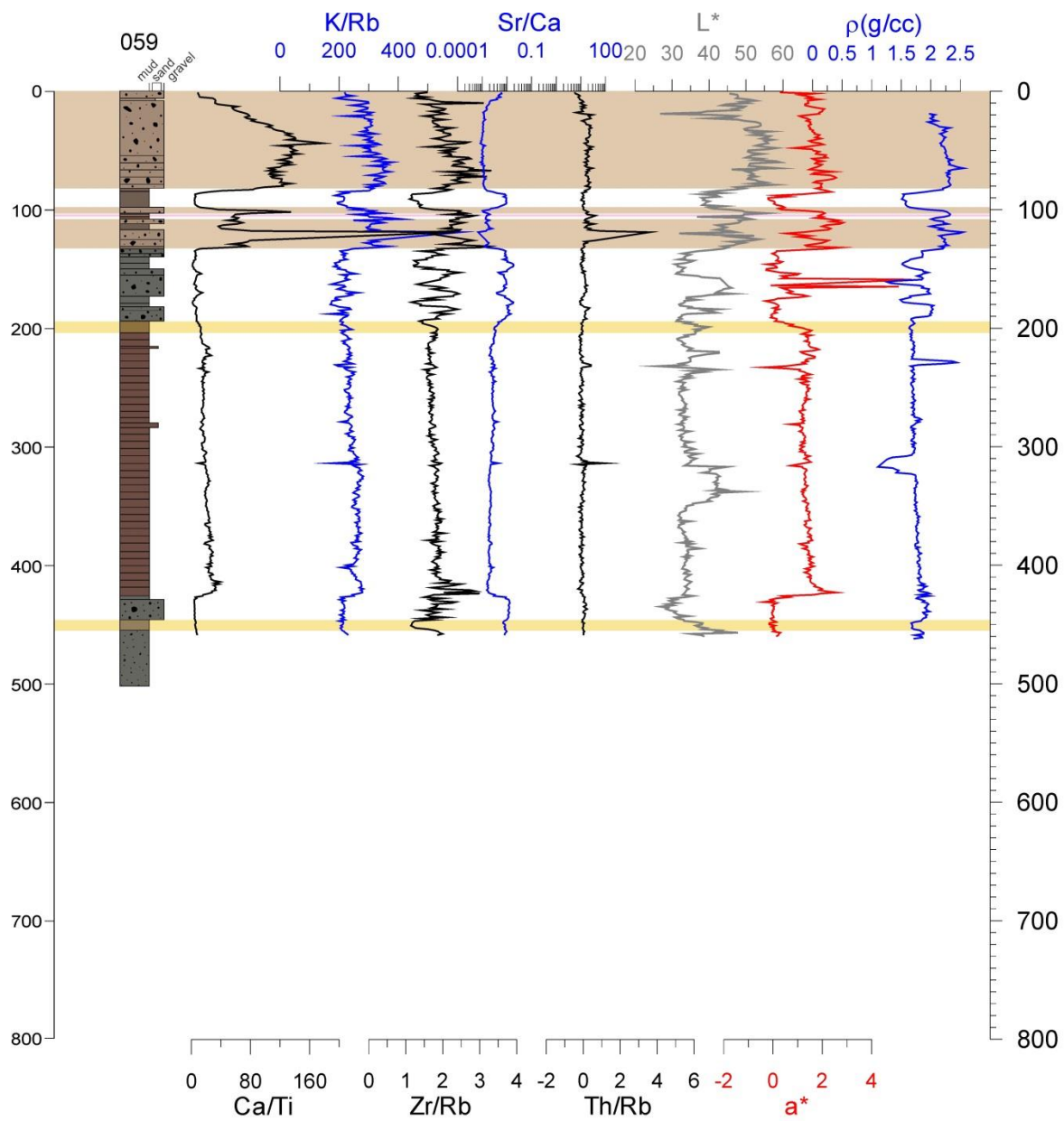


Figure 3.13. Down-core pXRF analysis for piston core 2013029-059. Tan highlighting indicates tan carbonate mud; rose highlighting indicates rose mud; gold brown highlighting indicates gold brown mud.

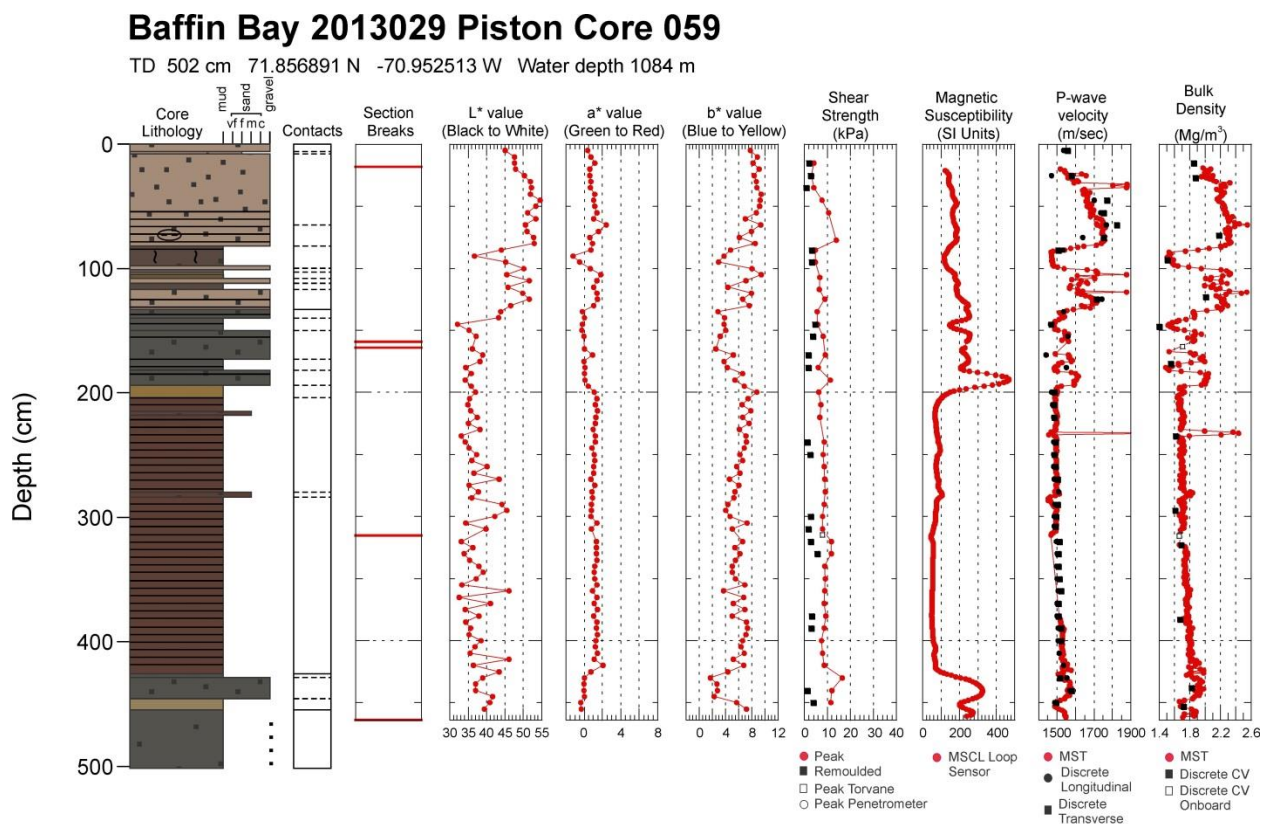


Figure 3.14a. Core plot summary for piston core 2013029-059.

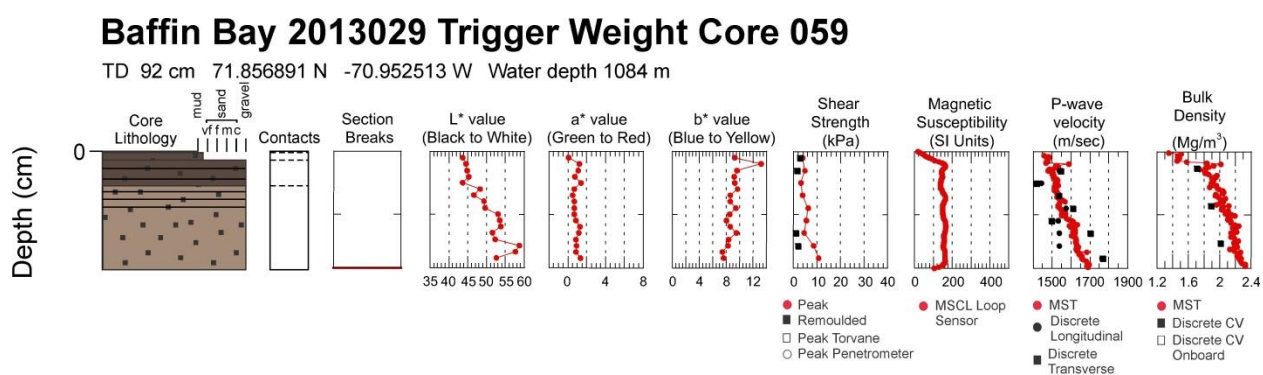


Figure 3.14b. Core plot summary for trigger weight core 2013029-059.

2013029 059 PC

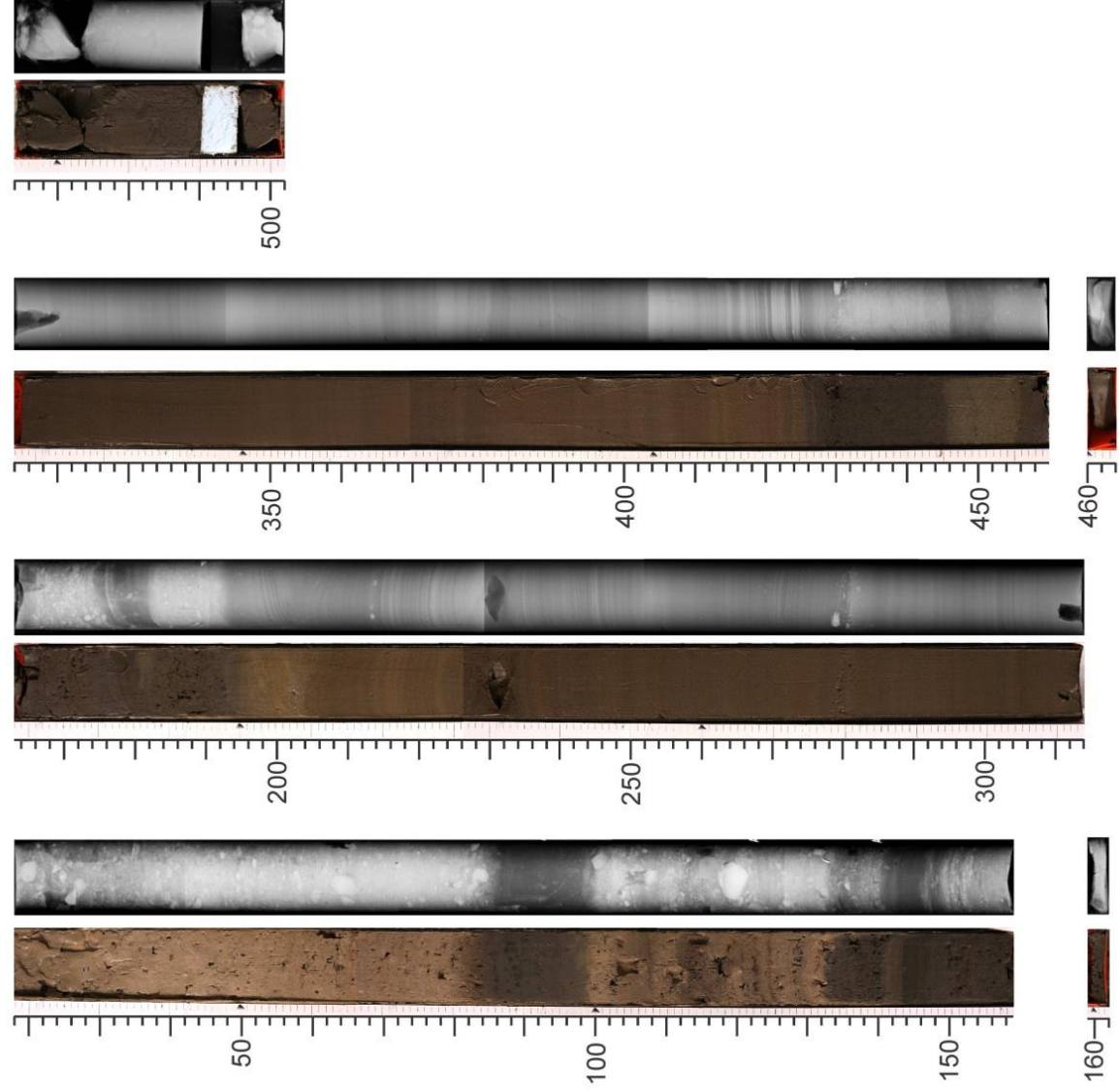


Figure 3.15a. Photography and X-radiography compilation for piston core 2013029-059.

2013029 059 TWC

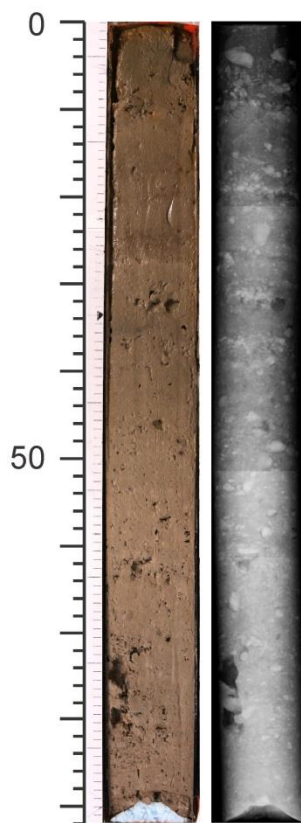


Figure 3.15b. Photography and X-radiography compilation for trigger weight core 2013029-059.

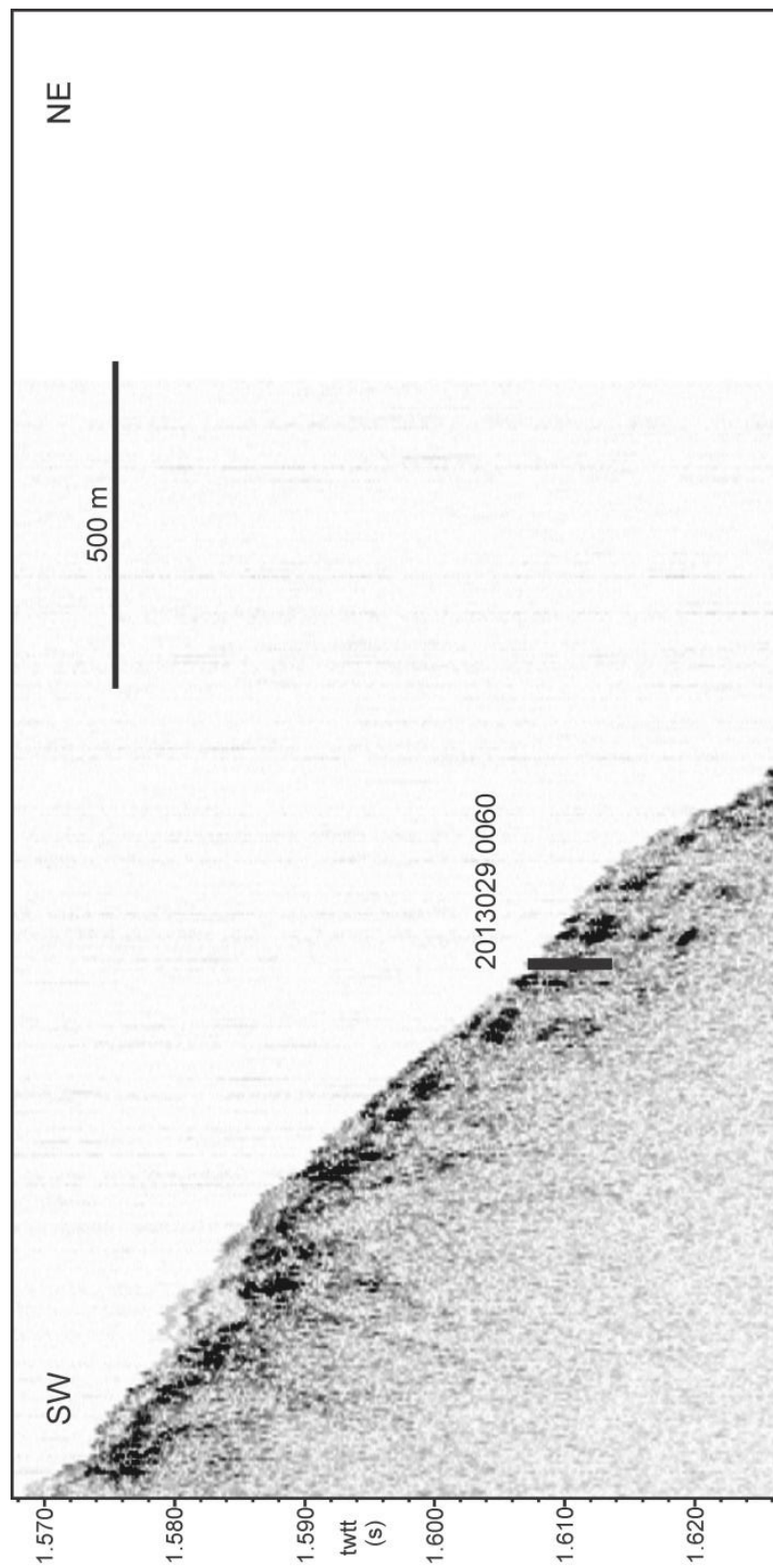


Figure 3.16. 3.5 kHz sub-bottom profile showing the acoustic stratigraphy and position of core 2013029-060.

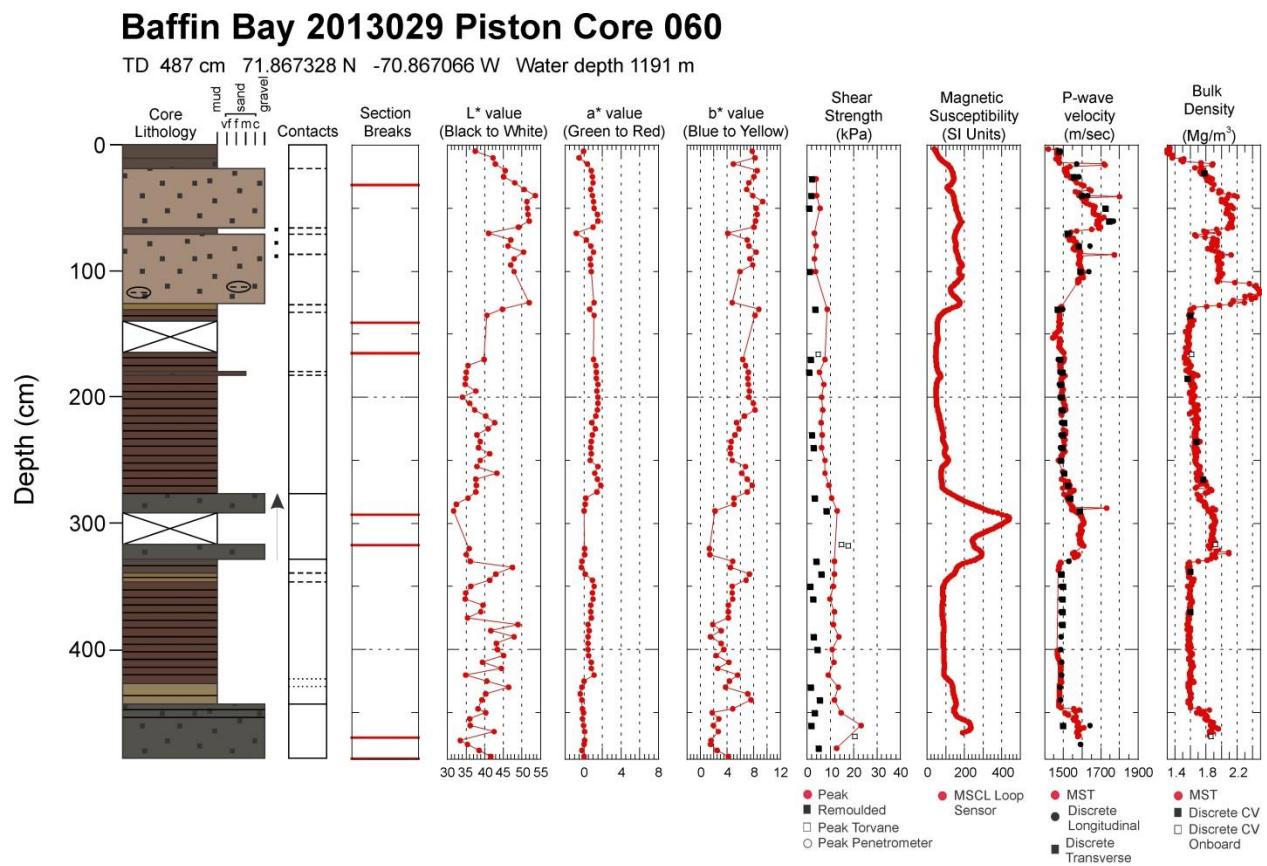


Figure 3.17a. Core plot summary for piston core 2013029-060.

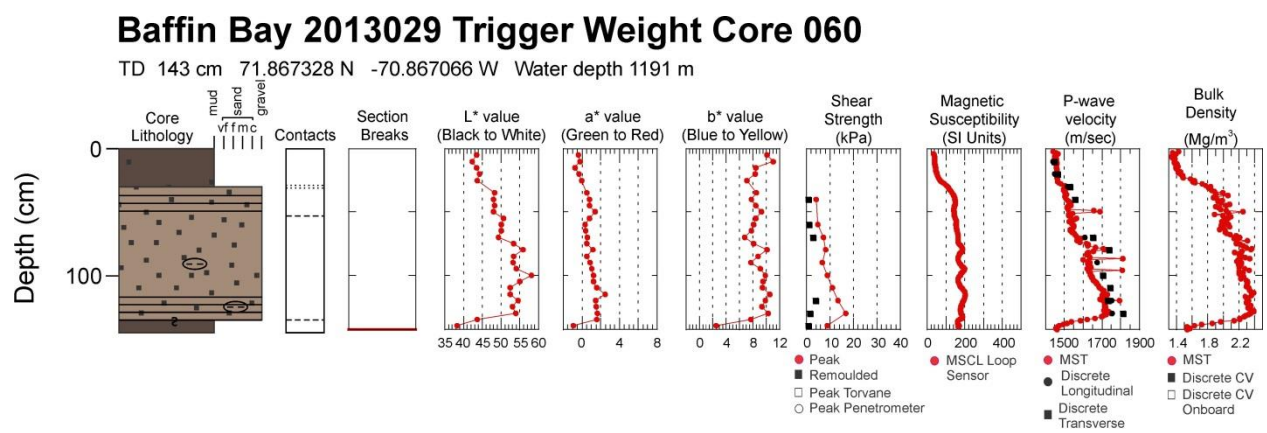


Figure 3.17b. Core plot summary for trigger weight core 2013029-060.

2013029 060 PC

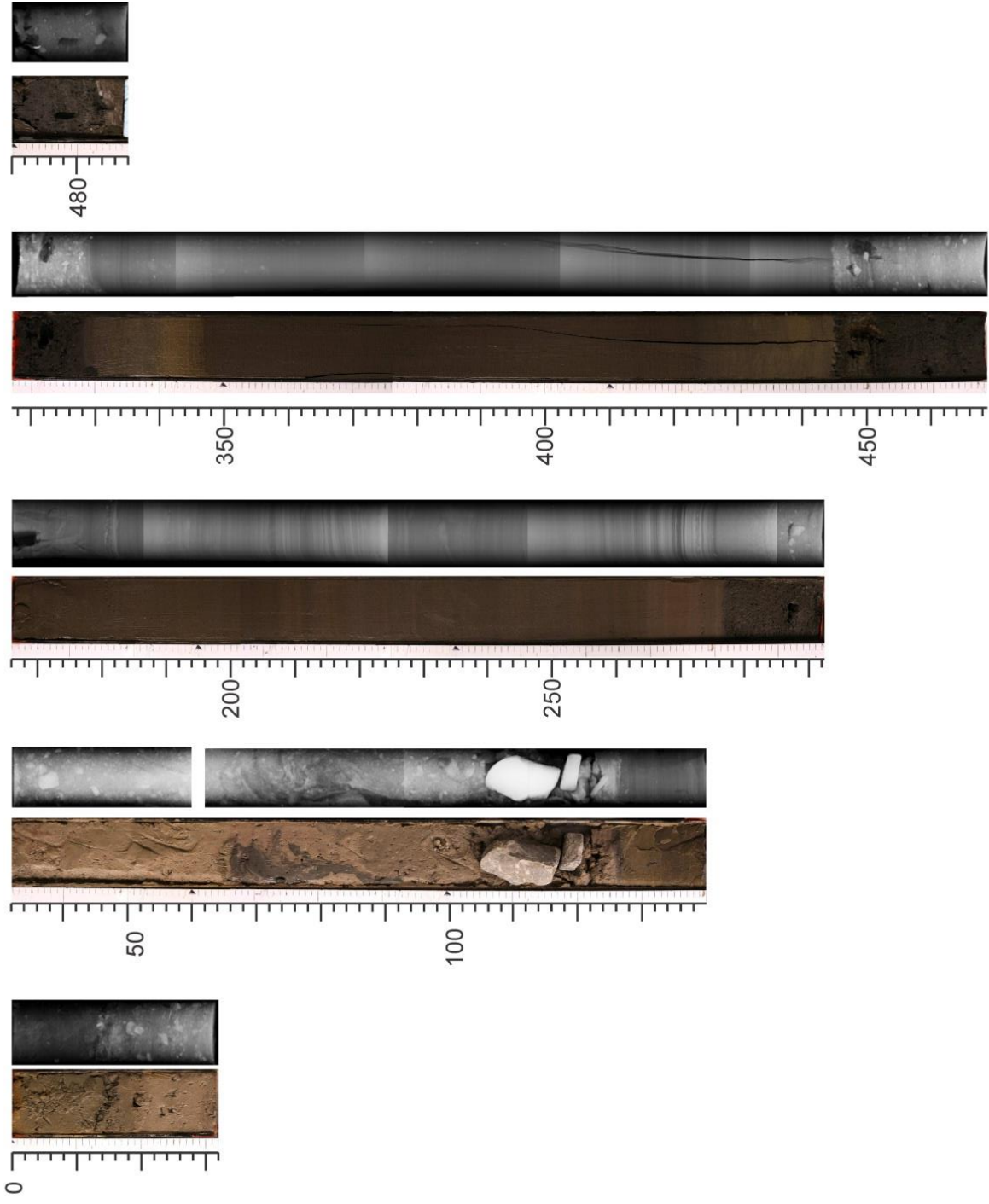


Figure 3.18a. Photography and X-radiography compilation for piston core 2013029-060.

2013029 060 TWC

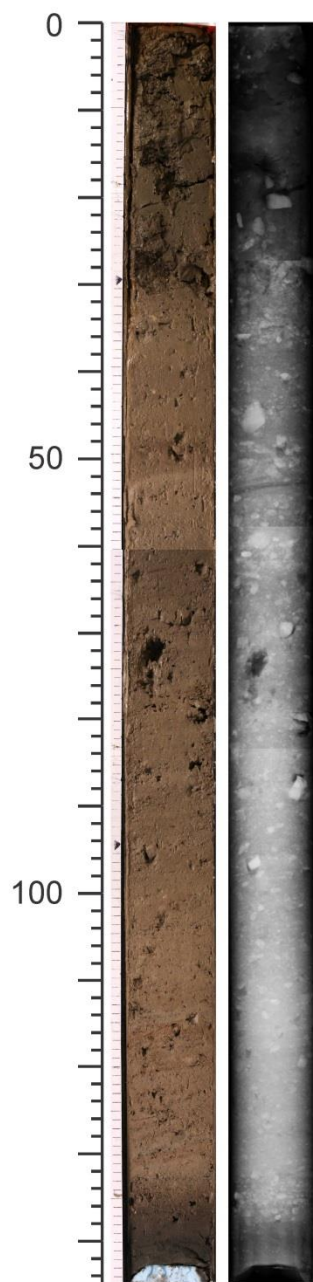


Figure 3.18b. Photography and X-radiography compilation for trigger weight core 2013029-060.

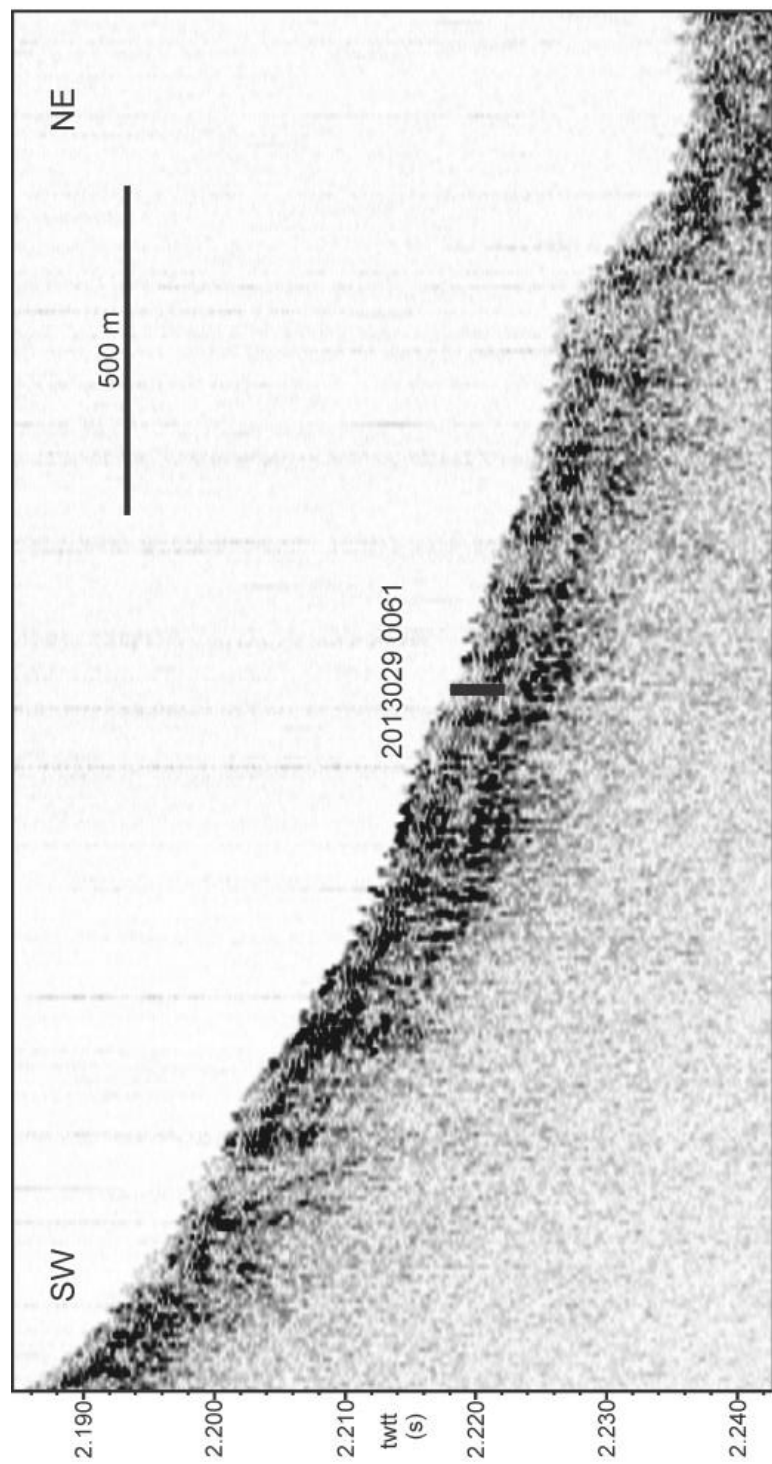


Figure 3.19. 3.5 kHz sub-bottom profile showing the acoustic stratigraphy and position of core 2013029-061.

Baffin Bay 2013029 Piston Core 061

TD 315 cm 71.919041N -70.458838 W Water depth 1635 m

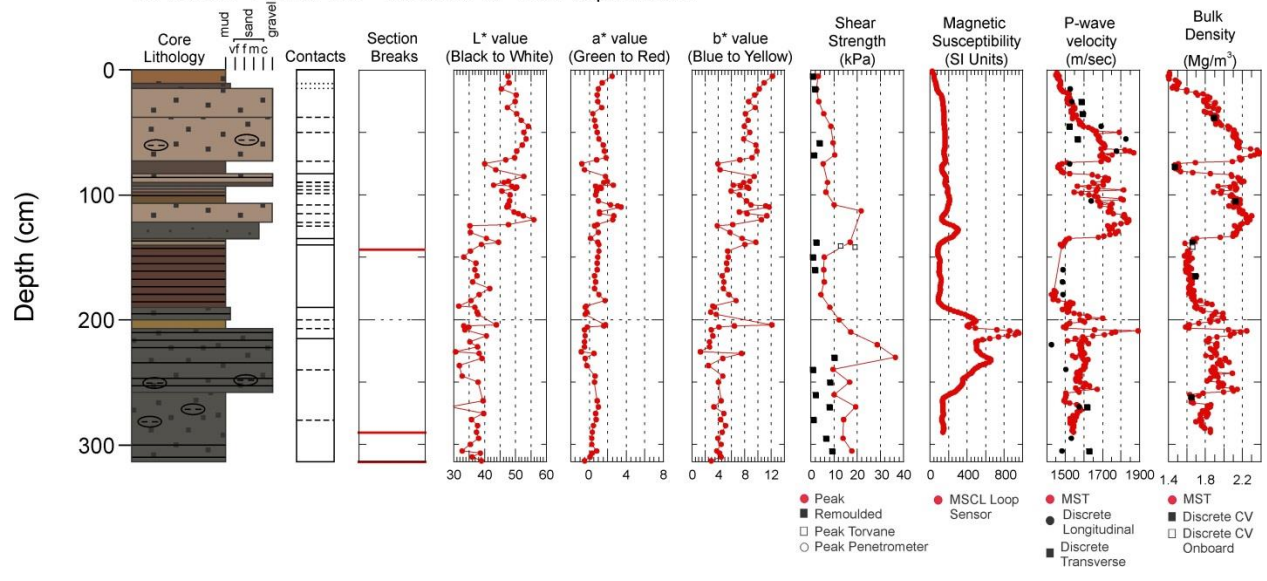


Figure 3.20a. Core plot summary for piston core 2013029-061.

Baffin Bay 2013029 Trigger Weight Core 061

TD 105 cm 71.919041 N -70.458838 W Water depth 1635 m

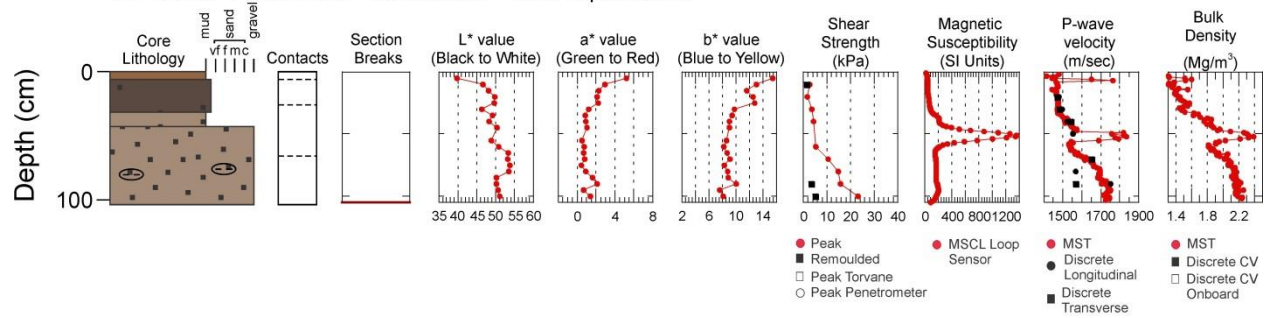


Figure 3.20b. Core plot summary for trigger weight core 2013029-061.

2013029 061 PC

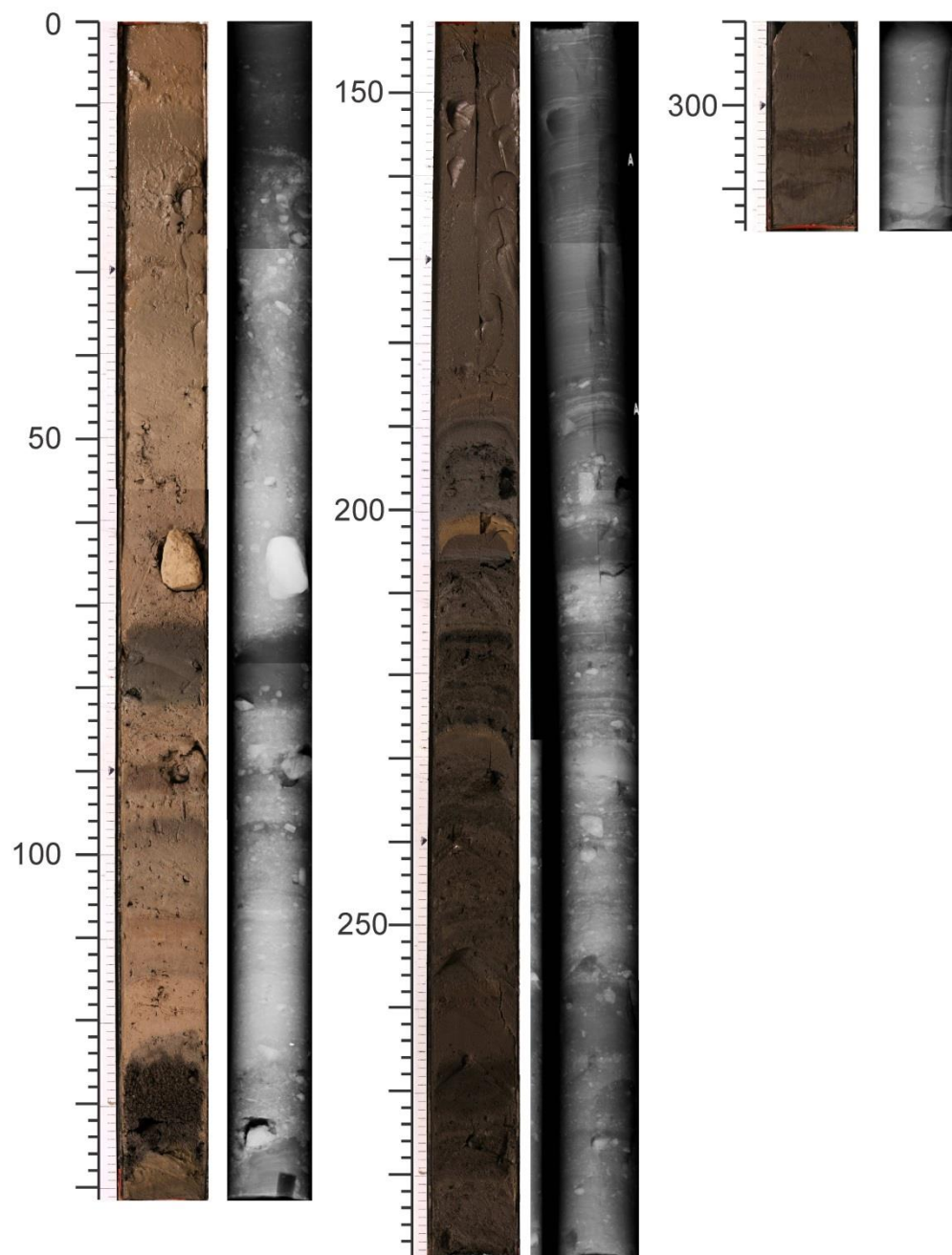


Figure 3.21a. Photography and X-radiography compilation for piston core 2013029-061.

2013029 061 TWC

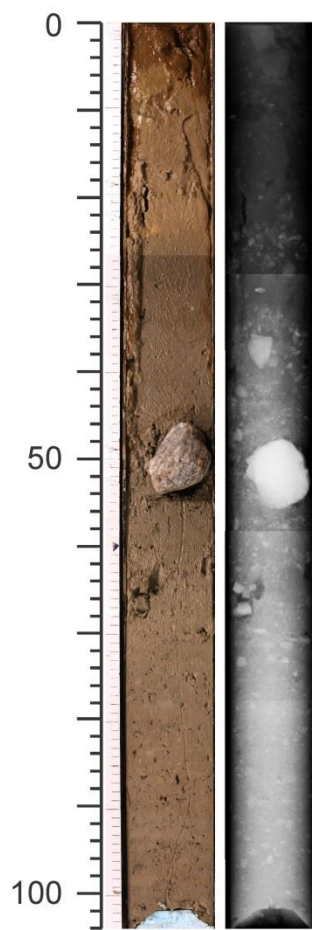


Figure 3.21b. Photography and X-radiography compilation for trigger weight core 2013029-061.

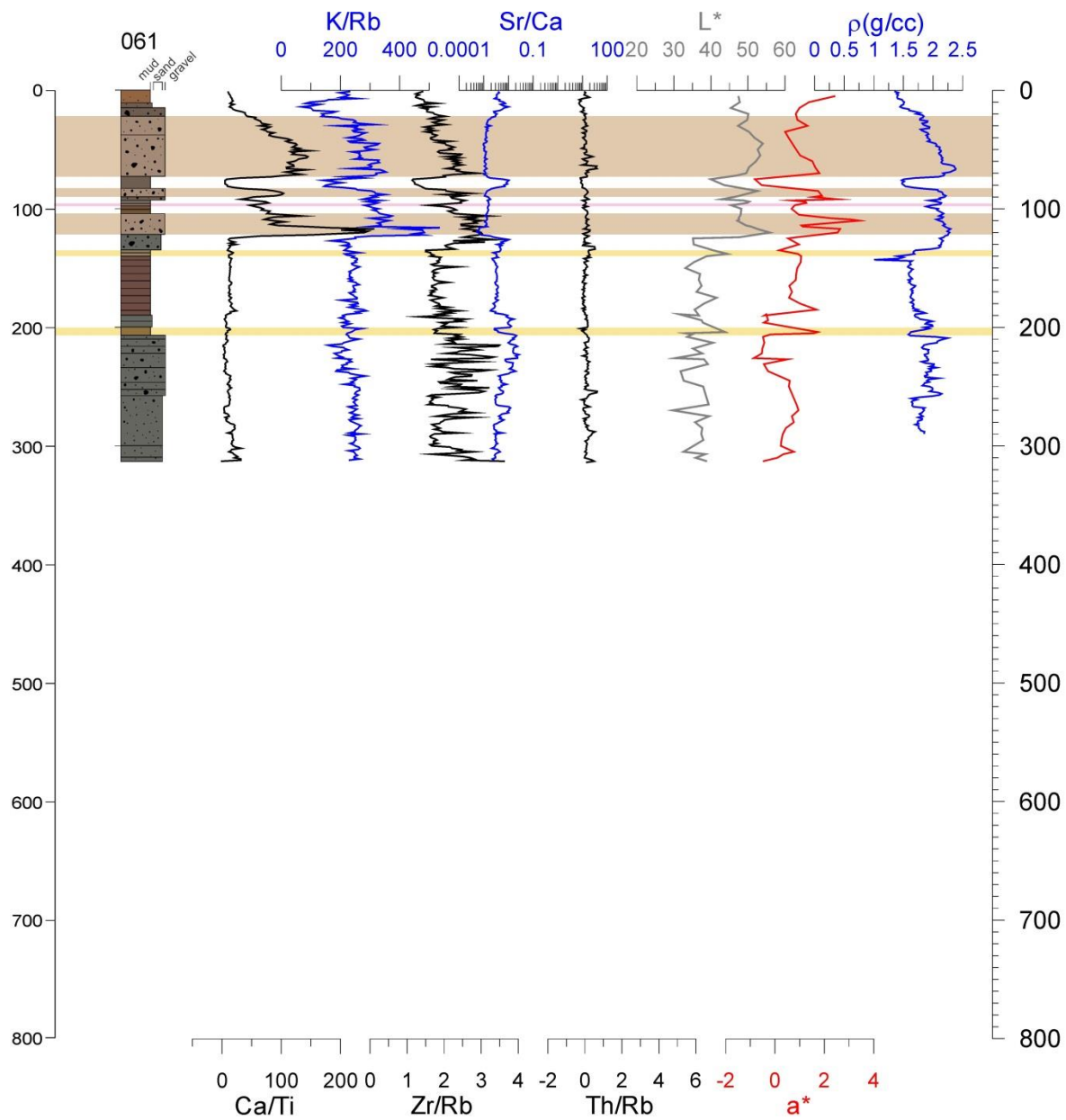


Figure 3.22. Down-core pXRF analysis for piston core 2013029-061. Tan highlighting indicates tan carbonate mud; rose highlighting indicates rose mud; gold brown highlighting indicates gold brown mud.

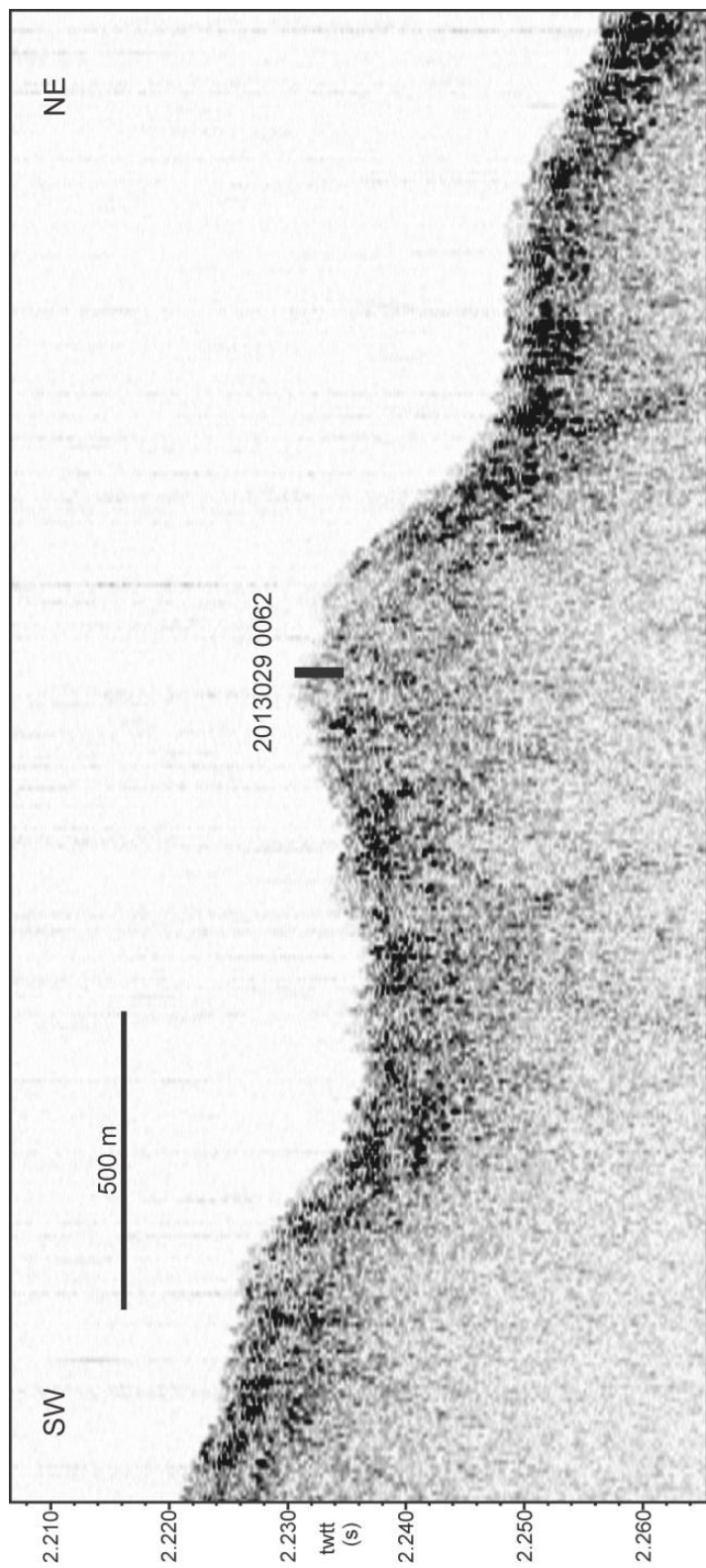


Figure 3.23. 3.5 kHz sub-bottom profile showing the acoustic stratigraphy and position of core 2013029-0062.

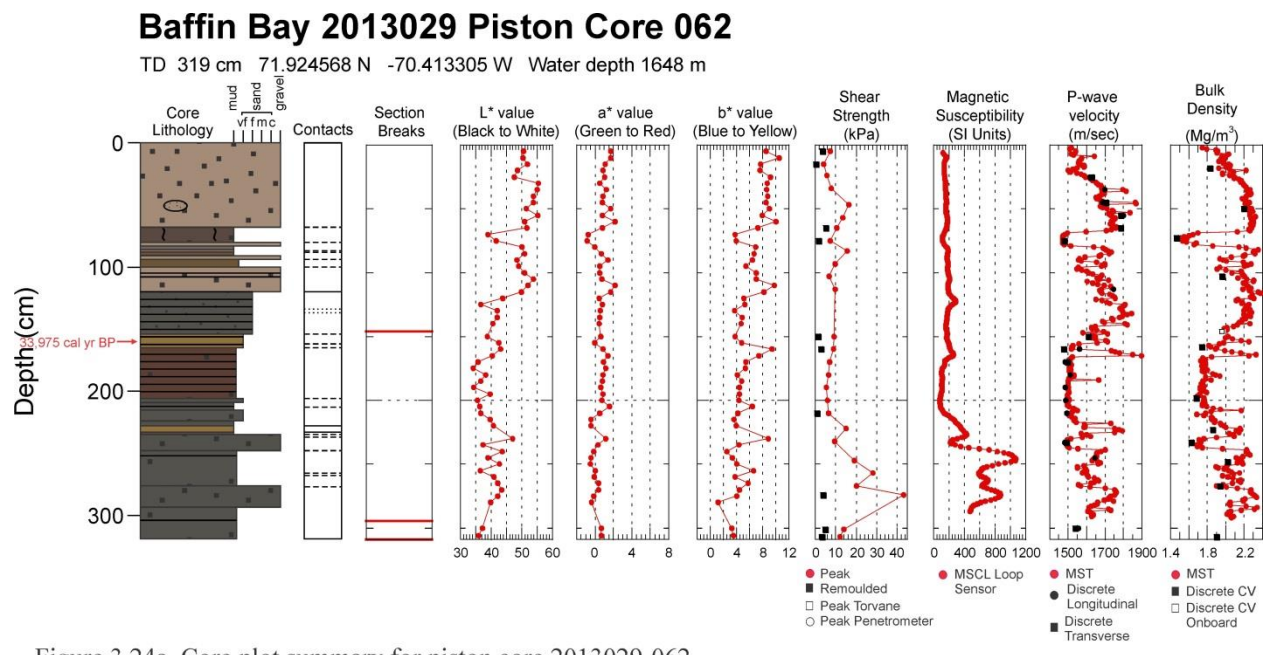


Figure 3.24a. Core plot summary for piston core 2013029-062.

Baffin Bay 2013029 Trigger Weight Core 062

TD 77 cm 71.924568 N -70.413305 W Water depth 1648 m

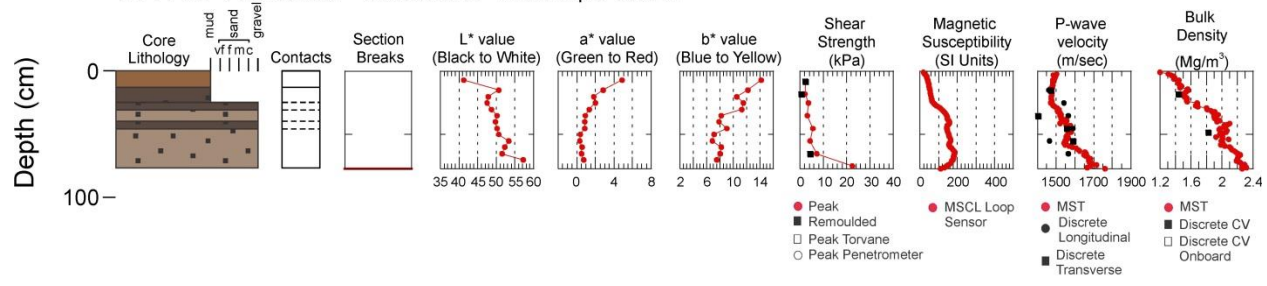


Figure 3.24b. Core plot summary for trigger weight core 2013029-062.

2013029 062 PC

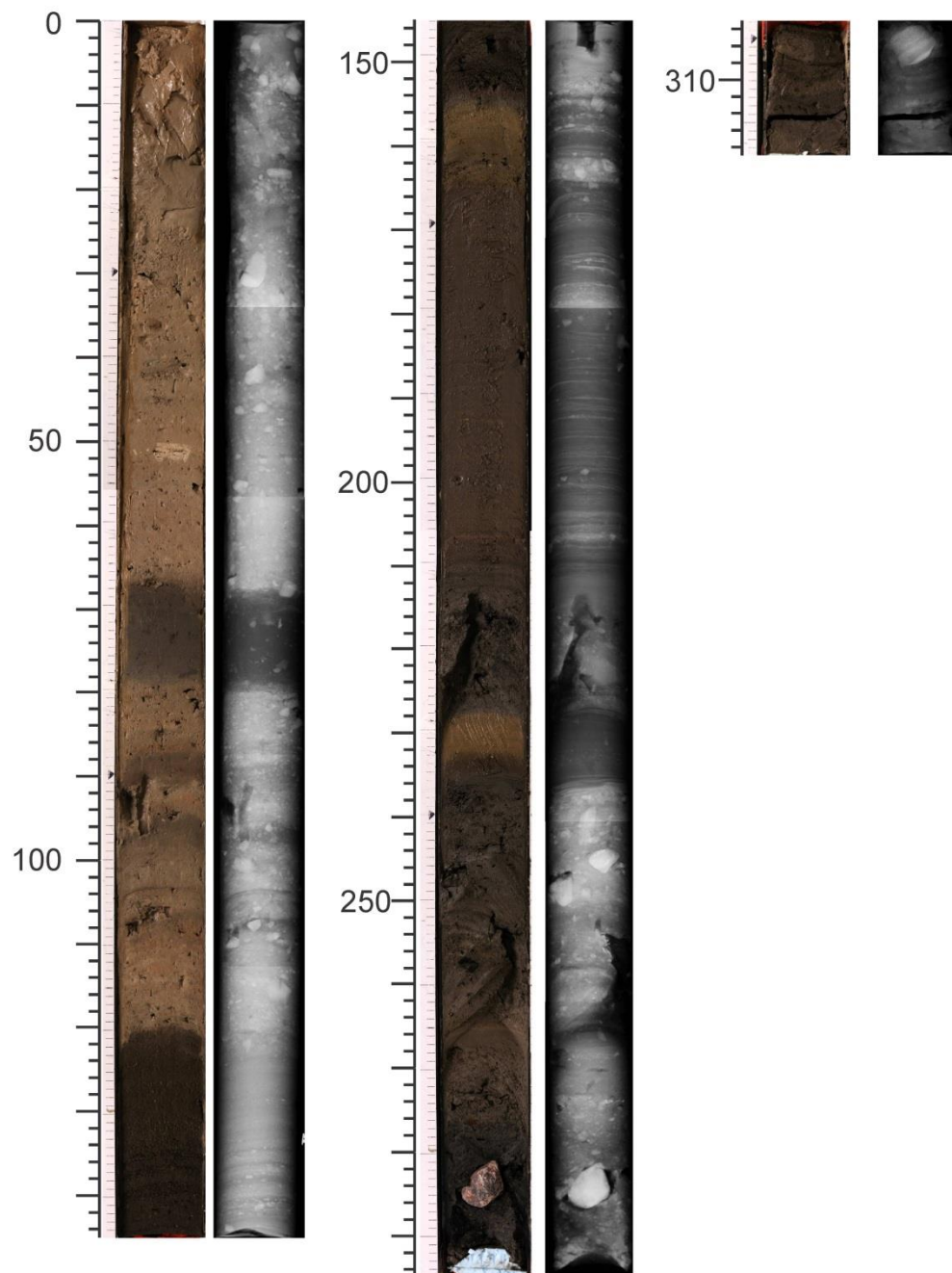


Figure 3.25a. Photography and X-radiography compilation for piston core 2013029-062.

2013029 062 TWC

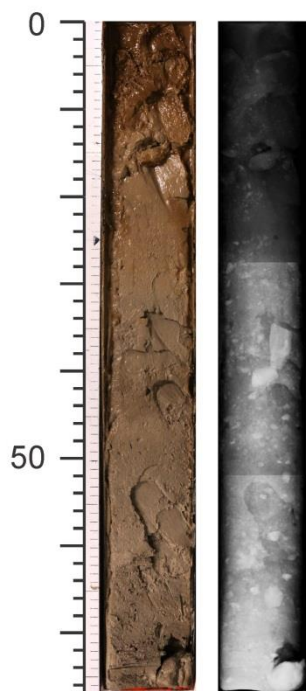


Figure 3.25b. Photography and X-radiography compilation for trigger weight core 2013029-062.

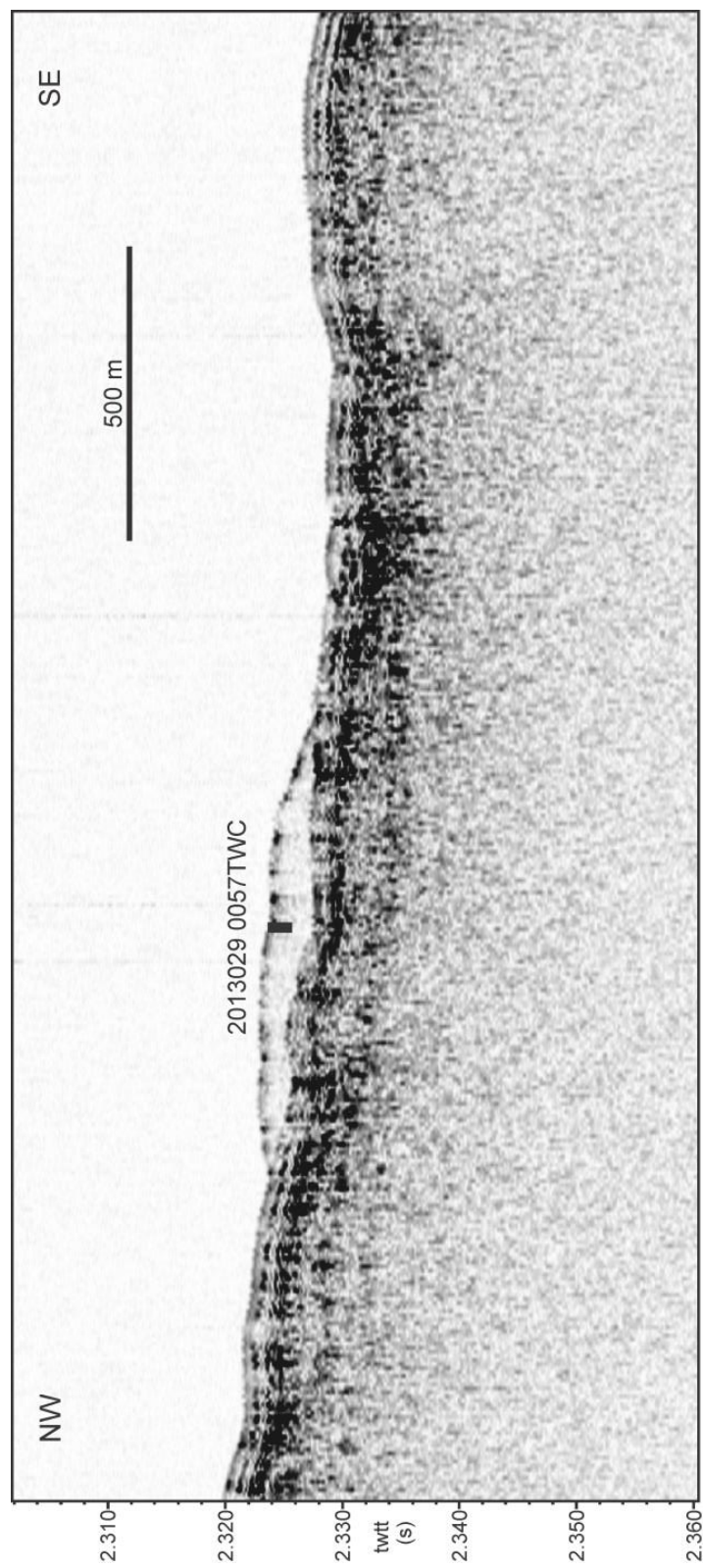


Figure 3.26. 3.5 kHz sub-bottom profile showing the acoustic stratigraphy and position of core 2013029-057.

Baffin Bay 2013029 Piston Core 057

TD 31.5 cm 71.701388 N -69.148798 W Water depth 1713 m

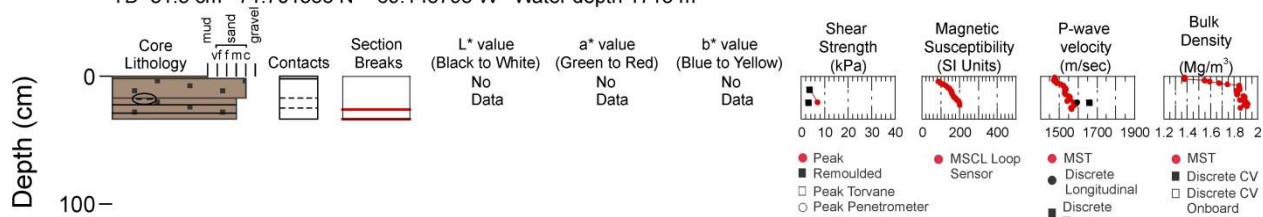


Figure 3.27a. Core plot summary for piston core 2013029-057.

Baffin Bay 2013029 Trigger Weight Core 057

TD 153 cm 71.701388 N -69.148798 W Water depth 1713 m

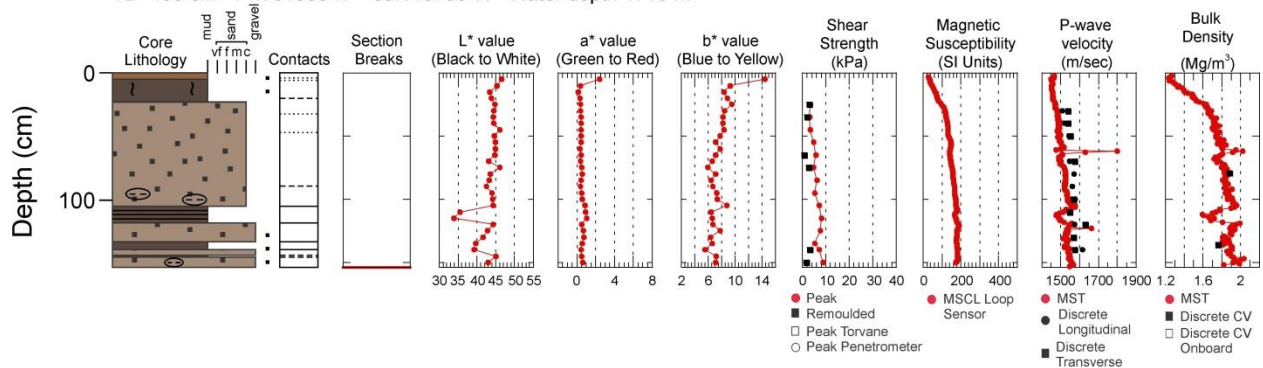


Figure 3.27b. Core plot summary for trigger weight core 2013029-057.

2013029 057 PC

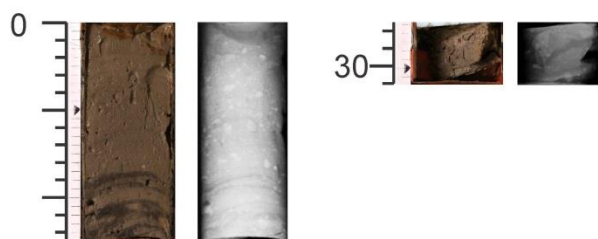


Figure 3.28a. Photography and X-radiography compilation for piston core 2013029-057.

2013029 057 TWC



Figure 3.28b. Photography and X-radiography compilation for trigger weight core 2013029-057.

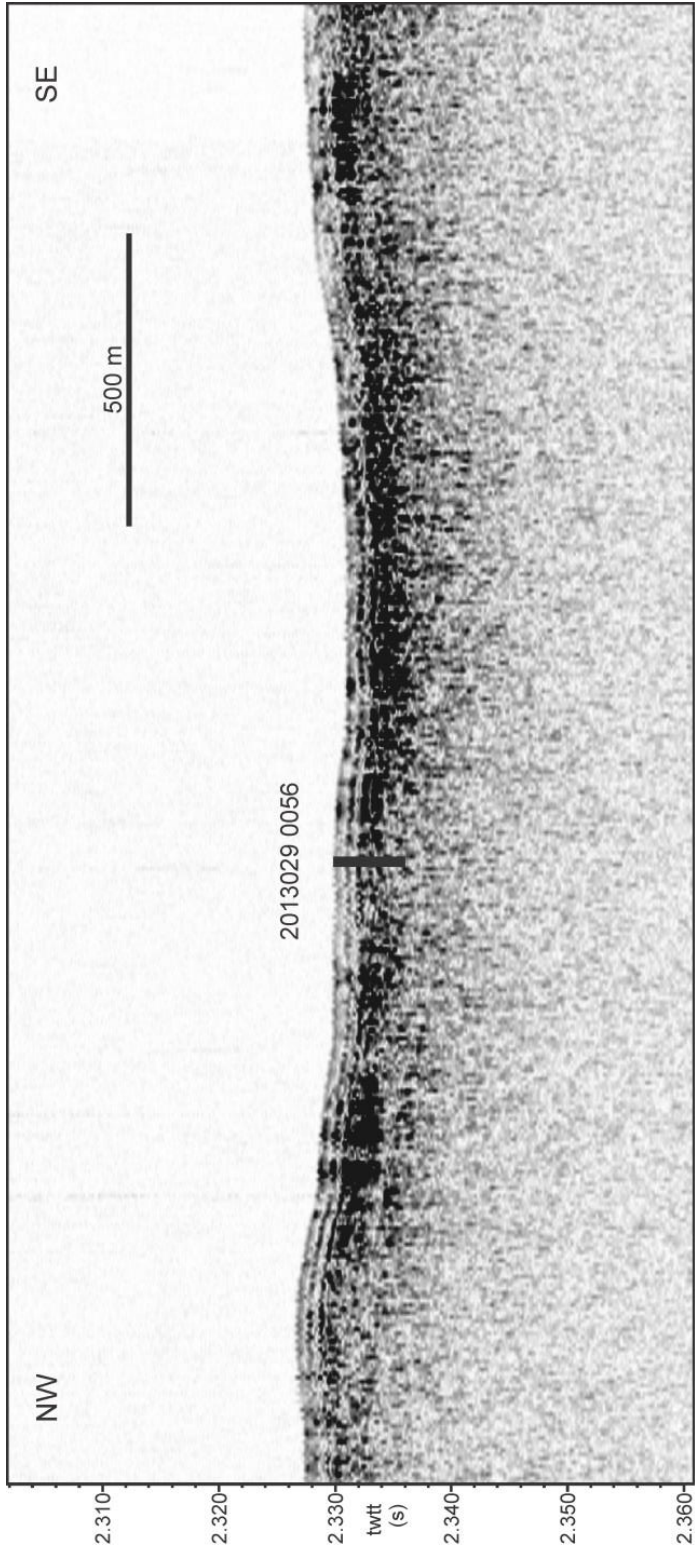


Figure 3.29. 3.5 kHz sub-bottom profile showing the acoustic stratigraphy and position of core 2013029-0056.

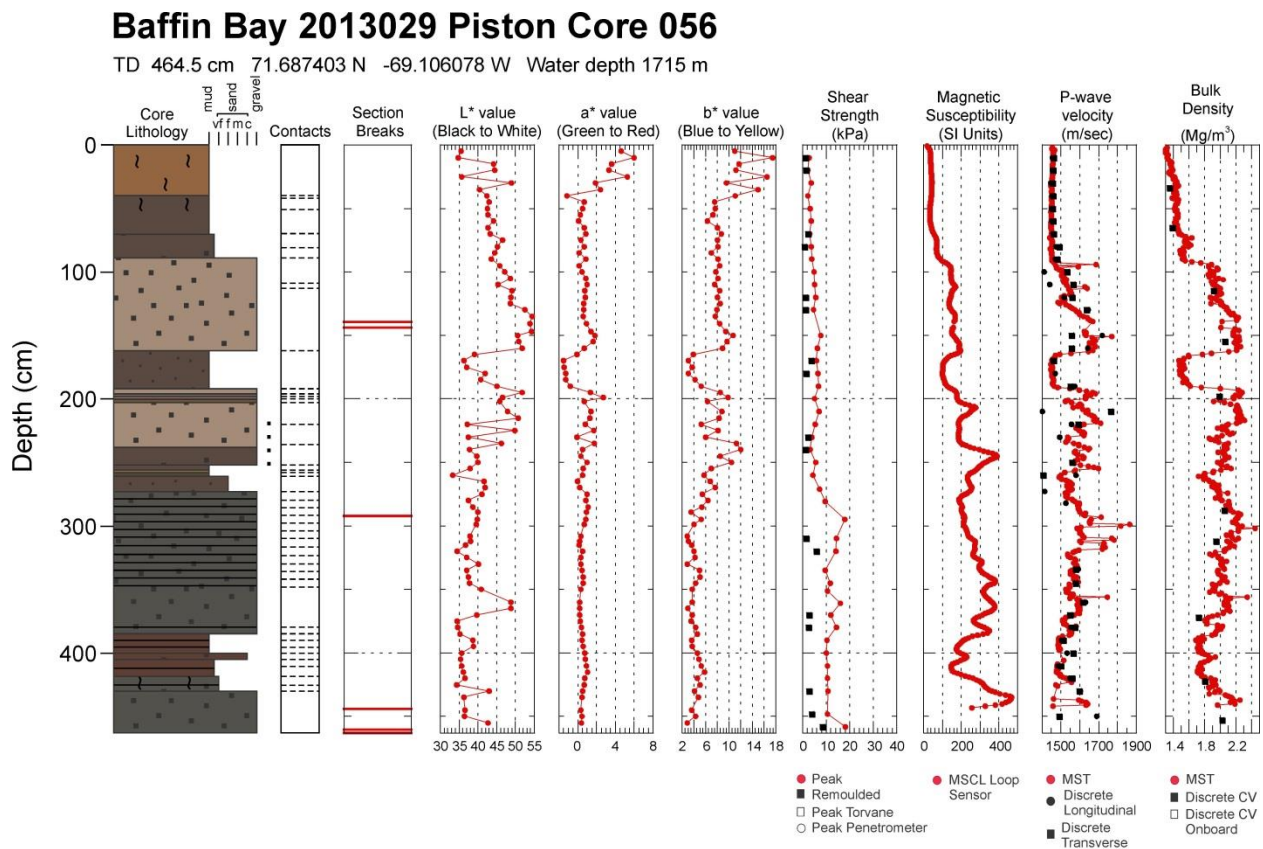


Figure 3.30a. Core plot summary for piston core 2013029-056.

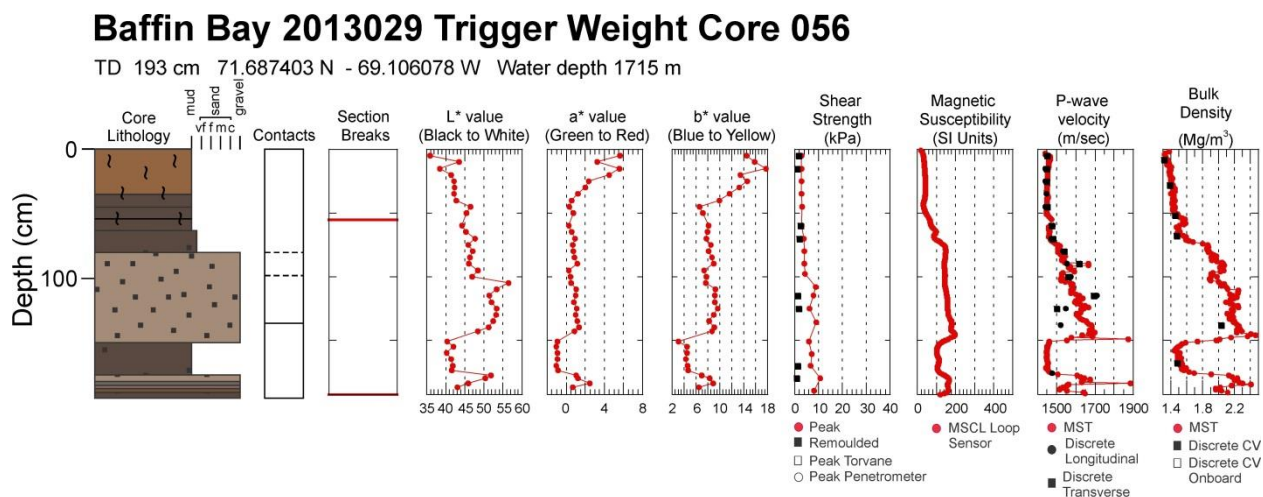


Figure 3.30b. Core plot summary for trigger weight core 2013029-056.

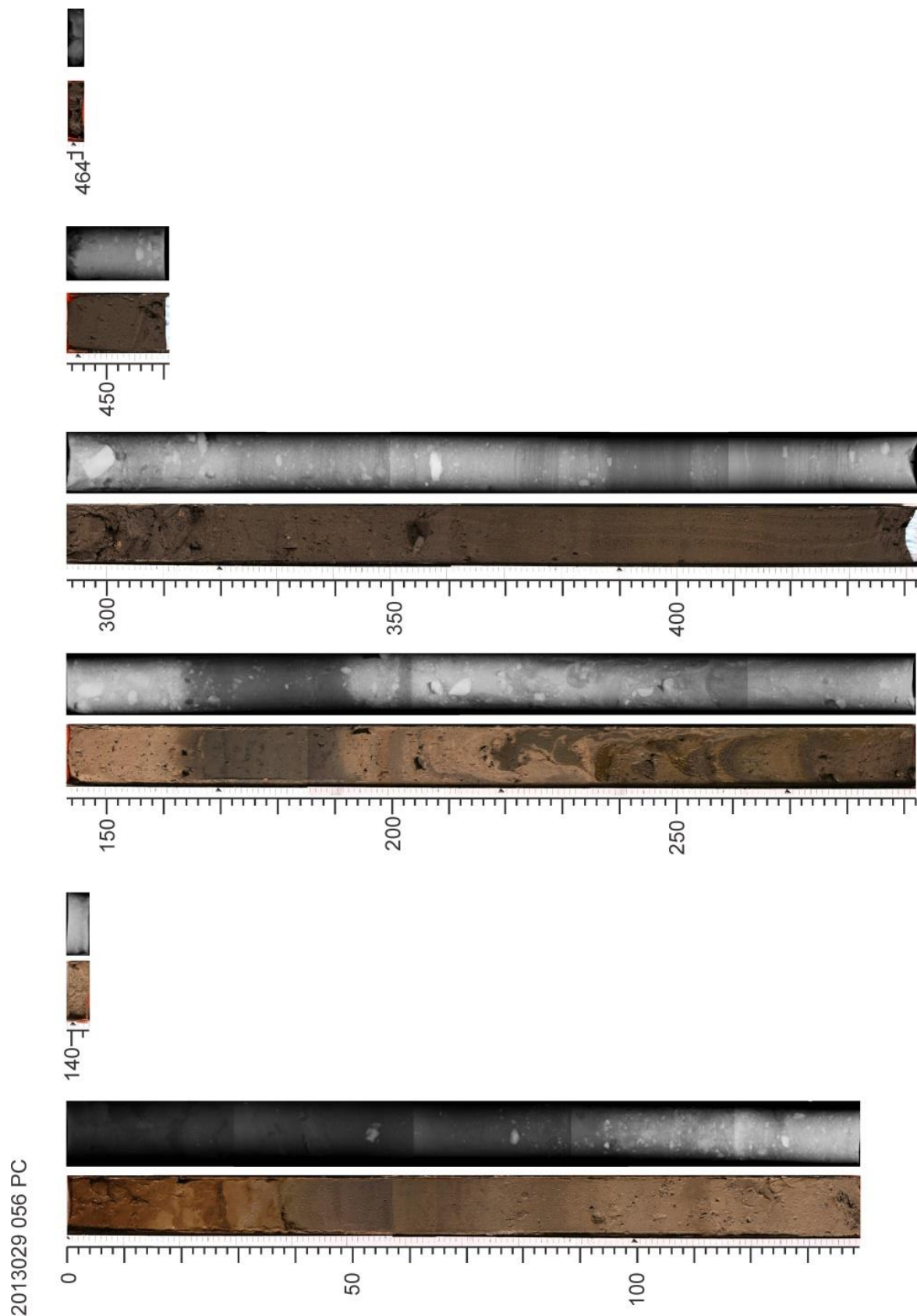


Figure 3.31a. Photography and X-radiography compilation for piston core 2013029-056.

2013029 056 TWC

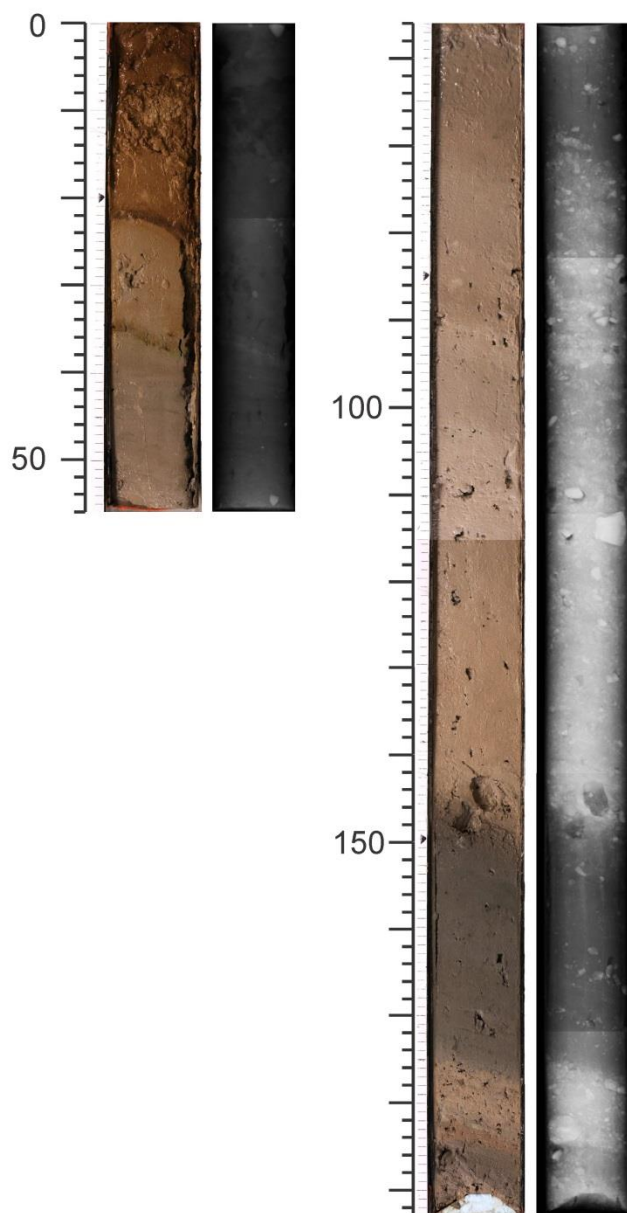


Figure 3.31b. Photography and X-radiograph compilation for trigger weight core 2013029-056.

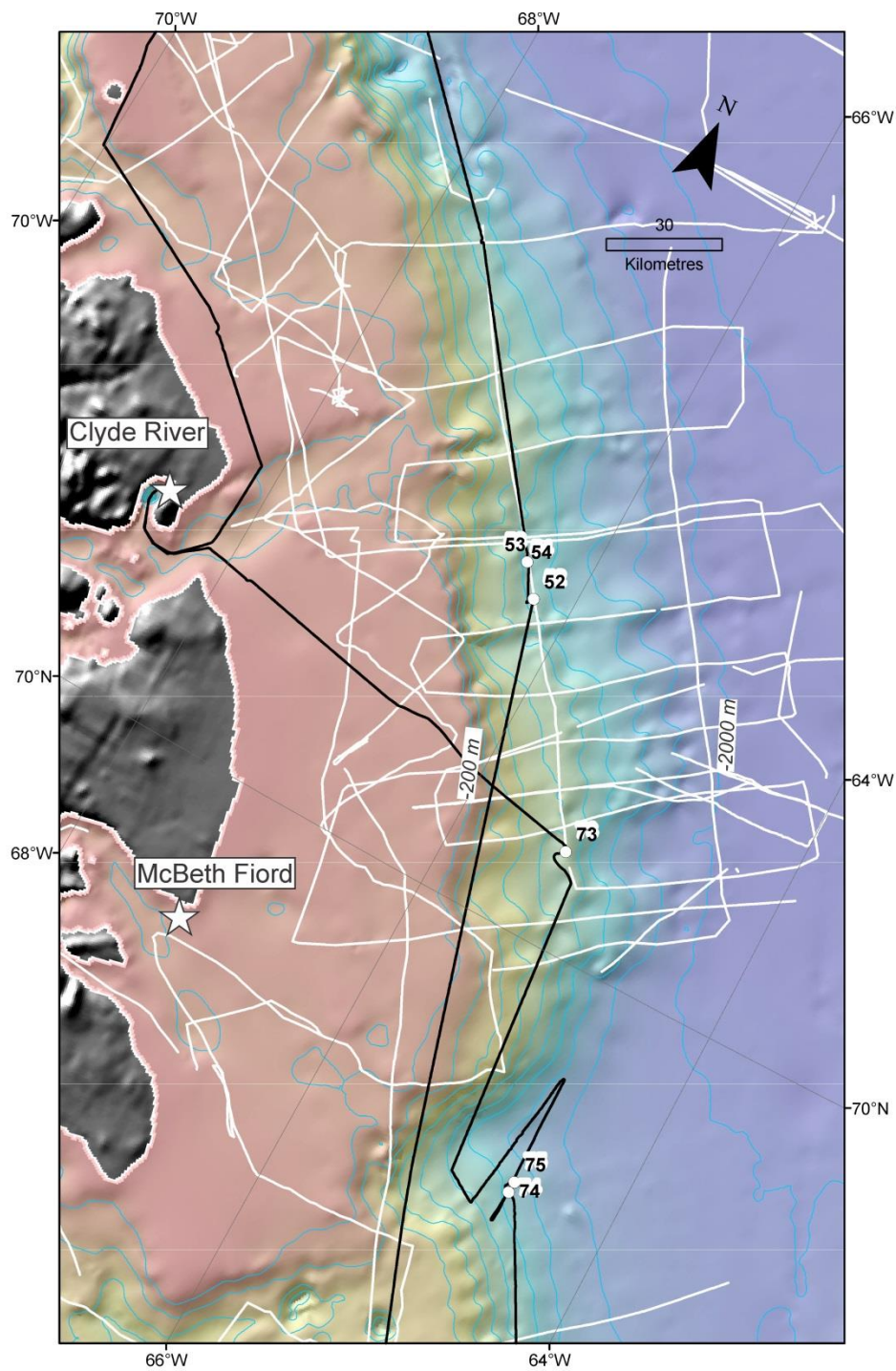


Figure 3.32. Regional map showing core locations and seismic coverage for the Clyde River region. 2013029 core locations are indicated by white circles and 2013029 sub-bottom profiler coverage by black lines. White lines indicate high resolution seismic reflection profiles collected by the GSC prior to the 2013 expedition. Bathymetric contour interval is 200 m.

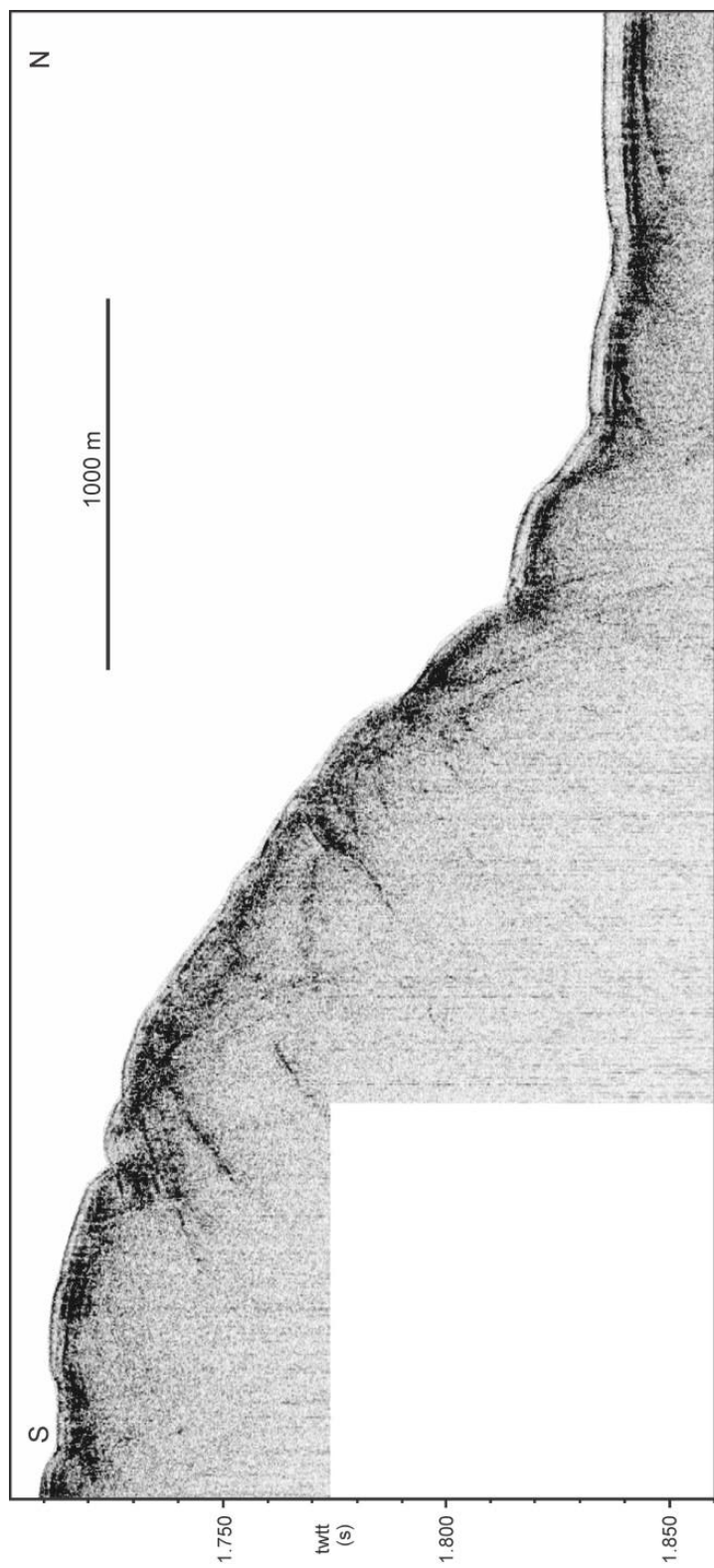


Figure 3.33. 3.5 kHz sub-bottom profile showing the regional acoustic facies of the Clyde River slope region.

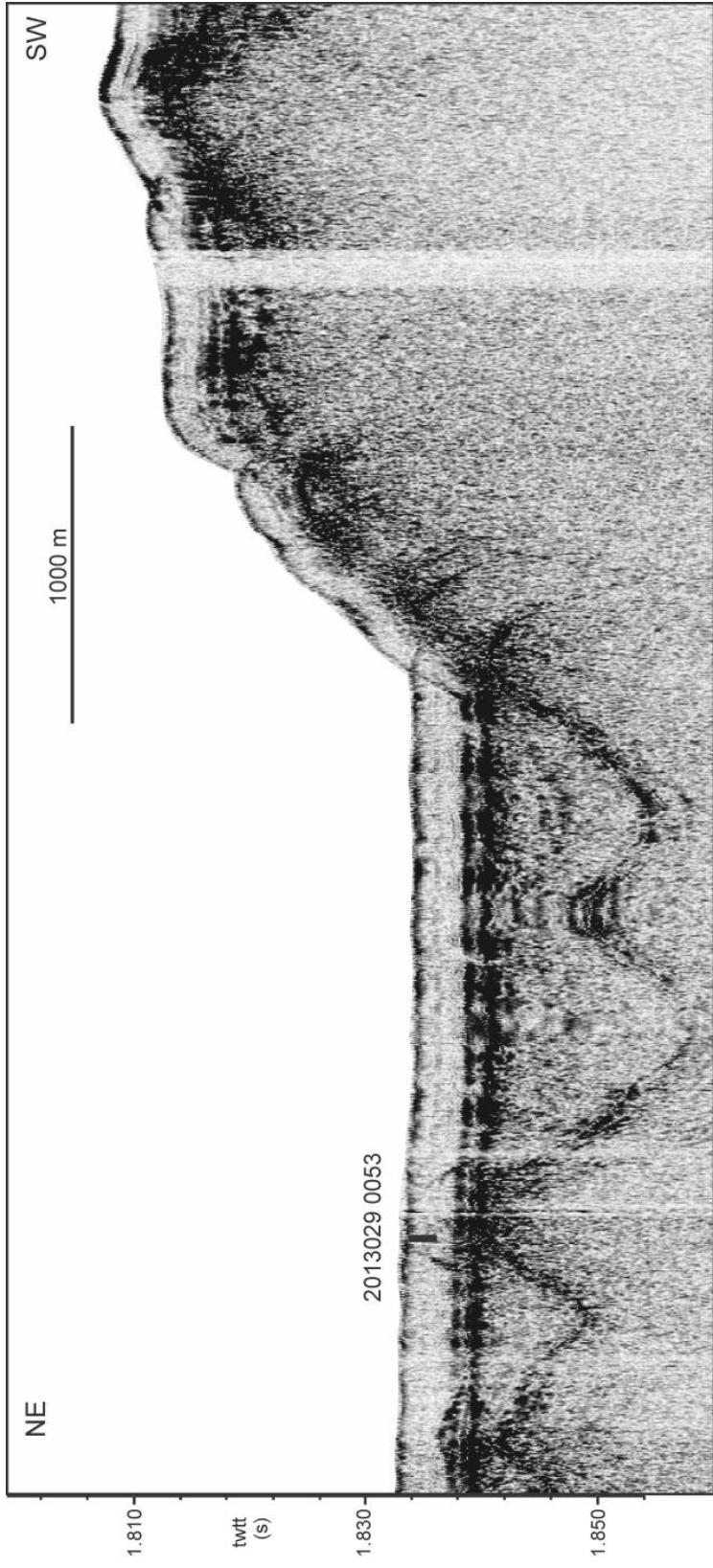


Figure 3.34. 3.5 kHz sub-bottom profile showing the acoustic stratigraphy and position of core 2013029-0053.

Baffin Bay 2013029 Trigger Weight Core 053

TD 165.0 cm 71.696770 N -66.395751 W Water depth 1349 m

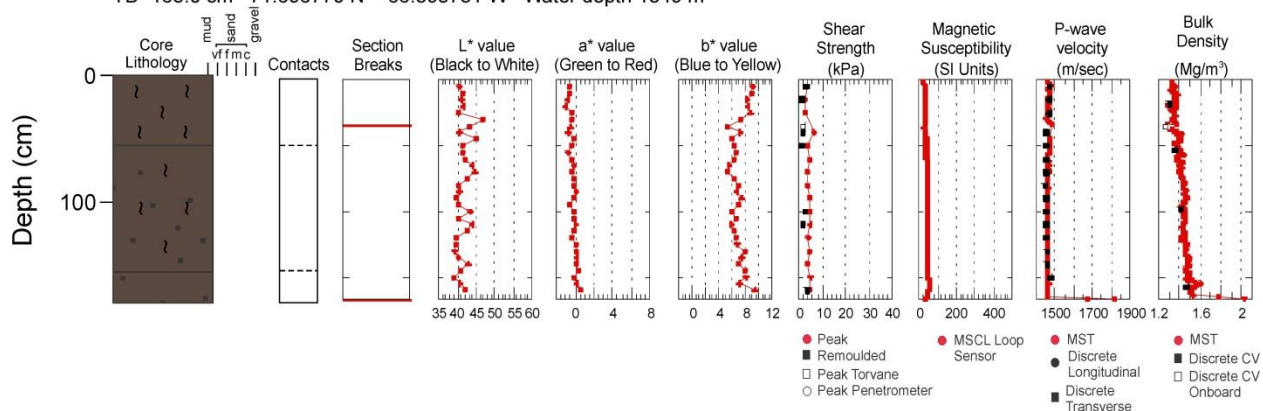


Figure 3.35a. Core plot summary for trigger weight core 2013029-052.

2013029 053 TWC

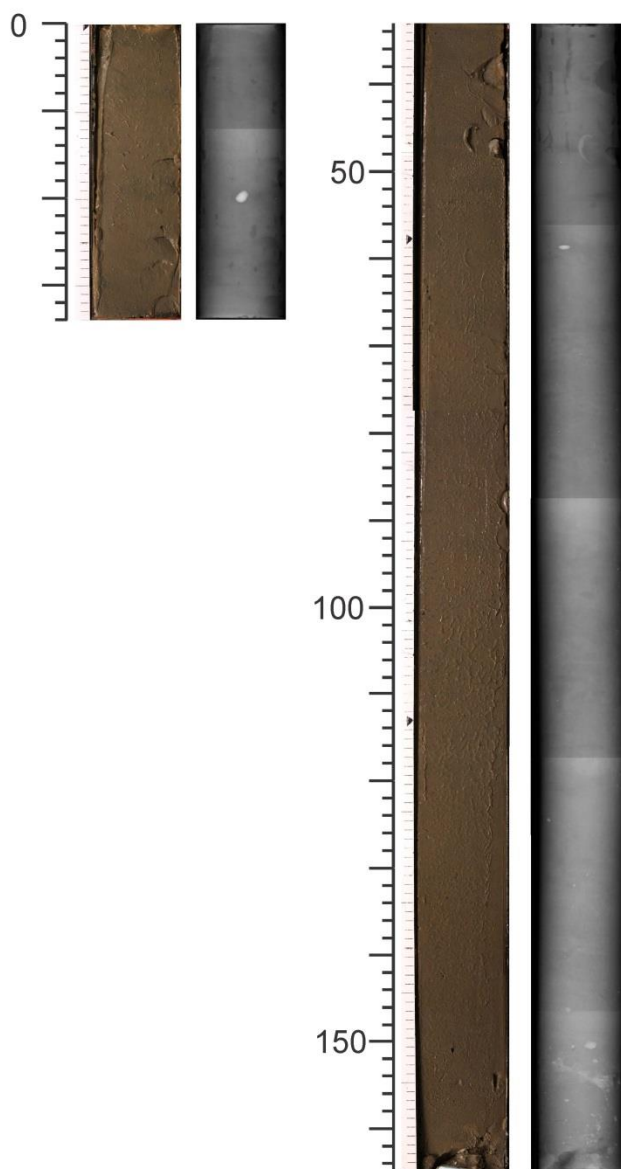


Figure 3.35b. Photography and X-radiography compilation for trigger weight core 2013029-053.

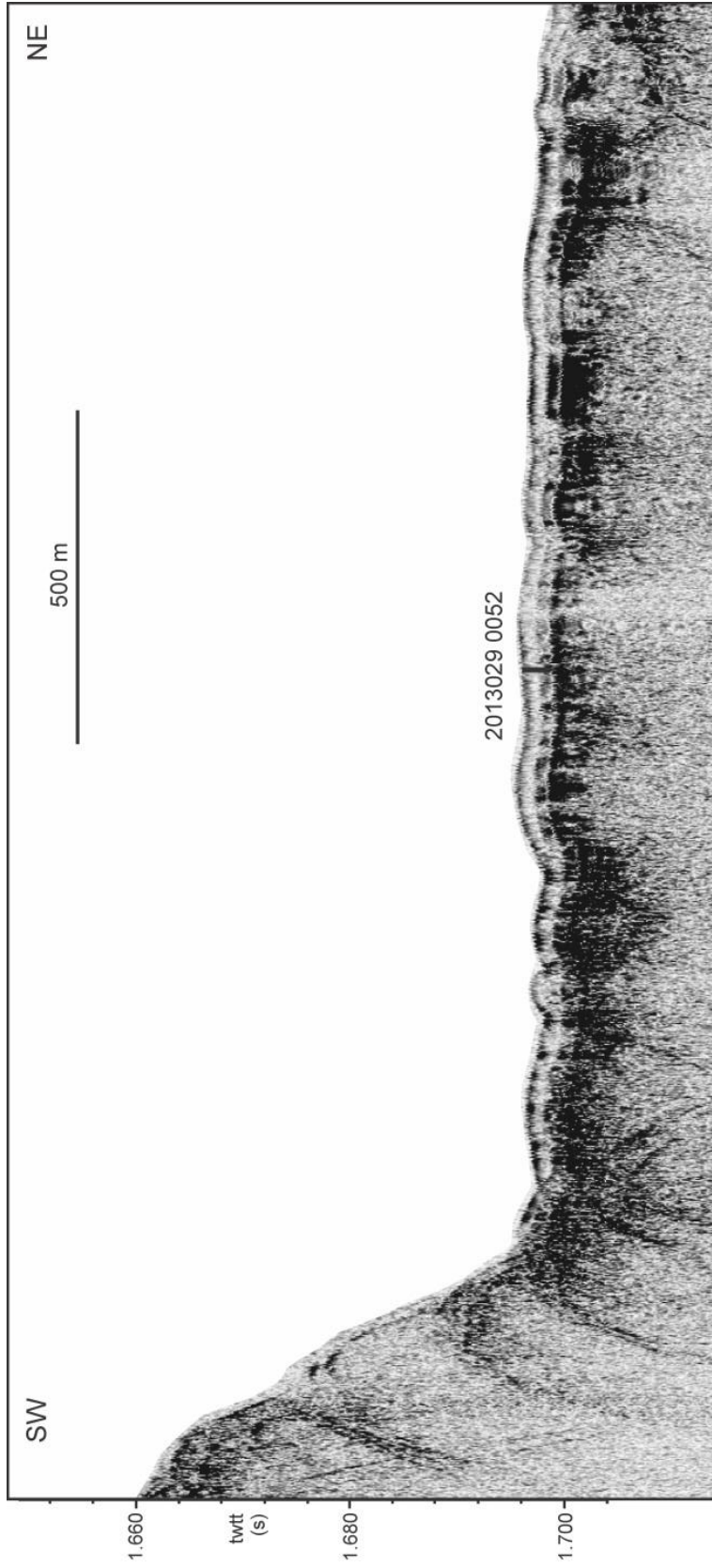


Figure 3.36. 3.5 kHz sub-bottom profile showing the acoustic stratigraphy and position of core 2013029-052.

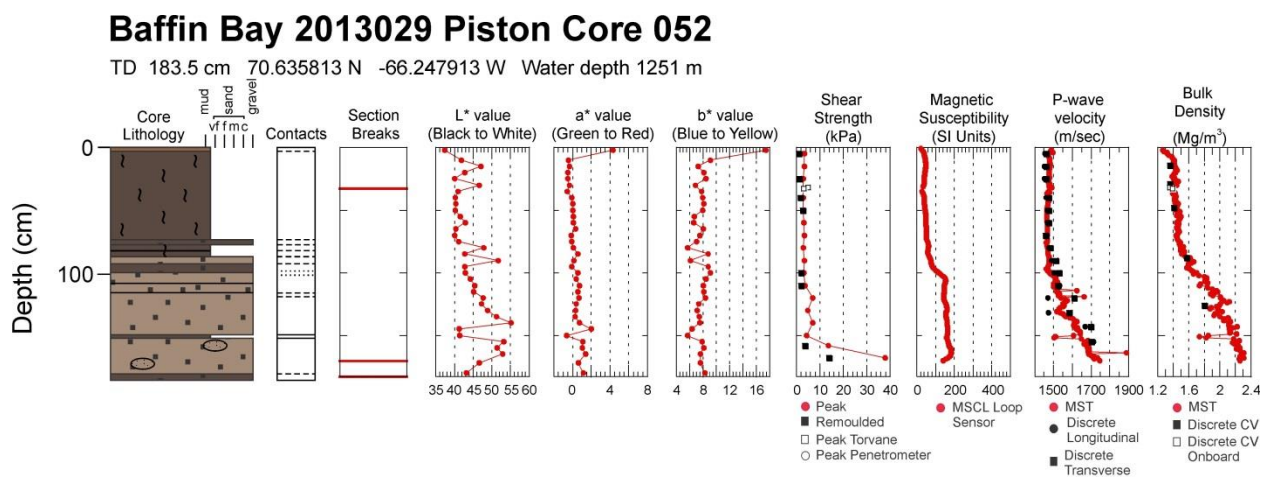


Figure 3.37a. Core plot summary for piston core 2013029-052.

Baffin Bay 2013029 Trigger Weight Core 052

TD 165 cm 70.635813 N -66.247913 W Water depth 1251 m

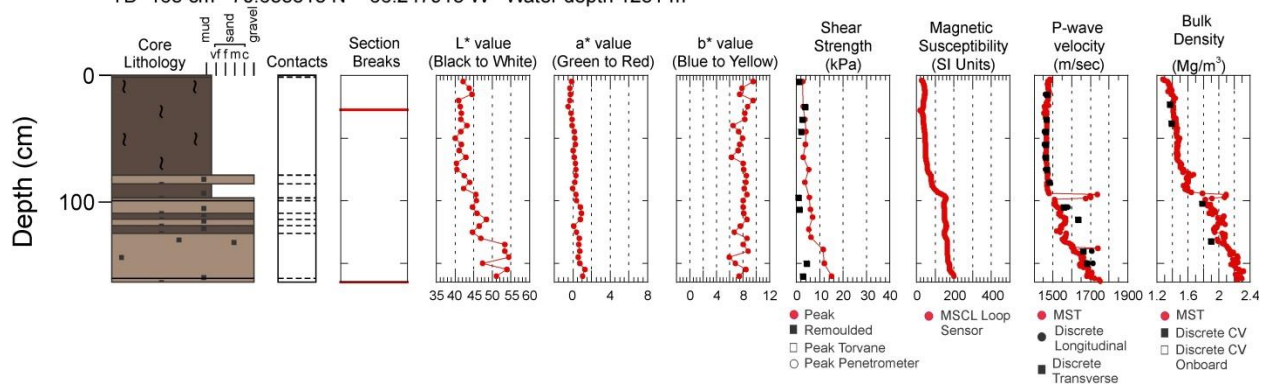


Figure 3.37b. Core plot summary for trigger weight core 2013029-052.

2013029 052 PC

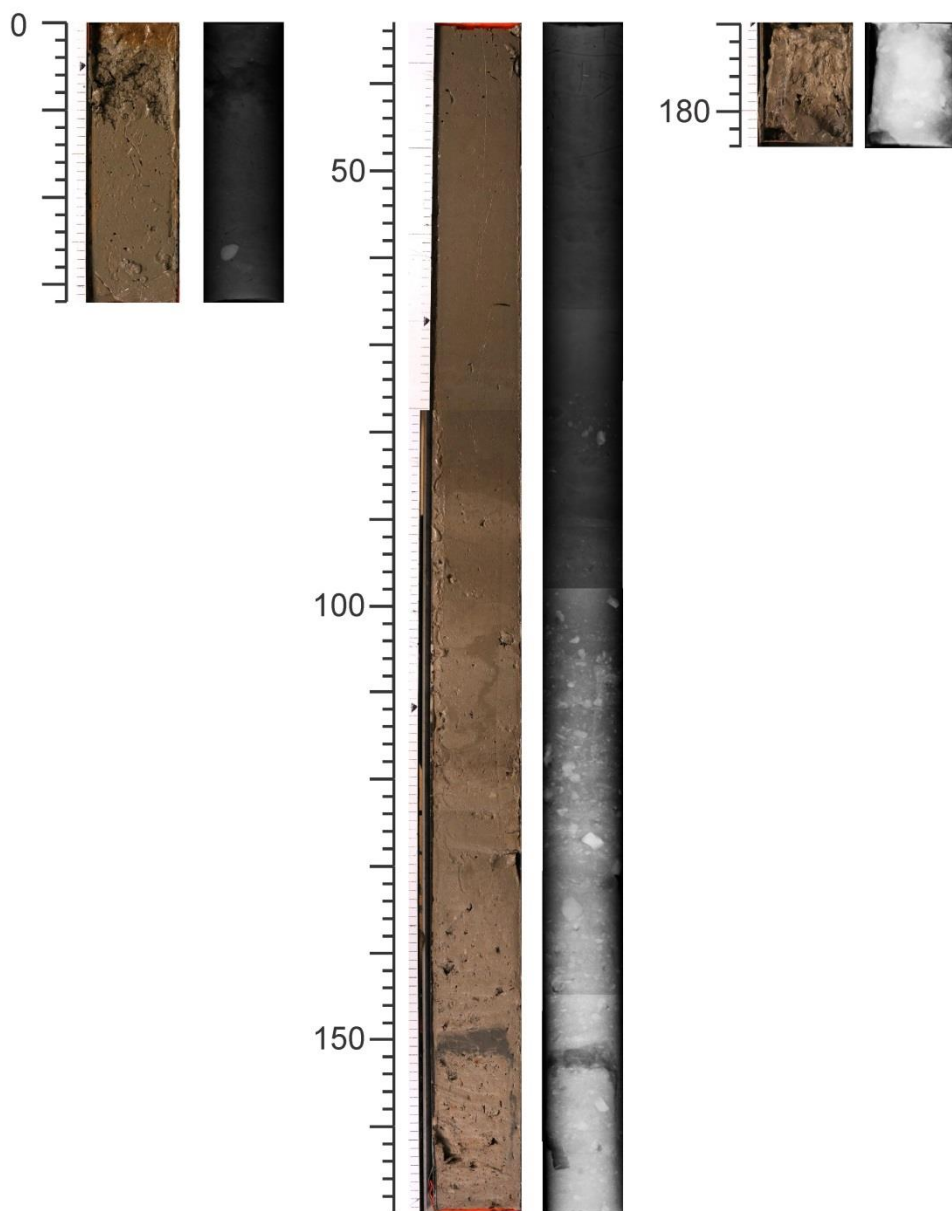


Figure 3.38a. Photography and X-radiography compilation for piston core 2013029-052.

2013029 052 TWC

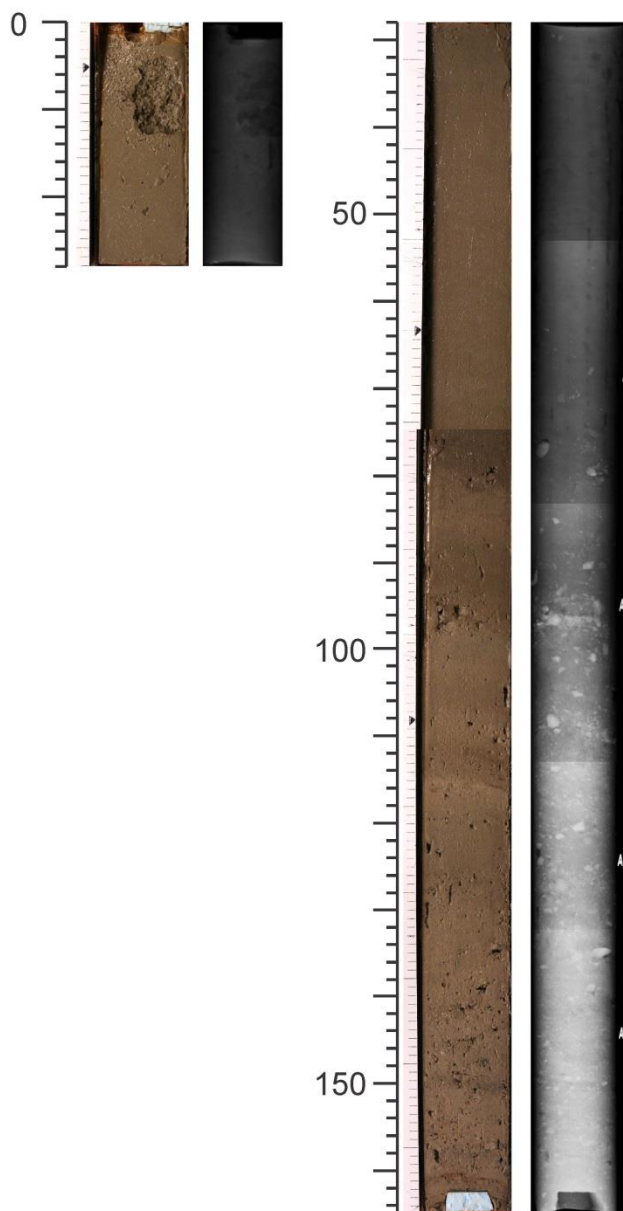


Figure 3.38b. Photography and X-radiography compilation for trigger weight core 2013029-052.

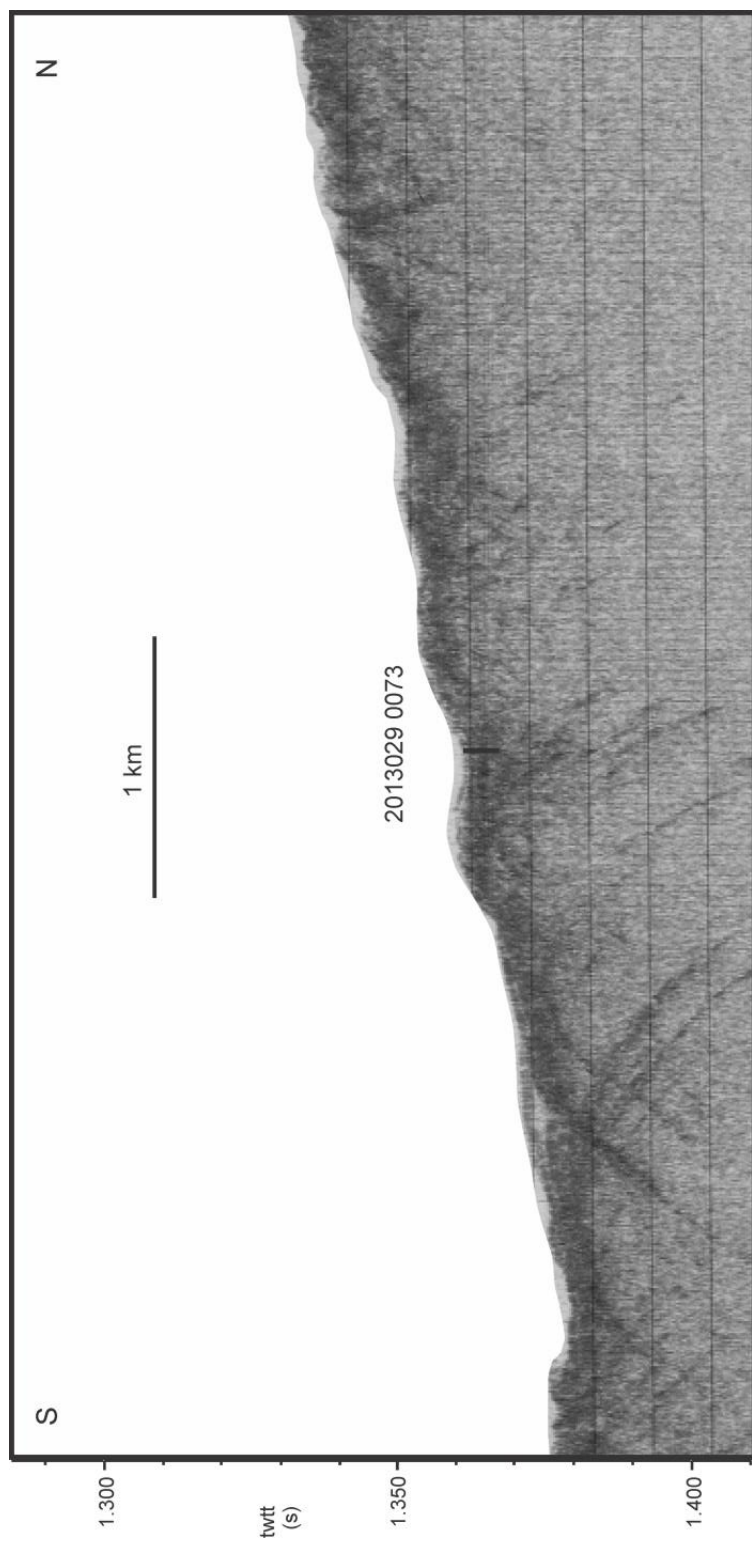


Figure 3.39. 3.5 kHz sub-bottom profile showing the acoustic stratigraphy and position of core 2013029-073.

Baffin Bay 2013029 Piston Core 073

TD 428 cm 70.208068 N -65.320780 W Water depth 1022 m

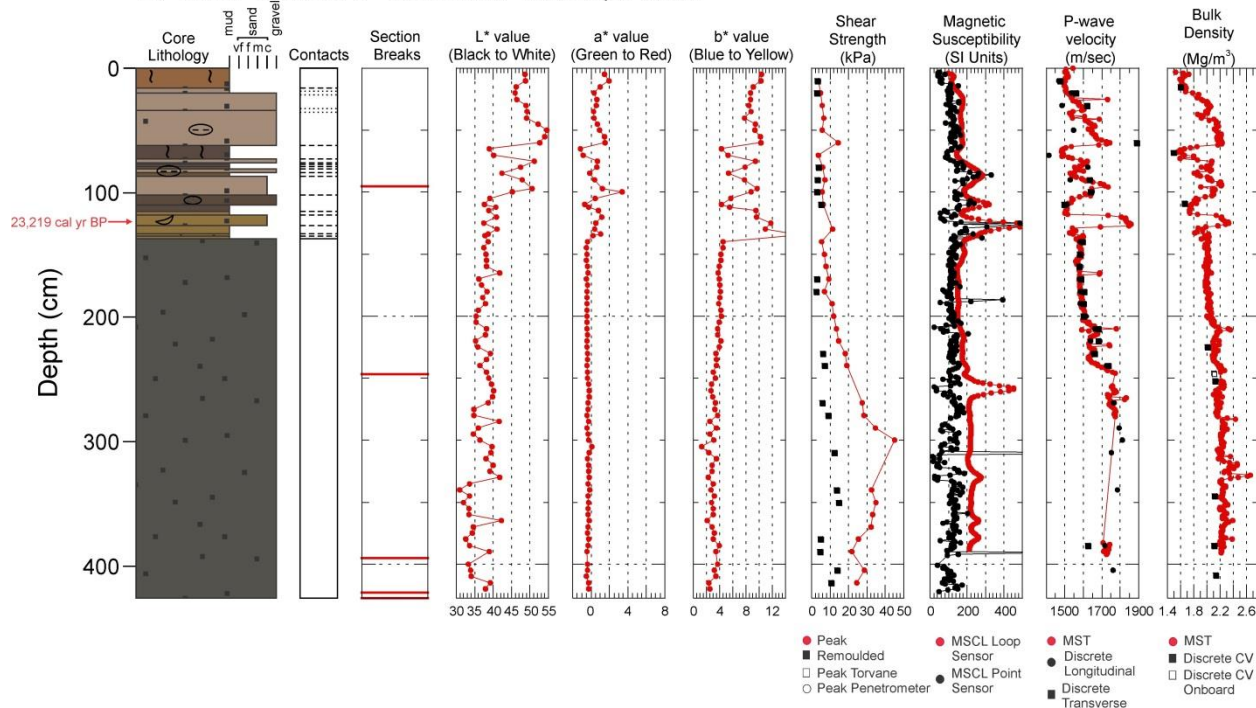


Figure 3.40a. Core plot summary for piston core 2013029-073.

Baffin Bay 2013029 Trigger Weight Core 073

TD 91 cm 70.208068 N -65.320780 W Water depth 1022 m

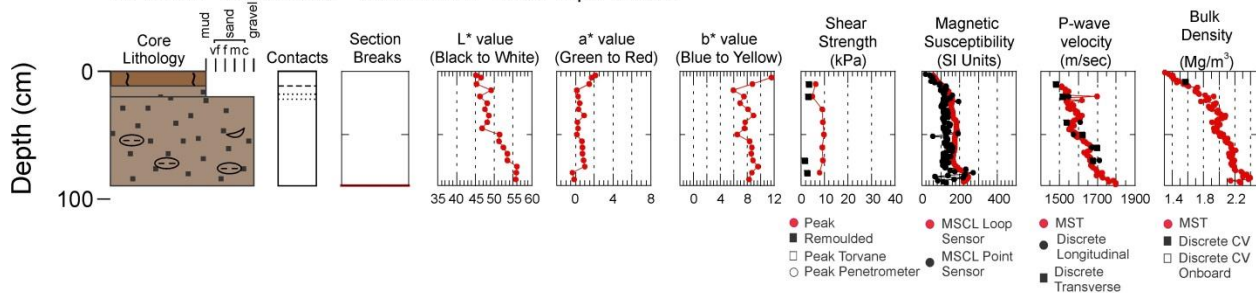


Figure 3.40b. Core plot summary for trigger weight core 2013029-073.

2013029 073 PC

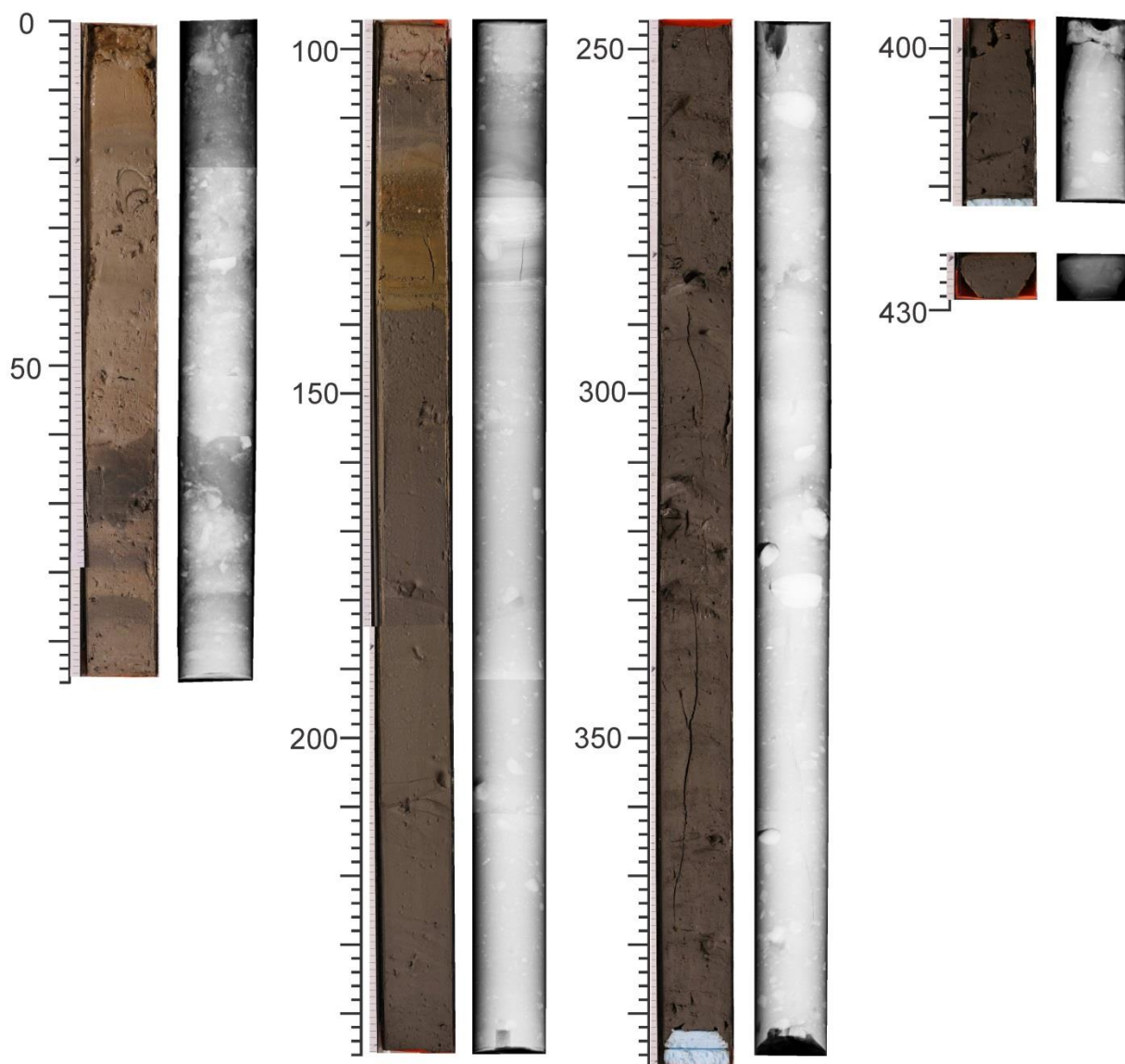


Figure 3.41a. Photography and X-radiography compilation for piston core 2013029-073.

2013029 073 TWC

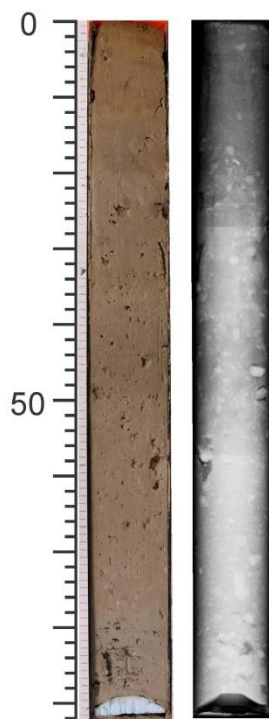


Figure 3.41b. Photography and X-radiography compilation for trigger weight core 2013029-073.

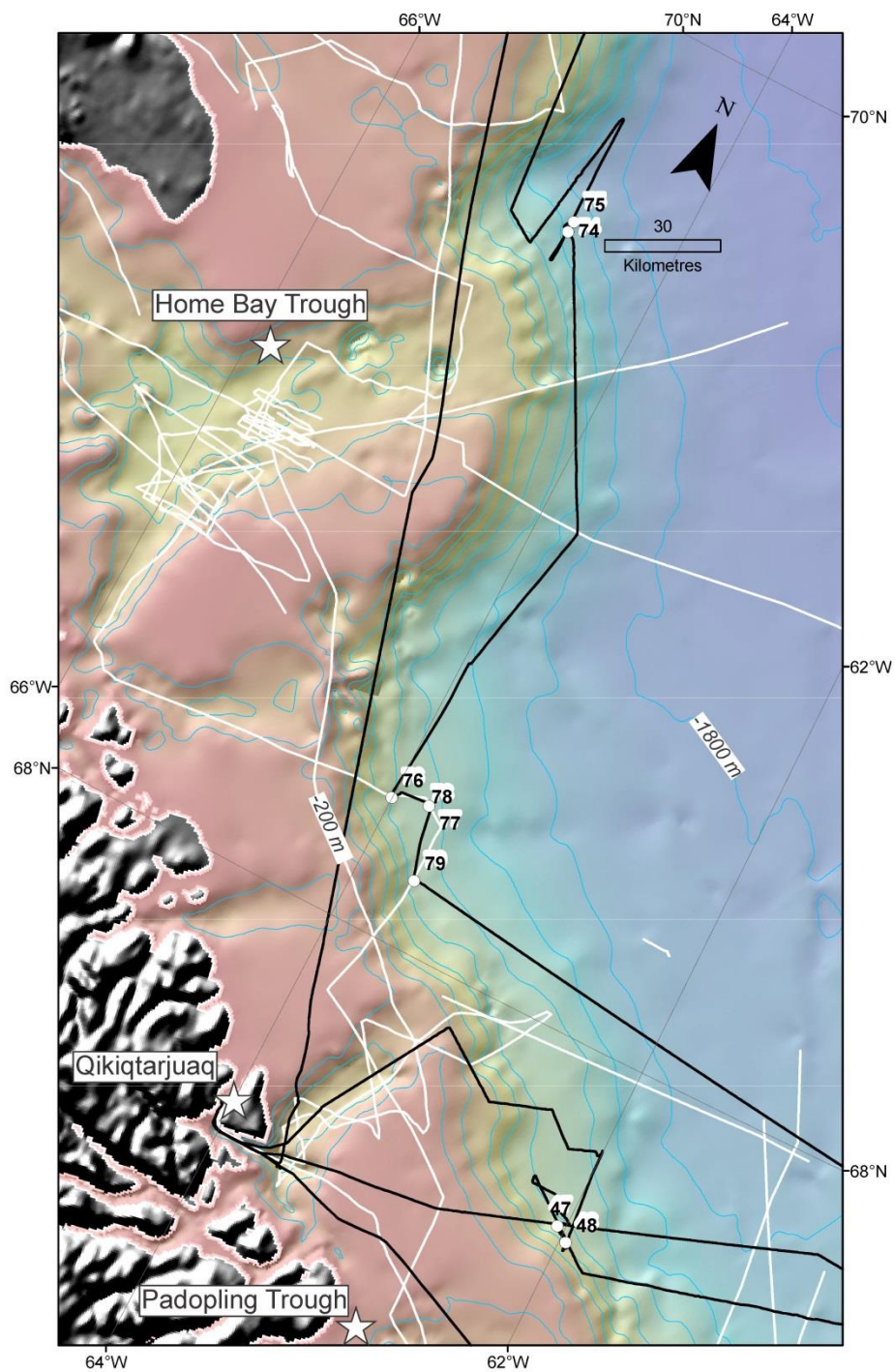


Figure 3.42. Regional map showing core locations and seismic coverage for the Home Bay region. 2013029 core locations are indicated by white circles and 2013029 sub-bottom profiler coverage by black lines. White lines indicate high resolution seismic reflection profiles collected by the GSC prior to the 2013 expedition. Bathymetric contour interval is 200 m.

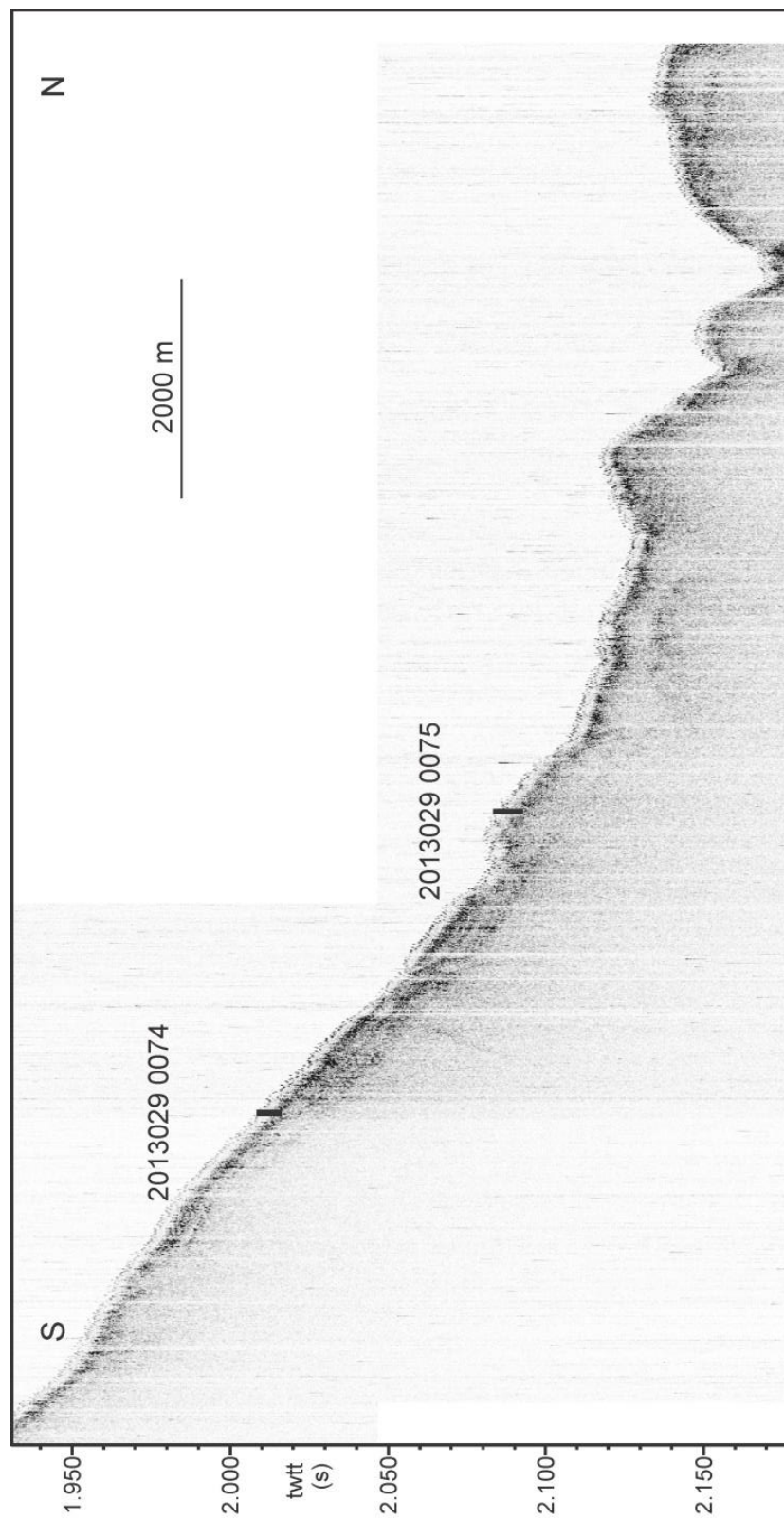


Figure 3.43a. 3.5 kHz sub-bottom profile showing the regional acoustic facies on the slope off Home Bay and location of piston cores 2013029-074 & 2013029-075.

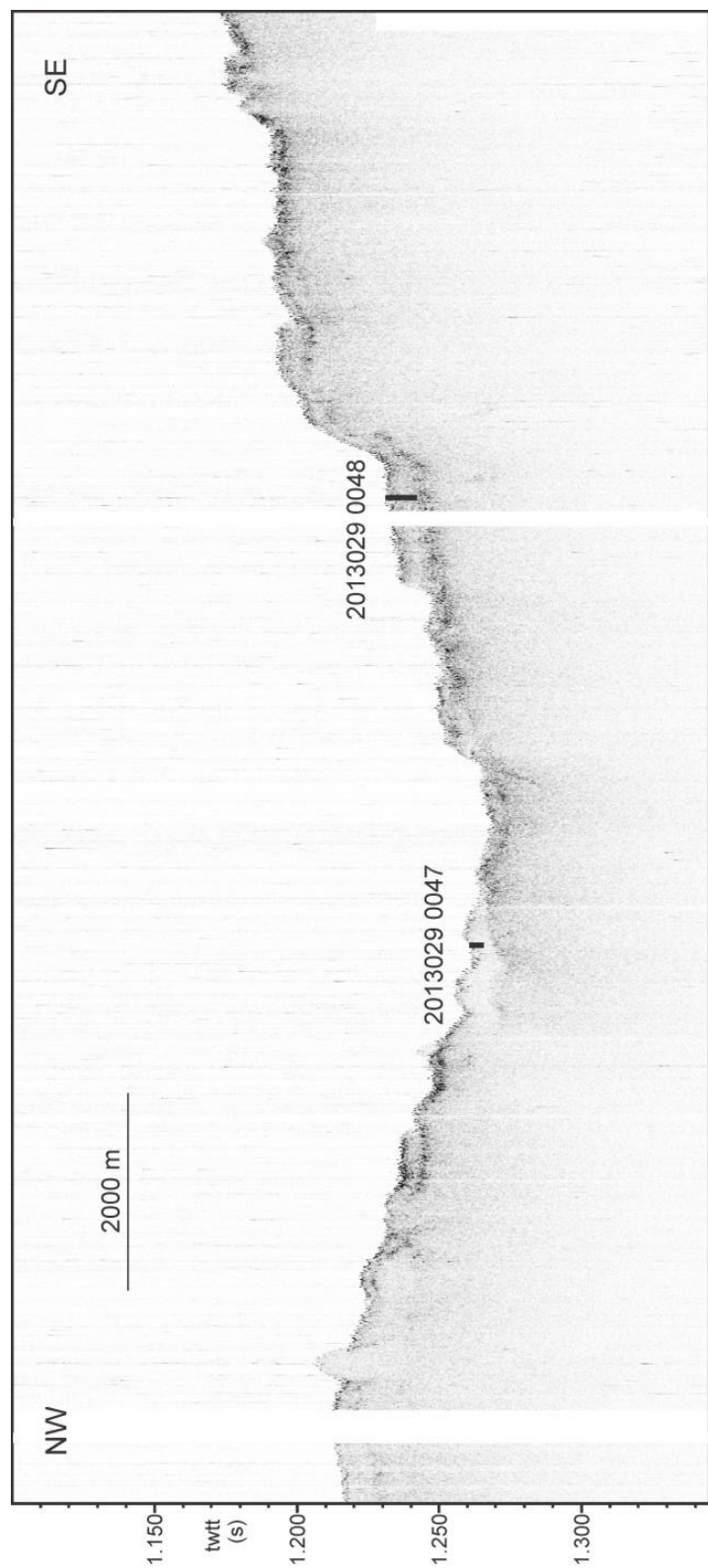


Figure 3.43b. 3.5 kHz sub-bottom profile showing the regional acoustic facies on the slope off Home Bay and location of piston cores 2013029-047 & 2013029-048.

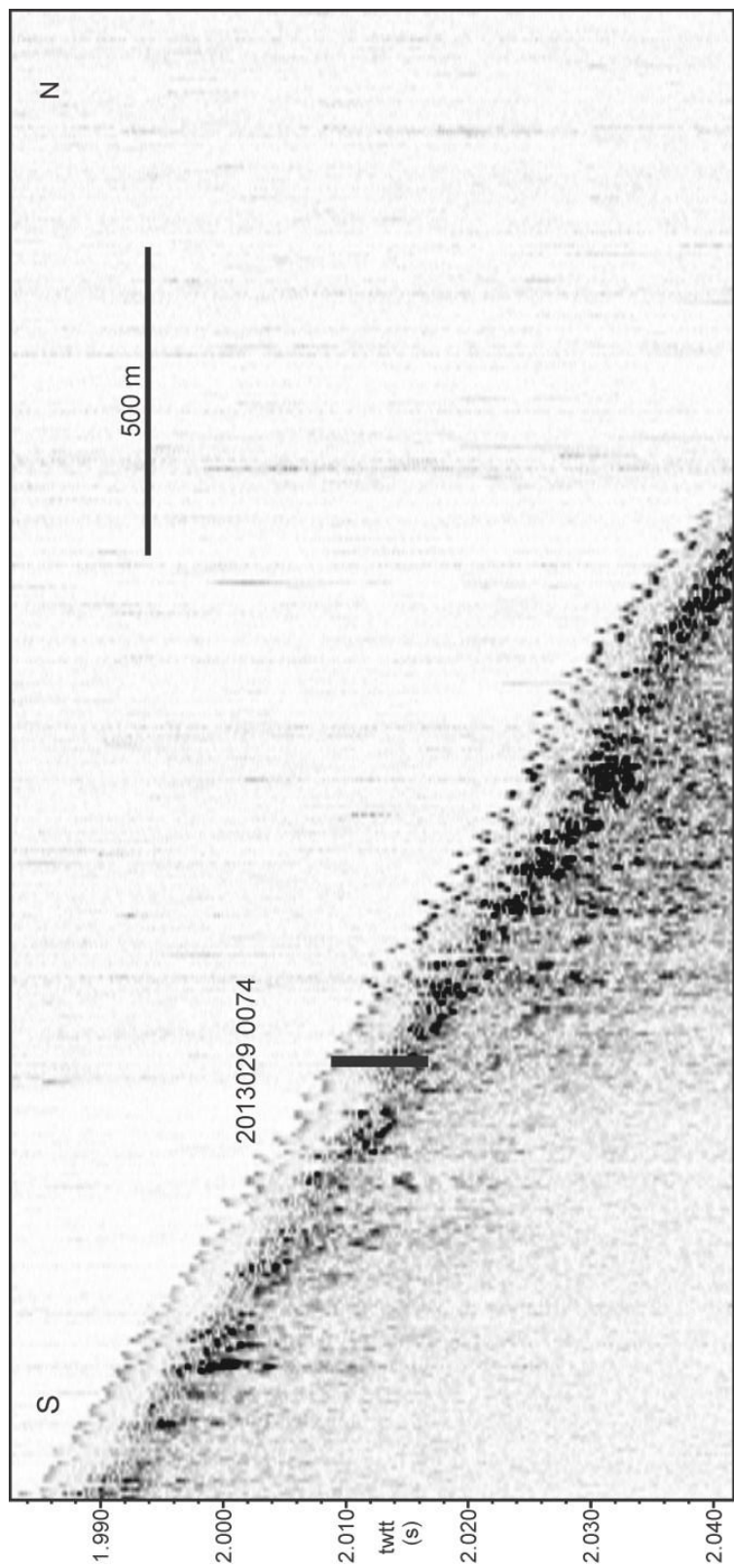


Figure 3.44. 3.5 kHz sub-bottom profile showing the acoustic stratigraphy and position of core 2013029-074.

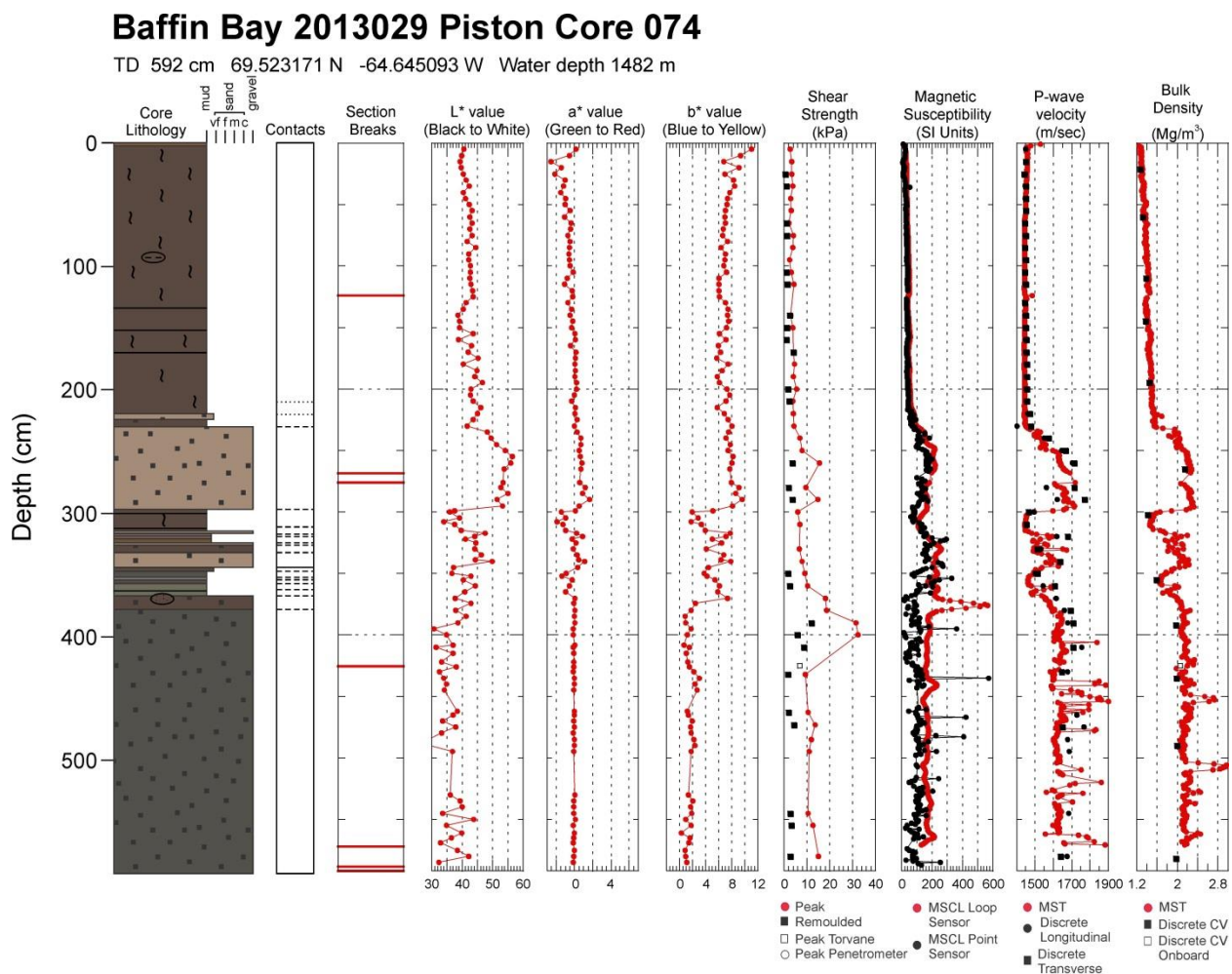


Figure 3.45a. Core plot summary for piston core 2013029-074.

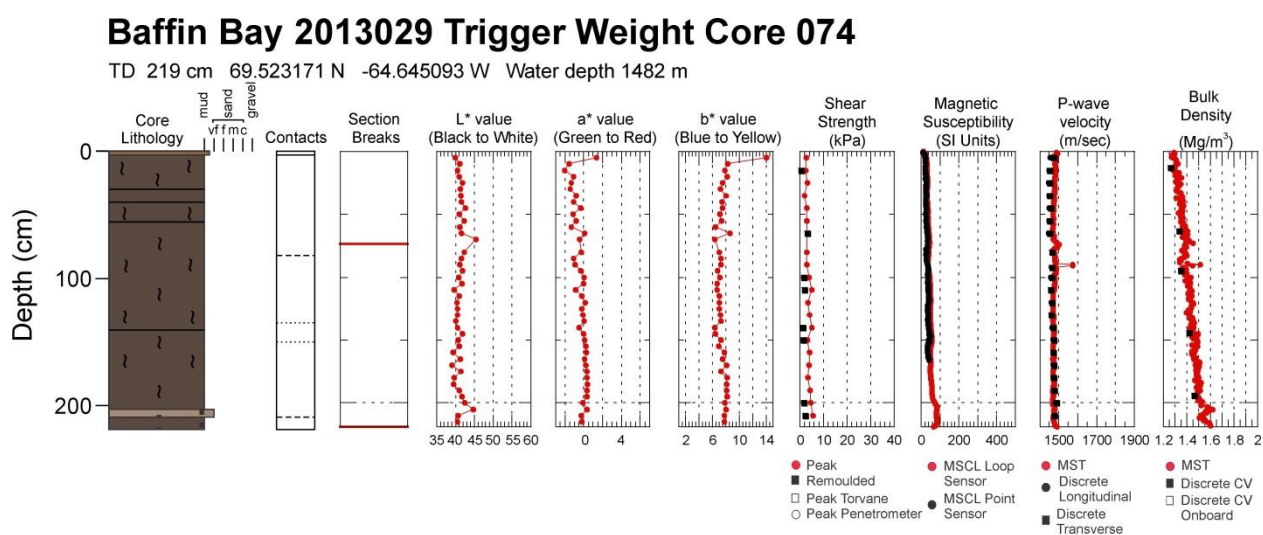


Figure 3.45b. Core plot summary for trigger weight core 2013029-074.

2013029 074 PC

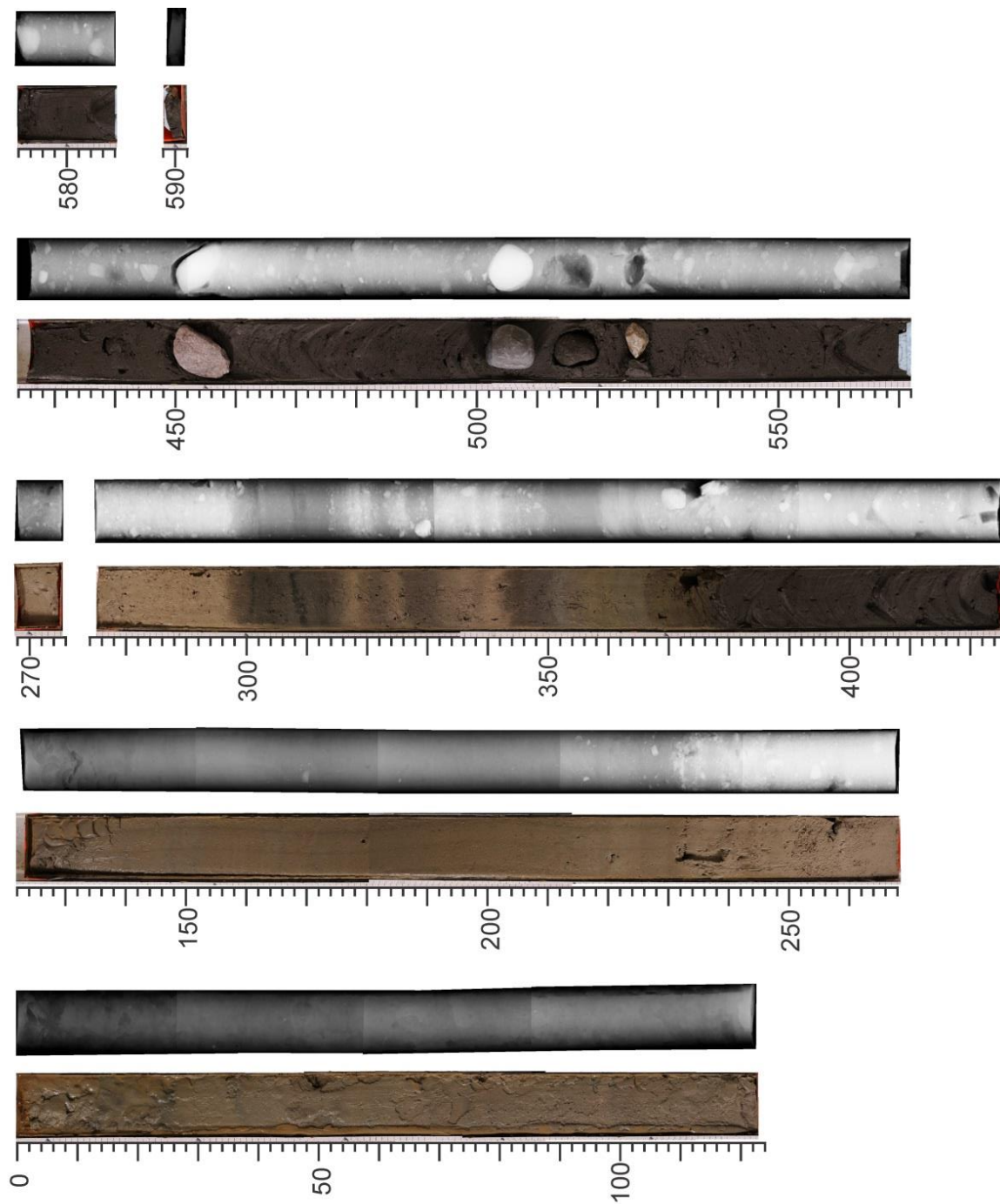


Figure 3.46a. Photography and X-radiography compilation for piston core 2013029-074.

2013029 074TWC

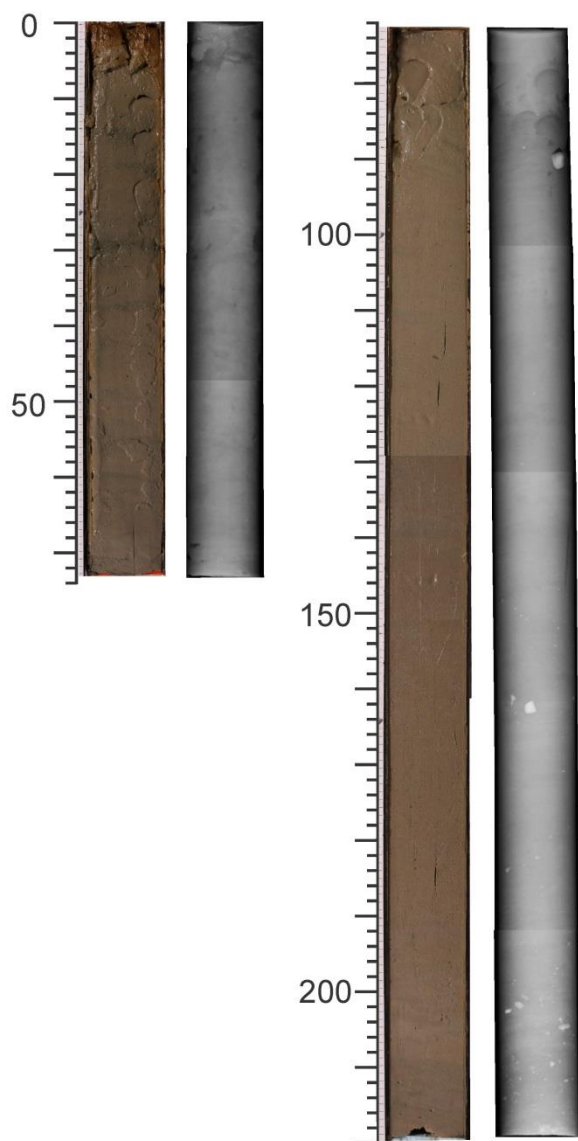


Figure 3.46b. Photography and X-radiography compilation for trigger weight core 2013029-074.

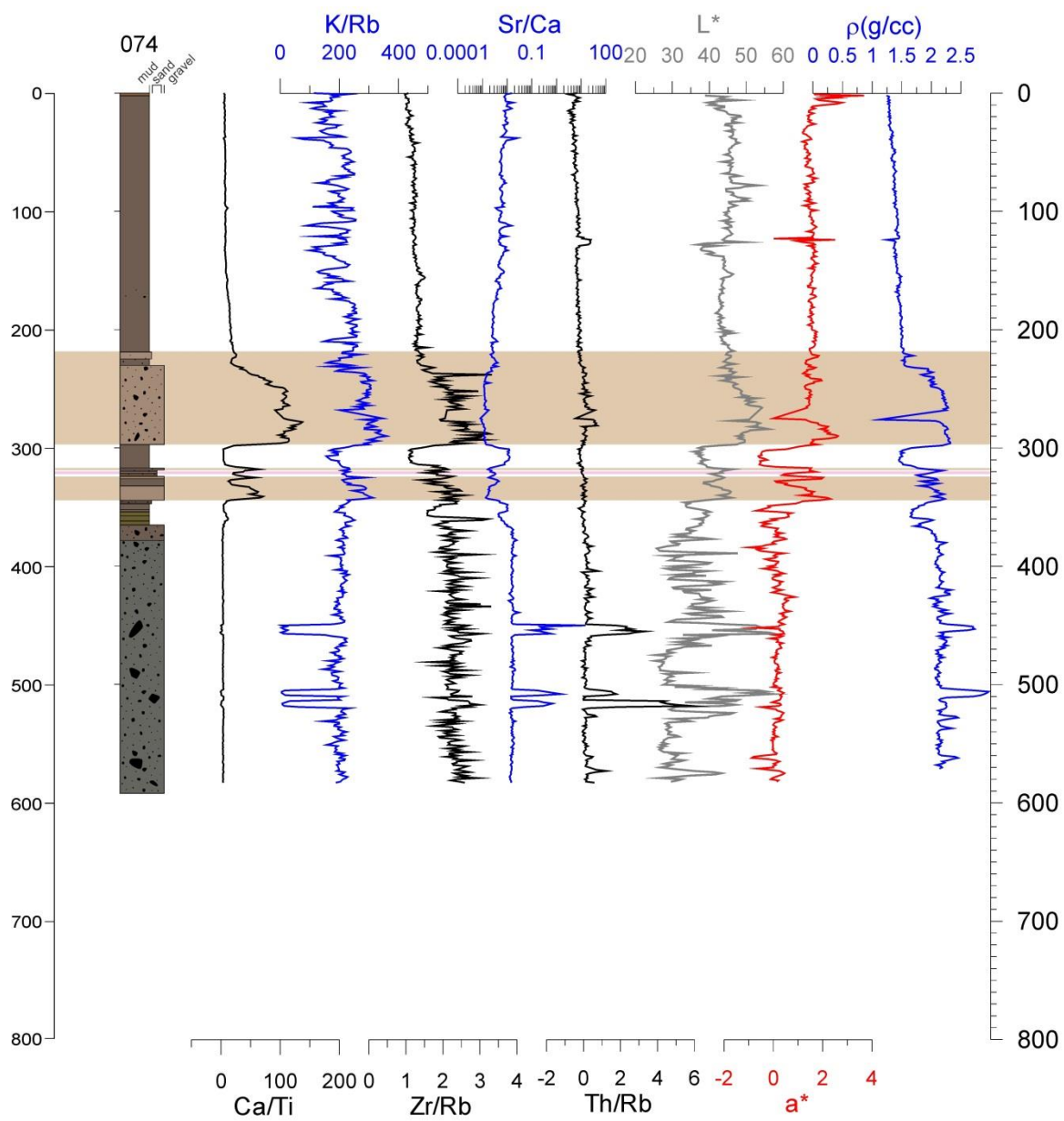


Figure 3.47. Down-core pXRF analysis for piston core 2013029-074. Tan highlighting indicates tan carbonate mud; rose highlighting indicates rose mud.

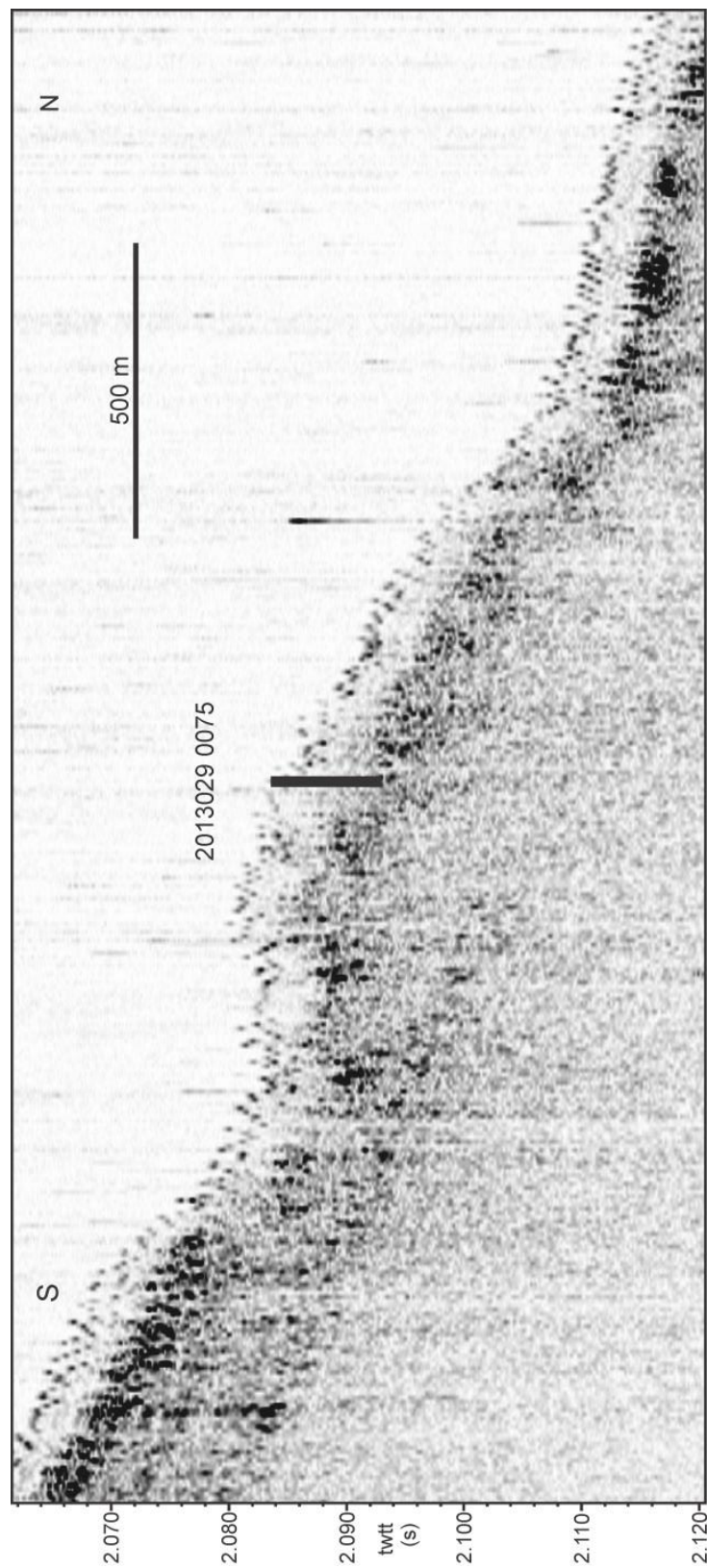


Figure 3.48. 3.5 kHz sub-bottom profile showing the acoustic stratigraphy and position of core 2013029-075.

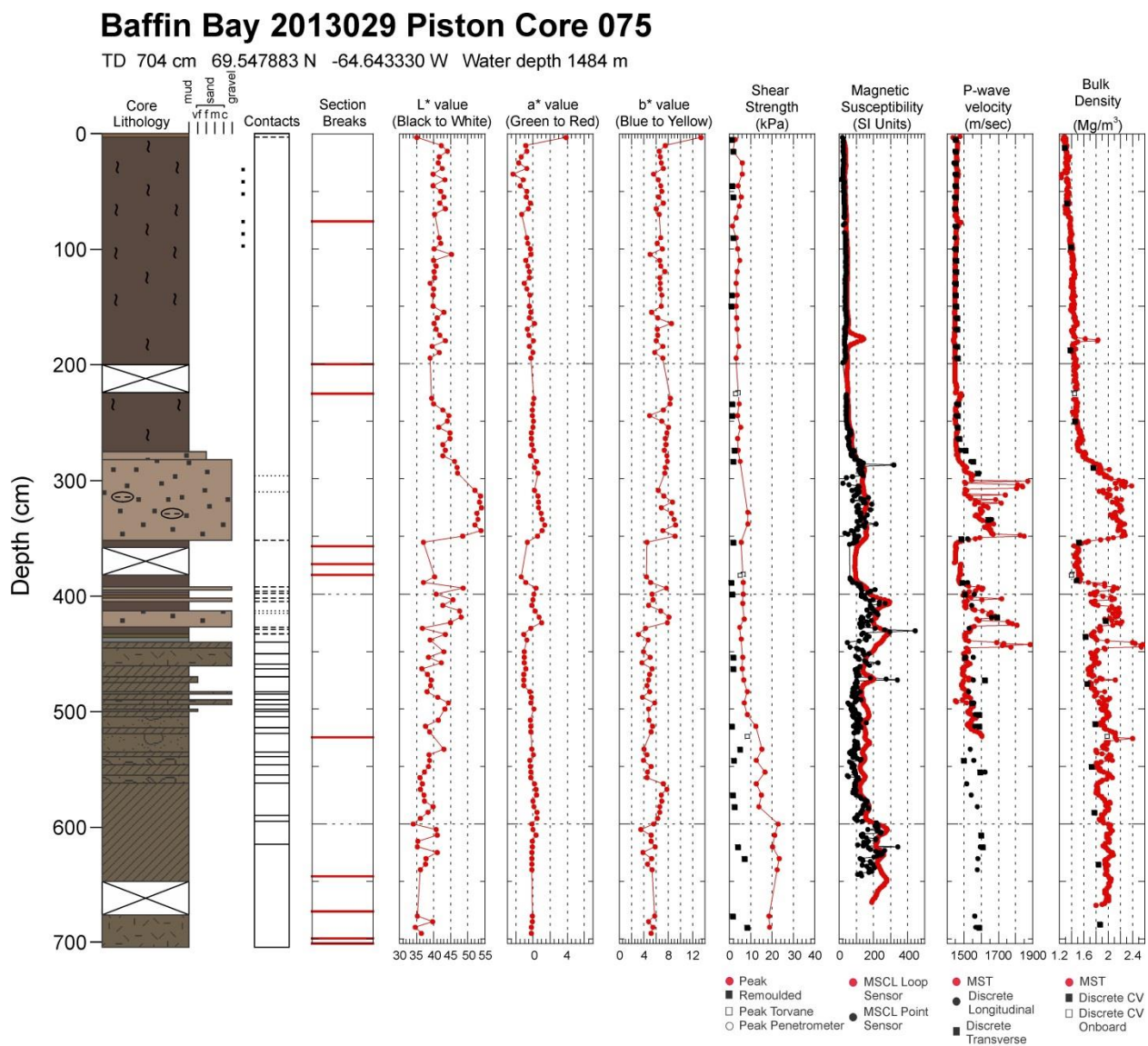


Figure 3.49a. Core plot summary for piston core 2013029-075.

Baffin Bay 2013029 Trigger Weight Core 075

TD 218.5 cm 69.547883 N -64.643330 W Water depth 1484 m

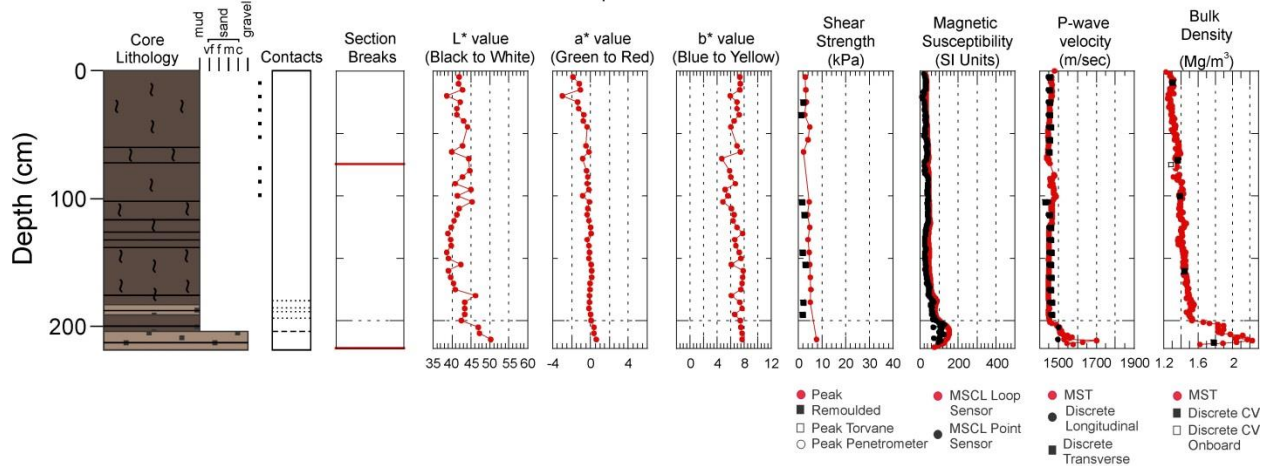


Figure 3.49b. Core plot summary for trigger weight core 2013029-075.

2013029 075 PC

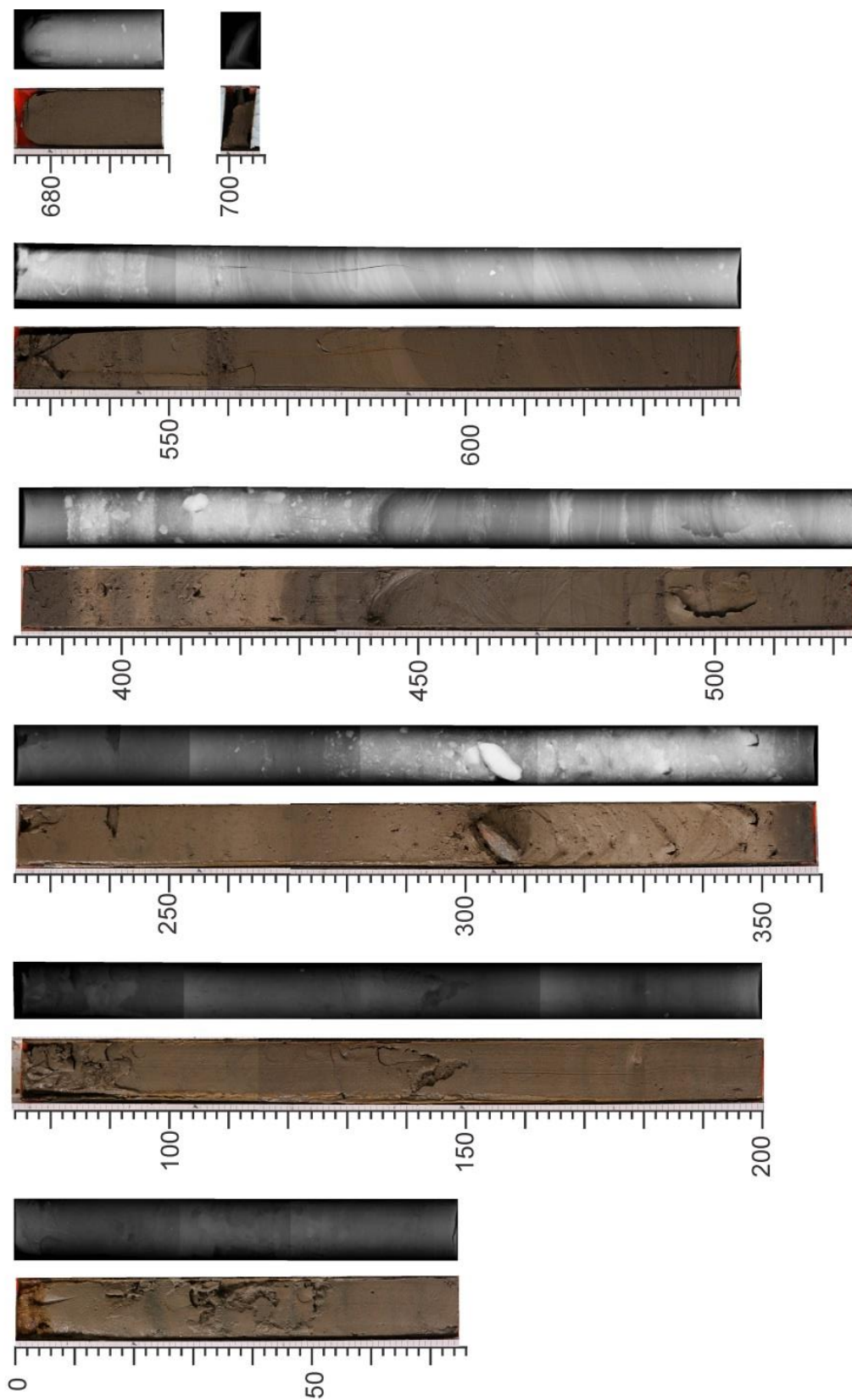


Figure 3.50a. Photography and X-radiography compilation for piston core 2013029-075.

2013029 075 TWC

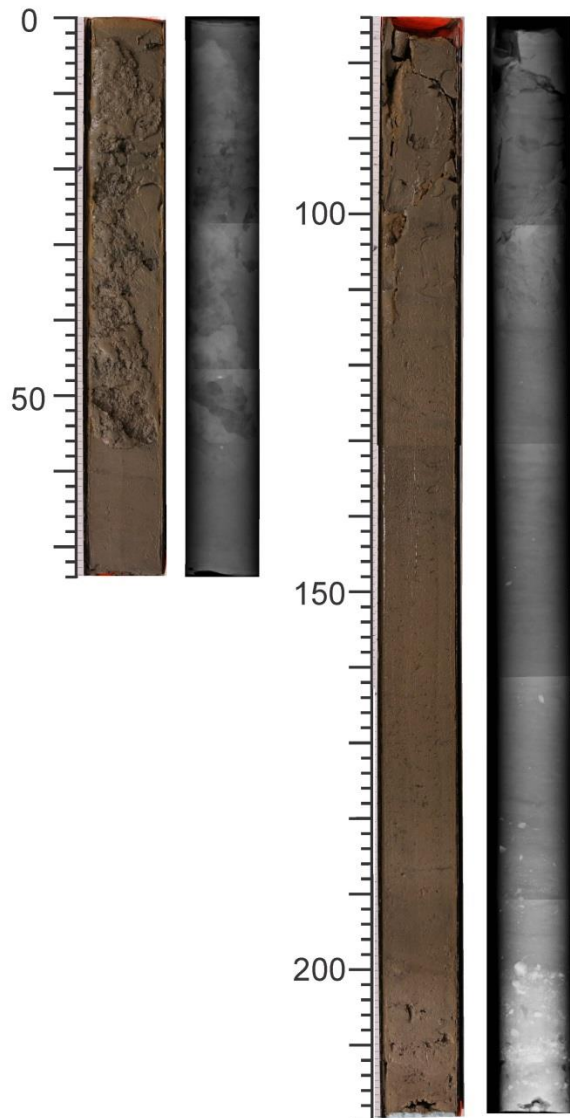


Figure 3.50b. Photography and X-radiography compilation for trigger weight core 2013029-075.

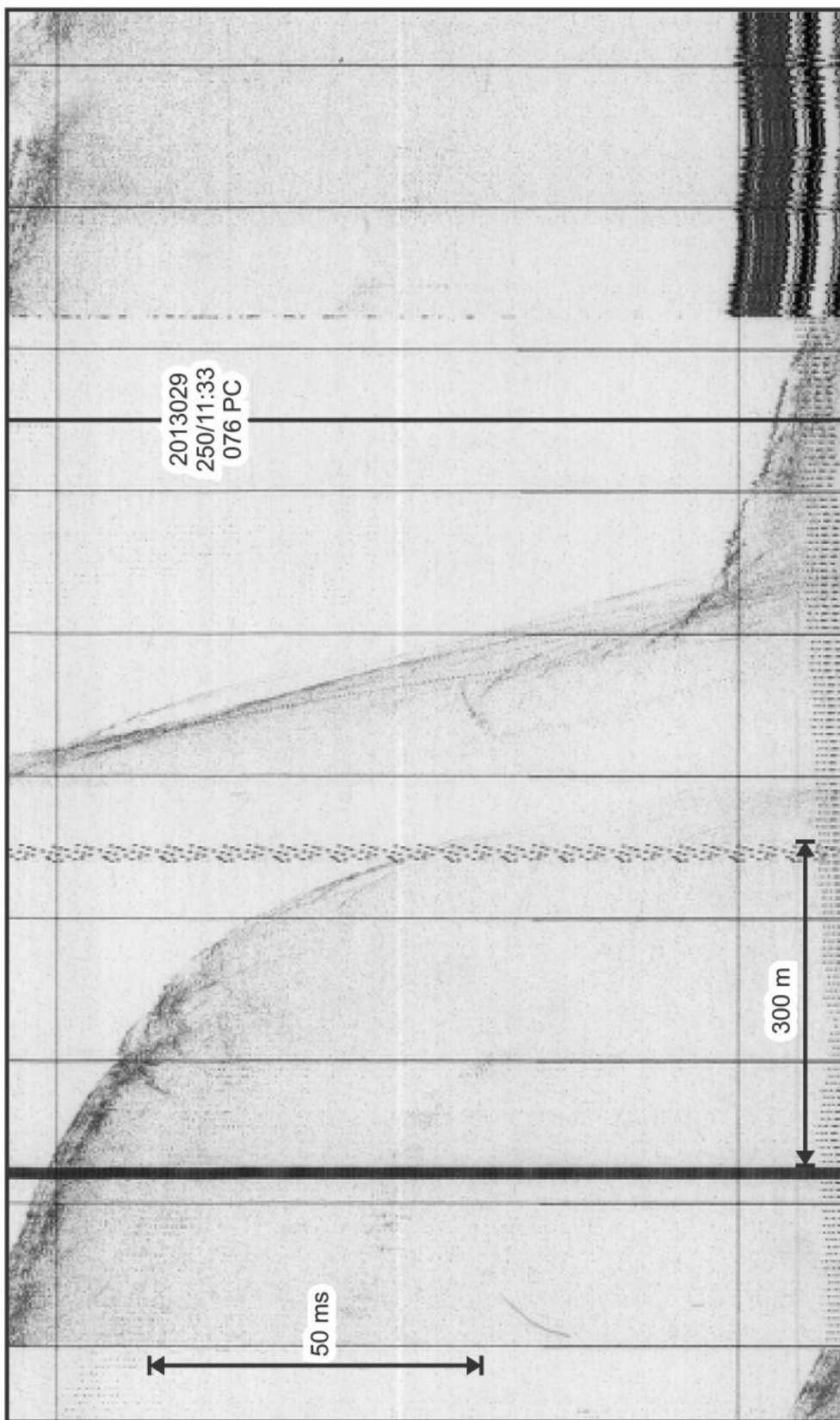


Figure 3.51. Hunttec profile showing the acoustic stratigraphy and position of core 2013029-076.

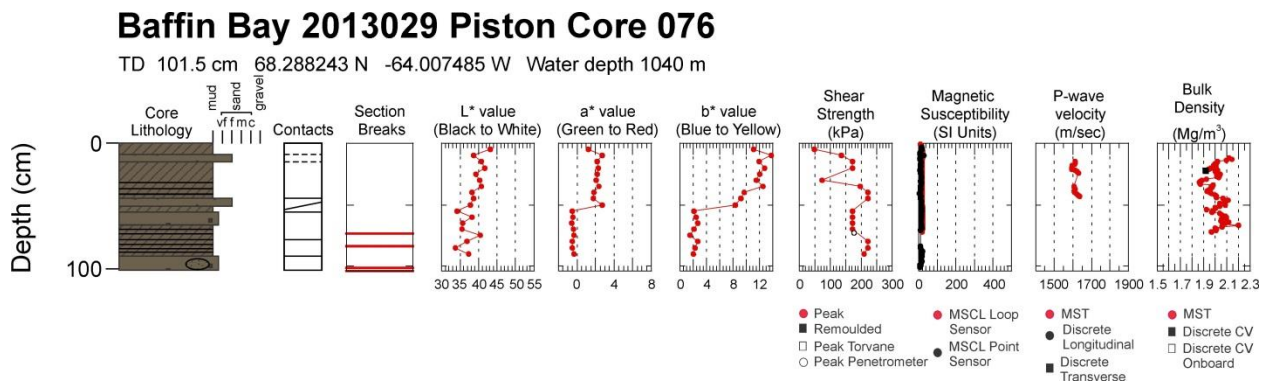


Figure 3.52a. Core plot summary for piston core 2013029-076.

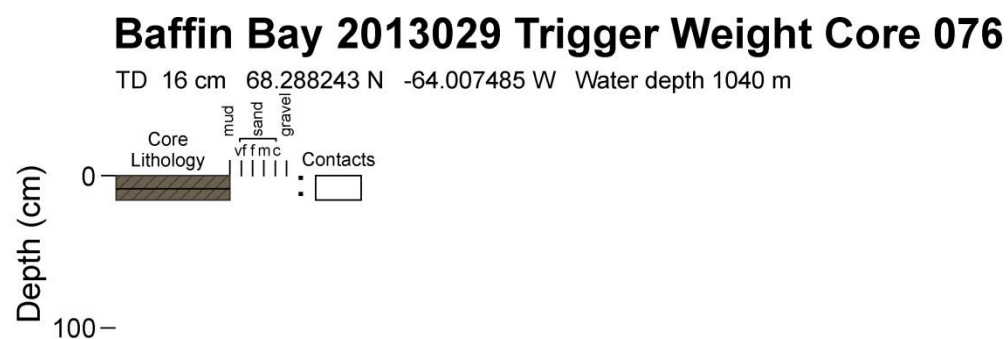


Figure 3.52b. Core plot summary for trigger weight core 2013029-076.

2013029 076 PC

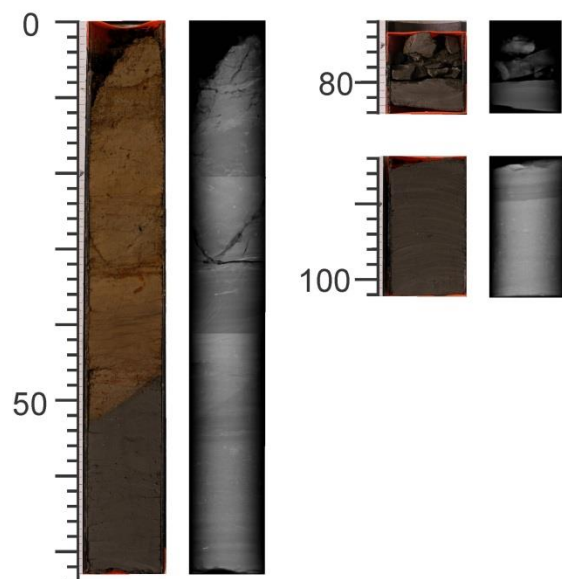


Figure 3.53a. Photography and X-radiography compilation for piston core 2013029-076.

2013029 076 TWC

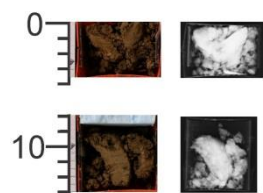


Figure 3.53b. Photography and X-radiography compilation for trigger weight core 2013029-076.

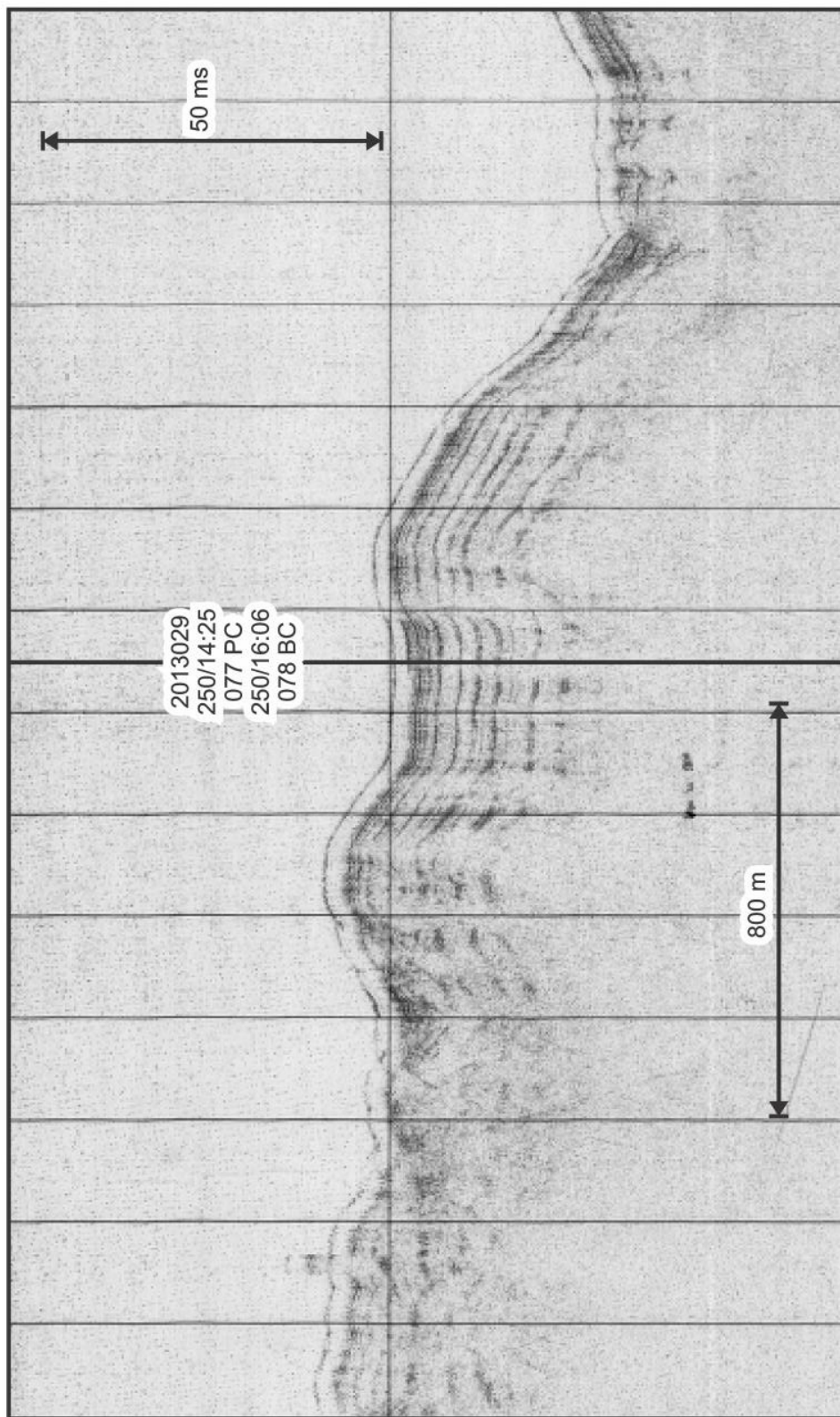


Figure 3.54. Hunttec profile showing the acoustic stratigraphy and position of core 2013029-077.

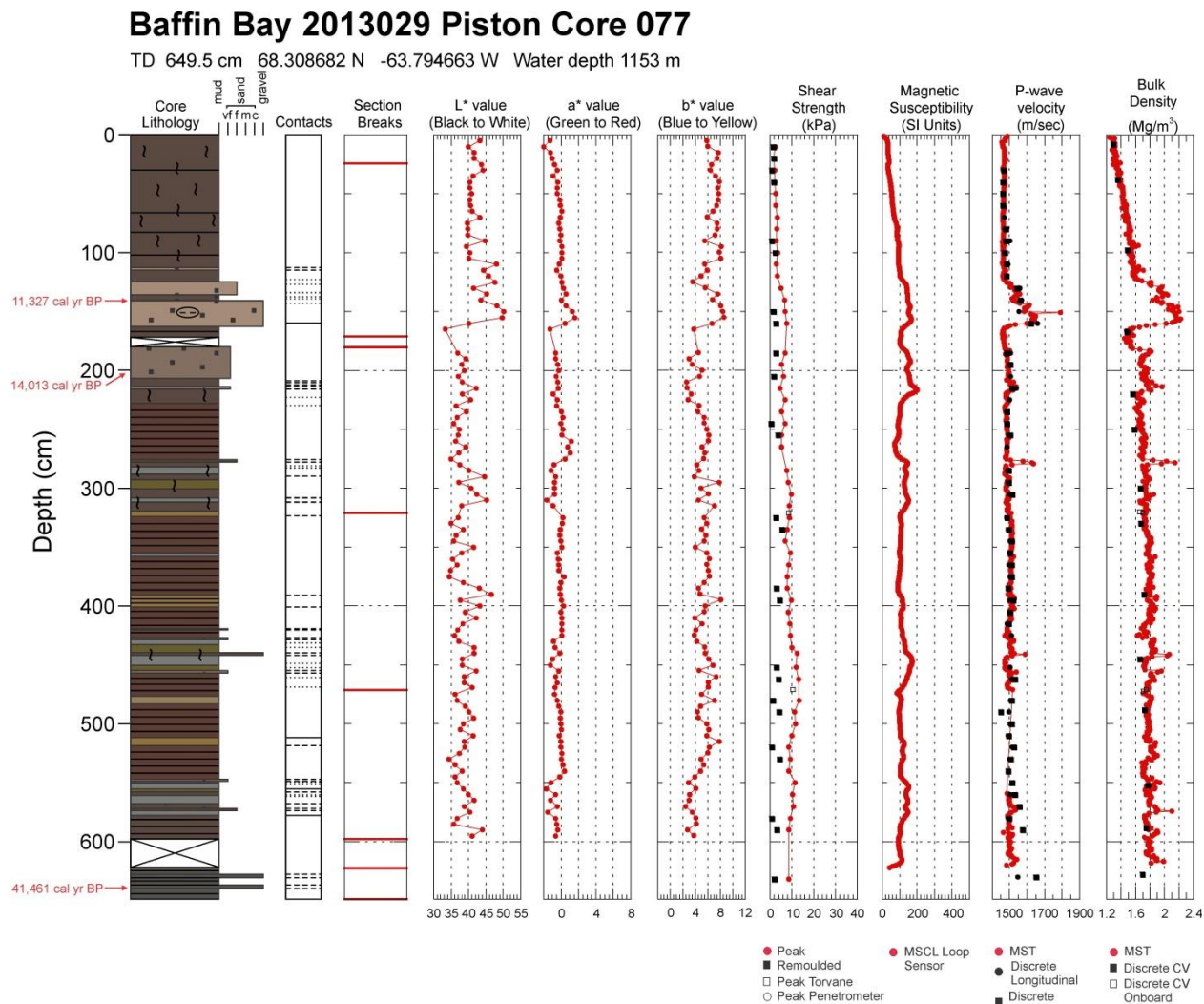


Figure 3.55a. Core plot summary for piston core 2013029-077.
Baffin Bay 2013029 Trigger Weight Core 077

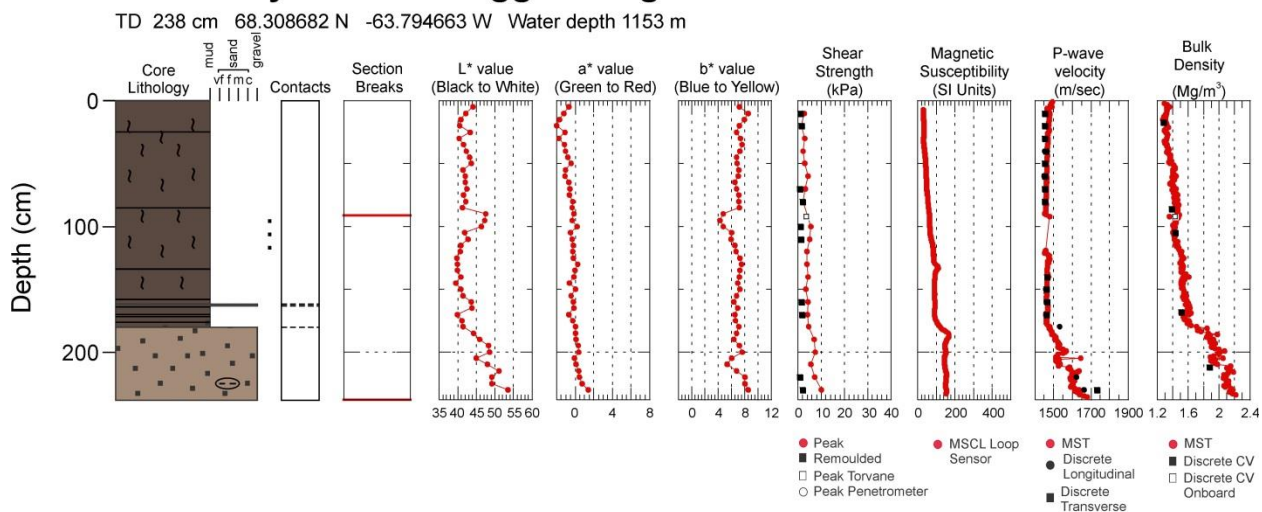


Figure 3.55b. Core plot summary for trigger weight core 2013029-077.

2013029 077 PC

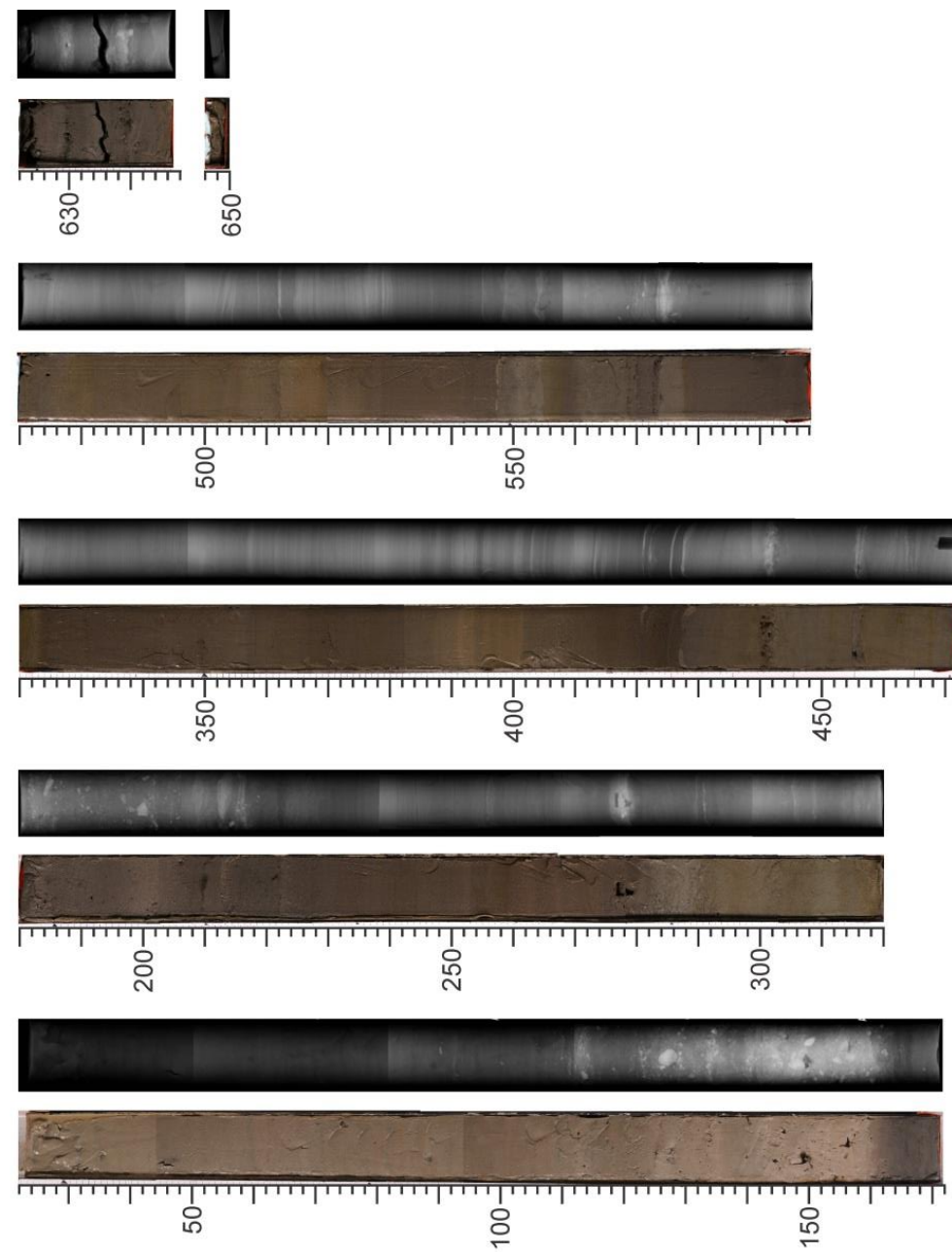


Figure 3.56a. Photography and X-radiography compilation for piston core 2013029-077.

2013029 077 TWC



Figure 3.56b. Photography and X-radiography compilation for trigger weight core 2013029-077.

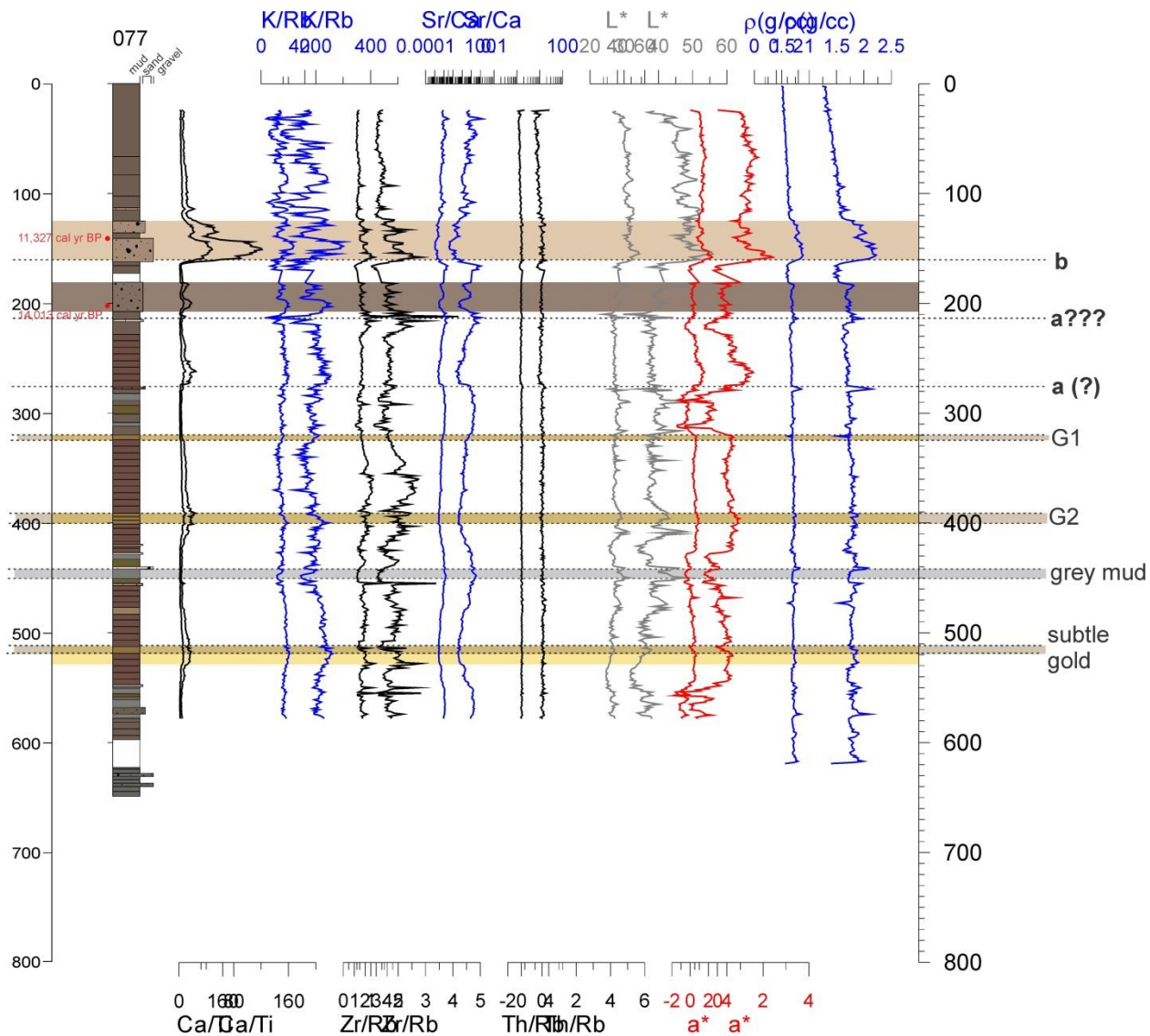


Figure 3.57. Down-core pXRF analysis for piston core 2013029-077. Tan highlighting indicates tan carbonate mud; gold brown highlighting indicates gold brown mud; light brown highlighting indicates light brown mud associated with an increase in the pXRF Ca/Ti ratio.

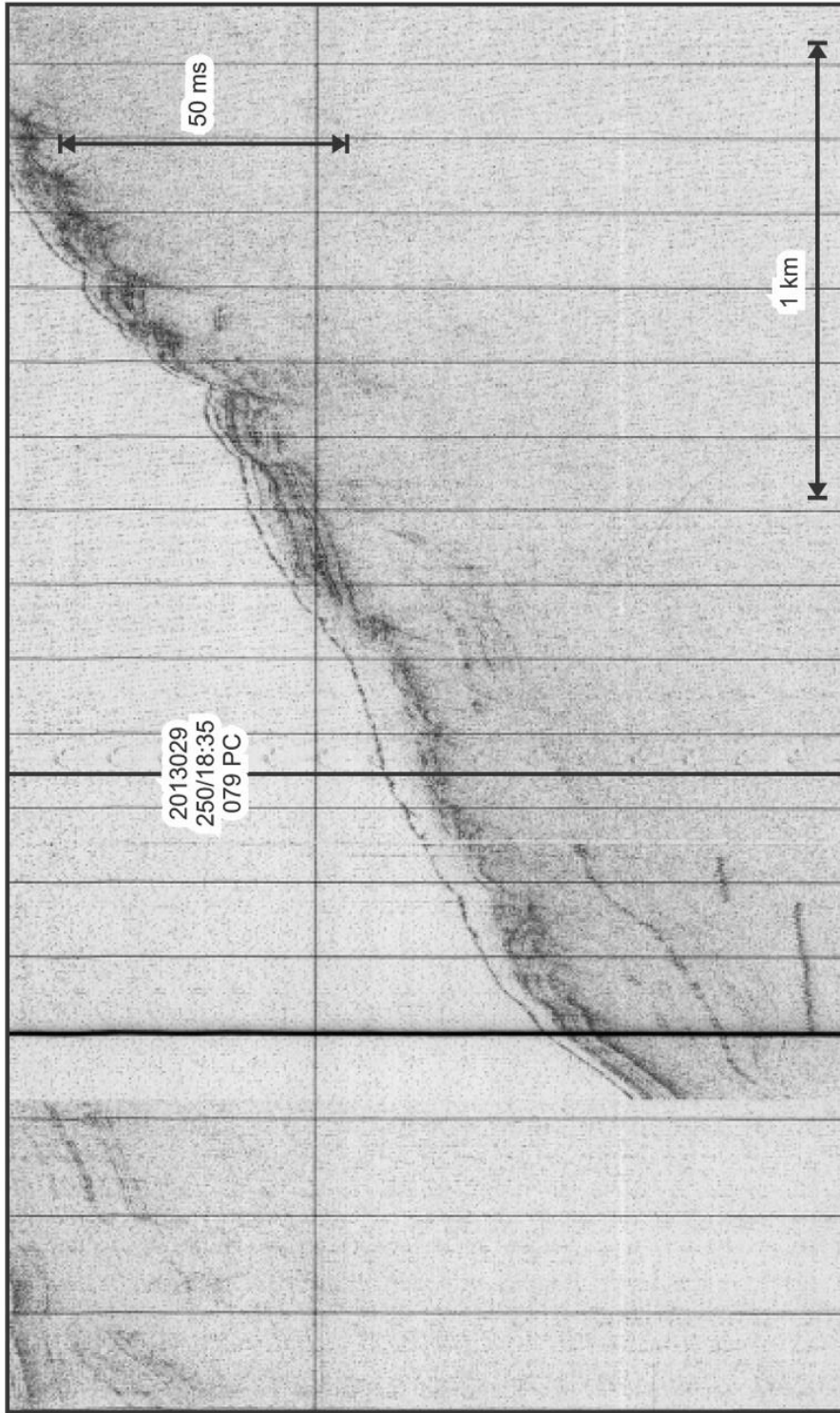


Figure 3.58. Hunttec profile showing the acoustic stratigraphy and position of core 2013029-079.

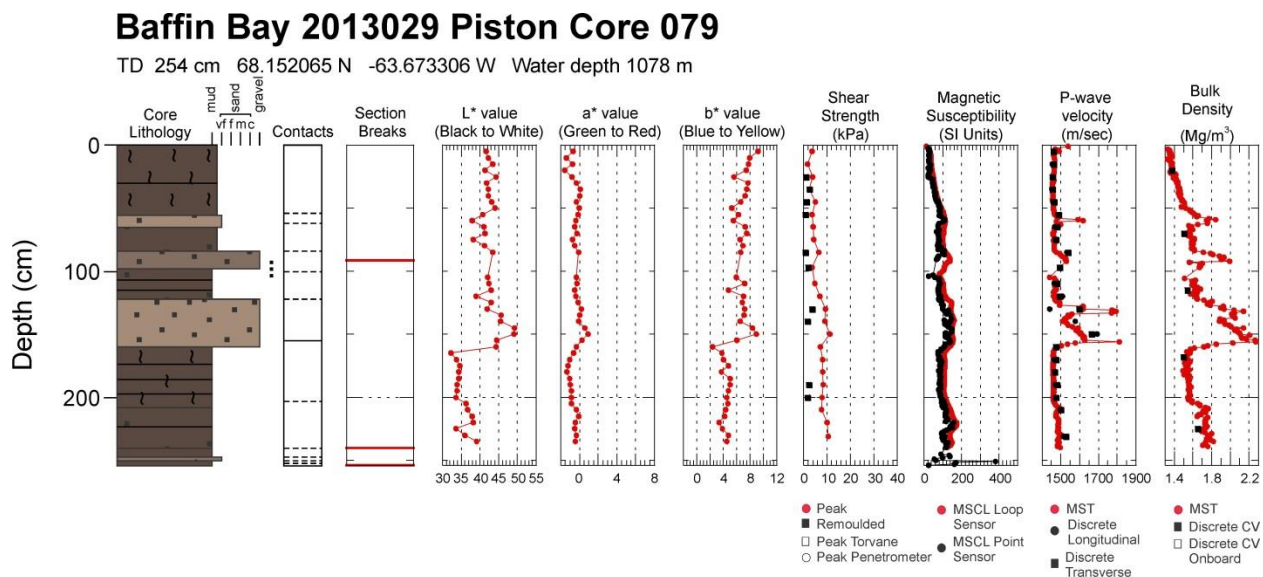


Figure 3.59a. Core plot summary for piston core 2013029-079.

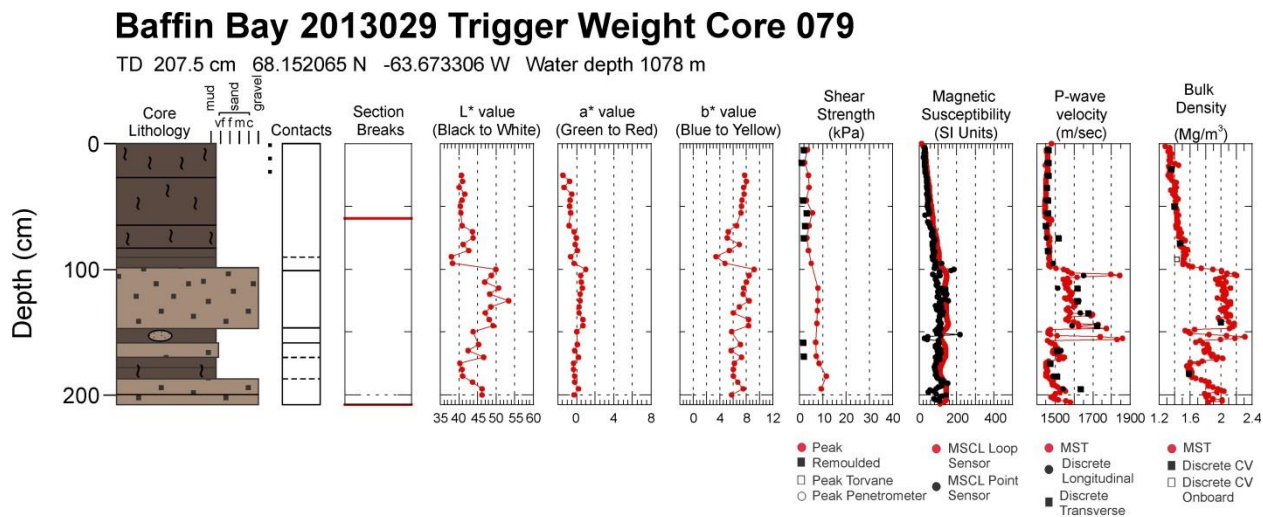


Figure 3.59b. Core plot summary for trigger weight core 2013029-079.

2013029 079 PC

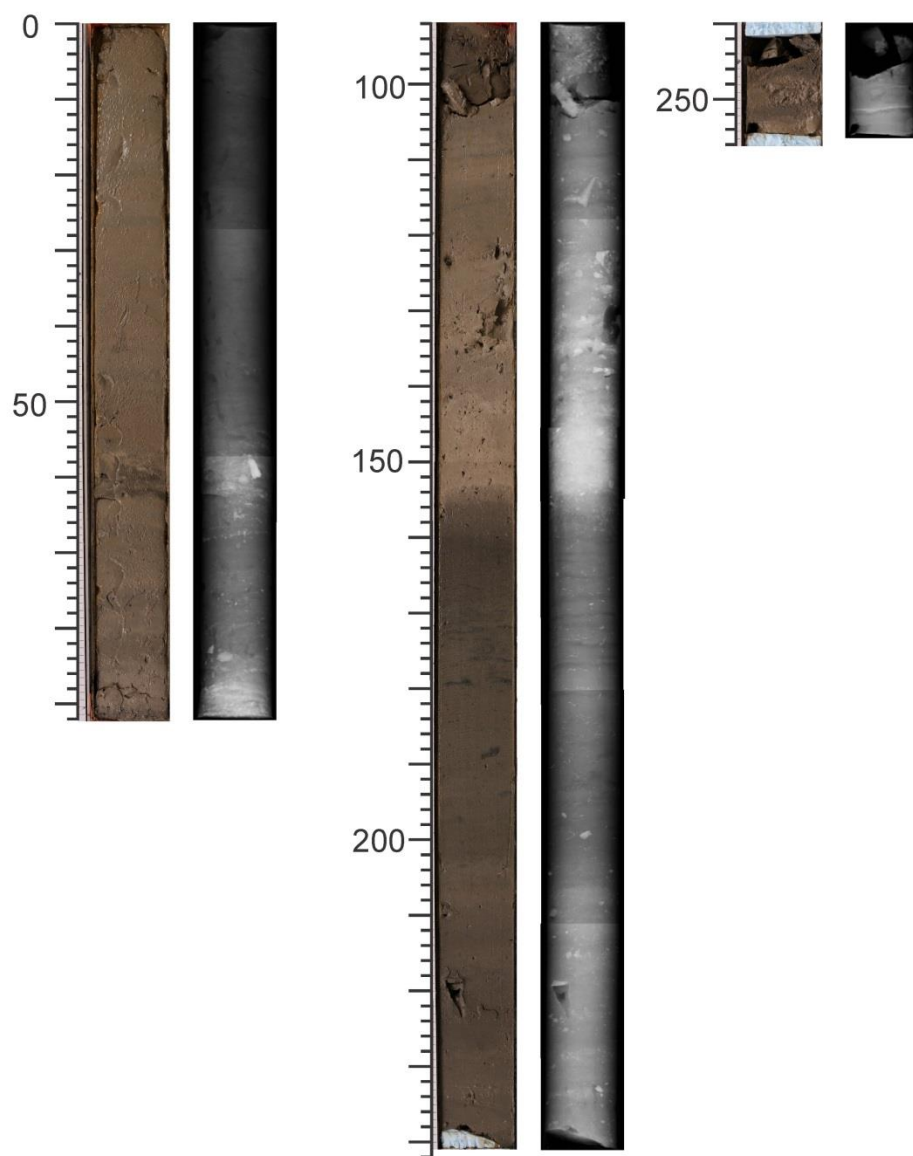


Figure 3.60a. Photography and X-radiography compilation for piston core 2013029-079.

2013029 079 TWC

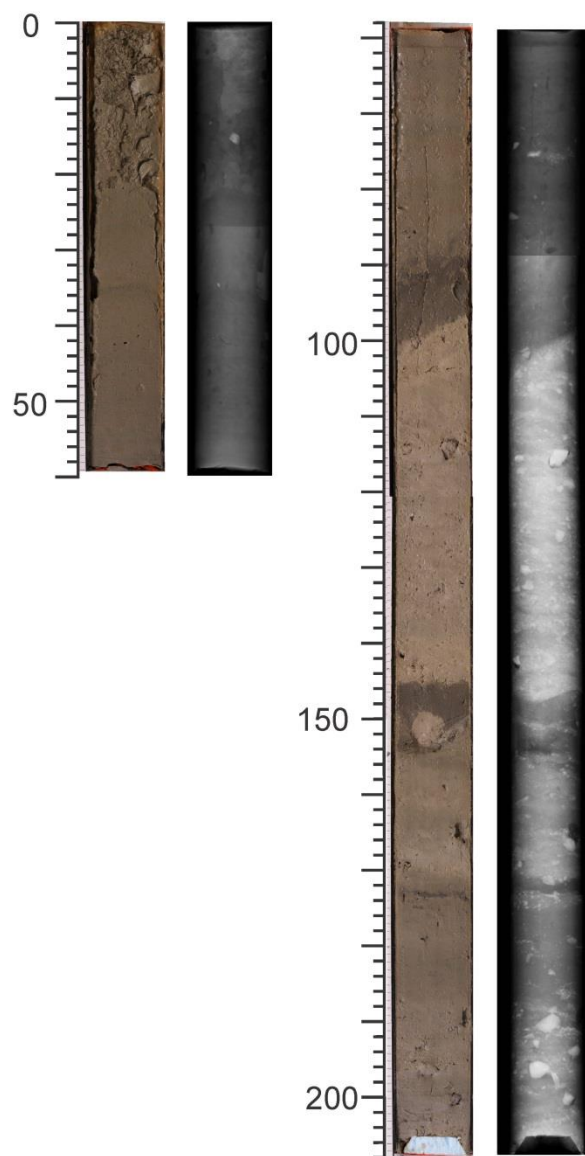


Figure 3.60b. Photography and X-radiography compilation for trigger weight core 2013029-079.

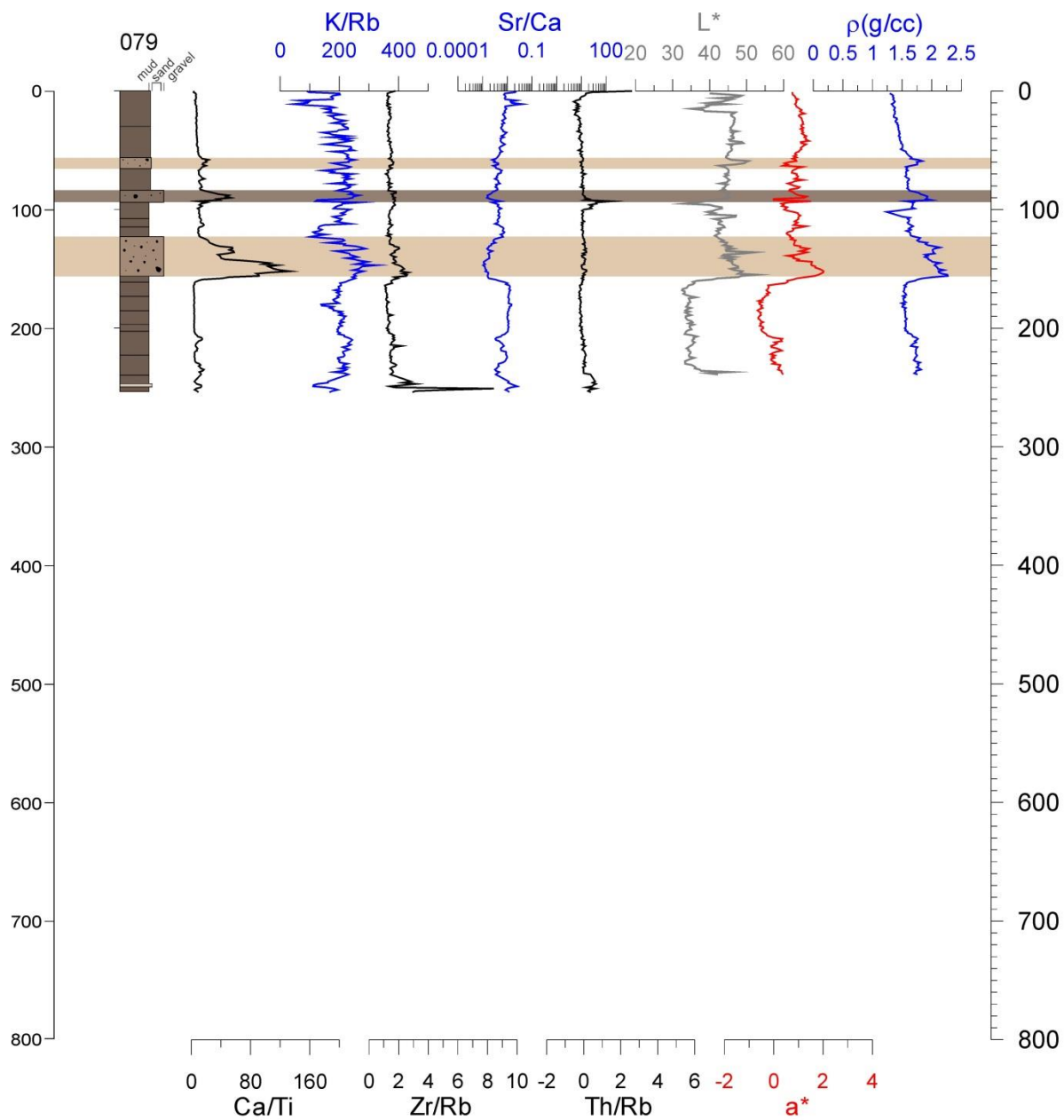


Figure 3.61. Down-core pXRF analysis for piston core 2013029-079. Tan highlighting indicates tan carbonate mud; light brown highlighting indicates light brown mud associated with an increase in the pXRF Ca/Ti ratio.

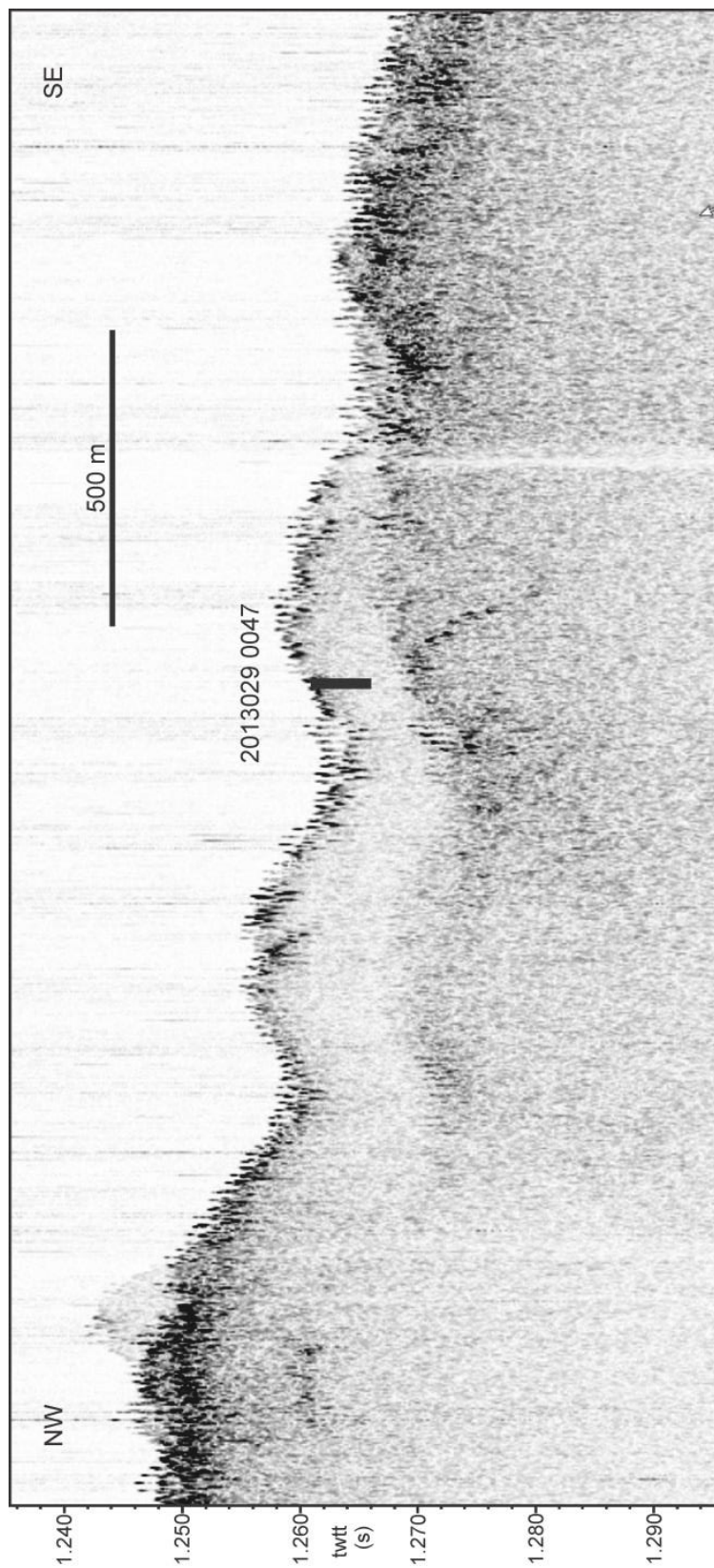


Figure 3.62. 3.5 kHz sub-bottom profile showing the acoustic stratigraphy and position of core 2013029-047.

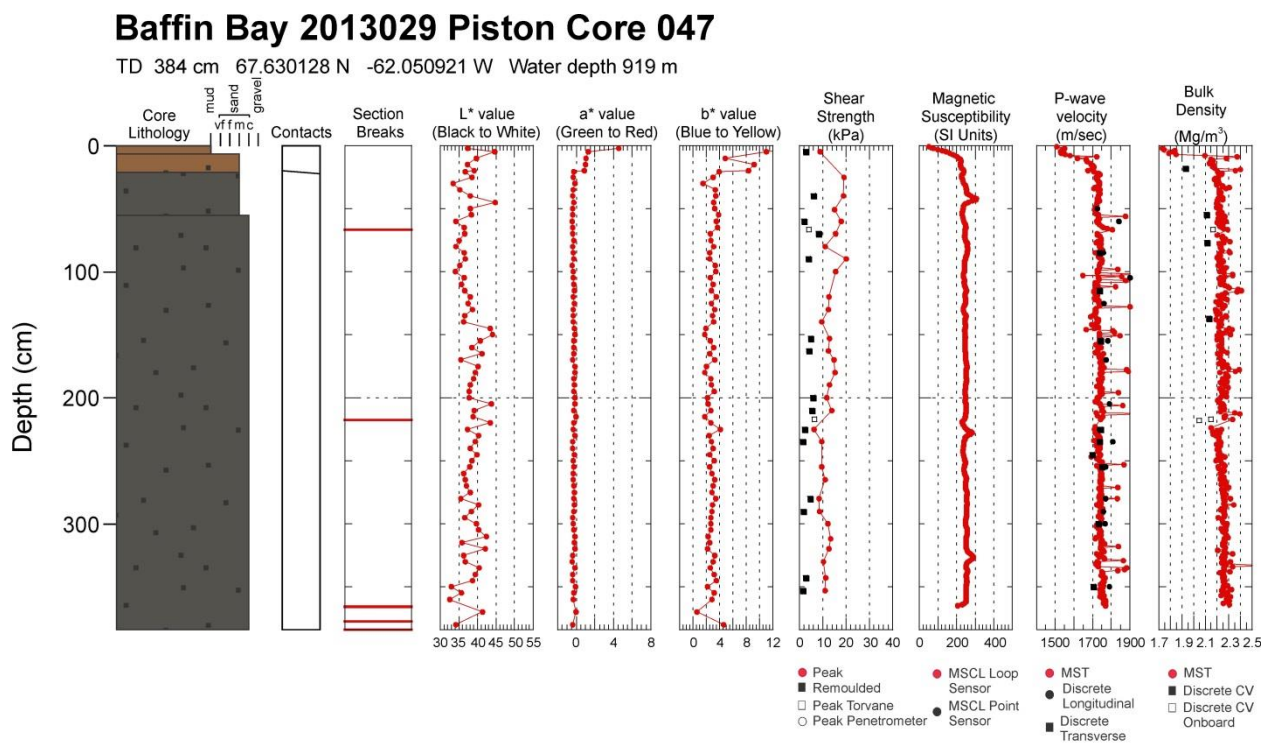


Figure 3.63. Core plot summary for piston core 2013029-047.

2013029 047 PC

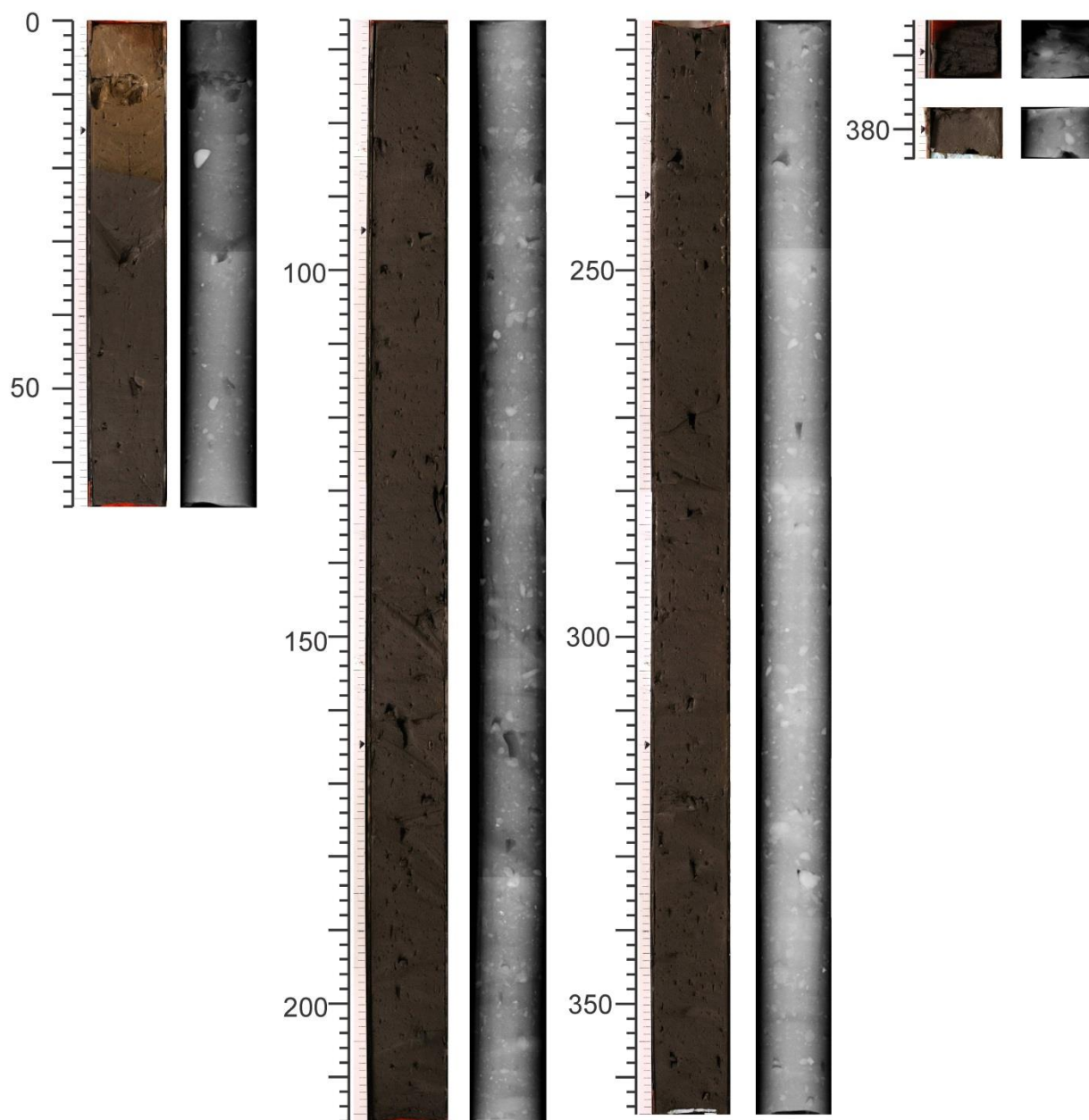


Figure 3.64. Photography and X-radiography compilation for piston core 2013029-047.

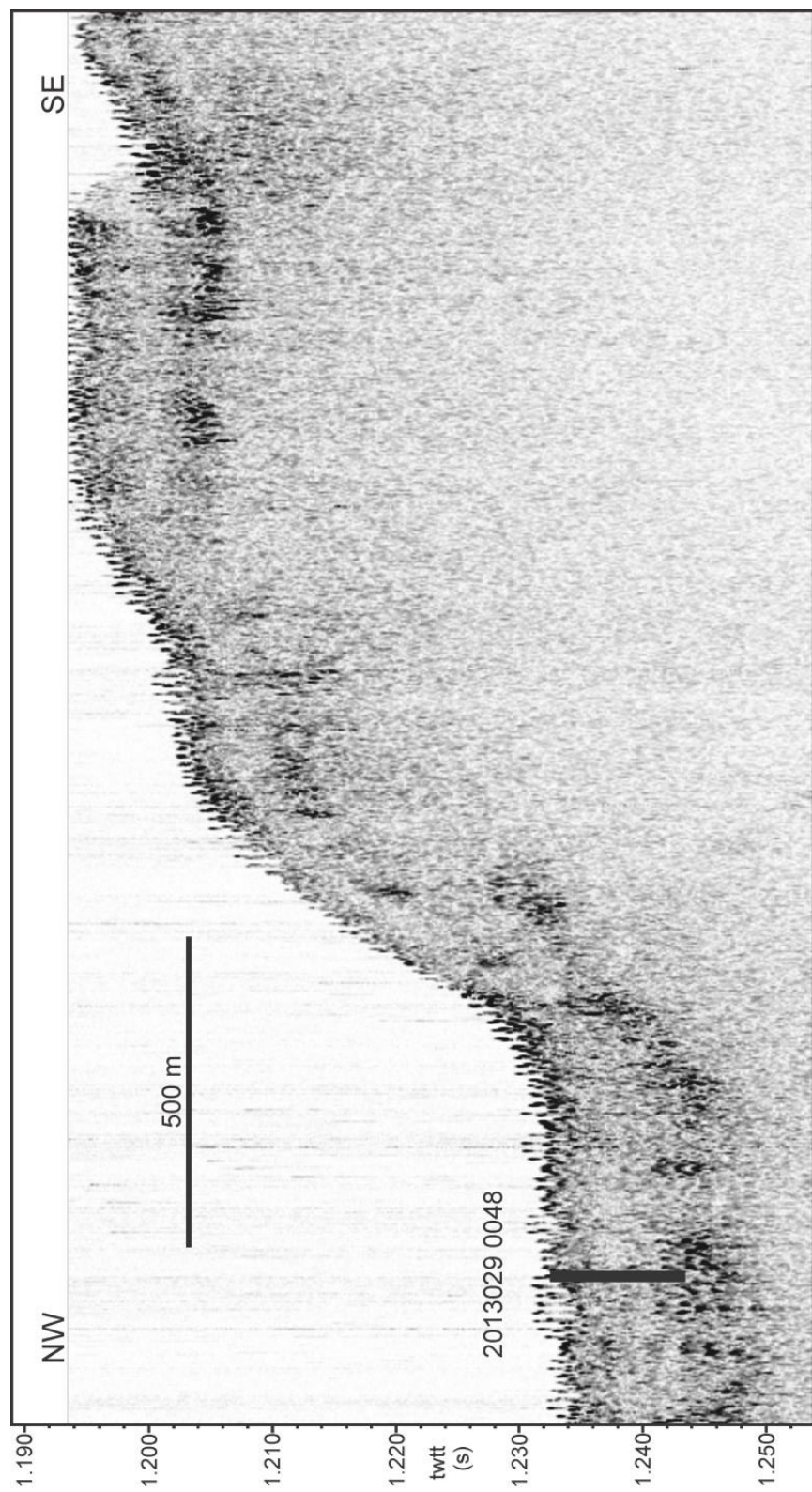


Figure 3.65. 3.5 kHz sub-bottom profile showing the acoustic stratigraphy and position of core 2013029-048.

Baffin Bay 2013029 Piston Core 048

TD 822.5 cm 67.605618 N -61.967451 W Water depth 935 m

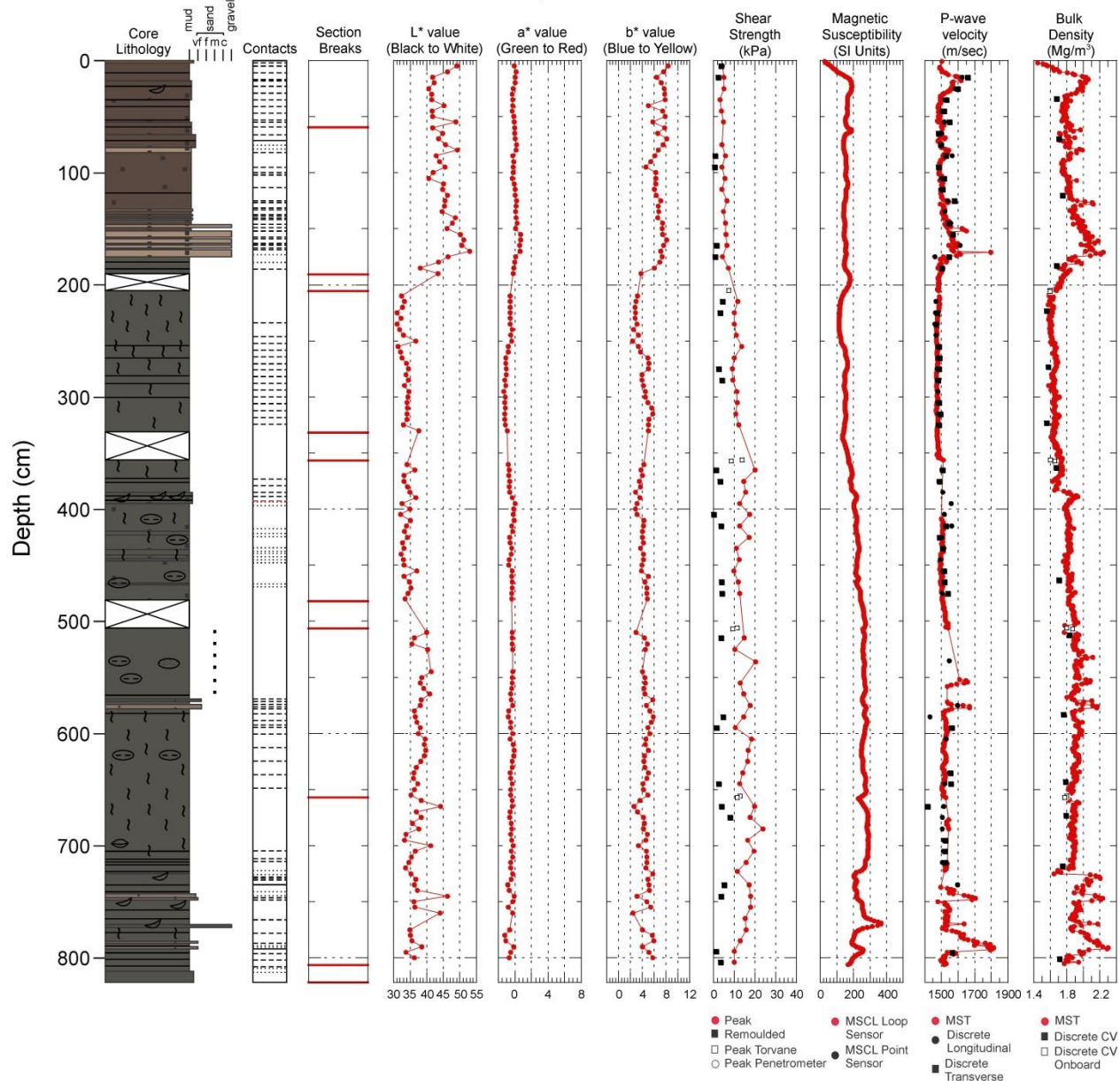


Figure 3.66a. Core plot summary for piston core 2013029-048.

Baffin Bay 2013029 Trigger Weight Core 048

TD 173 cm 67.605618 N -61.967451 W Water depth 935 m

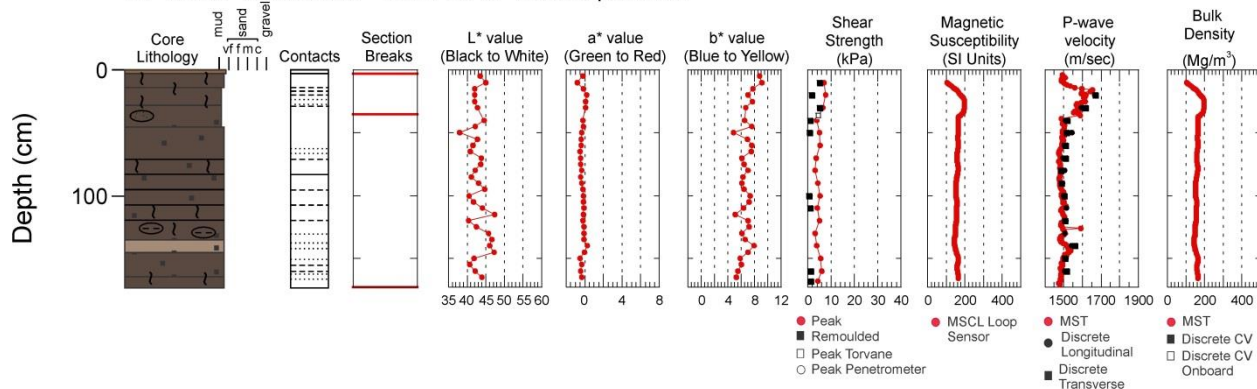


Figure 3.66b. Core plot summary for trigger weight core 2013029-048.

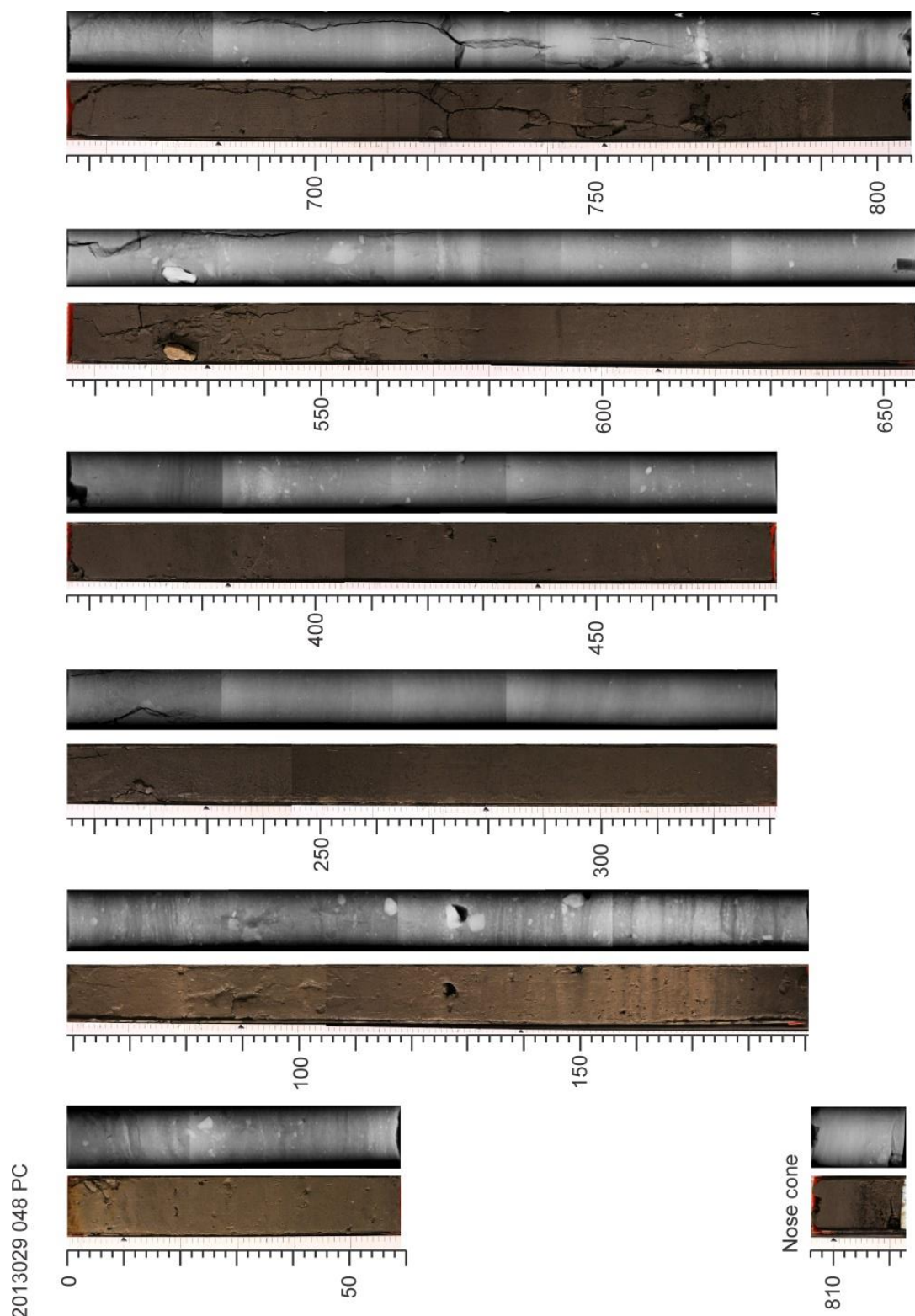


Figure 3.67a. Photography and X-radiography compilation for piston core 2013029-048.

2013029 048 TWC

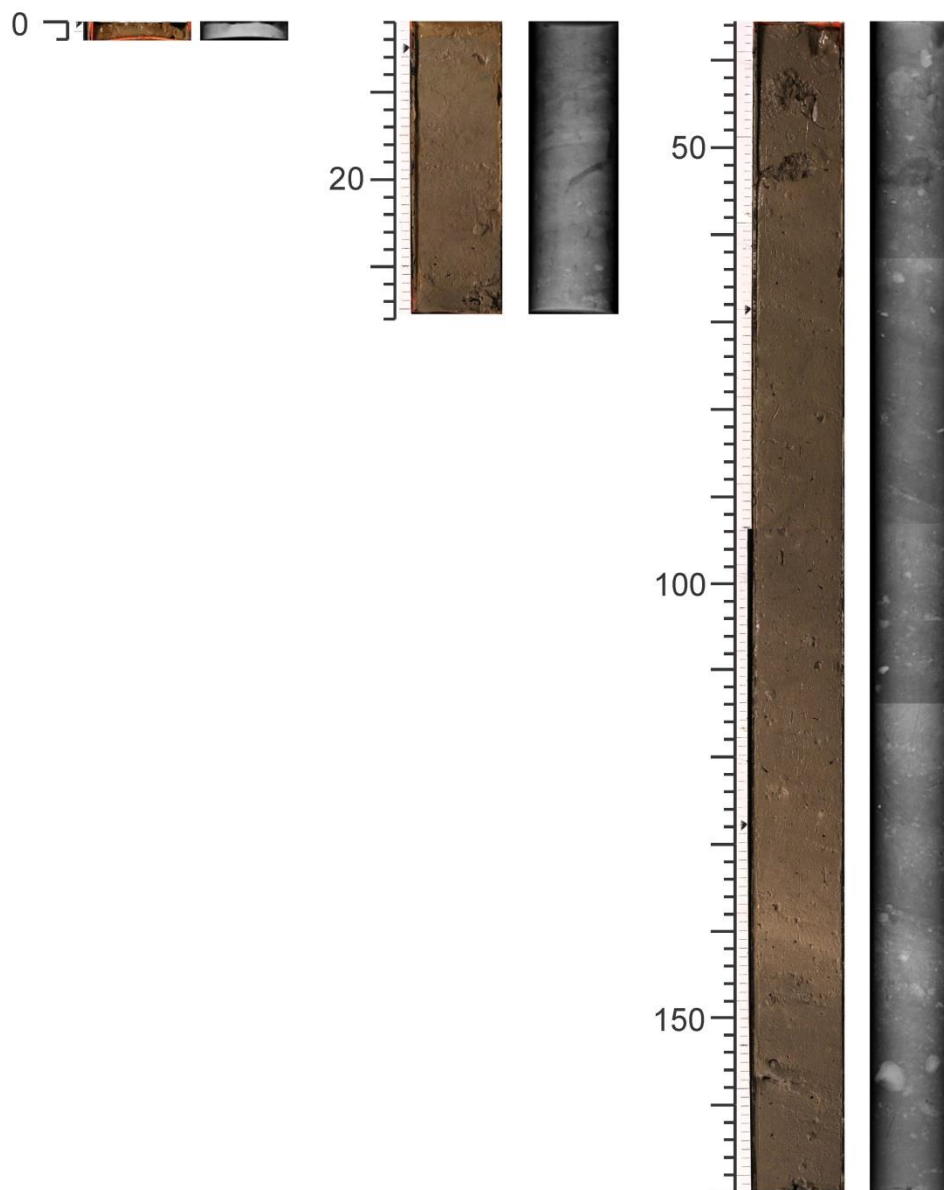


Figure 3.67b. Photography and X-radiography compilation for trigger weight core 2013029-048.

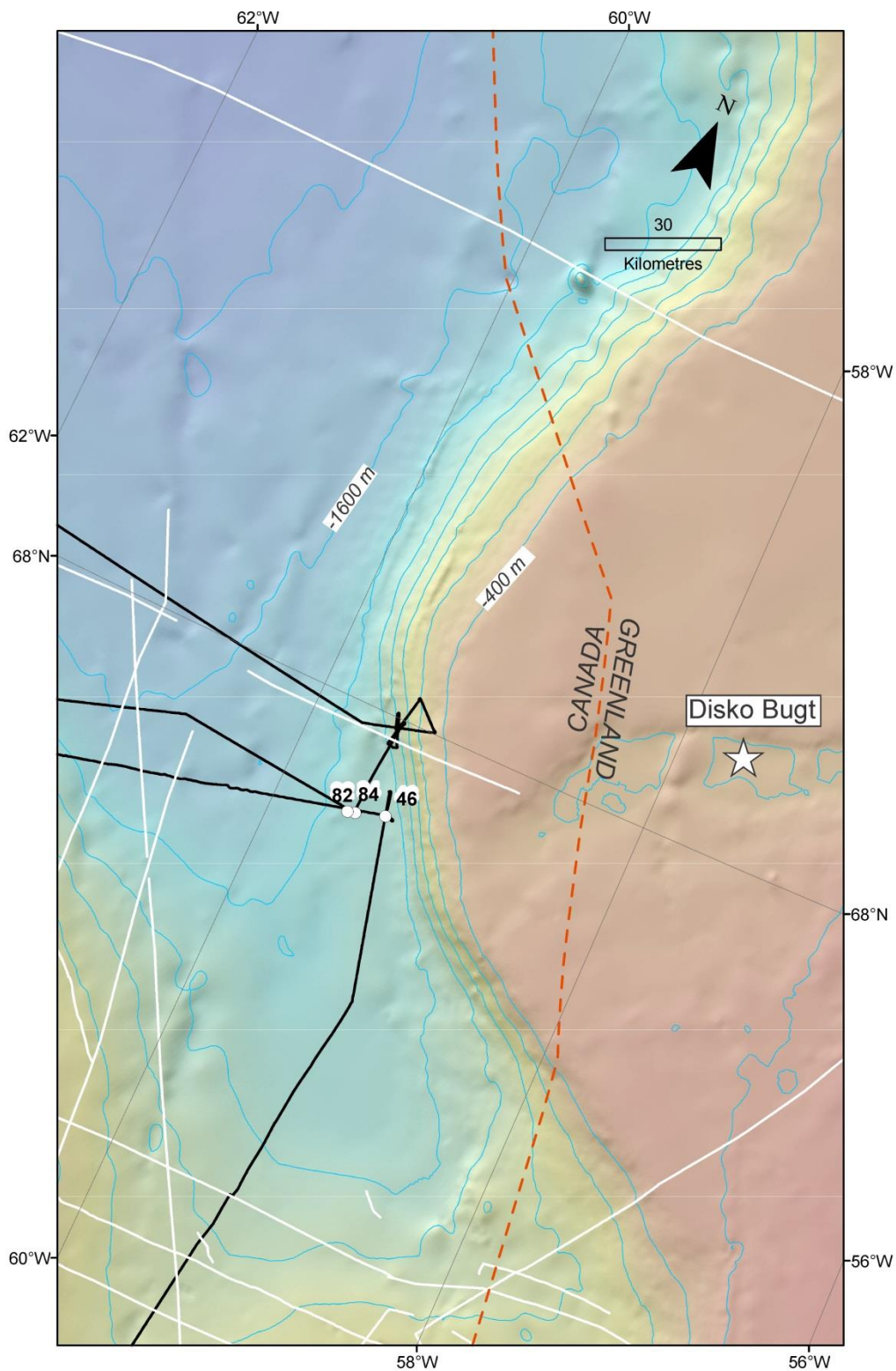


Figure 3.68. Regional map showing core locations and seismic coverage for the Disko Bugt region. 2013029 core locations are indicated by white circles and 2013029 sub-bottom profiler coverage by black lines. White lines indicate high resolution seismic reflection profiles collected by the GSC prior to the 2013 expedition. Bathymetric contour interval is 200 m.

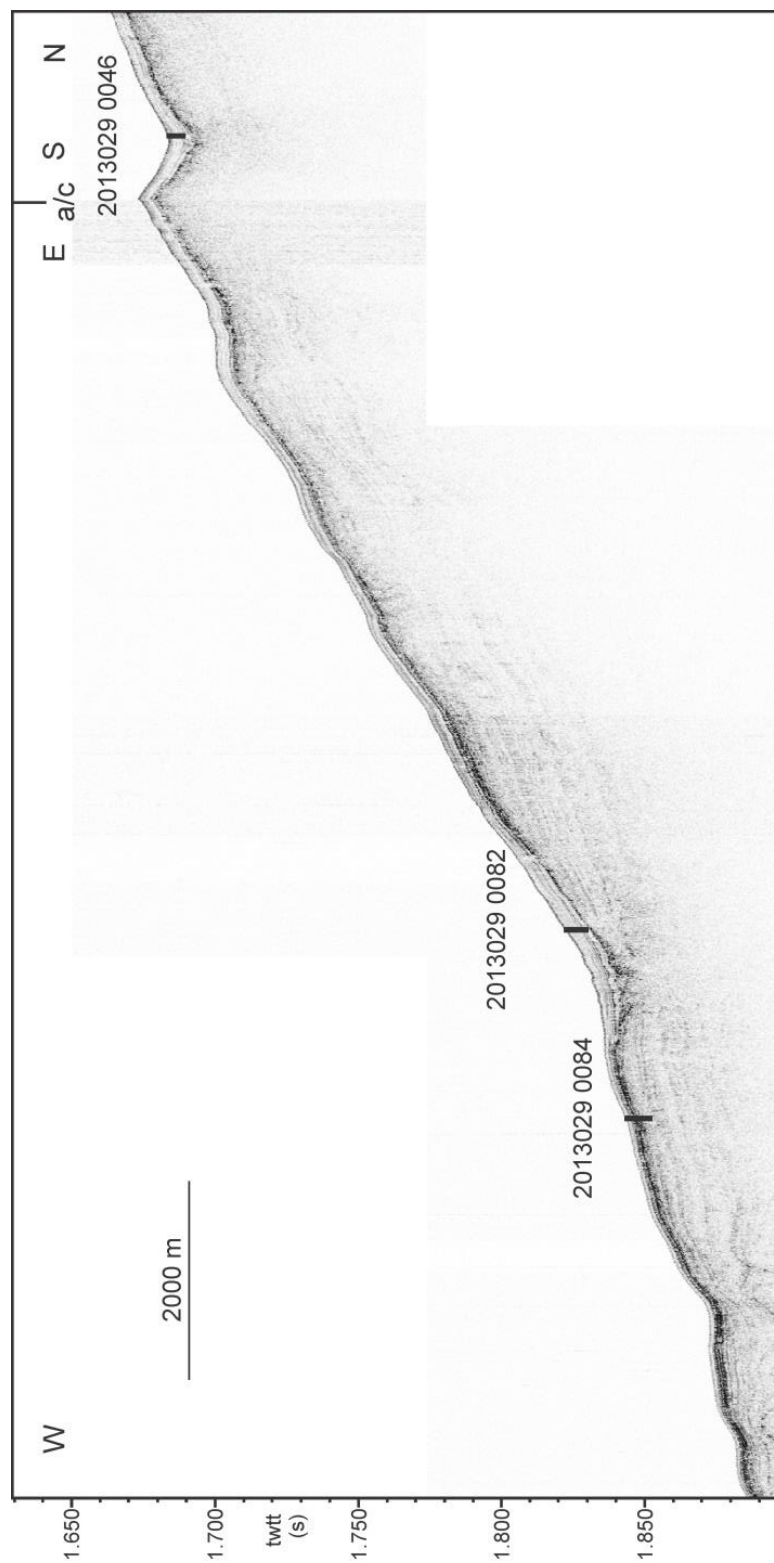


Figure 3.69 3.5 kHz sub-bottom profile showing the regional acoustic facies and location of piston cores 2013029-046, 2013029-082 & 2013029-84.

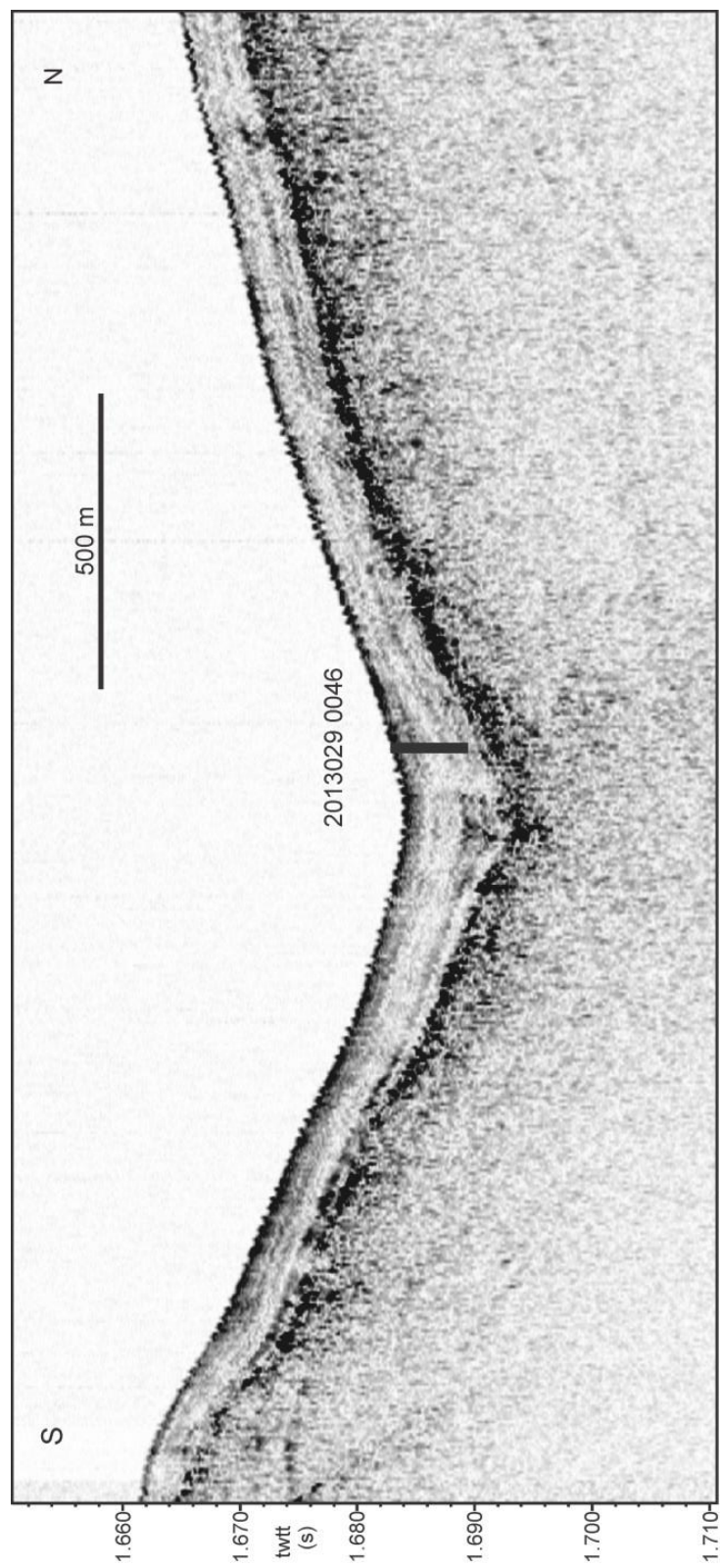


Figure 3.70. 3.5 kHz sub-bottom profile showing the acoustic stratigraphy and position of core 2013029-046.

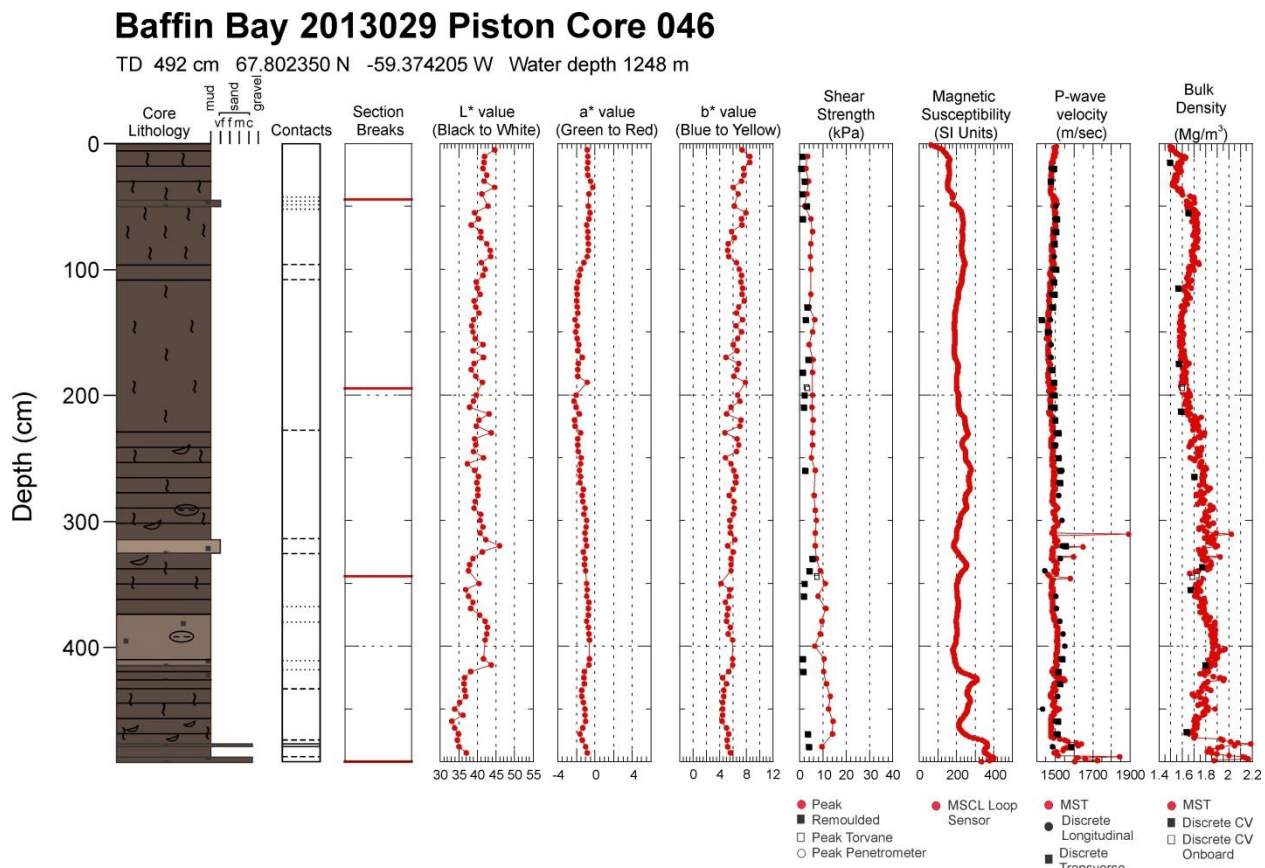


Figure 3.71a. Core plot summary for piston core 2013029-046.

Baffin Bay 2013029 Trigger Weight Core 046

TD 169.5 cm 67.802350 N -59.374205 W Water depth 1248 m

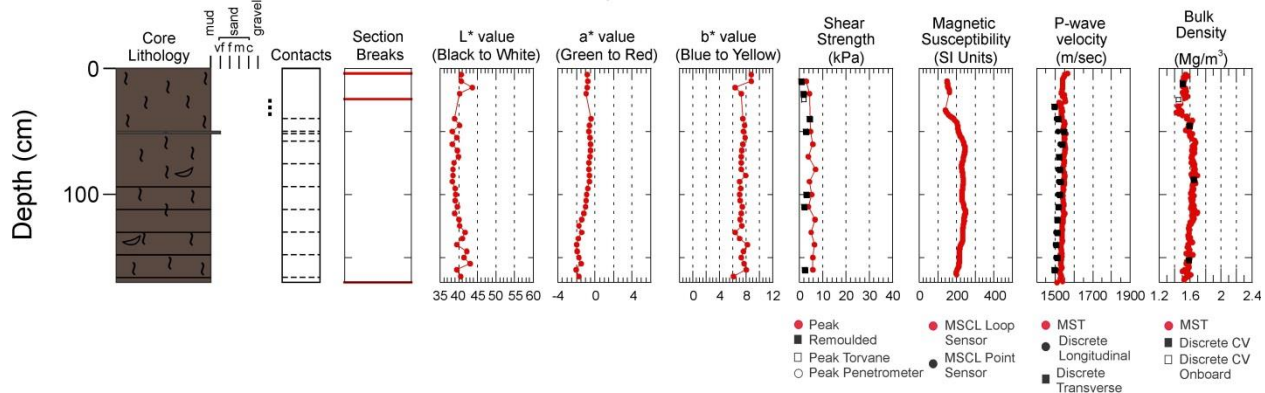


Figure 3.71b. Core plot summary for trigger weight core 2013029-046.

2013029 046 PC

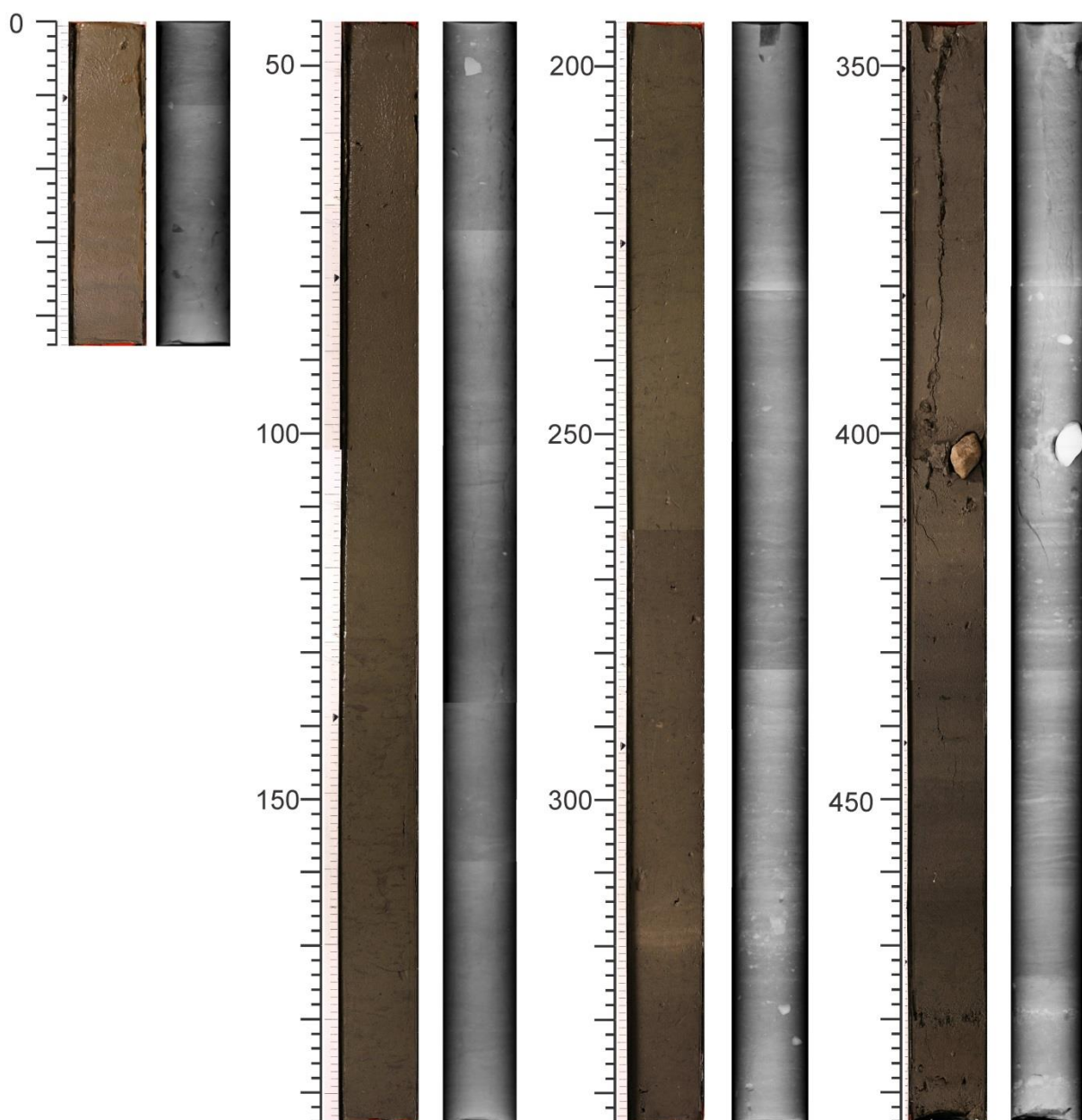


Figure 3.72a. Photography and X-radiography compilation for piston core 2013029-046.

2013029 046 TWC

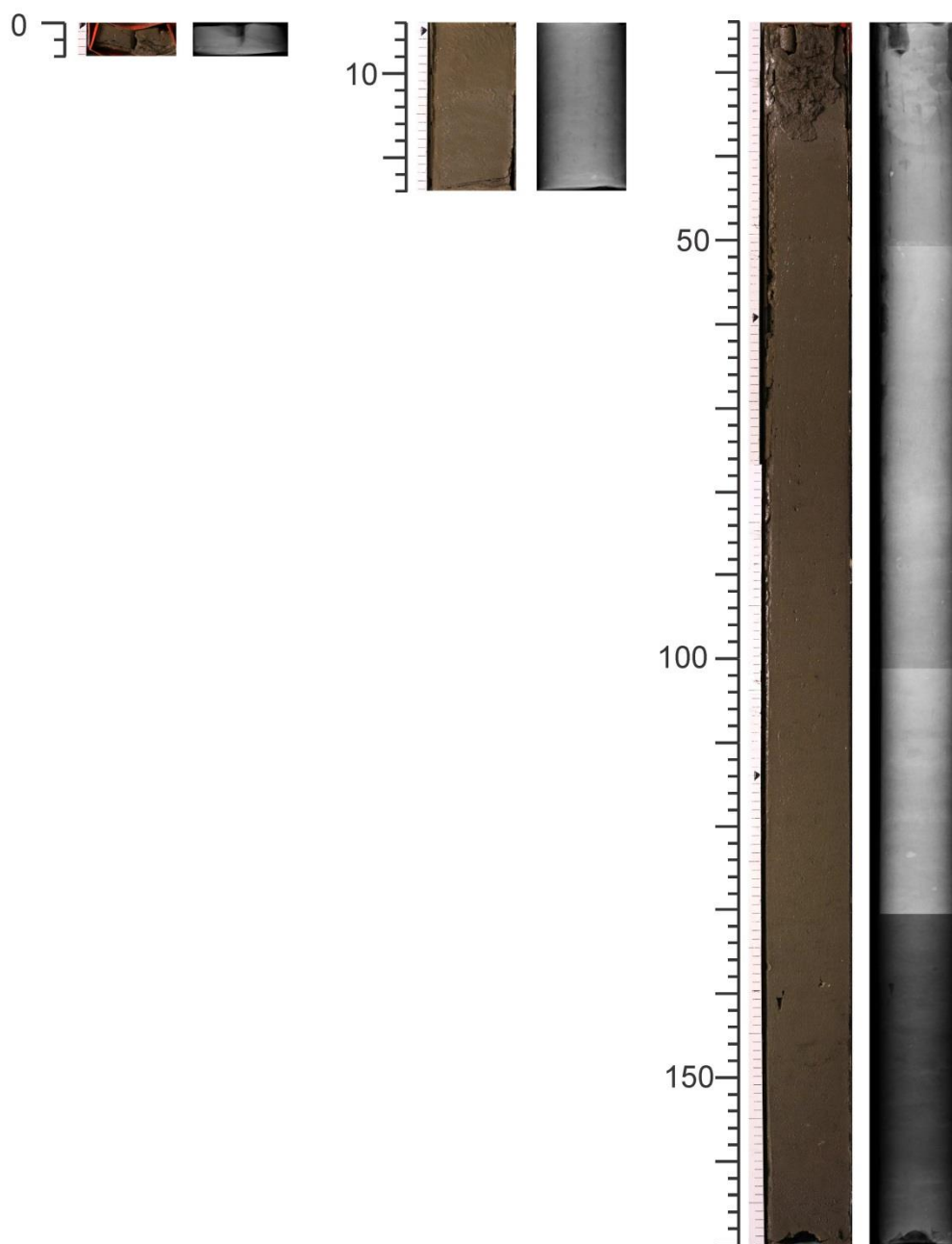


Figure 3.72b. Photography and X-radiography compilation for trigger weight core 2013029-046.

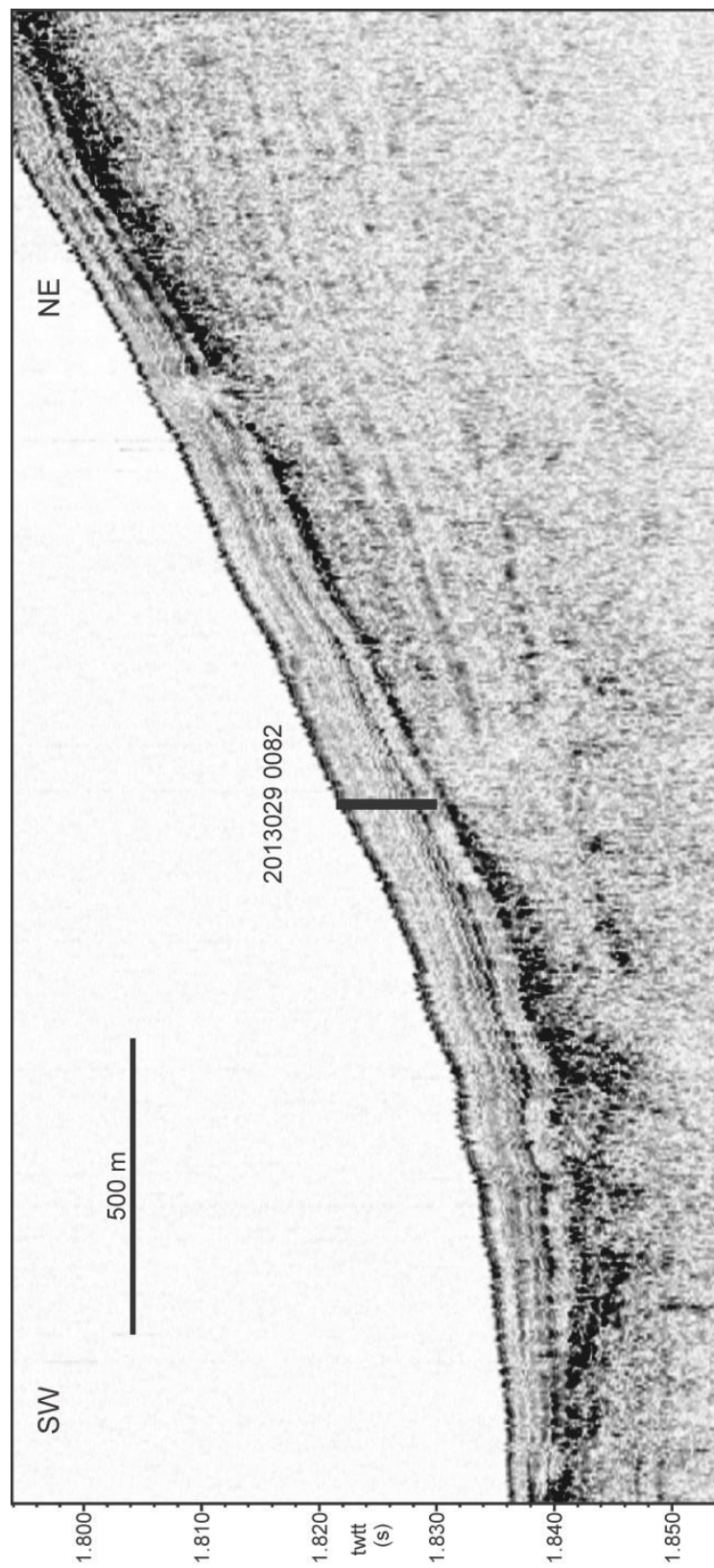


Figure 3.73. 3.5 kHz sub-bottom profile showing the acoustic stratigraphy and position of core 2013029-082.

Baffin Bay 2013029 Piston Core 082

TD 643 cm 67.781908 N -59.539071 W Water depth 1352 m

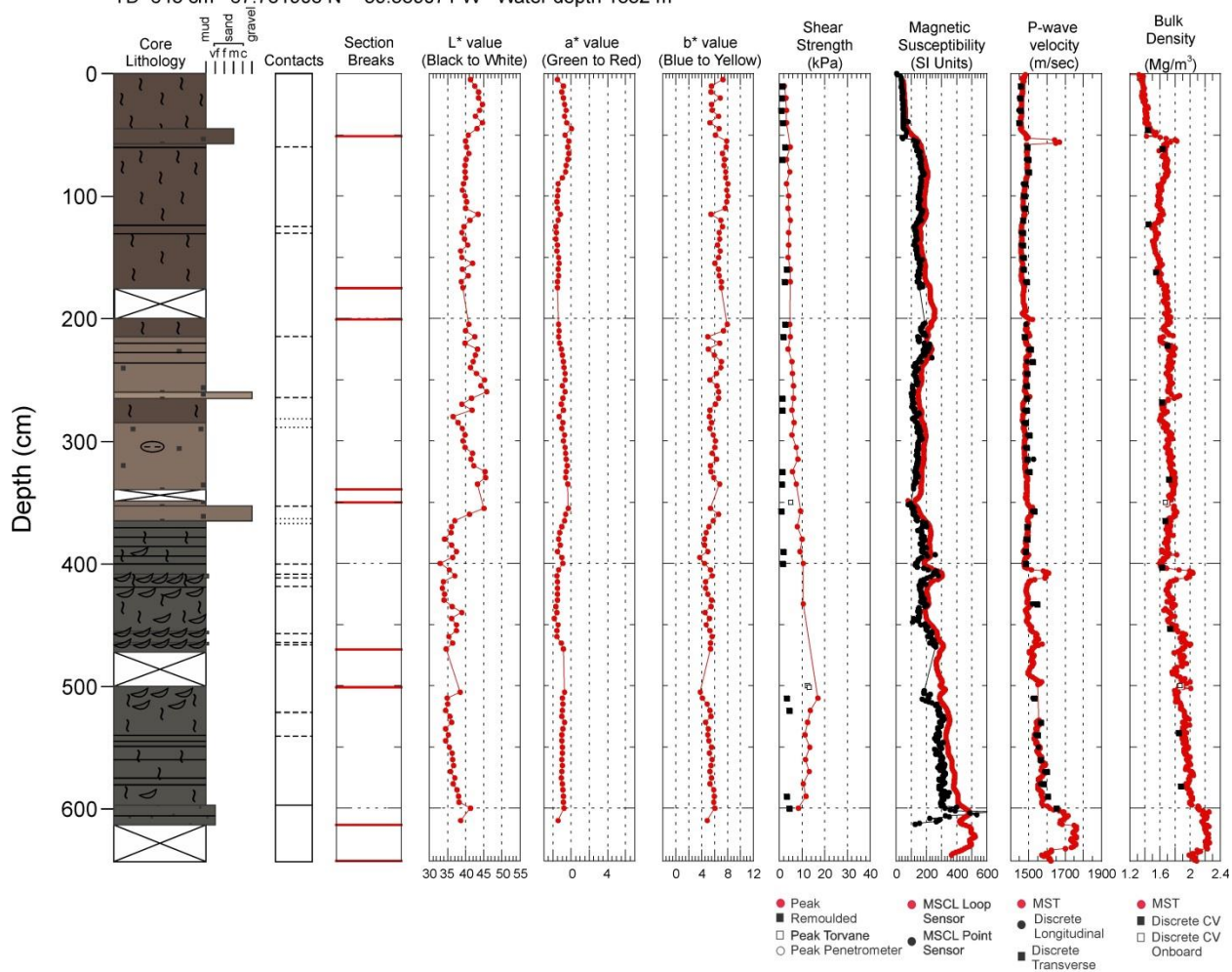


Figure 3.74a. Core plot summary for piston core 2013029-082.

Baffin Bay 2013029 Trigger Weight Core 082

TD 232.0 cm 67.781908 N -59.539071 W Water depth 1352 m

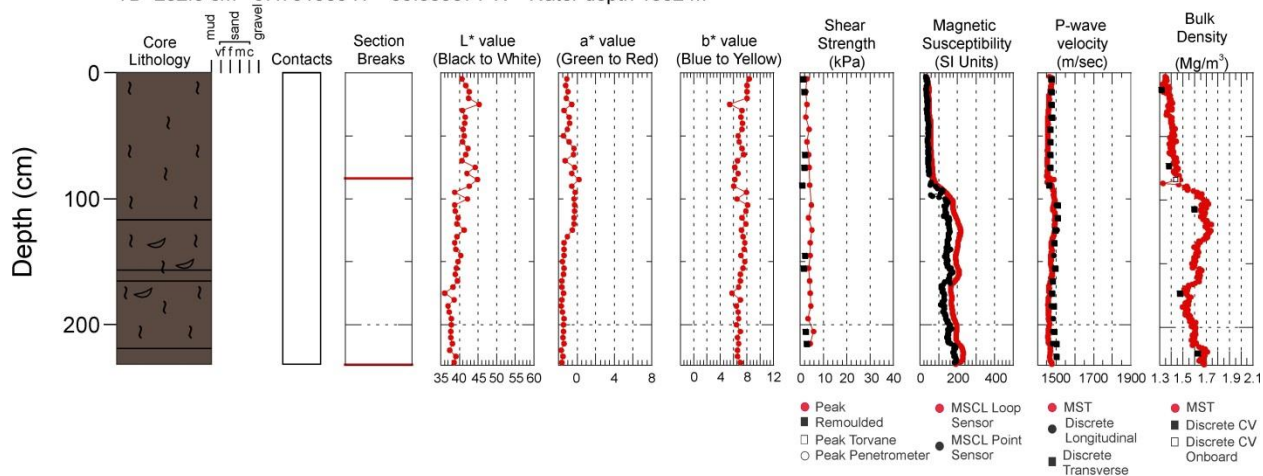


Figure 3.74b. Core plot summary for trigger weight core 2013029-082.

2013029 082 PC

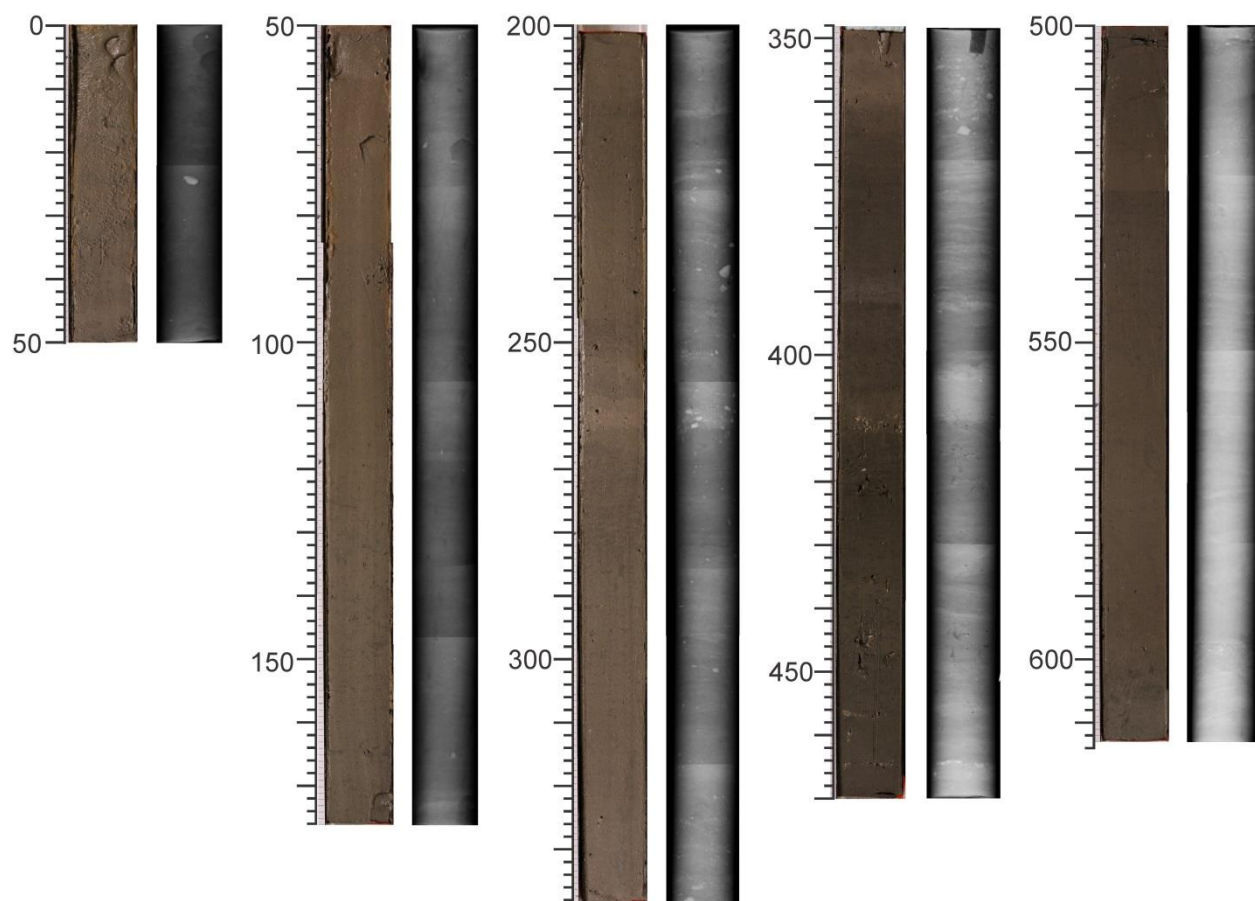


Figure 3.75a. Photography and X-radiography compilation for piston core 2013029-082.

2013029 082 TWC

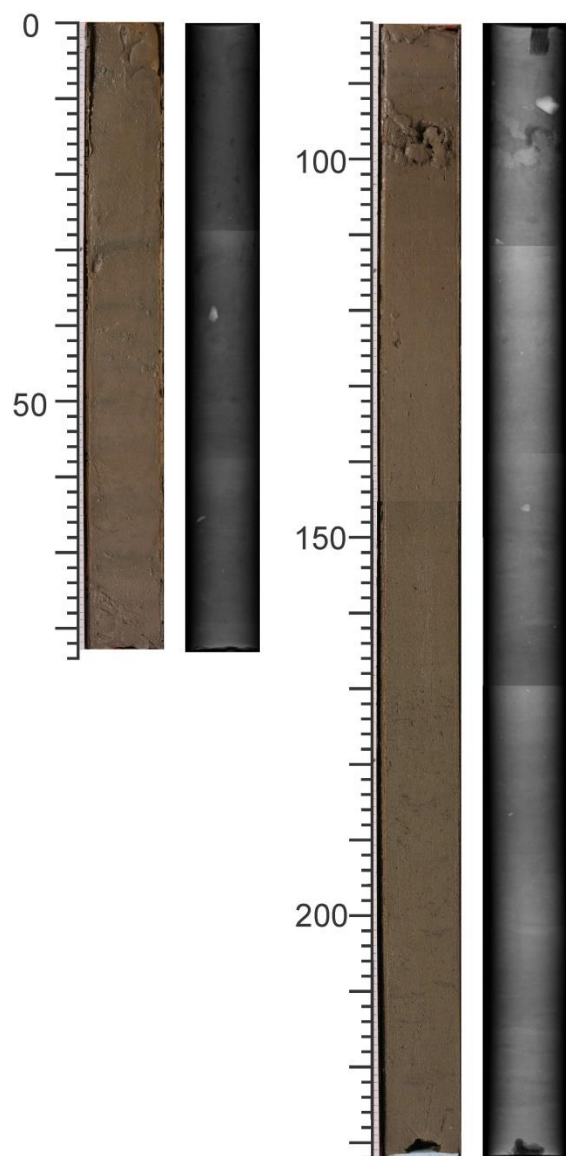


Figure 3.75b. Photography and X-radiography compilation for trigger weight core 2013029-082.

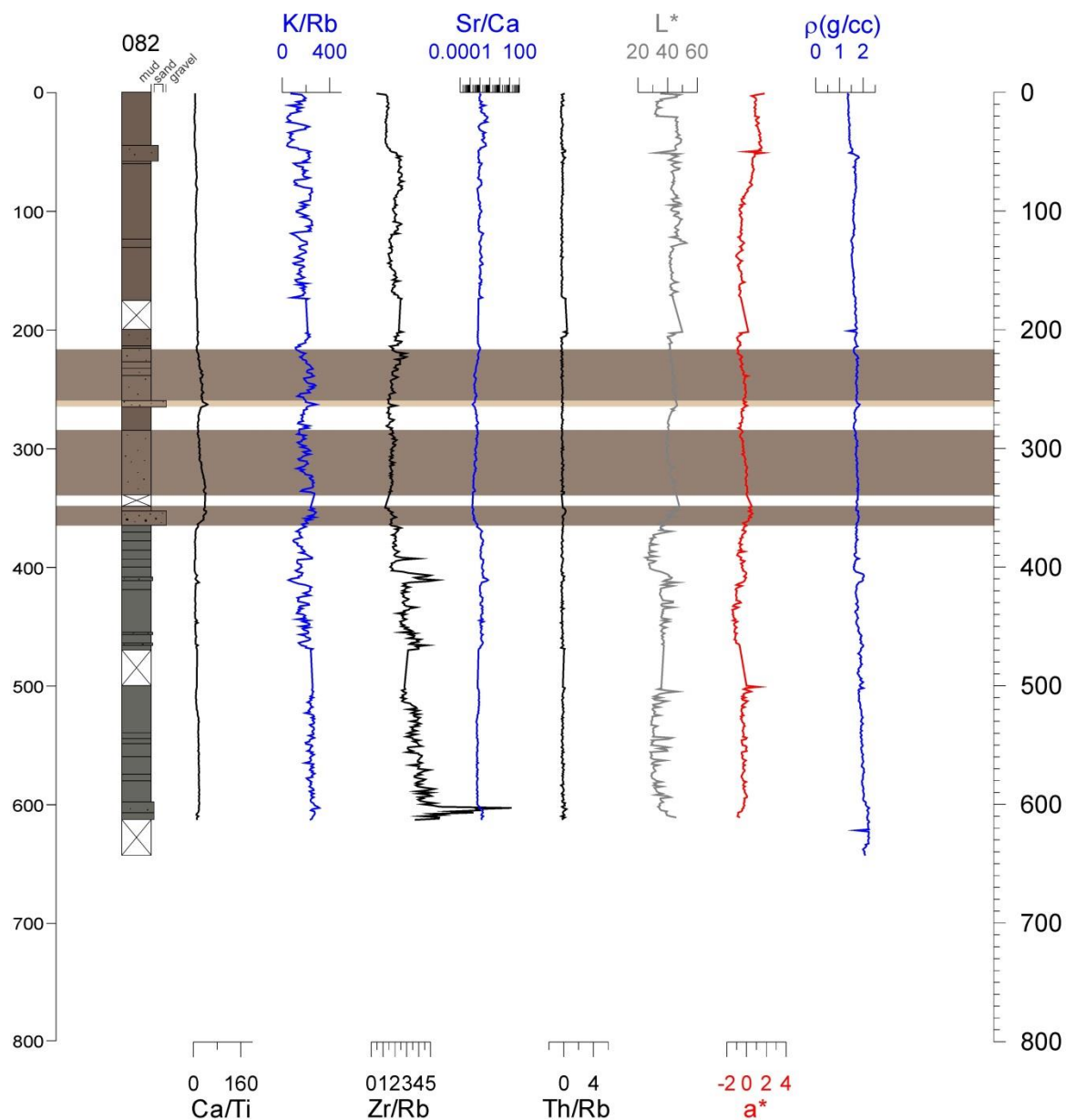


Figure 3.76. Down-core pXRF analysis for piston core 2013029-082. Tan highlighting indicates tan carbonate mud; light brown highlighting indicates light brown mud associated with an increase in the pXRF Ca/Ti ratio.

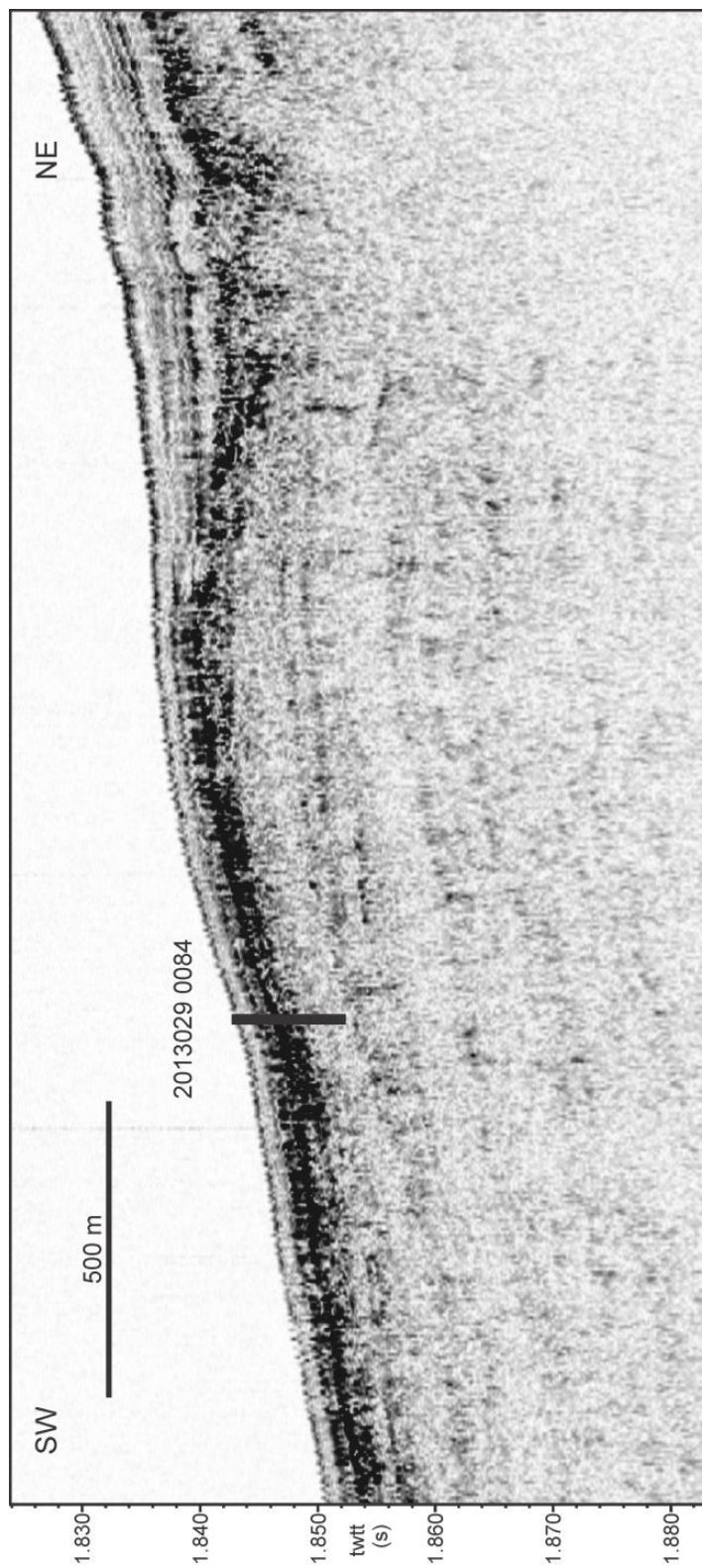


Figure 3.77. 3.5 kHz sub-bottom profile showing the acoustic stratigraphy and position of core 2013029-084.

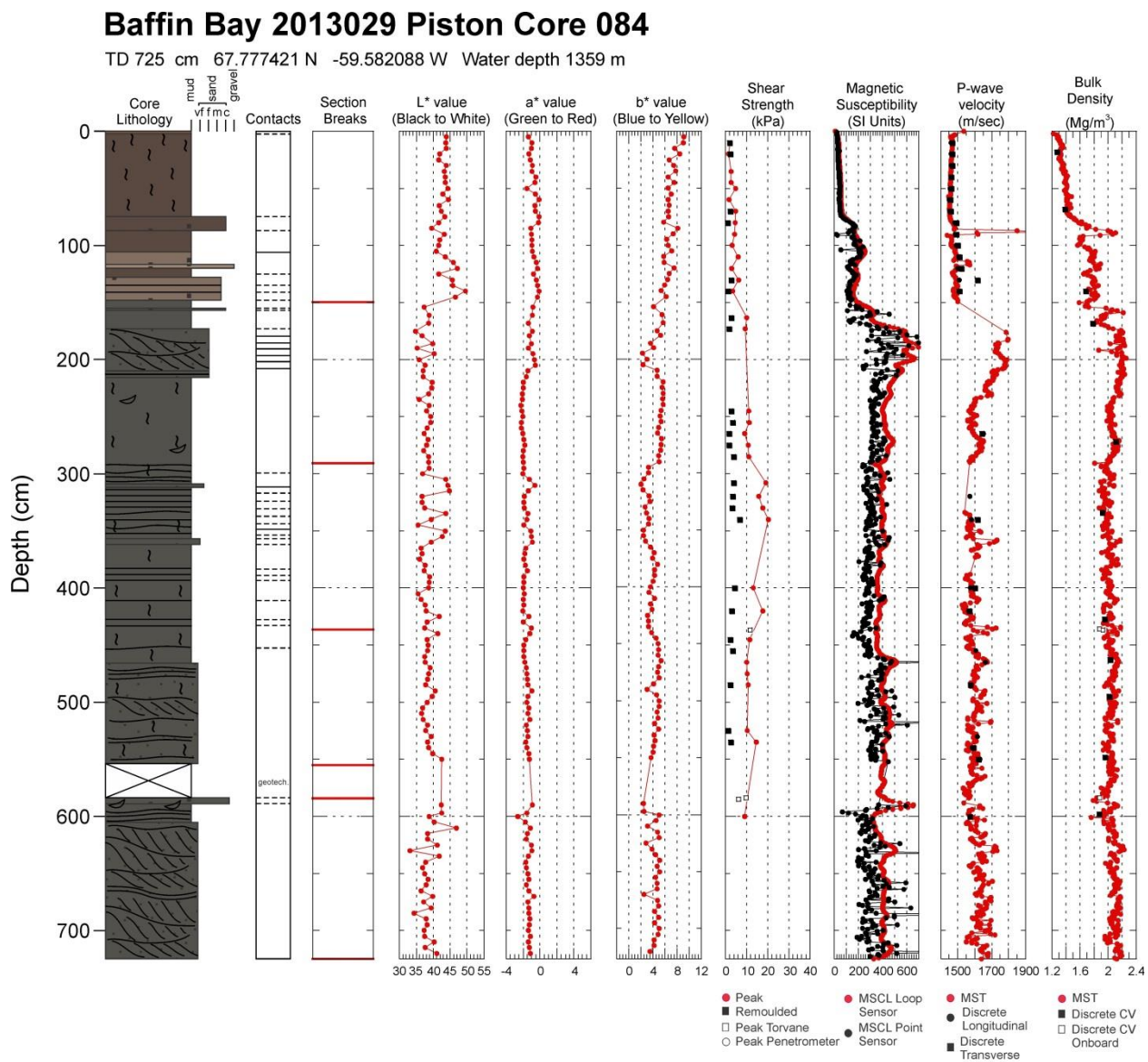


Figure 3.78a. Core plot summary for piston core 2013029-084.

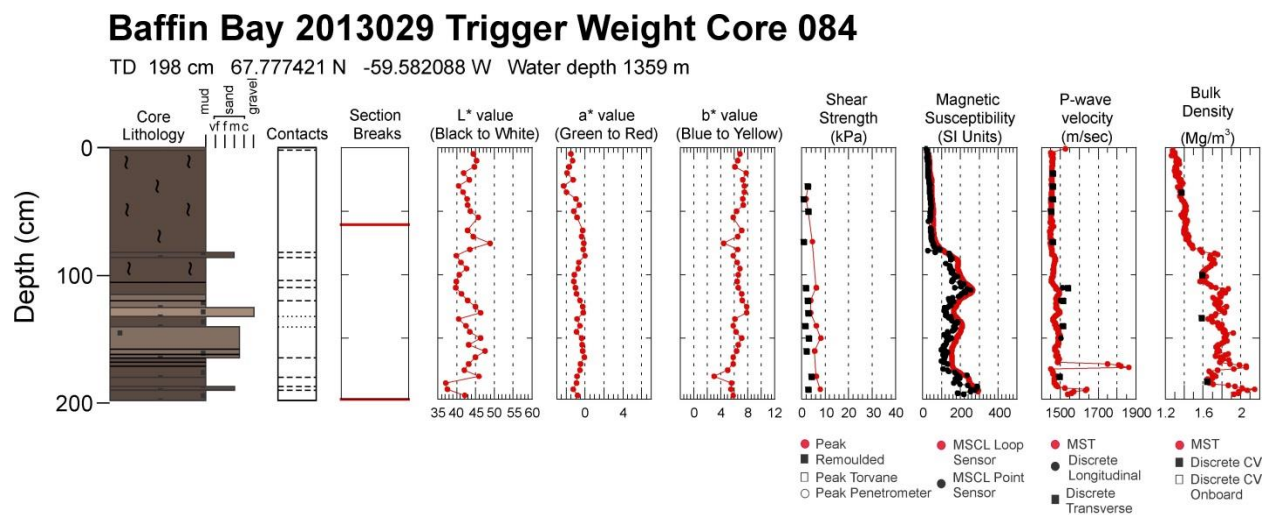


Figure 3.78b. Core plot summary for trigger weight core 2013029-084.

2013029 084 PC

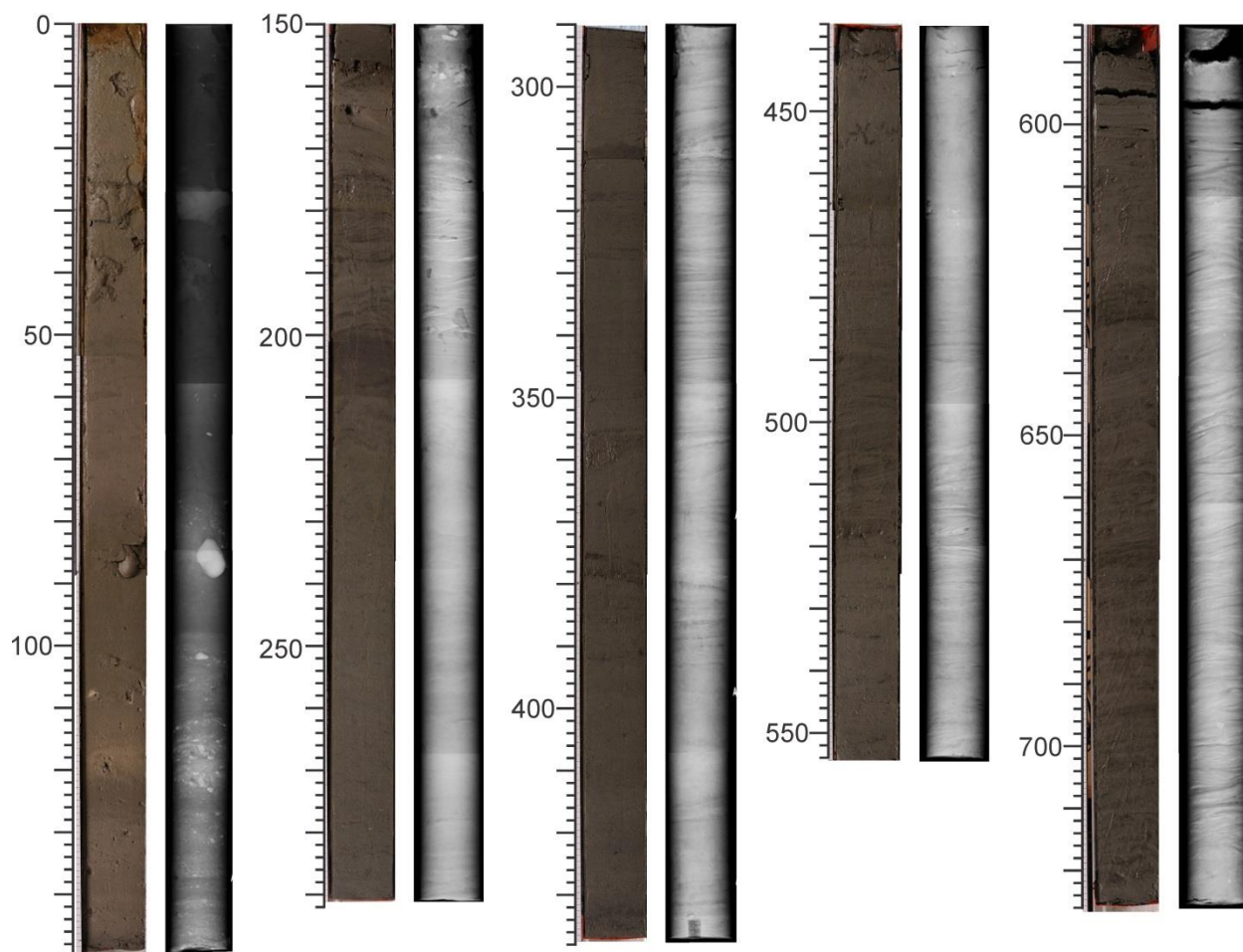


Figure 3.79a. Photography and X-radiograph compilation for piston core 2013029-084.

2013029 084 TWC

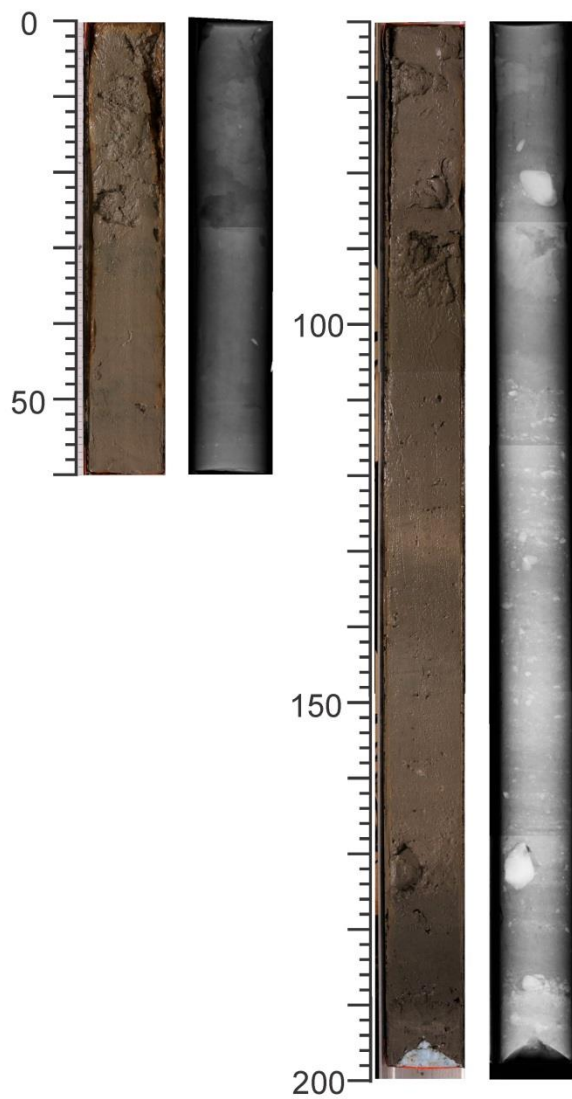


Figure 3.79b. Photography and X-radiograph compilation for trigger weight core 2013029-084.

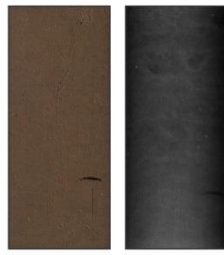
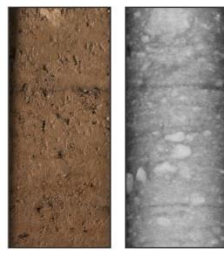

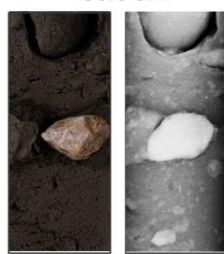
Image Xray	Facies	Sedimentary Features	Process/ Environment
<p>50 cm</p> <p>Core 052</p>  <p>70 cm</p>	<p>moderately to extensively bioturbated mud</p>	<p>massive to weakly stratified mud; burrows</p>	<p>hemipelagic deposition</p>
<p>250 cm</p> <p>Core 064</p>  <p>270 cm</p>	<p>tan carbonate IRD-rich mud</p>	<p>crudely stratified mud with randomly disseminated IRD; poorly sorted</p>	<p>significant ice-rafted deposition</p>
<p>325 cm</p> <p>Core 059</p>  <p>345 cm</p>	<p>red brown laminated mud</p>	<p>laminated clay and fine silt (1-4 mm); some angled laminae</p>	<p>turbidity current or turbid plume deposition</p>
<p>515 cm</p> <p>Core 074</p>  <p>535 cm</p>	<p>dark grey brown diamicton</p>	<p>massive, poorly sorted sand, granules and pebbles in a mud matrix</p>	<p>ice-proximal glacial debris flow deposition</p>

Figure 4.1. Summary figure of core lithofacies from the western margin margin of Baffin Bay.

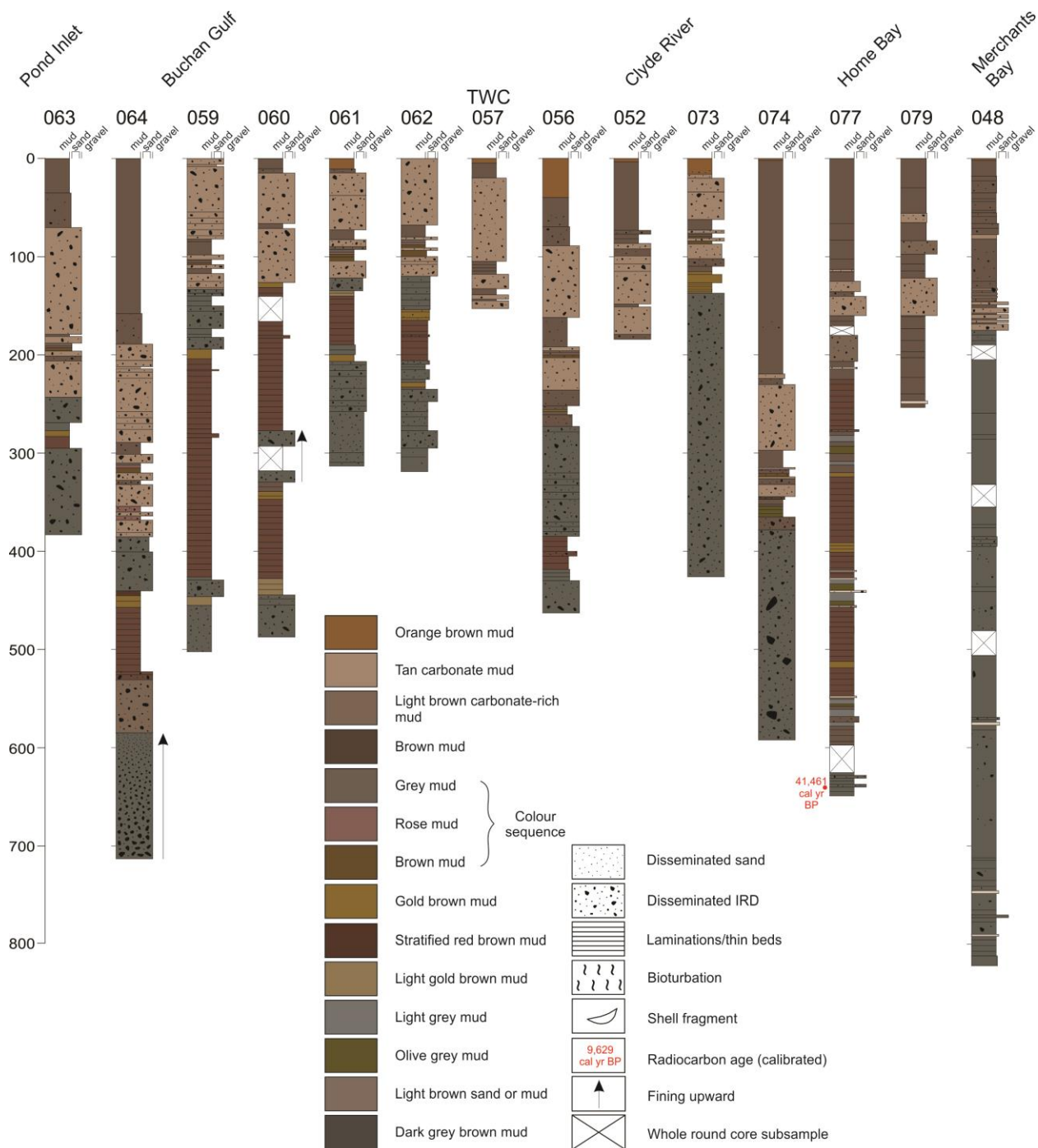


Figure 4.2. North to south along-slope variations of lithostratigraphy in cores from the western margin of Baffin Bay.

Diamicton

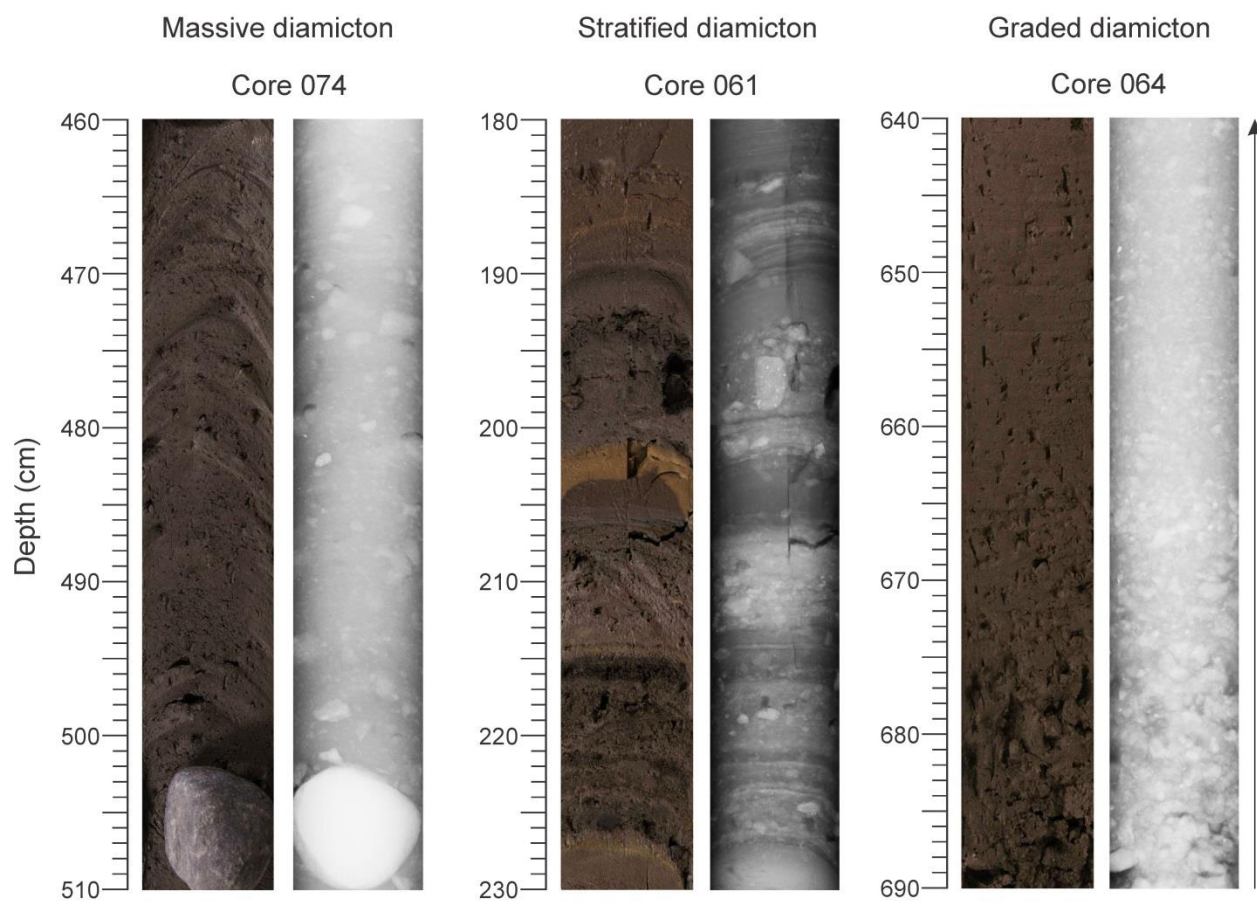


Figure 4.3. Examples of diamicton lithofacies.

Laminated red brown mud

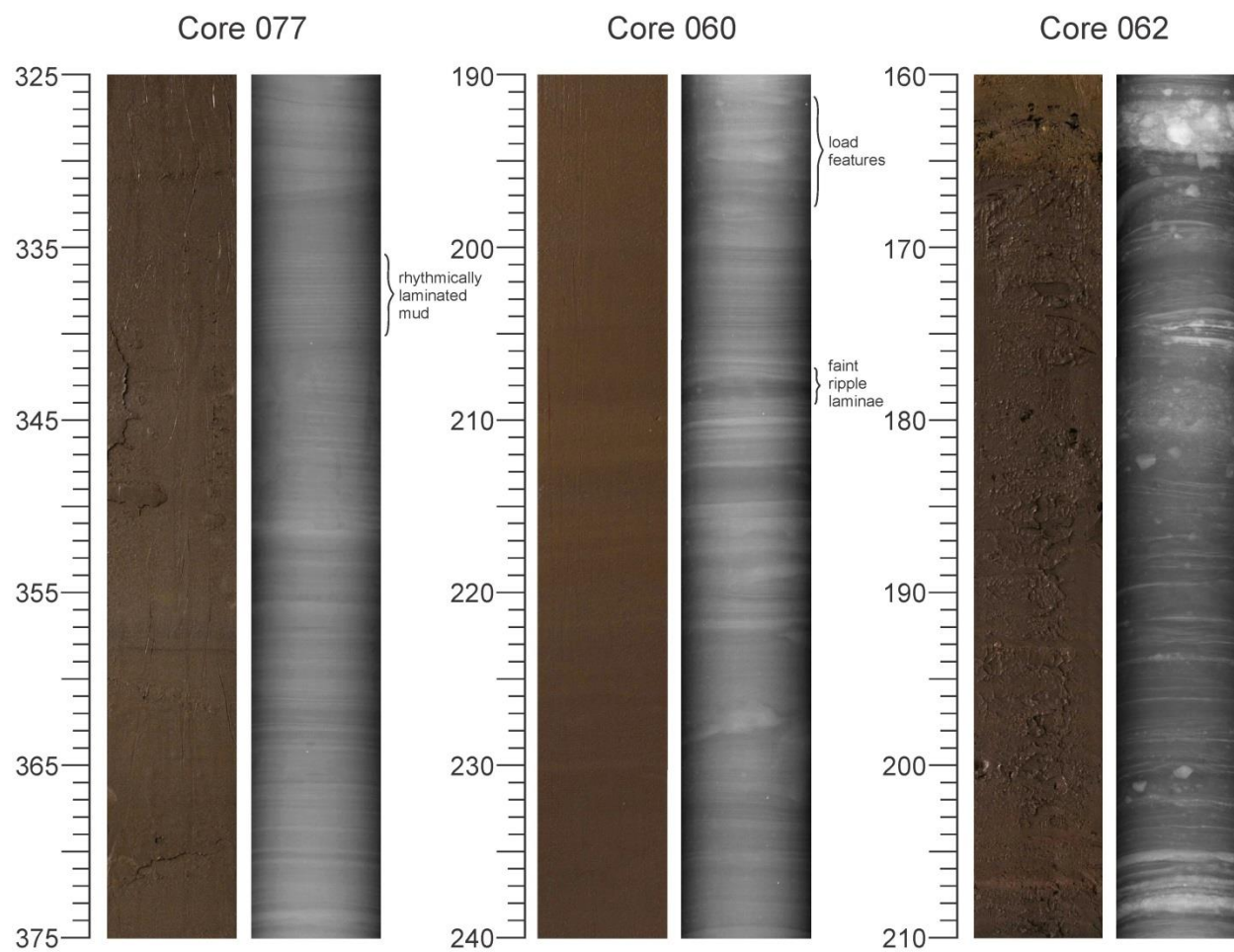


Figure 4.4. Examples of laminated red brown mud lithofacies.

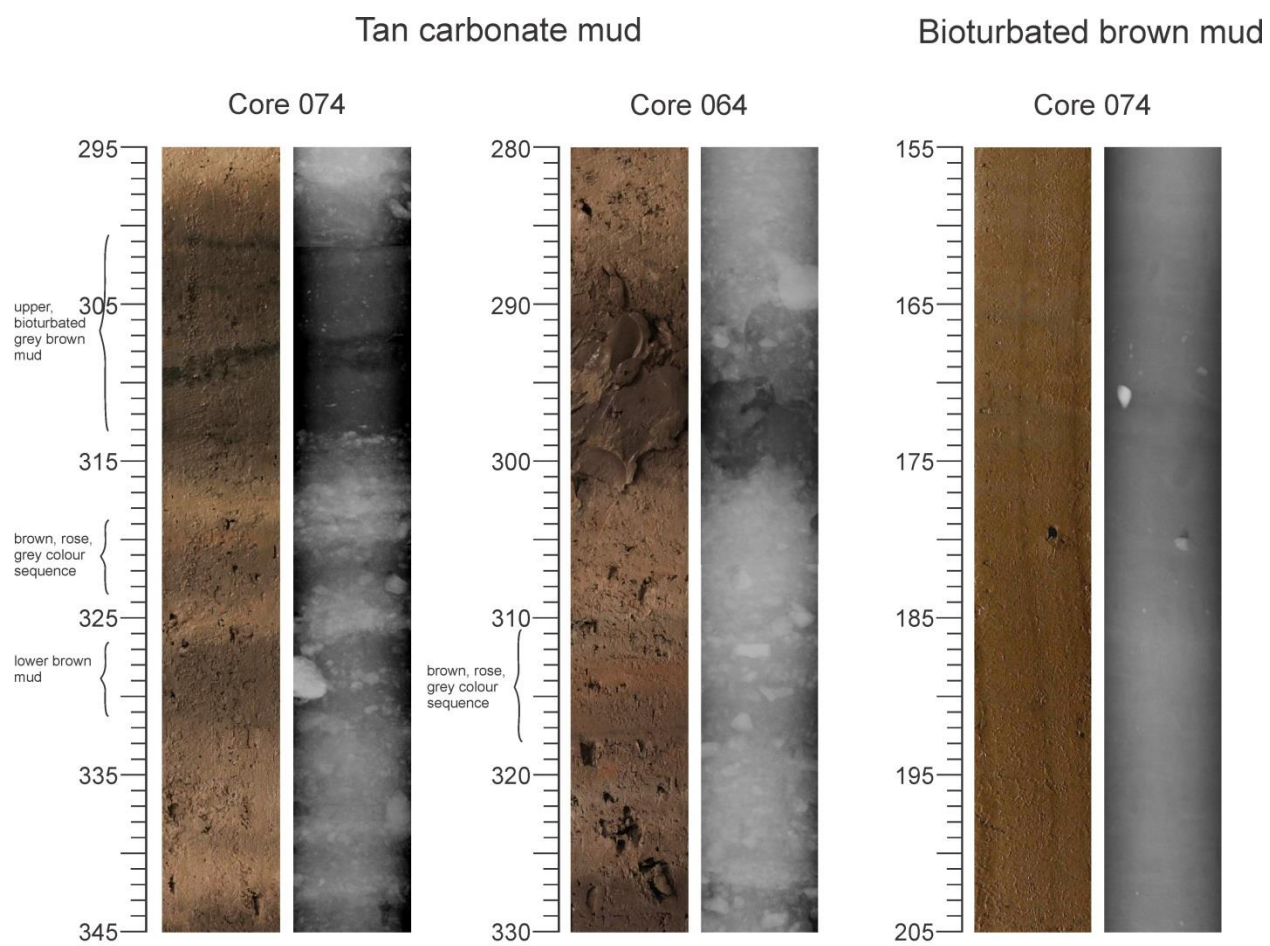


Figure 4.5. Examples of tan carbonate mud and bioturbated brown mud lithofacies.